

https://dspace.org/

Characterization of the mechanical and moisture absorption properties of kenaf reinforced polypropylene composites

Asumani, Oscar

2014-09-05
http://hdl.handle.net/10539/15415

Downloaded from a DSpace repository. https://dspace.org/

CHARACTERIZATION OF THE MECHANICAL AND MOISTURE ABSORPTION PROPERTIES OF KENAF REINFORCED POLYPROPYLENE COMPOSITES

Oscar Asumani

A thesis submitted to the Faculty of Engineering and the Built Environment, University of the Witwatersrand, Johannesburg, in fulfilment of the requirements for the degree of Doctor of Philosophy.

Johannesburg, February 2014

Declaration

I declare that this thesis is my own unaided work, expected where otherwise acknowledged. It is being submitted to the Degree of Doctor of Philosophy to the University of the Witwatersrand, Johannesburg. It has not been submitted before for any degree or examination to any other University.

Signed this 23rd day of May 2014



Oscar Asumani

Abstract

Great interest has been generated in the use of natural fibres as environmentally friendly reinforcing materials in polymeric composites, which do not require high load bearing capabilities. kenaf fibres extracted from kenaf plants (hibiscus cannabinus) have been identified as an attractive option due to its production cost and the ability of the kenaf plants to grow in a variety of climatic conditions. Polypropylene (PP) has a relatively low production cost, excellent corrosion resistance, good retention of mechanical properties and less recycling challenges in comparison to other matrix systems such as thermosets. Given the individual advantages of kenaf fibre and polypropylene, kenaf reinforced polypropylene composites (kenaf/PP composites) have considerable commercial interest in the composite industry. However, limitations arise with respect to the mechanical performance and to the resistance to moisture absorption when natural fibres are used.

This study focuses on the improvement of the mechanical properties (e.g. tensile, flexural, fatigue and impact properties) and the resistance to moisture absorption of kenaf reinforced polypropylene composites by means of fibre treatments (e.g. alkali and alkali-silane treatments) and the use of filler materials (e.g. functionalized multi-wall carbon nanotubes). Kenaf reinforced polypropylene composites are manufactured by a modified compression moulding using the film–stacking technique. The crux of this technique is that kenaf mats are impregnated with polypropylene powder in order achieve a uniform material distribution and to lower the manufacturing temperature, thereby preventing the thermal alteration of the composite constituents (e.g. kenaf fibres) and silano functional groups attached to the multi-wall carbon nanotubes. Fibre treatments including alkali treatments and alkali followed by silane treatments (alkali-silane) are considered in order to improve the fibre-matrix interfacial adhesion. The concentrations of the alkali solutions range from 1% to 8% in intervals of 1% by mass. Fibre contents ranging from 20% to 35% in interval of 5% by mass are considered for both kenaf and glass fibre reinforced plates. Functionalized multi-

wall carbon nanotubes are used as filler material in order to improve the mechanical properties of the composite plates. The concentrations of the multi-wall carbon nanotube (MWCNT) range from 0.1% to 1.25%.

Mechanical test and microscopic examination results showed that alkali treatments improve the mechanical properties of kenaf/PP composites. However, the improvements due to alkali-silane treatments were found to be more significant because additional silane treatments substantially enhanced the fibre-matrix interfacial adhesion. Material failures in untreated kenaf/PP composites and alkali treated kenaf/PP composites were mainly characterized by fibre pull-outs, whereas in alkali-silane treated kenaf/PP composites they were characterised by fibre breakage. Alkali concentrations of 5% and 6% NaOH are found to the optimum concentrations for both alkali treatment and alkali-silane treatment.

The use of functionalized MWCNTs as filler material improved furthermore the mechanical properties of kenaf/PP-MWCNT composites in comparison to those of kenaf/PP and glass/PP composites. The main contributing factors of the improvements were found to be the enhancement of the interfacial adhesion between the nanoparticles and the matrix, and also between the nanoparticles and kenaf fibres. Material failures in kenaf/PP-MWCNT composites were characterized by fibre breakage and matrix cracks. The optimum MWCNT concentrations were found to be 0.5% and 0.75%. 30% fibre contents was found to be the optimum fibre content for both kenaf/PP and kenaf/PP-MWCNT composites. Test results showed that the fibre treatments, especially alkali-silane treatment, improved the resistance to moisture absorption of the composites. Test results also showed that the manufacturing technique, which enables the manufacturing of composite plates with layers of different moisture diffusion resistances, has a significant influence on the resistance of kenaf/PP composites. The addition of multi-wall carbon nanotubes to the polypropylene matrix did not alter the moisture absorption resistance of kenaf/PP-MWCNT composites. The impregnation of kenaf and fibre glass mats with polypropylene powder significantly lowered the manufacturing temperature to below the typical melting temperature of the unreinforced polypropylene.

[i] For the purposes of this study, “composite” refers to fibre reinforced polymer composite laminate.

In memory of my late father

Gabriel Asumani Mwimba Lunyafu

Acknowledgements

I would like to thank the following people:

Professor Ratnam Paskaramoorthy for his supervision, support and commitments.

Professor Robert Grant Reid for his assistance.

Professor Ajay Mishra for making available the Haake PolyLab OS rheo-mixer

Dr. Jacob Mutu and Dr. Sabelo Mhlanga for their technical assistances.

My Dear wife Mylene Kamin Mutomb Asumani and my children Rita Asumani, Gabriel Asumani and Samuel Asumani for their prayer and encouragement.

Prophet Elize Bukasa and my brother Gaby Asumani for their prayer

My Line SASOL manager Ralf Paul Schaefer for his encouragement.

I would like to also thank SASOL and The National Research Foundation and Advanced Manufacturing Technology Strategy for their supports.

I give glory to the Almighty GOD for his grace and favour.

Published Works

Aspects of this thesis have been published in the following reference:

R.G. Reid, R. Paskaramoorthy and O.M.L. Asumani. The effects of alkali–silane treatment on the tensile and flexural properties of short fibre non-woven kenaf reinforced polypropylene composites. Composites: Part A, 43:1431-1440, 2012.

Aspects of this thesis are in process for publication.

Title: Effects of fibre treatments on the moisture absorption of kenaf fibre reinforced polypropylene composites.

Title: Effects of fibre treatments on the impact and fatigue properties of kenaf fibre reinforced polypropylene composites.

Title: Effects of the surface treatments of multi-wall carbon nanotubes on the impact and fatigue resistance of kenaf fibre reinforced polypropylene composites.

Contents

Declaration i

Abstract ii

Acknowledgements vi

Published Works vii

Contents viii

List of Figures xii

List of Tables xx

List of Abbreviations xxi

List of Symbols xxii

1 INTRODUCTION 1

2 LITERATURE SURVEY 5

2.1 Kenaf fibres 5

2.1.1 Origin of kenaf fibres 5

2.1.2 Production, trade and consumption of kenaf 9

2.1.3 Processing of kenaf fibres for polymeric composite utilization 11

2.1.4 Utilization of kenaf fibres as reinforcing material 11

2.2 Polypropylene matrix 13

2.3 Mechanical and moisture absorption properties of natural fibre reinforced polymer composites 16

2.3.1 Effects of fibre treatments on the mechanical properties of natural fibre reinforced polymer composites 17

2.3.2 Effects of fibre treatments on the resistance to moisture absorption of natural fibre reinforced polymer composites 26

2.4 Use of filler materials to improve the mechanical properties of natural fibre reinforced polymer composites 30

2.4.1 Improvement of the CNT dispersion and the CNT-matrix interfacial adhesion 32
2.4.2 Effects of the nanoparticle concentration on the mechanical properties of CNT reinforced polymer composites 37
2.4.3 Effects of nanoparticule alignments on the mechanical properties of CNTs reinforced polymer composites 39
2.5 Manufacturing of natural fibre reinforced polymer composites 40
2.6 Summary 41
2.7 Objectives 42
2.8 Outlines 42
3 PRODUCTION OF COMPOSITE PLATES 44
3.1 Fabrication materials 45
3.1.1 Matrix systems 45
3.1.1.1 Unreinforced PP matrix 45
3.1.1.2 MWCNTs reinforced PP matrix 46
3.1.2 Reinforcing materials 48
3.1.2.1 Glass fibres 48
3.1.2.2 Kenaf fibres 49
3.1.3 Multi-wall carbon nanotubes 52
3.2 Chemical treatments of kenaf mats 53
3.2.1 Alkali treatments 53
3.2.2 Alkali-silane treatments 56
3.3 Chemical treatments of MWCNTs 58
3.3.1 Treatments 61
3.3.1.1 Ultrasonic treatments 61
3.3.1.2 Acid treatment of MWCNTs 62
3.3.1.3 Silane treatment of acid treated MWCNTs 63

3.3.2 Characterization of MWCNTs 64
3.3.2.1 Dispersion and surface morphology of the MWCNTs 65
3.3.2.2 Characterization of the functional groups 69
3.3.3 Reaction mechanism of surface treatments 71
3.3.4 Thermal stability of functionalized MWCNTs 71
3.4 Fabrication of kenaf and glass fibre reinforced PP composites 73
3.5 Fabrication of polypropylene reinforced MWCNT plates 81
3.6 Material formulation 88
4 EXPERIMENTAL EVALUATION OF THE MECHANICAL AND MOISTURE PROPERTIES 91
4.1 Mechanical testing 91
4.1.1 Tensile tests 91
4.1.2 Flexural test 92
4.1.3 Fatigue test 93
4.1.3.1 Test control parameters 95
4.1.3.2 Test specimen characteristics and equipment 104
4.1.4 Izod notched impact test 105
4.2 Moisture absorption test 106
4.3 Microscopic examination 108
5 DISCUSSION 110
5.1 Effect of fibre treatment on the mechanical properties 110
5.1.1 Tensile strength and tensile modulus of kenaf/PP composites 111
5.1.1.1 Effect of alkali treatment on the tensile properties of kenaf/PP composites 111
5.1.1.2 Effect of alkali-silane treatment on the tensile properties of kenaf/PP composites 115
5.1.2 Flexural strength of kena/PP composites 121

5.1.2.1 Effect of alkali treatment on the flexural properties of of kenaf/PP composites 121

5.1.2.2 Effect of alkali-silane treatment on the flexural properties of kenaf/PP composites 123

5.1.3 Fatigue strength of kenaf/PP composites 124

5.1.3.1 Effect of alkali treatment on the fatigue properties of kenaf/PP composites 124

5.1.3.2 Effect of alkali-silane treatment on the fatigue properties of kenaf/PP composites 132

5.1.4 Izod notched impact strength of kenaf/PP composites 140

5.1.4.1 Effect of alkali treatment on the impact properties of kenaf/PP composites 140

5.1.4.2 Effect of alkali-silane treatment on the impact properties of kenaf/PP composites 144

5.2 Effects of fibre treatments on the resistance to moisture absorption 149

5.3 Effect of the inclusion of MWCNTs on the mechanical properties 156

5.3.1 Tensile strength and tensile modulus of kenaf/PP-MWCNT composites 161

5.3.2 Flexural strength of kenaf/PP-MWCNT composites 163

5.3.3 Fatigue strength of kenaf/PP-MWCNT composites 165

5.3.4 Izod impact strength of kenaf/PP-MWCNT-composites 168

5.4 Effect of the inclusion of MWCNTs on the resistance to moisture absorption 172

6 CONCLUSIONS 175

7 RECOMANDATIONS 177

REFERENCES 178

List of Figures

Figure 2.1: Kenaf: (a) Kenaf seed, (b) Kenaf plant, (c) Kenaf fibres and (d) Kenaf mat 7
Figure 2.2: Cross-sectional view of kenaf 7
Figure 2.3; Classification of natural fibres for use in the composite industry 11
Figure 2.4: Molecular structure of polypropylene 13
Figure 2.5: Process flow diagram of polypropylene 14
Figure 2.6: Interfacial fibre-matrix bonds caused by fibre treatments 19
Figure 2.7: Fatigue damage development in $[0/90]_s$ laminate 22
Figure 2.8: Impact test classification for fibre reinforced polymer composites ... 24
Figure 2.9: Intimate fibre-matrix contact and even fibre distribution 25
Figure 2.10: Fibre-matrix adhesion mechanism due to the use of coupling agent 26
Figure 2.11: water absorption and swelling at different silane concentration 28
Figure 2.12: TEM images of multi-wall carbon nanotubes 31
Figure 2.13: SEM images: (a) aggregates, (b) untreated carbon nanotubes, (c) uniform distribution of carbon nanotubes, (d) PP-g-MA carbon nanotube treated 34
Figure 2.14: TEM image of the MWCNTs (A and B: Raw nanotubes, C and: Oxidized and reduced, D: Silane treated) 35
Figure 2.15: Schematic of the reaction between the reduced carbon nanotube and the 3-Glycidoxypropyltrimethoxy silane 36
Figure 2.16: SEM images: (a) agglomerated of MWCNT, (c) uniform dispersion of nanoparticles) 38
Figure 3.1: Polypropylene: (a) PP pallets, (b) PP powder 46
Figure 3.2: MWCNT reinforced polypropylene matrix: 0.1% MWCNT-PP and 1.25% MWCNT-PP 47
Figure 3.3; Glass fibre chopped strand mats, 350 g/m^2 48
Figure 3.4: SEM picture of glass fibre 49
Figure 3.5: Kenaf fibres: (a) 125 g/m^2 mat, (b) 350 g/m^2 mats 50
Figure 3.6: Untreated kenaf fibre 50

Figure 3.7: Raw MWCNTs 52
Figure 3.8: Alkali and alkali-silane treated of kenaf mats 54
Figure 3.9: Alkali treatment mechanism of kenaf fibre 55
Figure 3.10: SEM of alkali treated kenaf fibres at: (a) 3%NaOH, (b) 4%NaOH, (c) 6%NaOH and (d) 8%NaOH 56
Figure 3.11: Alkali treated kenaf mats 56
Figure 3.12: Alkali-silane treatment mechanism of kenaf fibre 58
Figure 3.13: Silane treatments of MWCNTs 59
Figure 3.14: Ultrasonic treatment of MWCNTs 62
Figure 3.15: Damaged acid treated MWCNTs 63
Figure 3.16: Filtrate of acid-silane treated MWCNTs 64
Figure 3.17: Microanalysis equipment: (a) FEI Spirit 120 kV Transmission Electron microscope (b) SENTERA Raman spectroscope, (c) TENSOR 27 Infrared spectrometer 65
Figure 3.18: Dispersion of MWCNTs: (a) Untreated MWCNTs, (b) Sonicated MWCNTs, (c) Acid treated MWCNTs and (d) Acid-silane treated MWCNTs) .. 66
Figure 3.19: Suspension stability (A: Raw and untreated MWCNTs, B: Untreated MWCNTs, C: Acid treated MWCNTs, D: Acid-silane treated MWCNTs) 67
Figure 3.20: Surface morphology of MWCNTs: (a) Acid treated MWCNTs and (b) Acid-silane treated MWCNTs and (c) Acid-silane treated MWCNTs after 12 hours of ultrasonic treatment 68
Figure 3.21: RAMAN spectrums of untreated and treated MWCNTs 69
Figure 3.22: FTIR results of untreated MWCNTs, acid treated MWCNTs and acid-silane treated MWCNTs 70
Figure 3.23: Functionalization of a MWCNT 71
Figure 3.24: Suspension stability (D1: Heat-treated functionalized MWCNTs and D2: Non heat-treated functionalized MWCNTs) 72
Figure 3.25: RAMAN spectrums of heat-treated functionalized MWCNTs and none heat-treated functionalized MWCNTs 73
Figure 3.26: Detailed view of the mould assembly 74
Figure 3.27: Manufacturing arrangement 74

Figure 3.28: Carbon steel mould (A: Female, B: Male, C: Spacer) and laminate arrangement 74
Figure 3.29: Ovens 76
Figure 3.30: Uneven kenaf fibre distribution caused by excessive compaction load during impregnation phase 77
Figure 3.31: Manufacturing defects kenaf/PP composite plate: (a) Poor fibre impregnation, (b) Voids in matrix and fibre dominated regions 78
Figure 3.32: Embedded thermocouple in kenaf/PP composite plate 78
Figure 3.33: Voids and cavities: (a) kenaf fibre reinforced PP composite, (b) PP plate 79
Figure 3.34: Kenaf/PP composite plates 80
Figure 3.35: Optimum manufacturing parameters 80
Figure 3.36: Haake PolyLab OS rheo-mixer 84
Figure 3.37: Double screws and extrusion die 84
Figure 3.38: Flow process 85
Figure 3.39: Recorded operating conditions of rheo-mixer 85
Figure 3.40: (a) MWCNT-PP plates with 0.75% CNT, (b) packing arrangement 86
Figure 3.41: Optimum manufacturing parameters of the MWCNT-PP plate 87
Figure 4.1: Tensile test set up 92
Figure 4.2: Flexural test set up on Lloyd MX100 92
Figure 4.3: Schematic diagram of the computer-controlled closed-loop fatigue testing 94
Figure 4.4: Mid-plane delamination in fibre-dominated region of a 5A-KF/25PP composite 96
Figure 4.5: Crack in matrix dominated region of 6AS-KF/25PP composite at 410321 cycles 96
Figure 4.6: Crack and matrix yield in matrix dominated region in 6AS-KF/25PP composite 97
Figure 4.7: Splitting of UT-KF/35PP composite caused by local instability 97
Figure 4.8: Tensile modulus in terms of the load frequency at 30%UTS 99
Figure 4.9: Temperature increase in terms of the load frequency 100

Figure 4.10: Matrix yielding in matrix dominated region of a 2AS-KF/20PP specimen..... 101
Figure 4.11: Unreinforced PP specimen at 6Hz and 95% UTS 101
Figure 4.12: Figure E 1 Fatigue life of kenaf and glass /PP composites at different stress levels 103
Figure 4.13: Failure in matrix-dominated region of UT-KF/25PP at 15% UTS 104
Figure 4.14: Kenaf and glass/PP specimens 105
Figure 4.15: Kenaf/PP specimen under impact load..... 106
Figure 4.16: Moisture diffusion test set up and AE ADAM PW 184 scale..... 107
Figure 4.17: Test specimens: kenaf/PP and glass/PP composites..... 107
Figure 4.18: (a) FEI NOVA 600 Nanolab FBI and (b) EMITECH *K950X* 108
Figure 4.19: (a) MWCNT-PP and (b) Kenaf/PP-MWCNT specimens..... 109
Figure 4.20: (a) BX63 FM microscope and (b) Motic Images plus 2.0 ML..... 109
Figure 5.1: Tensile strength of alkali treated kenaf/PP and glass/PP composites113
Figure 5.2: Tensile modulus of alkali treated kenaf/PP and glass/PP composites 113
Figure 5.3: Improvement in the tensile strength of alkali treated kenaf/PP and glass/PP composites 114
Figure 5.4: Improvement in the tensile modulus of alkali treated kenaf /PP and glass/PP composites 114
Figure 5.5: Tensile strength of alkali-silane treated kenaf/PP and glass/PP composites..... 116
Figure 5.6: Tensile modulus of alkali-silane treated kenaf/PP and glass/PP composites..... 116
Figure 5.7: Improvement in the tensile strength of alkali-silane treated kenaf/PP and glass/PP composites 117
Figure 5.8: Improvement of the tensile modulus of alkali-silane treated kenaf/PP and glass/PP composites 117
Figure 5.9: Alkali-silane treated kenaf fibres: (a) Untreated kenaf, (b) 6%NaOH treated kenaf..... 118
Figure 5.10: Fibre dominated failure: (a) 5AS-KF/30PP, (b) 6AS-KF/30PP..... 118

Figure 5.11: PP matrix adhering to kenaf: (a) 4AS-KF/30PP, (b) 6AS-KF/30PP 118
Figure 5.12: Fibre pull-out followed by matrix yielding failure 119
Figure 5.13: Poor fibre impregnation and excessive voids: (a) 6AS-KF/35PP, (b) GF/30PP composites 121
Figure 5.14: Flexural strength of alkali treated kenaf /PP and glass/PP composites 122
Figure 5.15: Improvement in the flexural strength of alkali treated kenaf/PP and glass/PP composites 122
Figure 5.16: Flexural strength of alkali-silane treated kenaf/PP and glass/PP composites 123
Figure 5.17: improvement in the flexural strength improvement of alkali-silane treated kena/PP and glass/PP composites. 124
Figure 5.18: Fatigue life of alkali treated kenaf/PP and glass/PP composites at 30% of UTS 126
Figure 5.19: Fatigue life of alkali treated kenaf/PP and glass/PP composites at 45**%** UTS 126
Figure 5.20: Fatigue life of alkali treated kenaf/PP and glass/PP composites at 60% UTS 127
Figure 5.21: Fatigue performances of alkali treated kenaf/PP and glass/PP composites at 30% UTS 127
Figure 5.22: Fatigue performances of alkali treated kenaf/PP and glass/PP composites at 45% of UTS 128
Figure 5.23: Fatigue performances of alkali treated kenaf/PP and glass/PP composites at 60% UTS 128
Figure 5.24: Cracks initiating in the matrix-dominated region of 6A-KF/30PP composite loaded at 60% UTS 130
Figure 5.25: Localized structural irregularities on 5% NaOH treated kenaf 132
Figure 5.26: Fatigue life of alkali-silane treated kenaf/PP and glass/PP composites at 30% of UTS 133
Figure 5.27: Fatigue life of alkali-silane treated kenaf/PP and glass/PP composites at 45**%** UTS 134

Figure 5.28: Fatigue life of alkali-silane treated kenaf/PP and glass/PP composites at 60% UTS 134
Figure 5.29: Fatigue performances of alkali-silane treated kenaf/PP and glass/PP composites at 30% UTS 135
Figure 5.30: Fatigue performances of alkali-silane treated kenaf/PP and glass/PP composites at 45% UTS 135
Figure 5.31: Fatigue performances of Alkali-silane treated kenaf/PP and glass/PP composites at 60% UTS 136
Figure 5.32: PP matrix adhering to kenaf of a 6AS-KF/30PP specimen (45%UTS) 136
Figure 5.33: Cracks originating from the matrix-dominated layer of GF/30 composite loaded at 60% UTS 137
Figure 5.34: Failure of 6AS-KF/30PP: (a) 30% UTS, (b) 60% UTS 139
Figure 5.35: Fibre-matrix splits and fibre breakage in GF/30PP composite loaded at 60% UTS 139
Figure 5.36: Impact resistance of alkali treated kenaf/PP and glass/PP composites 142
Figure 5.37: Impact performances of alkali treated kenaf/PP and glass/PP composites 143
Figure 5.38: UT-KF/30PP composite: (a) kenaf fibres pulling out (b) smooth surface of the cavity 143
Figure 5.39: Matrix fragments emanating from PP matrix 144
Figure 5.40: Impact resistance of alkali-silane treated kenaf/PP and glass/PP composites 145
Figure 5.41: Impact performances of alkali-silane treated kenaf/PP and glass/PP composites 146
Figure 5.42: Fibre pull out and fibre breakage in 2AS-KF/30PP 146
Figure 5.43: Matrix crack and fibre breakage in AS6-KF/30PP composite 146
Figure 5.44: Crazing effect on 6AS-KF/30PP composites (a) Crazing effects, (b) Microcracks 147
Figure 5.45: Moisture content of alkali treated kenaf/PP composites at saturation 149

Figure 5.46: Moisture content of alkali-silane treated kenaf/PP composites at saturation 150
Figure 5.47: Morphological configuration of glass and kenaf fibre 152
Figure 5.48: Fibre and matrix dominated regions of 6AS-KF/20PP composite. 154
Figure 5.49: Tensile modulus of functionalized MWCNT-PP 158
Figure 5.50: Tensile strength of functionalized MWCNT-PP 158
Figure 5.51: Flexural strength of functionalized MWCNT-PP..... 159
Figure 5.52: Izod impact strength of functionalized MWCNT-PP..... 159
Figure 5.53: Typical fracture path of MWCNT-PP: (a) 0.25%, (b) 0.50%, (c) 0.75% and 1% MWCNT concentration 160
Figure 5.54: Tensile strength of kenaf/PP-MWCNT composites 162
Figure 5.55: Tensile modulus of kenaf/PP-MWCNT composites 163
Figure 5.56: Kenaf fibre: (a) Matrix adhering to the kenaf fibre and (b) fibre breakage 163
Figure 5.57: Flexural strength of kenaf/PP-MWCNT composites 164
Figure 5.58: (a) Fibre breakage and (b) Matrix yielding and a rough cavity surface 165
Figure 5.59: Fatigue life of alkali-silane treated kenaf/PP-MWCNT composites at 30% of UTS 166
Figure 5.60: Fatigue life of alkali-silane treated kenaf/PP-MWCNT composites at 45% of UTS 167
Figure 5.61: Fatigue life of alkali-silane treated kenaf/PP-MWCNT composites at 60% of UTS 167
Figure 5.62: Cracks in matrix dominated region of 6AS-KF/30PP-0.5CMWNT composite 168
Figure 5.63: Impact resistance of Alkali-silane treated kenaf/PP-MWCNT composites..... 169
Figure 5.64: Fibre splits and breakage 170
Figure 5.65: (a) Brightly facture and (b) Matrix yield and rough surface of the cavity..... 170
Figure 5.66: Moisture content of MWCNT-PP and kenaf/PP-MWCNT composites at saturation 173

Figure 5.67: Fibre and matrix dominated regions of 6AS-KF/20PP-0.5MWCNT composite 174

List of Tables

Table 2.1: Chemical composition of kenaf fibre in comparison with other natural fibres 8
Table 2.2: Properties of kenaf fibre in comparison with other natural fibres 8
Table 2.3: World production of kenaf and allied fibres in major producing countries 10
Table 2.4: Utilization of natural fibre in the automotive industry 12
Table 2.5: Utilization of polypropylene in the automotive industry 16
Table 3.1: Mechanical properties of polypropylene matrix 46
Table 3.2: Mechanical properties of MWCNT-PP 47
Table 3.3: Mechanical properties of glass fibre 49
Table 3.4: Mechanical properties of kenaf fibre 51
Table 3.5: Mechanical properties of MWCNTs 53
Table 3.6: Characteristics of reagents 53
Table 3.7: Alkali and silane treatment parameters 58
Table 3.8: Typical physical properties of silane 61
Table 3.9: Characteristics of reagents 61
Table 3.10: Optimum manufacturing parameters 81
Table 3.11: Optimum conditions of the shear-mixing process 85
Table 3.12: Optimum manufacturing parameters of MWCNT-PP plates 87
Table 3.13: Material formulation of alkali treated kenaf reinforced PP 89
Table 3.14: Material formulation of alkali-silane treated kenaf reinforced PP 90
Table 3.15: Material formulation of kenaf reinforced MWCNT-PP 90
Table 5.1: Moisture contents at saturation of Alkali treated kenaf /PP composites 154
Table 5.2: Moisture content at saturation of Alkali-silane treated kenaf/PP composites 155
Table 5.3: Moisture contents at saturation of MWCNT-PP and alkali-silane treated kenaf/PP-MWCNT 173

List of Abbreviations

CNT	Carbon nanotube
CMFST	Compression moulding using the film–stacking technique
FTIR	Fourier Transform Spectroscopy
MWCNT	Multi-wall carbon nanotube
PP-H	Polypropylene-homopolymer
RAMAN	Raman spectroscopy
SEM	Scanning electron microscopy
TEM	Transmission electron microscopy
UTS	Ultimate tensile strength

List of Symbols

$IE_{composite}$	Impact strength of the composite
$IE_{unreinforced\ PP}$	Impact strength of polypropylene
m_{kenaf}	Mass of the kenaf mat
$m_{PP\ sheet}$	Mass of the PP sheet weight
Mt	Mass of the specimen at a specific moisture exposure
Mo	Initial mass of the specimen for moisture absorption test
Ms	Mass of the specimen at saturation
$N_{composite}$	Number of cycle to failure of the composite
$N_{unreinforced\ PP}$	Number of cycle to failure of polypropylene
$TS_{composite}$	Tensile strength of the composite
$TS_{unreinforced\ PP}$	Tensile strength of polypropylene
wt	weight by mass

1 INTRODUCTION

The use of natural fibres as substitutes for synthetic fibres (e.g. glass fibres) in polymer base composites has raised great interest amongst material scientists and engineers for the past two decades. Accompanying this, new regulations (e.g. carbon emission tax and waste and recycling directives) which enforce the use of environmentally friendly materials are being implemented, further motivating the use thereof [1–4]. Consequently, strategies promoting the use of environmentally friendly and sustainable materials have recently been discussed during the 17th session of the Conference of Parties (COP 17) hosted by South Africa [5] and many other conferences [3, 21] to address certain environmental challenges that the world is facing. The need to investigate different applications of sustainable, environmental friendly reinforcing material has therefore increased, in order for the composite industry to comply with the new regulations [1, 2, 6].

Growth prediction of the composite industry e.g. car manufacturers) showed that it is actively considering the use of lignocellulosic fibres (e.g. kenaf, coir, flax, jute and hemp) as substitutes for synthetic fibres [8] in the fabrication of parts which do not require high load bearing capabilities. For example in the automotive industry, lignocellulosic fibres are preferred for weight reduction (e.g. natural fibres are half the weight of glass fibres) in order to optimize the fuel efficiency of the vehicle. Low production cost of lignocellulosic fibres (e.g. natural fibres are currently priced at 1/3 of the cost of glass fibres) also motivates their growing utilization [19]. Suddell [3] reported that studies conducted by Ellison and Mc Naught in 1999 showed that about 20 kg of natural fibres could be used in each of the 53 million vehicles produced globally each year. Table 2.4 lists different automotive manufacturers that make use of lignocellulosic fibres.

Among the wide variety of lignocellulosic fibres available in the composite market, kenaf fibres extracted from the kenaf plant (Hibiscus cannabinus) have been identified as an attractive option due to their low processing costs and the ability of the kenaf plant to grow in a variety of climatic conditions [3, 9, 21]. Thanks

to the innovation of the technology of processing kenaf plant (e.g. separation process of the inner woody core material, which constitutes the 60% of the plant from the outer bark which constitute the remaining 40%), different types of fibres can be produced as there is a possibility of using all the plant constituents [29]. Kenaf is not only produced for use in composites. It also serves a viable source of raw materials for applications such as food and bio-fuel processing. All these factors make kenaf a potential commodity of interest, especially in the emerging and developing countries [3, 21].

The use of natural fibres only partly satisfies the requirements of regulations that enforce the use of sustainable and environmentally friendly materials; the polymer matrix system must also be considered in this regard. The polymer matrix used for the fabrication of natural fibre reinforced polymer composites can either be thermoplastics, thermosets or bio-polymer [4, 8, 10, 11]. It is obvious that completely biodegradable materials such as cellulosic plastics, soy-based plastics, polylactic acids and polyhydroxyalkanoates (bacterial polyesters) would be the preferred matrix system [20]. But the current production cost constitutes a major disadvantage in comparison to polypropylene (PP) which has a relatively low production cost and less recycling challenges. Polypropylene is extensively used as matrix system in various applications because of its excellent corrosion resistance and good retention of mechanical properties (e.g. impact resistance) makes this material [3, 12]. A study of the economy of the polymer industry revealed that the production of polypropylene increased by 31.1% from 2002 to 2010 and the trend is expected to increase in the future [3, 21, 22]. Given the individual advantages of kenaf fibre and polypropylene, kenaf fibre reinforced polypropylene composites have considerable commercial interest in the composite industry.

Even though natural fibres have the potential to supplement glass fibres in some specific applications in polymeric composites, limitations arise with respect to the mechanical properties and the resistance to moisture absorption when natural fibres are used. The main cause of these limitations has been reported to be poor fibre-matrix interfacial adhesion between the hydrophilic natural fibres and the

hydrophobic matrix system. Various options including chemical treatments of fibres and the use of coupling agents are considered to achieve the necessary compatibility between the fibre and matrix. Li *et al* [13] conducted a comprehensive study to investigate different techniques currently used to improve the fibre-matrix adhesion. The authors listed several types of fibre treatments including alkali treatment, silane treatment, acetylation treatment, benzoylation treatment, etc. However, studies have also shown that the improvements of the mechanical properties achieved through fibre treatments were limited. Therefore, the use of filler materials (e.g. nano-clay, carbon nano-fibres and carbon nanotubes) is generally considered [14–16].

The manufacturing technique also has a significant influence on the resistance to moisture absorption and the mechanical properties of natural fibre reinforced thermoplastic composites. It affects the fibre content, fibre distribution, fibre aspect ratio and fibre orientation [17, 18]. There are several processing techniques (e.g. injection moulding, compression and extrusion) that are used in the composite industry. However, the compression moulding is preferred when non-woven mats are used for the fabrication of composite plates. Compared with other moulding techniques, the compression moulding has the advantages of producing composite plates with uniform material distribution and high fibre aspect ratio due to reduced fibre breakage. Rowell *et al* [19] reported that the fibres are generally oriented parallel to the extrusion flow direction in composite plates fabricated by extrusion technique and the probability of fibre breakage due to abrasion is high. Whereas in composite plates fabricated by compression moulding, the fibre orientation is not altered and the extent of fibre breakage is reduced.

Several studies on natural fibre reinforced PP composite plates fabricated by compression moulding technique were conducted, however investigations into the influences of processing variables (e.g. fibre treatment, inclusion of filler material and stacking sequence of the mates) on the mechanical properties (tensile, flexural, fatigue and impact properties) and the resistance to moisture absorption are limited [1, 18, 17]. It is therefore significant to get a better understanding of the influences of the manufacturing variables in order to fabricate kenaf fibre

reinforced PP composites plates with improved mechanical properties and improved resistance to moisture absorption.

Given the prospective commercial advantages of kenaf fibres and polypropylene, studies were initiated at the University of the Witwatersrand; Johannesburg to develop kenaf fibre reinforced polypropylene composites with improved mechanical properties and improved resistance to moisture absorption that can effectively be used in various applications.

2 LITERATURE SURVEY

Fibre reinforced polymer composite (FRP) is defined as a composite material made of a reinforcing material embedded in a polymer matrix system. The reinforcing material provides the structural strength and stiffness to the composite, whereas the matrix embeds the fibres. The reinforcing material can either be synthetic fibres (e.g. glass, carbon and aramid fibres) or natural fibres (e.g. lignocellulosic fibres). Either thermoset (e.g. epoxy, vinylester and phenol formaldehyde resins) or thermoplastic polymers (e.g. polypropylene, polyethylene, polyvinyl chloride and polystyrene) can be used as matrix systems [23].

2.1 Kenaf fibres

2.1.1 Origin of kenaf fibres

Kenaf fibres are natural fibres (lignocellulosic fibres) extracted from kenaf plants (hibiscus cannabinus). Kenaf plants shown in Figure 2.1 (b) are wild plants that can be cultivated under a wide variety of climatic conditions. They are annual plants and they grow to more than 3m high within 3 months with stem diameter of 25mm to 51mm [28, 30]. Kenaf plants have been used as raw materials for application such as food and fibre processing for many years. It is reported that the first cultivation of hibiscus cannabinus goes back to 3500 B.C in Asia; and they were introduced in several other countries including South Africa, Egypt, China, Thailand, America and Russia since the Second World War [23, 26].

Kenaf is a promising source of raw materials for various industrial applications. Studies suggest that kenaf has high percentage of digestible proteins. For example, the digestibility of dry matter and crude proteins in kenaf feeds ranges from 53% to 58%, and 59% to 71% respectively. Kenaf seeds, Figure 2.1 (a), produce edible vegetable oils which contain a wide variety of omega antioxidants. Kenaf oils are used for cosmetics, industrial lubricants and bio-fuel purposes [25].

Kenaf is made up of approximately 40% cellulose, 21.6% lignin and pectin, and other constituents such as ash and silica. However, the amount of these constituents may differ depending on several factors including the climatic and soil conditions, the age of the plant and the stage of the growing season [28, 29, 30]. The chemical composition of kenaf fibres in comparison with other natural fibre is shown in Table 2.1 [29, 30], whereas the mechanical properties of kenaf fibre in comparison with other natural fibres are shown in Table 2.2 [29, 30].

The processing technique to extract fibres from kenaf plant has significantly improved. For example, the separation process of the inner woody core material, (which constitutes the 60% of the plant) from the outer bark (which constitutes the remaining 40%) has significantly improved in such a way that different types of fibres (coarser fibres and finer fibres) can be produced as there is a possibility of processing either the entire plant or its constituents [28]. Kenaf fibres shown in Figures 2.1 (c) and 2.1 (d) are used in several domestic and engineering applications. Coarser fibres have traditionally been used as raw materials in the manufacturing of cordage products such as ropes and twines whereas finer fibres are mainly used in the manufacturing of carpet, wallpaper, roofing felt, copy machine paper and fast-food containers. In the construction and transportation industry, kenaf fibres are generally used as reinforcing material for parts, which do not require considerable load bearing capabilities (e.g. door panels). Cross-section view of a 4 months old kenaf is shown in Figure 2.2.

With regard to its environmental attributes, the cultivation of kenaf plants can significantly contribute to the sequestration of CO_2. This is because kenaf plant absorbs carbon dioxide gas (CO_2) from the atmosphere more than any other crop. As an example, approximately 1.5 tons of CO_2 is required to produce 1 ton of dry matter of kenaf. This suggests that every hectare of kenaf requires 30 to 40 tons of CO_2 for each production cycle. Comparing the amount of CO_2 required for a single production cycle and the amount of CO_2 produced by a car engine (e.g. combustion engine) it was found that 1 hectare of kenaf can consume the amount of CO_2 that 20 car engines release for the whole year [31].



Figure 2.1: Kenaf: (a) Kenaf seed, (b) Kenaf plant, (c) Kenaf fibres and (d) Kenaf mat

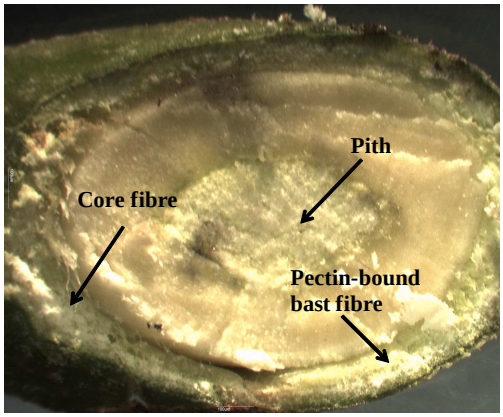


Figure 2.2: Cross-sectional view of kenaf

Table 2.1: Chemical composition of kenaf fibre in comparison with other natural fibres

Type of fibre	Cellulose (%)	Lignin pentosan (%)	Ash (%)	Silica (%)
Kenaf				
Bast fibre	31 - 39	15 - 19	22 - 23	5
Core fibre	31 - 34	15 - 21	-----	2.2
Jute				
Bast fibre	45 - 53	21 - 26	18 - 21	0.5 - 2
Core fibre	41	24	22	0.8
Wood				
Coniferous	40 - 45	26 - 34	7 - 14	-----
Deciduous	38 - 49	23 - 30	19 - 26	-----

Table 2.2: Properties of kenaf fibre in comparison with other natural fibres

Fibre	Density (g/cm3)	Tensile strength (MPa)	Young's modulus (GPa)	Elongation at break (%)	Specific tensile strength (MPa/ g.cm^3)
Kenaf	1.5	450.24	43.36	3.1	319.4 [7]
Sisal	1.45	468-640	9.4-22.0	3-7	323-441 [38]
Jute	1.3-1.45	393-773	13-26.5	1.16-1.5	286-562 [38]
Coir	1.15	131-175	4-6	15-40	114-152 [38]
Ramie	1.5	400-938	61.4-128	1.2-3.8	267-625 [38]

2.1.2 Production, trade and consumption of kenaf

Market survey showed that the annual world production of kenaf largely depends on various factors such as the market demand, climate conditions as well as agricultural outputs. Forecasts of kenaf production in major producing countries are presented in Table 2.3 [22]. Studies have shown that the demand for natural fibre reinforced polymer composites is expected to increase, especially in the automotive and construction industries. Luncintel [22] indicated that the global market of natural fibre reinforced polymer composites reached $2.1 billion in 2010, with compound annual growth rate of 15% in the last five years. It is expected to reach $ 3.8 billion by 2016. Suddell [3] reported that the predicted increase of kenaf trade volume is justified by the sustained demand of sustainable and environmentally friendly materials, especially in the construction and automotive industries. Furthermore, the author argued that political drive towards new environmental regulations (e.g. carbon emission tax) aimed to tackle the global pollution issues will also contribute to the increase of the trade volume. Studies showed that the Far East countries including China, India and Thailand account for 80 percent of the global cultivated area allocated to kenaf. These three countries produce more than 90% of the global production. However, a major portion of the global trade of kenaf fibres is focused on developed countries such as the United States of America and Western European countries. This is due to scientific innovation, increasing awareness on climatic challenges and acceptance of natural fibre composites by various players (e.g. civil societies, governments and industries) [22].

Other factors which also contribute to the increase of the production of kenaf plants are the improvement of farming practices and the biotechnology breakthroughs. Liu [21] reported that scientists from the Biotechnological Research Centre, Chinese Academy of Agricultural Sciences have successfully produced the first transgenic kenaf plant by transferring the fungal resistance genes chitinase and glucanase into the kenaf plant. Hybrid kenafs (e.g. KB2 and KB11 varieties) developed by the Institute of Bast Fiber Crops China are capable of producing 3.7 ton/ha of fibres, which is about 16% higher than the control variety.

Table 2.3: World production of kenaf and allied fibres in major producing countries

	Production					
	----------Thousand tonnes----------					
	2004/05	2005/06	2006/07	2007/08	2008/09	2009/10
World	**352.1**	**325.4**	**314.1**	**323.3**	**279.8**	**290.1**
Far East	**302.3**	**262.1**	**250.3**	**260.2**	**217.3**	**227.6**
China	86.9	82.8	86.8	86.8	80.0	80.0
India	156.4	153.0	144.0	139.7	120.0	131.2
Indonesia	7.0	7.0	3.1	4.0	3.8	3.8
Thailand	35.7	4.6	3.6	2.2	2.9	1.8
Vietnam	14.2	12.6	10.6	25.7	8.8	9.0
Cambodia	0.9	0.8	0.6	0.3	0.3	0.3
Pakistan	1.2	1.3	1.6	1.5	1.5	1.5
South America	**25.9**	**39.4**	**39.9**	**39.1**	**38.5**	**38.5**
Brazil	12.6	26.1	26.0	25.7	25.1	25.1
Cuba	10.0	10.0	10.0	10.0	10.0	10.0
Other	3.3	3.3	4.0	3.4	3.3	3.3
Africa	**13.2**	**13.2**	**13.3**	**13.3**	**13.3**	**13.3**
Near East	**3.7**	**3.7**	**3.7**	**3.7**	**3.7**	**3.7**
Developed countries	**7.0**	**7.0**	**7.0**	**7.0**	**7.0**	**7.0**

2.1.3 Processing of kenaf fibres for polymeric composite utilization

Several methods are used to produce kenaf fibres. These are: mechanical separation, bacterial retting, chemical retting and sugar cane separation method are used to process kenaf. Kenaf fibres extracted from the kenaf plant can be processed into yarns (continuous strand of fibre) or short fibre non-woven mats (Figure 2.1). A comprehensive review of different extraction and fabrication processes of kenaf fibres can be found in report published by Zhang [28]. Non-woven kenaf fibre mats are generally fabricated through the needle punching method [21].

2.1.4 Utilization of kenaf fibres as reinforcing material

As previously mentioned, the composite industry is actively considering the use of lignocellulosic fibres (e.g. kenaf, coir, flax, jute and hemp) as substitutes for synthetic fibres. Suddell [3] reported that about 20 kg of natural fibres could be used for the parts that do not require high bearing load in each of the 53 million vehicles produced globally each year. Different automotive manufacturers that make use of lignocellulosic fibres are listed in Table 2.4 [3]. Considering the economical and environmental advantages of lignocellulosic fibres over synthetic fibres (e.g. glass fibres) in conjunction with the public awareness towards green products, it is evident that kenaf fibre has a potential prospective in the composite industry [3, 22]. Classification of natural fibres for use in the composite industry is shown in Figure 2.3 [38].

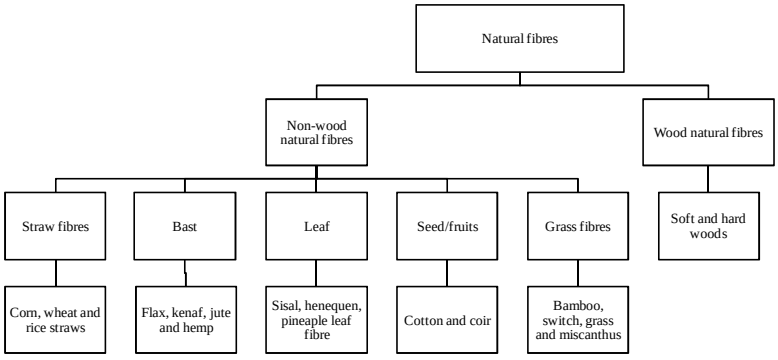


Figure 2.3; Classification of natural fibres for use in the composite industry

Table 2.4: Utilization of natural fibre in the automotive industry

Automotive manufacturers	Model applications
AUDI	A2, A3,A4 (& Avant), A6, A8, Roadster, Coupe Seat backs, side and back door panels, boot lining, hat rack, spare tyre lining
BMW	3,5,7 series Door panels, headliner panel, boot lining, seat backs, noise insulation panels, moulded foot well linings
MERCEDES-BENZ	TRUCKS Internal engine cover, engine insulation, sun visor, interior insulation, bumper, wheel box, roof cover
VOLKSWAGEN	Golf, Passat, Bora Door panel, seat back, boot lid finish panel, boot liner
PEUGEOT	406 Seat backs, parcel shelf
ROVER	2000 and others Insulation, rear storage shelf/panel
VOLVO	C70, V70 Seat padding, natural foams, cargo floor tray
DAIMLER-CHRYSLER	A, C, E and S-class models, EvoBus (exterior) Door panels, windshield, dashboard, business table, pillar cover panel
FORD	Mondeo CD 162, Focus Door panels, B-pillar, boot liner
LOTUS	Eco Elise (July 2008) Body panels, Spoiler, Seats, Interior carpets
TOYOTA	Brevis, Harrier, Celsior, Raum Door panels, seat backs, Spare tyre cover

2.2 Polypropylene matrix

Polypropylene is a polymer with linear structure based on the monomer C_nH_{2n}. Based on its molecular structure, polypropylene is a vinyl polymer with a methyl group attached to every alternate carbon atom in the main structure. It can be manufactured from the polymerization of propylene gas in presence of a catalyst such as titanium chloride. Polypropylene is also a by-product of oil refining processes [12, 36]. The molecular structure of the polypropylene chain is presented in Figure 2.4.

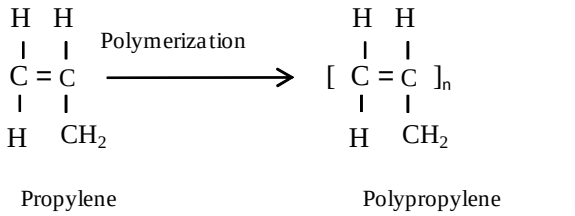


Figure 2.4: Molecular structure of polypropylene

The manufacturing technology of polypropylene has tremendously improved because of the continued demands from the market. The improvement of the polymerization process for the manufacturing of polypropylene is summarized in Figure 2.5. More detail on different manufacturing process of polypropylene can be found on report published by Sato and Ogawa [12].

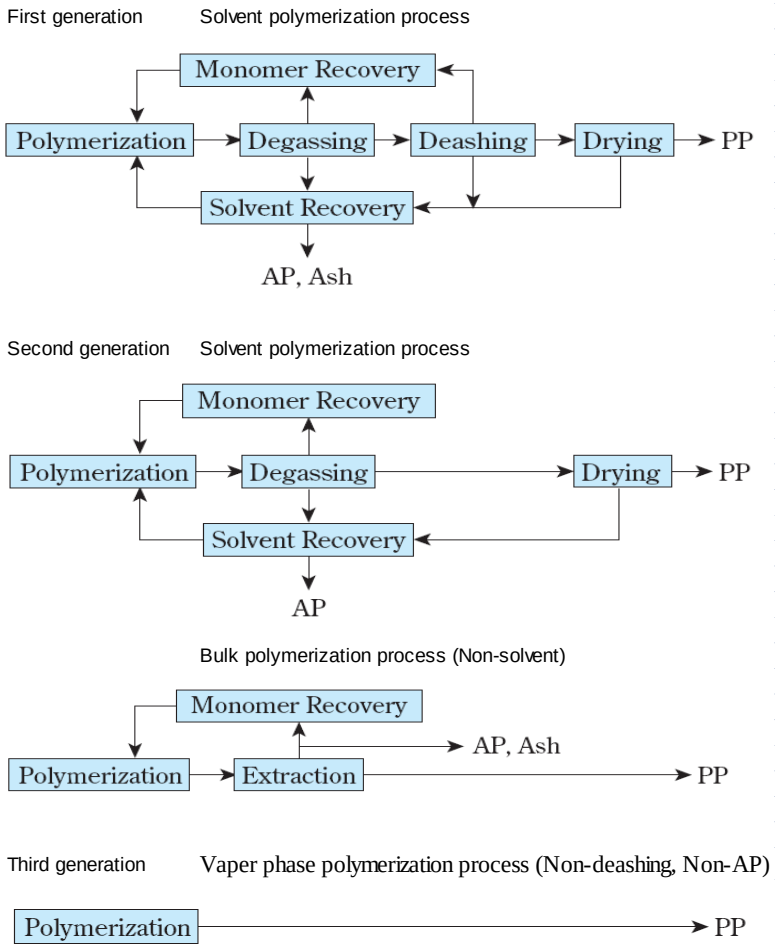


Figure 2.5: Process flow diagram of polypropylene

Polypropylene has several advantages when compared to other thermoplastic polymers. For example, it has excellent impact and fatigue strengths, low specific mass (e.g. 0.90 - 0.92 g/cm3) and a broad spectrum of corrosion resistance. It is highly resistant to organic solvents, most of the alkalis and acid, degreasing agents and electrolytic attack. Due to its high melting temperature (164°C), polypropylene has a relatively high service temperature. The use of polypropylene materials for domestic and commercial applications (e.g. delay life commodities) does not have any significant effects from an occupational health and safety point of view in terms of chemical toxicity.

In terms of the processability, polypropylene is easy to process due to its extraordinary melt-flow characteristics. This allows the fabrication of polypropylene parts in a low cycle time. In addition, polypropylene can be processed several times without significant loss its mechanical properties. Thermoplastic polymers, including polypropylene, are susceptible to degradation when exposed to ultraviolet radiation. However this can be significantly reduced by the use of filler materials (e.g. carbon black) [12, 35].

Over the last five decades, polypropylene has played a significant role in the polymeric composite due to its reduced environmental impacts and manufacturing cost. For example, light weight, optimal balance of mechanical properties and excellent surface finish of polypropylene found use in the automotive industry. This allowed the automotive manufacturers to replace several metallic parts which do not require considerable load bearing capabilities at lower cost and with less environmental impact. The consumption of polypropylene in the automotive industry is shown in Table 2.5. The processing of the polypropylene material has a very small carbon footprint when compared to synthetic fibres (e.g. glass and carbon fibres), and its water footprint is significantly smaller than that of glass fibres. Also, less energy is required for the production of the polypropylene polymer [12, 35].

Based on this survey, it is evident that the advantages of kenaf fibres and polypropylene definitely position natural fibre reinforced polypropylene composites as an important economic resource for the composite industry to address the environmental challenges the world is currently facing.

Table 2.5: Utilization of polypropylene in the automotive industry

	Production ----------Thousand tonnes----------				
	2002	2003	2004	2007	2010
World	142284	199384	234110	344000	442600
Australia	12275	14624	13638	15600	16400
China	44068	80755	92650	160000	220000
India	28158	36319	47134	60000	80000
Indonesia	7739	8128	10000	14000	16000
Iran	18810	21996	28000	40000	48000
Malaysia	15200	12996	14594	20000	23200
Pakistan	-----	1687	1730.4	2400	2800
Philippines	-----	1546	1600	2200	2400
Taiwan	9260	10594	11985	12000	12600
Thailand	6773	10067	11977	16800	20000
Vietnam	-----	671	800	1000	1200

2.3 Mechanical and moisture absorption properties of natural fibre reinforced polymer composites

Lignocellulosic fibres have an enormous potential to substitute conventional synthetic fibres, such as glass fibres, in many applications that do not require high load bearing capabilities [(6)]. However, natural fibres reinforced composites still have limitations with respect to mechanical performances and resistance to moisture absorption. These limitations are more pronounced when hydrophobic thermoplastics such as polypropylene matrix are used as matrix a system [(39)]. Previous researchers reported that the level of the chemical incompatibility

between the natural fibre molecules and the thermoplastic molecule is the main factor that dictates the mechanical performances of lignocellulosic fibre reinforced thermoplastic composites. This incompatibility leads to difficulties in ensuring proper bonding on fibre–matrix interfaces, which in turn causes ineffective load transfer between the fibre and matrix [40, 41].

Good resistance to moisture absorption is essential to guaranty extended service life of natural fibre reinforced composites when exposed to a moist environment. Moisture uptake can result in reduced mechanical properties due to fibre degradation (e.g. leaching, biodegradation and swelling) and dimension stability. To eradicate entirely the moisture uptake in fibre reinforced polymer composites is a big challenge. However, it can be minimized by ensuring a good encapsulation of the fibres by the matrix or by applying layers of corrosion barriers onto the composite surface.

Chemical treatments of fibres and the use of compatibilizers have been suggested as a means to create a strong interfacial bond between the fibre and matrix in order to improve the mechanical properties and the resistance to moisture absorption of natural fibre reinforced composites [39, 41]. Previous works related to the influences of fibre treatments on the mechanical properties and the resistance to moisture absorption of natural fibre reinforced composites are reviewed. The influences of the manufacturing process are also reviewed.

2.3.1 Effects of fibre treatments on the mechanical properties of natural fibre reinforced polymer composites

Tensile and flexural properties of natural fibre reinforced polymer composites

Li *et al* [13] carried out an investigation study on various chemical treatments for improving the compatibility between the natural fibres and the polymer matrix. Fibre treatments using chemicals such as alkali, silane, permanganate, benzoylation, acrylation, acetylation, isocyanates have been reviewed. The researchers reported that alkali treatment can be used to improve the overall

properties of the composite. They argued that alkali treatment modifies the texture of the fibre surface, increases the amount of cellulose on the fibre surface, which in turns increases the number of the reaction sites. They also reported that alkali treatment enhances the fibre strength. Edeerozey *et al* [40] studied the morphological changes of kenaf fibres caused by alkali treatments at different temperatures (ambient and 95°C). Sodium hydroxide solutions with different concentrations (3%, 6% and 9% NaOH) were used for fibre treatments. It was found that the concentration of the sodium hydroxide solutions influences the cleanness and the mechanical properties of the fibre. Scanning electron microscopy revealed that alkali treatment with 3% NaOH does not remove the impurities on the fibre surface in an effective manner. Surface impurities were removed completely at 6% NaOH. The researchers claimed that 9% NaOH alkali treated kenaf fibres had the cleanest surface. However, material degradations caused by excessive alkali concentration (9% NaOH) compromised the mechanical properties of the fibres. The tensile strengths of 9% NaOH alkali treated fibres were found to be even smaller than those of the untreated fibres. They finally concluded that 6% NaOH is the optimum concentration for alkali treatment at 95°C since kenaf fibres were sufficiently clean and exhibited improved tensile strength. Van de Weyenburg *et al* [98] reported up to 30% increases in the tensile strength and modulus of flax reinforced epoxy composite.

Silane solutions are also used to improve the fibre-matrix interfacial bonds. Lee *et al* [59] reported the effects of the three glycidoxypropyltrimethoxy silane treatement on kenaf fibre reinforced poly (lactic acid) bio-composites. They indicated that silane solution with a concentration of 1% improved the flexural strength and stiffness of a composite of 50% mass fraction by approximately 20% and 25%, respectively, when compared against the untreated kenaf/PLA composites. Cho *et al* [97] considered kenaf fibres as reinforcement for PP and polyester. Three different silanes were considered: gamma-aminopropyltriethoxysilane, gamma-glycidopropytriethoxysilane and three-methacryloxypropyltrimethoxy silane. They reported that gamma-glycidopropytriethoxysilane treatment was the most effective when using a concentration of 0.5% by mass. Mechanical test results showed that the flexural

and tensile strengths increased relative to those of the composite made from untreated fibre by 26% and 17%, respectively. Whereas the corresponding increases in the moduli were about 8% and 20%.

Although several researchers have looked at either alkali or silane treatments, the combined effects of the two treatments have been considered as well. Masud *et al* [(42)] investigated on the effects that the fibre treatments (e.g. alkali treatment, silane treatment and alkali−silane treatment) have on the mechanical properties of kenaf reinforced polylactic acid composites. They reported that chemical treatments of kenaf fibres improved the tensile and flexural properties of the composites. The researchers argued that silane treatment was the predominant contributing factor for the improvement of matrix−fibre interfacial bond. They explained the effects of silane as follow: When the three aminopropyltriethoxysilane is dissolved in water, the ethoxy groups hydrolyze and produce silanol molecules. Subsequently the silanol molecules react with the hydroxyl group (OH^-) of alkali treated kenaf fibres and establish stable covalent links. Thereafter, the silanol radicals connect to kenaf fibres and create stable ties that enhance the fibre-matrix bonding strength by ensuring strong cross-linkages and interlocking between the fibre and polymer matrix. The mechanism of the improvement of the fibre-matrix bond reported by Loan [(38)] is summarized in below in Figure 2.6.

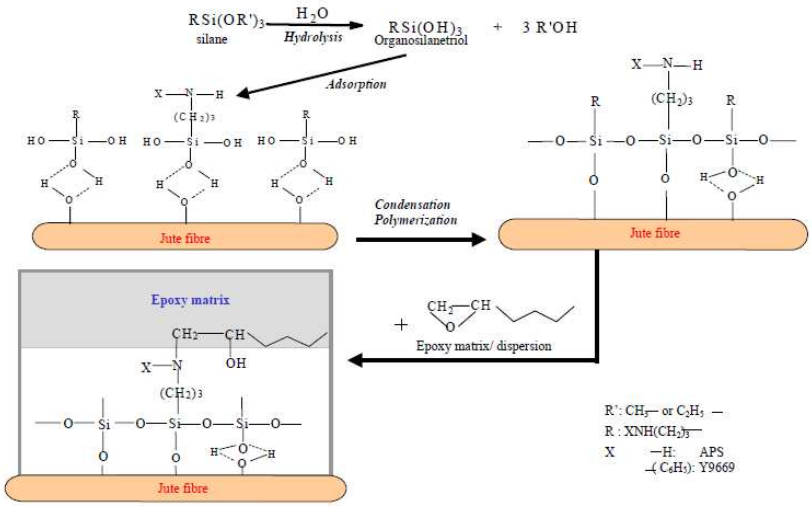


Figure 2.6: Interfacial fibre-matrix bonds caused by fibre treatments

The improvement of the fibre-matrix interfacial bond caused by alkali-silane treatment was also reported by Reid *et al* [7]. They used compression moulding techniques to fabricate composite plates using kenaf fibre mats and polypropylene as reinforcing and matrix system, respectively. As an example, they tensile modulus and strength improved by more than 100%, where the flexural strength improved by 70% in comparison to unreinforced polypropylene. The authors reported that alkali-silane treatment of kenaf fibres improved the specific tensile and flexural strength of kenaf reinforced polypropylene composites with 30% fibre contents to such extent that they compare well with those of glass reinforced polypropylene composites.

Fatigue properties of natural fibre reinforced polymer composites

Several studies related to the improvement of the mechanical properties of natural fibre reinforced polymer composites by means of fibre treatments mainly focus on the tensile and flexural properties of the material. Hardly any have been focused on the fatigue behaviours [43, 44]. Still, the studies devoted to the fatigue characteristics are generally orientated towards synthetic fibre reinforced thermoset composites, [10]. Understanding the fatigue behaviours of these materials is therefore indispensable in order to comprehend the fatigue characteristics of natural fibre reinforced polypropylene composites.

Gassan [45] conducted tension-tension fatigue tests at a stress ratio of 0.1 and a 10Hz frequency to investigate the influences of the fibre characteristics and fibre-matrix bond on the fatigue behaviour of natural fibre composites. Natural fibres including flax fibre yarns, tossa jute fibre yarns and woven textile were used as reinforcing materials. Epoxy resin, unsaturated polyester resin and polypropylene were used as a matrix system. The author reported that the effectiveness of the fibre-matrix bond significantly affects the fatigue behaviours of both reinforced thermoset and thermoplastic composites. He argued that the critical load for initiating and propagating damage through the material could be increased by means of fibre treatments. This proposal was validated by inferior values of the critical load to initiate and propagate damage in untreated fibre composites.

Microscopic examination has shown that cracks initiate at the weakest points of the material (e.g. fibre-matrix interfaces) and propagate preferentially along the fibres before spreading through the matrix.

Mallik [10] also reported complex failure mechanism in cross-ply and multidirectional continuous fibre reinforced composites. The author stated that the damage grows in size and intensity in a progressive manner until the ultimate failure occurs. The sequence of damage development events in cross-ply laminates was found to be similar to those of multidirectional laminates containing off-axis fibres. The author argued that the initiation of fatigue damage in $[0/90]_s$ laminates was characterized by the formation of transverse microcracks at the fibre-matrix interface in the 90° laminae. As cycling progresses, the initial damages (microcracks) develop toward the adjacent 0° laminae. Depending of the stress level, these microcracks may deflect parallel to the 0° laminae, thereby causing delamination between the adjacent laminae. Delamination generally occurs at the early stage of the cycling load, they become stable overtime and rapidly increase during the last stage of the fatigue cycle of the laminate. Fatigue damage growth in $[0/90]_s$ laminate is depicted in Figure 2.7. Mallick [10] concluded that that the fatigue strengths of composites that have strong fibre-matrix interfacial bond were significantly affected by the fibre contents. This is because test results showed that the critical load to initiate and propagate damage increases with the increase in fibre content. No clear correlation between the critical load and the fibre content was noticed for untreated fibre reinforced PP composites. It is believed that such behaviours were caused by poor fibre-matrix interfacial bond.

It is evident that the fatigue behaviours of fibre reinforced polymer composites is a very complex mechanism. It is often analyzed as a progressive phenomenon. The sequence of the damage events largely depend on several factures such as the laminate configuration (packing sequences of laminae), resin characteristics (e.g. thermoset or thermoplastic), test temperature, stress level, load frequency and test control mode. As such a rigorous and systematic approach was considered to study the fatigue behaviours of kenaf reinforced polypropylene composites.

Details on the preliminary fatigue tests conducted to determine the optimums test control parameters (e.g. stress ratio, load frequency and stress levels) can be found in Chapter 4.

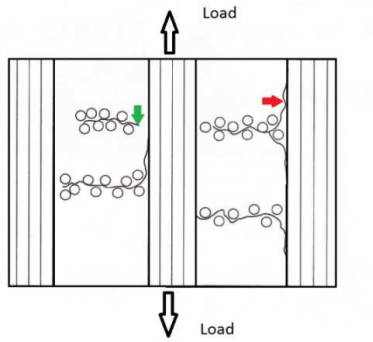


Figure 2.7: Fatigue damage development in $[0/90]_s$ laminate

Towo and Ansell [46] evaluated the effects of alkali treatments on the fatigue behaviours of sisal reinforced thermoset composites manufactured through the hot press process. Sisal fibres were treated with 0.06M NaOH alkali solution. The authors reported that the improvement of the fatigue performances was caused by the strong fibre-matrix bond between the fibre and the matrix. The researchers also indicated that factors including load frequency, stress ratio significantly influenced the test results. They suggested that 0.1 (Non-reversing stress cycles) was the appropriate stress ratio to prevent local instability of the specimens and maximize the load amplitude.

Although most of the previous works focus more on fibre reinforced thermoset composites, the survey however, shows that there is a possibility of improving the fatigue strength of natural fibre reinforced composites through fibre treatments. Therefore investigation into the effects of fibre treatments on the fatigue performances of kenaf fibre reinforced polypropylene composites is indispensable.

Impact properties of natural fibre reinforced polymer composites

Alterations of the viscoelasticity of the polymer matrix often take place when fibre reinforced thermoplastic composites are exposed to a hostile environment

(e.g. ultraviolet radiations). These alterations may compromise the impact performances of the composites by causing matrix embrittlements [30, 47]. The matrix embrittlements generally cause the transitions of the material behaviours from ductile to brittle, which in turns create favourable conditions for brittle failure. For example, prolonged exposure of polymer based composites to ultraviolet radiations (e.g. sunlight) generally reduces the impact resistance of the material even at temperatures below the glass transition temperature [47]. Besides the changes in the viscoelasticity of the polymers chains, factors associated to the design and manufacturing (e.g. poor fibre-matrix bond) also affect the impact properties of the polymer based composites [8, 42].

Designing fibre reinforced polymer composites against deformation within the elastic regions is an obvious task since typical material properties such as the elastic modulus and the tensile strength properties can be used. However, designing against crack initiation and subsequent crack propagation in fibre reinforced polymer materials under impact loading is far more complex. Impact tests are generally performed to assess the integrity of the material at the earlier stage of the design process. As an example, impact test results are used to specify the maximum impact loads that the material can withstand at the operating temperature.

Several impact test procedures are specified. These procedures generally depend on the material characteristics and the engineering requirements pertaining to the manufacturing process, operating conditions (e.g. loading conditions and operating temperature) and service life of the material. The choice of a specific impact test methodology is largely dictated by these variables. As an example the impact test procedure specified for the evaluation of the impact resistance of fibre reinforced composite plates subjected to static and high speed impact load would be different to that of composite plates subject to recurring and low speed impact loads [48, 49]. The impact test procedures commonly used for plastics and fibre reinforced polymer composites are summarized in Figure 2.8.

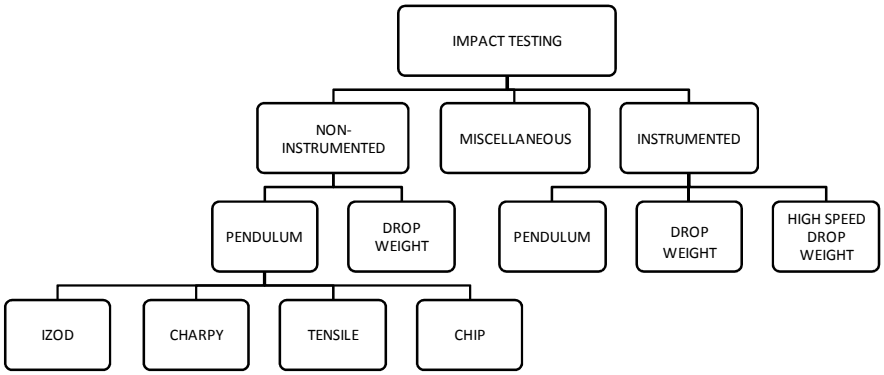


Figure 2.8: Impact test classification for fibre reinforced polymer composites

Several studies have been carried out to evaluate the influences of the fibre treatments on the impact properties of fibre reinforced polymer composites. Few works however have been devoted to lignocellulosic fibres reinforced thermoplastic composites. Ramires and Frollini [11] conducted Izod unnotched impact tests in accordance with ASTM D256 [48] to evaluate the impact properties of sisal fibre reinforced tannin-phenolic composites. The authors reported that the enhancement of the fibre-matrix adhesion was the main cause of the improvement of the impact strength. They argued that the predominance of acid sites at the surface of the sisal fibres improved the fibre-matrix adhesion. The researchers also reported that the increase of the fibre content improved the Izod impact strength of the composites. The optimum fibre content was found to be 50%. However, the impact resistance dropped at fibre content greater than 50%, probably because of poor fibre impregnation. They concluded that the use of sisal fibres as reinforcing material in tannin-phenolic resin was beneficial since it significantly improves the impact properties of the composite. The researchers also reported that the fibre distribution also (Figure 2.9) contributed to the improvement of the impact strength since they guarantee uniform load distribution within the material.

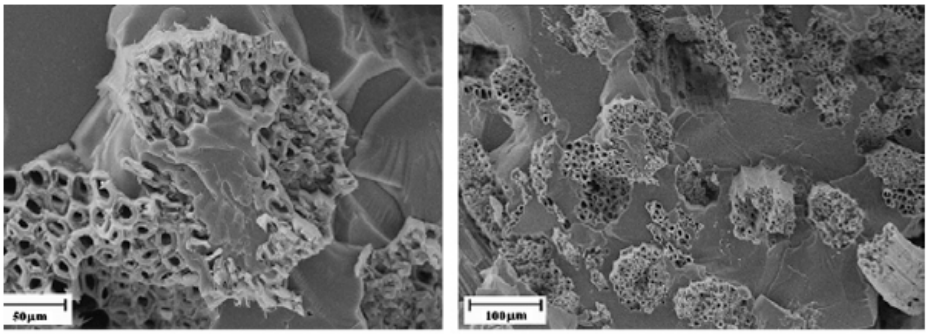


Figure 2.9: Intimate fibre-matrix contact and even fibre distribution

Kim *et al* [50] investigated the effect of different compatibilizing agents, including maleated polypropylene and maleated polyethylene on the tensile and Izod impact strength properties of lignocellulosic material filled polyethylene bio-composites fabricated through extrusion. Low and high-density polyethylene were used as matrix whereas rice-husk flour and wood flour were used as reinforcement. Different compatibilizing agents (e.g. maleated polypropylene and maleated polyethylene) were used to improve the fibre-matrix adhesion. The researchers reported that maleated polyethylene improves the Izod impact strength notched specimens because of the enhancement of the fibre-matrix interfacial adhesion. They argued that the Izod impact strengths of the maleated polypropylene incorporated composites slightly dropped following the incorporation of the compatibilizing agent at a content of 3% by mass. On the other hand, those of the maleated polyethylene incorporated composites slightly improved because a better wetability of the polyethylene matrix polymer was achieved. The fibre-matrix adhesion mechanism as suggested by the authors is shown in Figure 2.10.

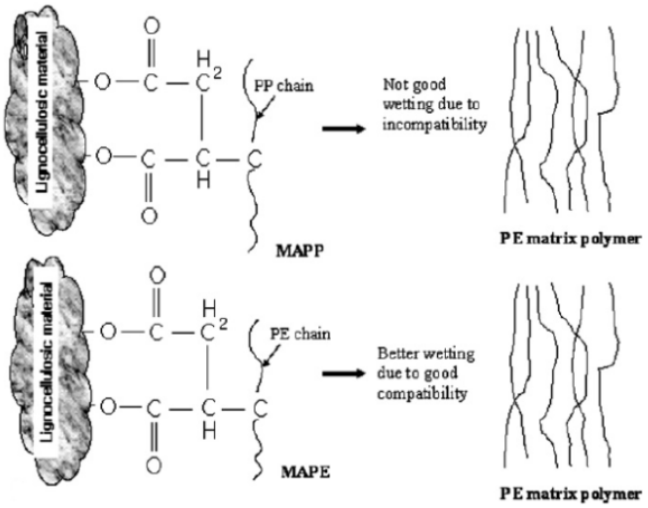


Figure 2.10: Fibre-matrix adhesion mechanism due to the use of coupling agent

In view of these results the improvement of the mechanical properties (e.g. tensile, flexural, fatigue and impact properties) of natural fibre reinforced thermoplastic composites due to fibre treatment (e.g. alkali and alkali-silane) is evident. However the improvement is still somewhat deficient in comparison to that of glass fibre reinforced composites.

2.3.2 Effects of fibre treatments on the resistance to moisture absorption of natural fibre reinforced polymer composites

Natural fibres reinforced composites have limitations in terms of moisture absorption. However, considerable efforts are made to address these drawbacks given the potential benefits of natural fibres. It is therefore imperative that a better understanding of the moisture absorption mechanism in natural fibre reinforced composites and its effects on the material properties of the composites is achieved. Several diffusion models describing the moisture absorption mechanism in lignocellulosic fibres reinforced polymer composites have been proposed. Various concepts (e.g. Finite element analysis, Fickian Laws, Percolation theory and the semi empirical methods) are used to elaborate these models [51, 53 – 55], Experimental test results showed that these models are valid only at the early stage of the diffusion process and at ambient temperatures. The accuracies of these models become inadequate as the immersion time and the temperature

considerably increase, because the diffusion process could be driven by the synergy of uncontrolled factors [52, 56 – 58]. These factors could be:

- The variation of the diffusion coefficients due to the plasticization of the matrix polymer chains and the changes in the microstructure configuration of the fibres.
- The increase of the amount of voids within the composite causing the diffusion process to behave as a macroscopic phenomenon rather than a microscopic mechanism.

Studies have shown that the hydrophilic nature of natural fibres and the level of the chemical incompatibility between the fibre and the matrix are the main factors that compromise the resistance to moisture absorption of natural fibre reinforced polymer composites. Chemical and mechanical treatments are commonly used to improve the fibre-matrix interfacial adhesion [42, 59, 52, 60].

Alkali treatment is used to clean the fibre and improve the bonding strength between the lignocellulosic fibres and the polymer matrix. It is believed that alkali treatment improves the moisture resistance and enhances the adhesion between the natural fibres and the polymer matrix since it modifies the external structure of the fibre and chemically modifies the fibre surface composition by removing the surface impurities. Sharifah *et al* [61] investigated the improvement of the moisture resistance caused by chemical treatment. The composite specimens were made of kenaf fibres and unsaturated modified Crystic 2-406PA polyester resin. They reported that alkali treatment using 6% NaOH solution contributed to the improvement of the resistance to moisture of the composites. They concluded that strong bonding and interfacial adhesion between the kenaf fibre and matrix increased the resistance to moisture of the composites.

Silane solutions (e.g. Three–aminopropyltriethoxysilane) can also be used to improve the resistance to moisture absorption of natural fibre reinforced polymer composites. Lee *et al* [59] investigated the effects silane treatments on the resistance to moisture absorption of kenaf fibre reinforced poly (lactic acid) bio-composites. The researchers reported that silane treatments improved the the

resistance to moisture absorption of the composites. They indicated that the reaction between the silane molecules and hydroxyl groups of kenaf fibres reduces the hydrophilic nature of the fibres due to the reduction in the amount of hydroxyl groups. Furthermore, they mentioned that the swellings and moisture absorption rates were significantly reduced with the increasing of the silane concentrations. The water absorption and swelling curves are illustrated in Figure 2.11. The researchers argued that the increase of the resistance to moisture absorption could be explained as follow: First, the silane molecules react with the hydroxyl groups and rend kenaf fibres less attractive to water molecules. Secondly, the intimate fibre- matrix adhesion caused by silane treatment leads to less voids and eliminates possible paths for water molecules through the composite.

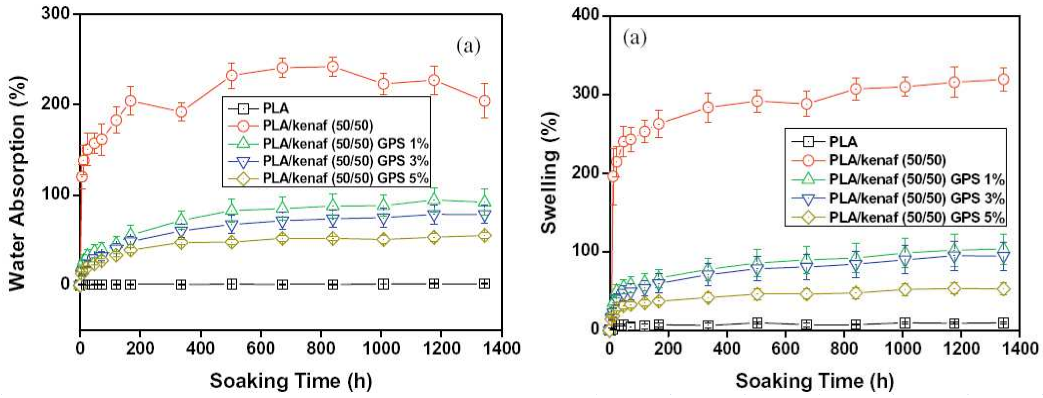


Figure 2.11: water absorption and swelling at different silane concentration

Alkali treatment followed by silane treatment (alkali-silane) is also used for improving the fibre–matrix adhesion. Sgriccia *et al* [60] conducted experimental works to characterize the surfaces of treated and untreated kenaf and hemp fibres. They also evaluated the effects of alkali and alkali-silane treatments on the water absorption resistance by comparing the saturation mass gain of untreated, alkali treated and alkali-silane treated epoxy composites. Three different types of natural fibres were used: kenaf, flax and hemp fibres. It was found that all three types of composites had similar moisture contents at saturation. Flax reinforced epoxy composites had a saturation mass of 17.2%, hemp reinforced epoxy composites

had a saturation mass of 18.4% and kenaf reinforced epoxy composites had a saturation mass of 17.8%. The researchers reported that alkali-silane treatments at 5% NaOH and 1% silane significantly improve the resistance to moisture absorption. It was found that 5% NaOH is the optimum alkali concentration to remove surface impurities such as lignin, pectin, waxy substances, and natural oils.

The effects of the moisture on the mechanical properties of natural fibre reinforced polymer composites have been investigated by several researchers. Karlsson *et al* [62] investigated the mechanism of water uptake and its influences on the mechanical properties of lignocellulosic reinforced polypropylene composites. The researchers argued that the water absorption severely affects the mechanical properties of the composites since the testing results have shown that the water-saturated samples exhibit poor tensile modulus and tensile strength as compared to those of dried composites. Li *et al* [52] also investigated on the effects of water absorption on the tensile and impact strengths of sisal fibre reinforced polypropylene composites manufactured by injection moulding. They reported that the tensile modulus and tensile strength of the composites decrease continuously with the increase of the water immersion time. The researchers argued that the changes in the mechanical properties of the composites were attributed to the combined effects of the matrix plasticization and the fibre degradation. Contrarily to the tensile characteristics, the Izod impact strength improved at the early stage of the diffusion process and dropped as the immersion time increases. They argued that these contradictory behaviours were caused by the swelling of the sisal fibres, which probably enhanced the frictional force and thereby preventing the fibre from pulling out of the matrix. The researchers also reported that reduced Izod impact strength was caused by excessive leaching of water soluble substances from the sisal fibres causing changes in the microstructure configuration of the fibres.

It is obvious that there is a possibility of improving the mechanical properties and resistance to moisture absorption of natural fibre reinforced composites by means of fibre treatments (e.g. alkali and silane treatments). However the use of natural

fibre reinforced thermoplastic composites in moisture environment are still limited.

2.4 Use of filler materials to improve the mechanical properties of natural fibre reinforced polymer composites

Besides fibre treatments and functionalization of the fibres, the use of filler material in particular carbon nanotubes (CNTs), is being considered as a potential mean of improving the mechanical properties of reinforced polymer composites [14-16, 64, 66]. As an example, the cost of multi-wall carbon nanotubes (MWCNTs) for use as reinforcing material in polymeric composites and ceramics is estimated to be $200 million dollars [64]. A TEM image of MWCNTs manufactured by vapour deposition is shown in Figure 2.12. CNTs, developed by Iijima in 1991, have exceptional nano-scale physical properties. These include high mechanical strengths (e.g. young modulus of 1 to 5TPa, and high elongation to failure in the range of 20% to 30%), excellent thermal stability and low electrical resistance [15, 64, 65, 72, 73]. The strength and the adaptability of the carbon-carbon bonds, one of the strongest encountered in nature, are the reason behind the strength of carbon nanotubes. The stiffness is attributed to the hybridization phenomenon [15, 64]. The low density of CNTs (1.3 - 1.4 g/cm^{-3}) leads to a high specific strength of the nanoparticles (4.8×10^7 N.m.kg^{-1}) when compared with that of carbon steel (1.54×10^7 N.m.kg^{-1}).

Various techniques are used for the fabrication of CNTs, a detailed review thereof can be found elsewhere [64]. Considering the high surface area (500 times more than carbon fibre) and aspect ratios (of about 1000) of CNTs, it would be logical that such materials should be regarded as potential reinforcing materials for polymeric composites. It is expected that the inclusion of a small quantity of CNTs into the matrix system will substantially improve the mechanical properties of reinforced polymer composites [68].

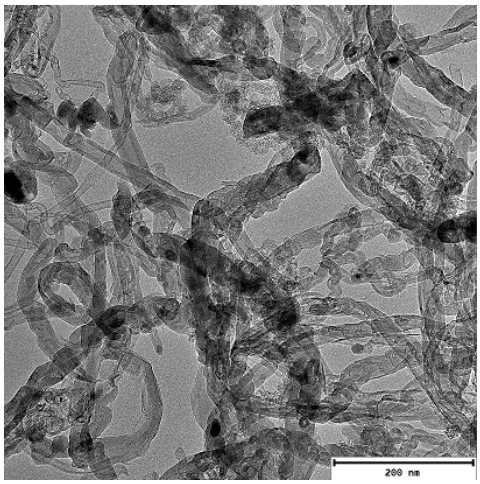


Figure 2.12: TEM images of multi-wall carbon nanotubes

Unfortunately, the polymeric composite industry is still facing challenges in using CNTs as a reinforcing material in an effective way. Studies have shown that the exceptional mechanical properties of CNTs have not yet been fully exploited in reinforced polymer composite applications. Numerous studies have indicated that the mechanical properties of CNT reinforced polymer composites are generally significantly lower than the predicted values obtained through different approaches, such as the rule of mixtures and Halpn-Tsai approach [74]. The major limiting factors in utilizing CNTs as reinforcing material in polymer composites are: poor interfacial bond between the carbon nanotube and the matrix, poor dispersion of CNTs within the polymer matrix, improper CNT alignment and degradation of the CNT due to processing [14, 15, 66, 68]. For example, poor interfacial bond between the CNT and the matrix prevents effective stress transfer, subsequently leading to poor mechanical properties. Studies have also shown that although the tensile strength of individual CNT shells can be extremely high, they are weak under compressive loads. In addition, weak shear interactions between adjacent grapheme sheets, especially in MWCNTs, tend to significantly lessen the effective strength of the nanotube [64].

2.4.1 Improvement of the CNT dispersion and the CNT-matrix interfacial adhesion

Studies have been carried out to explain the causes of several drawbacks, such as poor interfacial bonding between the CNTs and matrix, poor dispersion of CNTs within the polymer matrix and improper CNT alignment; and subsequently to suggest techniques for achieving optimal reinforcement of polymer composites with CNTs. These techniques include chemical treatments (e.g. oxidation, reduction and functionalization), coating (e.g. plasma coating) and mechanical treatments (e.g. ball mixing, sonication and shear mixing) [14, 15, 68]. A survey of previous studies is therefore of interest in order to appraise the potential and challenges of CNTs as reinforcing materials for polymeric composite materials.

Andrews *et al* [14] reviewed the state of research on the use of nanotube reinforced polymer composites; particular emphasis was placed on the effectiveness of the interfacial bonding between the carbon nanotubes and polymer matrices in order promote CNT–matrix load transfer. They reported that the surface of the CNT, an exposed grapheme sheet, could be the main cause of the weak inter-planar interaction of graphite due to its lubricant characteristics, which in turn prevents strong adhesion to the polymer matrix. They also stated that the lubricant characteristics of the grapheme were exaggerated due to it being chemically inert. The authors indicated that functionalization of the CNT surface has been regarded as an effective means of improving the CNT–matrix interfacial bonding strength and increasing the dispersion of the CNTs in various polymer matrices and organic solvents by creating CNT–matrix compatible functional groups on the surface of CNTs. Acid treatments (e.g. nitric acid treatment) have been reported to successfully oxidize MWCNTs by attaching carboxylic groups on to MWCNT surface, which in turn improved the bonding between the CNTs and the resin by reacting with the matrix epoxy terminated molecules.

Prashantha *et al* [68] investigated the effects of adding a coupling agent such as polypropylene grafted maleic anhydride (PP-g-MA) on the dispersion and mechanical properties of the MWCNT filled polypropylene nanocomposites. The researchers indicated that the intermolecular van der Waals interactions between

the nanotubes, in combination with large surface areas and high aspect ratio were the main causes of ineffective CNT reinforcement abilities since they prevent proper CNT–matrix load transfer due to poor dispersion of CNTs within the composite. They suggested that the van der Waals forces between CNTs and the entanglement thereof inherited from the synthetic manufacturing process have to be minimized in order to guarantee a consistent dispersion of CNTs within the polymers. The researchers concluded that the PP-g-MA, when added in a ratio of 2% by weight, was an effective additive for uniform dispersion of the MWCNT's and to improve the interfacial bonding between the MWCNTs and the polypropylene matrix. The results were validated by means of morphological characterization (SEM) and mechanical testing, which indicated improved impact, tensile and flexural properties of the MWCNT filled polypropylene. The tensile modulus of the composites treated with PP-g-MA increased, on average, 10% as compared to composites without PP-g-MA. SEM images of untreated and treated MWCNTs are shown below [(68)]. Figure 2.13 (a) shows the aggregates and Figure 2.13 (b) shows untreated carbon nanotubes. Whereas Figure 2.13 (c) and (d) depict good dispersion of carbon nanotubes and PP-g-MA carbon nanotube treated respectively.

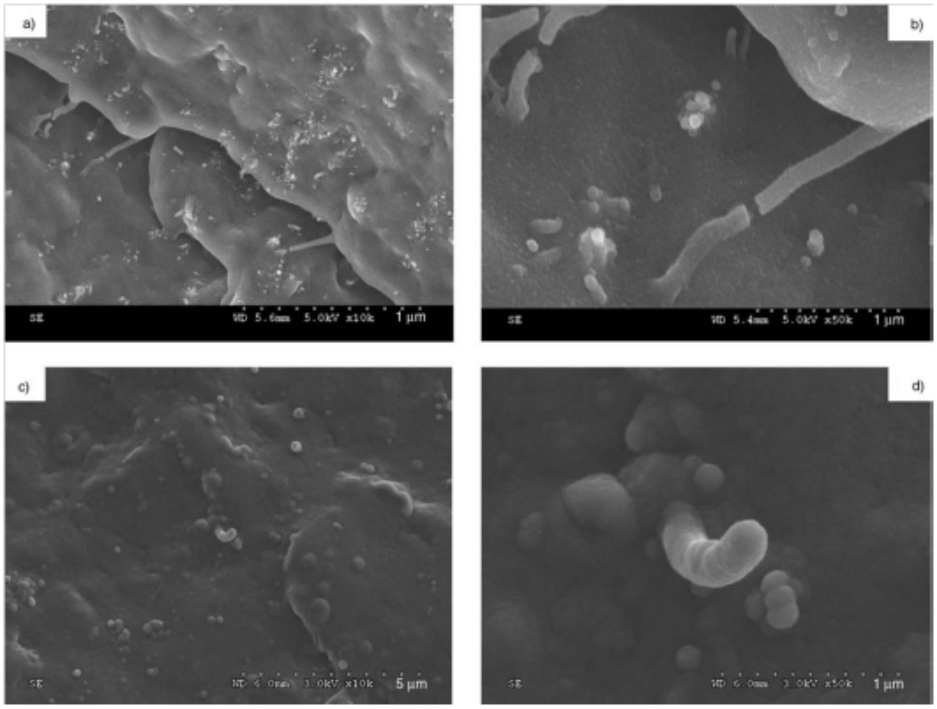


Figure 2.13: SEM images: (a) aggregates, (b) untreated carbon nanotubes, (c) uniform distribution of carbon nanotubes, (d) PP-g-MA carbon nanotube treated

Although acid treatment of the CNTs surface has been reported as successful means of functionalizing CNTs, studies have indicated that it may damage the nanotubes, therefore limiting the use thereof. Andrews *et al* [(14)] reported that excessive acid treatment can dislocate the bonding of the CNT grapheme sheets and consequently compromise the mechanical properties of functionalized CNTs in the fabricated composite. Ma *et al* [(66)] also reported similar results. The authors stated that a surface treatment with concentrated acid successfully attached functional groups (carboxyl groups) onto the CNTs surface. The treatment, however, can also degrade the mechanical properties of CNTs by causing defects on the CNT sidewalls, and decreasing the aspect ratio of CNTs by dividing the CNTs into shorter segments during the oxidative process. To address these limitations, alternative treatment, such as silane treatment, which consist of broadening the chemical reactivity of the CNTs by depositing active moieties onto the surface of the carbon nanotubes has been developed. Ma *et al* [(66)] presented a new method which consisted of chemical functionalization of the MWCNTs. This was achieved through the combined process of: oxidation by exposing MWCNTs

to a UV/O_3 environment, reduction of the MWCNTs in a solution of Lithium aluminium hydride (LiAlH4) and hydrochloric acid, and silanization using 3-Glycidoxypropyltrimethoxy silane. The authors argued that the intent of the oxidation was to create active sites and moieties (–OH groups) on the surface of the carbon nanotubes. The presence of these groups was confirmed by Fourier transform infrared analysis (FTIR). The aim of the reduction step was the reduction of the – COOH groups to –OH groups. Silane treatment was carried out to enable the reaction between the –OH groups of MWCNTs and the –OCH_3 groups of the 3-Glycidoxypropyltrimethoxy silane. Ma *et al* [66] claimed that the method was effective as it lead to good dispersion of the carbon nanotubes in ethanol without damage; and it created strong bonds between the epoxy groups attached to the MWCNT surface and the –OCH3 groups of the silane molecules. The dispersion of the MWCNTs at different steps of the functionalization process is shown in Figure 2.14. The schematic of the reaction between a reduced carbon nanotube and the three-Glycidoxypropyltrimethoxy silane is depicted in Figure 2.15 [66].

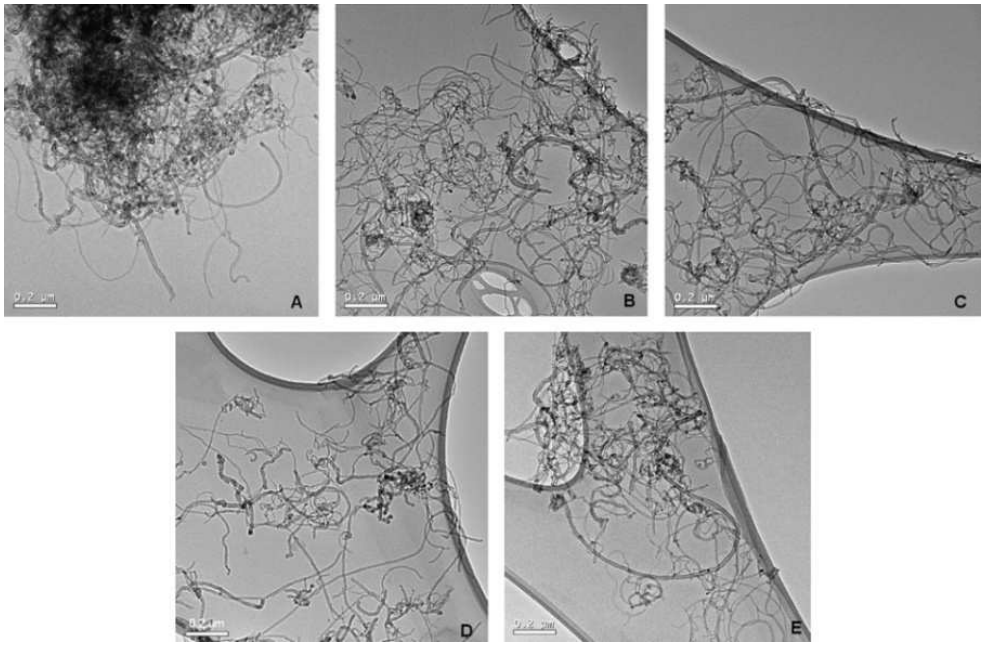


Figure 2.14: TEM image of the MWCNTs (A and B: Raw nanotubes, C and: Oxidized and reduced, D: Silane treated)

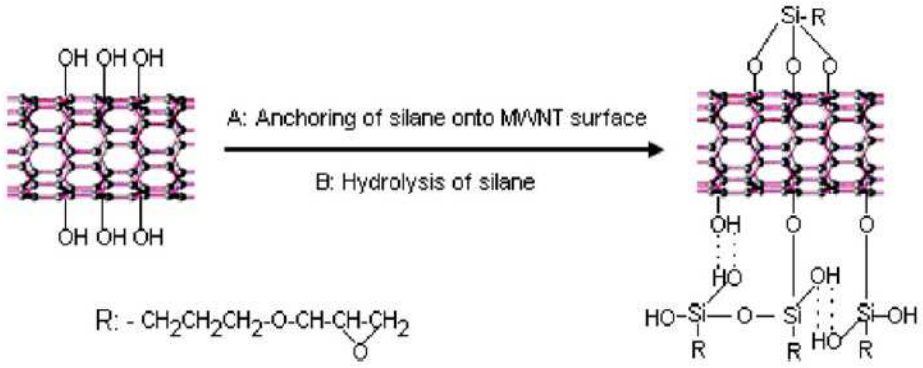


Figure 2.15: Schematic of the reaction between the reduced carbon nanotube and the 3-Glycidoxypropyltrimethoxy silane

Zhou *et al* [16] investigated the functionalization of MWCNTs with silane and its influences on the tensile properties of CNT reinforced PP composites. The functionalization process consisted of coating the MWCNTs with a uniform layer of inorganic silica by the sol-gel process and then treating the coated nanoparticles with silane (3-methacryloxypropyltrimethoxysilane). The authors stated that the main advantage of this process was the attachment of functional groups (–Si–O–Si–) onto the nanotubes without degradation the grapheme layers. The CNT reinforced PP composites sheets (2 mm thick) were fabricated by compression moulding. Different nanoparticle concentrations (0.25%, 0.5%, 1, 2% and 5% by weight) were considered. TEM revealed that sufficient dispersion of the nanoparticles was achieved at lower filler contents. TEM revealed that there was a uniform layer of silica gel on the surface of the nanoparticles after silane functionalization. The presence of functional groups such as –Si–O–Si– was proven by FTIR analysis. Mechanical testing was conducted in order to evaluate the effects of the functionalization on the mechanical properties of the composites. Test results showed that the functionalization slightly improved the tensile strength by about 2%.

Chemical treatments and mechanical dispersion (sonication and shear mixing) is commonly used to achieve desirable dispersion of CNTs in polymers and to prevent phase separation during processing. However, these two techniques have limitations. It was found that inappropriate energy or shear forces applied to

disperse the CNTs could severely compromise the mechanical strengths of the derived composites. In fact, CNTs can randomly be dispersed in liquid or molten polymer matrix by sonication or shear mixing during processing. Excessive energy input tends to decrease the aspect ratio by breaking the CNTs into shorter segments. Ma *et al* [66] reported that sufficient dispersion of CNTs in toluene was successfully achieved after mechanical treatment (ball milling) followed by 30 minutes of sonication treatments. The authors did, however, realize that breakage of carbon-carbon bonds along the grapheme layers of the co-axial tubes of the carbon nanotubes occurred after the treatments. The breakages were characterized by the opening of the end tips of several MWCNTs.

2.4.2 Effects of the nanoparticle concentration on the mechanical properties of CNT reinforced polymer composites

The effects of CNT concentration on the improvement of the mechanical properties of CNT reinforced composites have previously been investigated. Many authors reported that a large concentration of CNT reduce the mechanical strength of the composite. The researchers suggested that difficulty of homogeneously dispersing aggregates of CNTs within the polymer matrix was the main cause of an increase in voids [14, 15].

Khare *et al* [15] conducted an extensive review on carbon nanotube reinforced composites. They concluded that reduced levels of improvement in the mechanical properties of carbon nanotube reinforced composites were caused by inefficient and incomplete dispersion of CNTs. They referenced of several studies, which indicated similar observations. As part of the conclusion, the authors indicated that 1 wt% was the optimum MWCNT content for effective improvement of the tensile properties of MWCNT reinforced composites when fabricated through the screw extruder. A CNT concentration of 1% by weight was reported to increase the strain energy and the ductility by 150% and 140%, respectively.

While investigating the effects of the functionalization of the CNTs on the tensile properties of CNT reinforced PP composites fabricated by melt mixing Zhen

Zhou *et al* [16] found that the tensile strength of the composites increased up to 39 MPa with the increase of the MWCNT content. They considered different nanoparticle concentrations including 0.25wt%, 0.5wt%, 1wt%, 2wt% and 5wt%. Test results indicated that 1wt% was the optimal concentration for the improvement of the tensile strength of the composites since homogeneous dispersion of the nanoparticles could be achieved. The hypothesis was additionally supported by the TEM analysis that confirmed good dispersion at lower nanoparticle concentration. The SEM images in Figure 2.16 show agglomeration of the MWCNT caused by poor dispersion and uniform dispersion of nanoparticles through the matrix system [16]. Mechanical test results also indicated that an increase in MWCNT concentration compromised the tensile strength because many defects, such as voids, were introduced into the polypropylene matrix due to the difficulty of dispersing homogeneously the MWCNTs by melt mixing.

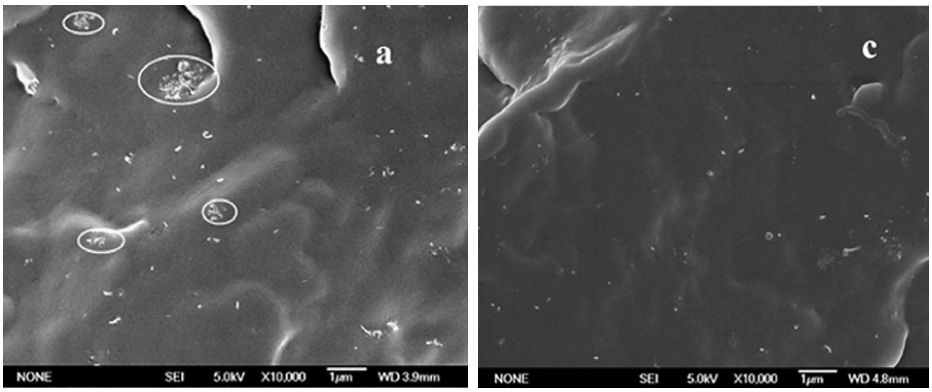


Figure 2.16: SEM images: (a) agglomerated of MWCNT, (c) uniform dispersion of nanoparticles)

Prashantha *et al* [68] concluded that the quantity of nanotubes incorporated in to the matrix had significant effects on the mechanical properties of polypropylene reinforced with MWCNTs. An average improvement of 35% in tensile strength was observed. They reported that 5wt% was the optimum nanotube concentration to improve the tensile and flexural properties, whereas 2wt% to 3wt% was the optimum concentration for improvement the impact properties. However, the

optimum CNT concentration reported by Prashantha *et al* [68] is significantly higher in comparison with the value (1wt%) reported by Zhou *et al* [16] and Khare *et al* [15].

2.4.3 Effects of nanoparticule alignments on the mechanical properties of CNTs reinforced polymer composites

The effects of the CNT alignment of on the mechanical properties of carbon nanotube reinforced polymers have been investigated by previous researchers. Andrews *et al* [14] reverenced several preceding studies that investigated on the alignment of CNTs. They indicated that the alignment in the loading direction of the test specimen was achieved in polymeric matrices by means of shear flow and recently by a magnetic field, resulting in film and fibre geometries. As an example, the researchers indicated that a twofold increase in the tension-tension fatigue strength for aligned single wall carbon nanotube reinforced epoxy resin composites compared well with that of a typical carbon fibre reinforced epoxy composite. Although the improvement of the mechanical properties due to CNT alignment could be achieved, the practicality of the CNT alignment was questionable. Up-scaling and reproducibility was reported to be extremely difficult, because the CNTs are in general randomly dispersed by the sonication or shear mixing during fabrication process of the composite [14, 15, 68]. Given these processing constraints, the fabrication of polymer matrixes reinforced with aligned CNTs is only practical on micro-scale.

It is evident that the chemical functionalization and the use of coupling agents are extensively used to enhance the interfacial bond between the carbon nanoparticles and the matrix system; and to improve the dispersion of carbon nanoparticles in the matrix in order to improve the mechanical properties of the resulted composites. Nevertheless, the potential of carbon nanotubes as reinforcing material in polymeric composites has still has to be fully explored as their exceptional nano scale mechanical properties have not yet been fully transferred to the carbon nanotube reinforced polymers on a macro scale. Furthermore, when other reinforcing materials such as natural fibres are used in addition to carbon

nanotubes, the main challenges will be to achieve optimal reinforcement by improving the interfacial compatibility between the matrix and the two reinforcing materials. It is thus imperative that a better understanding of the relationships between the manufacturing process and the interfacial bonds is achieved.

2.5 Manufacturing of natural fibre reinforced polymer composites

Studies suggest that the manufacturing technique has a great influence on the mechanical properties of natural fibre reinforced thermoplastic composites. It affects the content, fibre distribution, fibre aspect ratio and fibre orientation [17, 18]. There are several manufacturing techniques (e.g. injection moulding, compression and extrusion) that are used in the composite industry. However, the compression moulding is preferred when non-woven kenaf mats are used as reinforcing material for the fabrication of composite plates. Compared to other moulding techniques, the compression moulding has the advantages of producing composite plates with uniform material distribution and high fibre aspect ratio due to reduced fibre breakage. Rowell *et al* [19] reported that the fibres are generally oriented parallel to the extrusion flow direction in composite plates fabricated by extrusion technique and the probability of fibre breakage due to abrasion is high. Whereas in composite plates fabricated by compression moulding, the fibre orientation is not altered and the extent of fibre breakage is reduced.

The manufacturing process also has a great influence on the moisture diffusion characteristics. Thwe and Liao [63] investigated on the mechanical and moisture absorption properties of short bamboo fibre reinforced polypropylene composites; and short bamboo-glass fibre reinforced polypropylene hybrid composites. The laminates were fabricated by the compression moulding method. They reported that the inclusion of glass fibre as additive (20 wt%) and the use of coupling agent (maleic anhydride polypropylene) noticeable improved the resistance to moisture absorption since the results indicated substantial drop in the moisture content at saturation. Similar findings were reported by Kamal *et al* [51] who investigated on the long-term water absorption and its effects (e.g. swelling) on two types of composites. These were hot-press moulded composites made of wood flour filled

recycled and wood flour-virgin polyolefin. They reported that the water absorption was largely affected by the fibre content. They reported that diffusion characteristics such as the diffusion coefficient, the solubility and the permeability, increase as the wood flour content increases regardless the type of composites. They also argued that the permeability characteristics decrease with the addition of the maleated polypropylene. Bhagawan *et al* [39] investigated on the effects of the moisture absorption on pineapple-leaf fibre reinforced low-density polyethylene composites at different fibre loadings (10%, 20%, and 30% by weight). They mentioned that the moisture content at saturation increased almost linearly with the fibre loading increase. Lance Paiken [99] also reported the increase of the moisture absorption rate with the increase of the fibre content in natural fibre reinforced thermoplastic composites. He argued that as the fibre content increase, hemp fibres sticking out of the surface of the composites are the low impedance pathways for water molecules to penetrate into the material, thereby leading to a higher moisture absorption rate and a higher saturation value. These findings clearly show that the manufacturing process has a significant impact on the mechanical properties and moisture characteristics of natural fibre reinforced polymer composites.

2.6 Summary

From the literature survey, it is evident that:

- Lignocellulosic fibres are an important resource for the composite industry.
- There is a possibility of improving the mechanical properties and resistance to moisture absorption of natural fibre reinforced composites by means of fibre treatments.
- Functionalized multi-wall carbon nanotubes can be used to improve the mechanical properties of natural fibre reinforced composites.

2.7 Objectives

The overall objective of this experimental research work is to develop kenaf fibre reinforced polypropylene composite plates with improved mechanical properties (tensile, flexural, fatigue and impact properties) and resistance to moisture absorption.

To achieve this objective the following are required:

- Evaluate the influences of the fibre treatments (e.g. alkali treatments and alkali treatments followed by three-aminopropyltriethoxysilane treatments) on the mechanical properties (tensile, flexural, fatigue and impact properties) and on the resistance to moisture absorption of kenaf/PP composites.
- Evaluate the influences of the filler material (e.g. functionalized multi-wall carbon nanotubes) on the mechanical properties (tensile, flexural, fatigue and impact properties) and on the resistance to moisture absorption of kenaf/PP composites.

2.8 Outlines

This report comprises 7 chapters. Chapter 1 provides an introduction to the subject and highlights the motivation of the research work.

Chapter 2 emphasizes the potential prospective of kenaf fibre and polypropylene matrix in the composite industry. It also highlights the limitations of natural fibre reinforced polymer composites with regards to the mechanical properties and the resistance to moisture absorption. Different techniques used to improve the mechanical properties and the resistance to moisture absorption of natural fibre reinforced polymer composites are reviewed. Thermoset and thermoplastic based composites are both considered. This Chapter 2 also gives the objectives of the study and the outline of the thesis.

The materials of constructions (e.g. resins, filler material and reinforcing materials) and the manufacturing process of the kenaf reinforced polypropylene composites are described in Chapter 3.

The mechanical tests (tensile tests, flexural test, fatigue test and impact test) and moisture absorption test are explained in Chapter 4. The microscopic examination techniques used in this project are also described.

In Chapter 5, the mechanical test results, the failure characteristics and the moisture absorption results are presented and discussed in relation to the microscopic examination findings. This Chapter 5 comprises 4 sections:

- Section 5.1 discuses the effects of the fibre treatments on the mechanical properties (e.g. tensile, flexural, fatigue and impact properties).
- Section 5.2 discuses the effects of the fibre treatments on the resistance to moisture absorption.
- Section 5.3 discuses the effects of the filler material (multi-wall carbon nanotubes) on the mechanical properties (e.g. tensile, flexural, fatigue and impact properties).
- Section 5.4 discuses the effects of the filler material (multi-wall carbon nanotubes) on the resistance to moisture absorption.
- Section 5.5 gives a summary of the results.

Chapter 6 summarizes the findings of the work and Chapter 7 provides the recommendations for future works.

3 PRODUCTION OF COMPOSITE PLATES

The kenaf and glass reinforced polypropylene composites are fabricated by compression moulding using the film–stacking technique (CMFST). This technique enables the fabrication of composite plates with layers of significantly different material properties toward moisture absorption. It also prevents possible changes in the matrix crystallinity and inhibits the thermal degradation of kenaf fibres and associated functional groups due to the reduction in fabrication temperature [7].

Two treatment methods of kenaf mats are considered: Alkali treatments and alkali treatments followed by three-aminopropyltriethoxysilane treatments (alkali-silane treatments). Multi-wall carbon nanotubes are chemically treated in order to improve the nanoparticles dispersion and enhance the interfacial bonding with the polymer matrix [6, 16, 40, 41, 66, 68]. The treatment of the MWCNTs is a combination of process, namely ultrasonic, acid and silane treatment.

This chapter is divided into six sections: Section 3.1 discusses the fabrication material including the matrix systems (e.g. unreinforced polypropylene and MWCNT reinforced polypropylene matrix), the reinforcing materials (e.g. glass and kenaf fibre) and the filler material (e.g. functionalized MWCNTs). Section 3.2 discusses the chemical treatments of kenaf mats (e.g. alkali and alkali-silane treatments). The changes in the surface morphologies of kenaf fibres are also investigated. Section 3.3 describes the surface treatment for improving the dispersion of the MWCNTs and attaching functional groups (silano and oligomers) onto the nanoparticles. It also discusses the results of the analytical examination, including TEM, RAMAN and FTIR analysis. The thermal stability of the functional groups (silano and oligomers) is also investigated since the functionalized MWCNTs will be exposed to high temperatures (approximately 180°C) during the fabrication of the MWCNT-PP plates and kenaf/MWCNT-PP composites. Section 3.4 provides the manufacturing details of the kenaf and glass fibre reinforced polypropylene composite plates along with the advantage and limitation of the manufacturing techniques. Section 3.5 describes the fabrication

process of the polypropylene reinforced MWCNTs plates (MWCNT-PP plates). However, the influences of the CNT concentration on the mechanical properties of MWCNT-PP plates (e.g. tensile modulus, tensile strength, flexural strength and impact strength) are discussed in Chapter 5. Section 3.6 describes the material formulation, indicating the manner in which the composite plates are indentified.

3.1 Fabrication materials

3.1.1 Matrix systems

Polypropylene-homopolymer (PP-H) in the form of pellets and micro powder was used as the matrix system. Both the polypropylene pallet and micro powder were donated by SASOL. Two types of matrix formulations comprising of unreinforced polypropylene (PP) and polypropylene reinforced with multi-wall carbon nanotubes (MWCNT-PP) were used.

3.1.1.1 Unreinforced PP matrix

Polypropylene sheets were fabricated by compression moulding using the PP pallets, Figure 3.1 (a). The tensile properties (e.g. tensile modulus and tensile strength) of unreinforced polypropylene and MWCNT-PP were determined experimentally using a test procedure implemented in accordance with the BS ISO 527 and ASTM D 3039/D 3479M-96 standards [75, 76]. The flexural properties were determined in accordance with the requirements of BS ISO 178 and ASTM D790-10 [77, 78]. Specific gravity was determined in accordance with ASTM D792 [79]. The results of the mechanical tests are shown in Table 3.1.



a **b**

Figure 3.1: Polypropylene: (a) PP pallets, (b) PP powder

Table 3.1: Mechanical properties of polypropylene matrix

Properties	Unit	Unreinforced PP
Density	Kg/m^3	902
Elastic modulus	GPa	1.25
Tensile strength	MPa	28.5
Flexural strength	MPa	31
Izod notched Impact	J/m	78.38
Elongation at break	%	12

3.1.1.2 MWCNTs reinforced PP matrix

The MWCNT-PP matrix (Figure 3.2) was produced using the direct incorporation method, a shear-mixing process commonly used in the industry for the blending of thermoplastic matrices. The Rheo-mixer apparatus was made available by the Department of Chemical Technology of the University of Johannesburg. The apparatus comprises of three units: the driver (Haake PolyLab OS), the Rheo-mixer (Rheomex) and the extruder (Rheomex). The concentration of the CNT in the matrix investigated in this study ranges from 0.1% to 1.25%. An interval of 0.25% by mass was considered for concentrations greater than 0.25%. Earlier studies reported that high CNT concentration in the thermoplastic matrix can be achieved by using the shear-mixing process. Liu and Choi [83] indicated that a

concentration of 7 wt% was achieved by this technique, but the authors did not indicate the effects thereof on the mechanical properties of the resulted composite. They acknowledged that, in order to achieve sufficient dispersion within the matrix, increased processing time will be required at higher concentration. However, in this study, the processing time had to be reduced in order to prevent thermal degradation of the composite constituents (e.g. the PP matrix, kenaf fibres and functional groups). The mechanical properties of MWCNT-PP made of functionalized MWCNTs are presented in Table 3.2. Detailed description of the manufacturing of MWCNT reinforced PP plates can be found in Section 3.5.



Figure 3.2: MWCNT reinforced polypropylene matrix: 0.1% MWCNT-PP and 1.25% MWCNT-PP

Table 3.2: Mechanical properties of MWCNT-PP

Properties	Unit	MWCNT-PP					
		0.1%	0.25%	0.50%	0.75%	1.0%	1.25%
Density	Kg/m^3	902	901	903	902	902	903
Elastic modulus	GPa	1.26	1.41	2.31	2.29	1.95	1.12
Tensile strength	MPa	27.5	29.5	42.2	42.8	38.5	27.50
Flexural strength	MPa	31.1	32.4	42.1	42.6	39.8	30.50
Izod notched Impact	J/m	75.45	85.6	120.4	123.2	75.6	71.10

3.1.2 Reinforcing materials

Single fibre tension tests were conducted to determine the tensile properties of glass and kenaf fibres. The testing was conducted in accordance with the requirements of ASTM D3379 [80] because the standard provides guidelines for the testing of individual fibres. Although discrepancies in the results were present (especially for kenaf fibres), the average test results compared well with typical values reported in literature [8, 81, 24].

3.1.2.1 Glass fibres

Glass fibre in the form of 350 g/m^2 chopped strand mats (Figure 3.3) were donated by RP/Composites Facility Laboratory of the University of the Witwatersrand, Johannesburg. The mechanical properties of glass fibre determined experimentally are shown in Table 3.3. The density of the glass fibre could not be determined experimentally. Therefore theoretical value was considered. The test results of glass fibre showed appreciable consistency, even though slight discrepancies were observed which could have been caused by uncontrollable test variables (e.g. load-cell sensitivity). In contrast of kenaf fibres, microscopic examination (Figure 3.4) showed that glass fibres have a uniform geometric configuration, which probably led to consistent test results.



Figure 3.3; Glass fibre chopped strand mats, 350 g/m^2

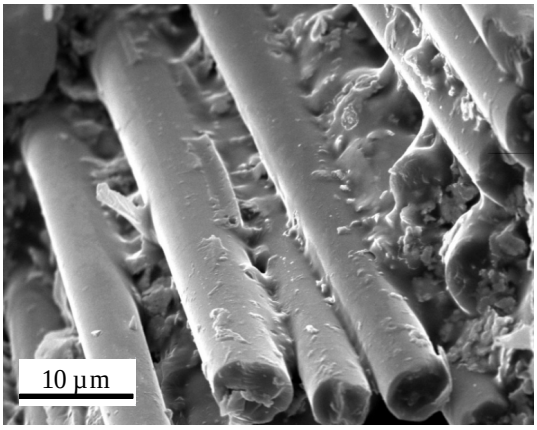


Figure 3.4: SEM picture of glass fibre

Table 3.3: Mechanical properties of glass fibre

	Tensile modulus	Tensile strength
	GPa	MPa
Specimen 1	68.3	1763.2
Specimen 2	73.1	1689.3
Specimen 3	68.4	1817.6
Specimen 4	68	1644.6
Specimen 5	70.3	1687.1
Average	**69.6**	**1720.4**
Standard Deviation	**2.15**	**69.10**

3.1.2.2 Kenaf fibres

Kenaf fibres used in this work were in the form of non-woven kenaf fibre mats, Figure 3.5. The two areal masses, 125 g/m^2 and 350 g/m^2, were selected in order to achieve the predicted fibre contents by using a maximum of 3 polypropylene sheets per composite plate. Kenaf plants used for the fabrication of the mats used in this study were cultivated in South Africa. The mats were fabricated using the needle punching method. The lengths of kenaf fibre varied between 5.0 mm and 22.4 mm with an average of 14 + 0.5 mm. Three forms of kenaf fibres were used:

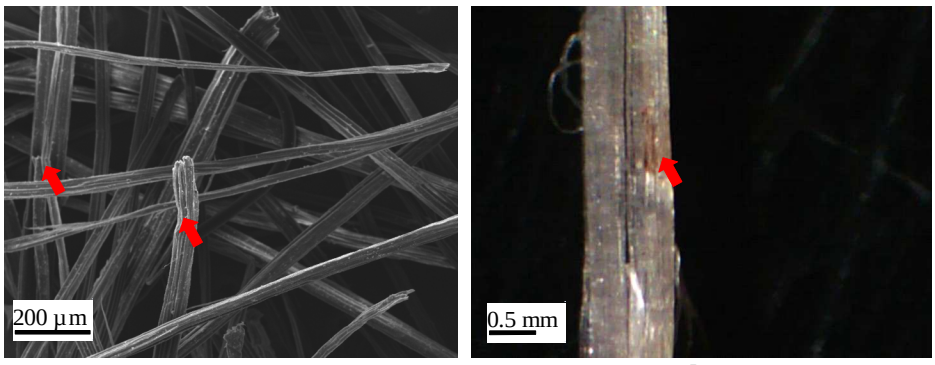
untreated fibres, fibres treated with a sodium hydroxide solution and kenaf treated with a sodium hydroxide solution followed by three-aminopropyltriethoxysilane.

The mechanical properties of kenaf fibre are shown in Table 3.4 and significant discrepancies in the test results (e.g. tensile strength and modulus) can be noted. Material irregularities (geometrical and chemical irregularities in the wall cells) of the individual kenaf fibres were found to be the cause. This was confirmed by microscopic examination, which revealed typical geometrical irregularities and possible chemical anomalies in kenaf fibres, Figure 3.6. It is believed that these geometrical irregularities shown in Figure 3.6 (a) were caused by the mechanical loads applied to the mats during the fibre processing. Localized changes in colour on untreated fibres, Figure 3.6 (b), point to the possibility of chemical decomposition that took place during the processing of kenaf fibres.



a **b**

Figure 3.5: Kenaf fibres: (a) 125 g/m^2 mat, (b) 350 g/m^2 mats



a **b**

Figure 3.6: Untreated kenaf fibre

Table 3.4: Mechanical properties of kenaf fibre

	Tensile modulus	Tensile strength
	GPa	MPa
Specimen 1	46.1	469.6
Specimen 2	58.4	361.3
Specimen 3	32	496.2
Specimen 4	41.3	406.6
Specimen 5	39	517.5
Average	**43.4**	**450.2**
Standard Deviation	**9.82**	**64.86**

Effects of fibre aspect ratio

Research [95] has shown that the fibre aspect ratio plays a significant role in the mechanical characteristics of kenaf reinforced PP composites. The effects of the fibre aspect ratio of kenaf fibres were consequently investigated by comparing the calculated critical length to the actual average fibre length. Thus, the formula reported by Shibata *et al* [95] was used to calculate the critical fibre length, *Lc*, of the kenaf fibre, and is expressed in equation 3.1.

$$L_c = \frac{T_f \, r_f}{T_m} \tag{3.1}$$

Where, T_f and T_m are the tensile strength of the fibre and matrix. r_f denotes the fibre radius.

The critical length, *Lc*, was determined to be 1.16 mm. Comparing *Lc* to the average length of the fibre, one can see that the fibre length used as reinforcing material is well above the calculated critical length. This suggests that the tensile and flexural behaviours exhibited by kenaf/PP composites are not influenced by the fibre aspect ratio, rendering further investigation into the effects of aspect ratio irrelevant. Similar findings were also made for glass/PP composites.

3.1.3 Multi-wall carbon nanotubes

Previous studies showed that the functionalization of carbon nanotube can alter the mechanical properties [64, 65]. By treating it with strong acids, the molecular structure is damaged due to breakage of the carbon – carbon bonds (C=C). This is more prominent in single wall carbon nanotubes (SWCNTs) than MWCNTs. Therefore, for the purposes of this study, MWCNTs were used as filler material because of the superior resistance of the grapheme layers to damage.

Multi-wall carbon nanotubes (MWCNTs) with a specified purity of 98% were supplied by the School of Chemistry of the University of the Witwatersrand, Johannesburg. The MWCNTs (Figures 3.7) were fabricated using the chemical vapour deposition process. Details on the manufacturing process of the MWCNTs have been discussed in a report published by Mhlanga *et al* [69]. According to the supplier, the inner diameter of the CNT is 10 nm, whereas the outer diameter of the MWCNTs ranges between 20 and 30 nm. The length of the MWCNTs ranges between 10 and 50 µm. The typical material characteristics of a MWCNT are summarized in Table 3.5.



Figure 3.7: Raw MWCNTs

Table 3.5: Mechanical properties of MWCNTs

Properties	Unit	MWCNTs
Density	Kg / m^3	1300 – 1400 [7]
Elastic modulus	GPa	1000 – 5000 [7]
Tensile strength	GPa	150 [97]
Compressive strength	GPa	100 [80]
Bending strength	GPa	14 [80]
Elongation at break	%	24 [7, 79]

3.2 Chemical treatments of kenaf mats

The descriptions of the reagents are shown in Table 3.6. The characteristics of the solutions of three-aminopropyltriethoxysilane and methanol, used for the silane treatment of kenaf fibres, are similar to those of the solutions used for the treatment of MWCNTs, described in section 3.3.

Table 3.6: Characteristics of reagents

	NaOH	Toluene	Acetic Acid
Physical form	Solid	Liquid	Liquid
Density (g/ml)		0.87	1.049
Concentration		99% (ace)	98% (uniLAB)

3.2.1 Alkali treatments

As discussed in Chapter 2, the effectiveness of natural fibres as reinforcing material largely depends on the load transfer between the fibre and matrix [6, 40]. It was therefore imperative to ensure that the surface impurities of the kenaf fibres were removed in order to facilitate an effective load transfer by increasing the contact area and improving the bonding strength [7]. The alkali treatments considered in this study, consist of soaking kenaf mats in an alkali solution. Kenaf mats were immersed in the NaOH solution for 24 hours at a temperature of 45ºC,

Figure 3.8. After immersion, the mats were washed with running tap water and then immersed in distilled water containing 1% acetic acid to neutralize the remaining NaOH acid. The alkali treated kenaf mats were then dried in the oven at 45°C for 12 hours, ready to be used as reinforcing material for the fabrication of alkali treated kenaf/PP composites. The concentration of the alkali solution ranged from 1% to 8% (by mass), increasing in intervals of 1%.

The results from preliminary microscopic examinations indicated that the cleanliness of the fibre after treatment is largely determined by the concentration of the alkali solution Figure 3.10. This resulted in a wide range of concentrations that had to be investigated in order to determine the effectiveness. With the selection of this wide range, results of earlier studies indicating that 5-6% NaOH was optimal, and this could also be verified [24]. The expected reaction mechanism governing the alkali treatment process is summarized in Figure 3.9

The objectives of the alkali treatments are:

- to clean the fibres and to remove surface impurities such as lignins, oils and wax covering the external surface of the fibre cell wall.
- to increase the cellulose quantity, thereby providing additional hydroxyl groups (−OH) on the fibres. These hydroxyl groups are then intended to act as sites for the attachment of silano radicals (silano and oligomers) on the fibres [13, 24].



Figure 3.8: Alkali and alkali-silane treated of kenaf mats

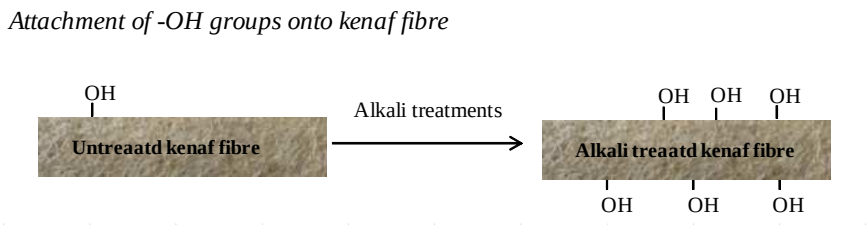


Figure 3.9: Alkali treatment mechanism of kenaf fibre

Microscopic examination revealed that treatment using solutions with a concentration less than 5% NaOH is not effective due to the retention of surface deposits. It should be noted that the surface impurities are significant factors contributing to the poor mechanical properties of natural fibre reinforced polymer composites by preventing effective fibre–matrix interfacial bonding [7].

In agreement with results found in literature, an optimal concentration of 5-6% NaOH effectively removes impurities and modifies the surface texture of the fibres. These results were obtained using SEM; the surface morphology of kenaf fibres treated with different alkali concentrations are depicted in Figure 3.10. It is evident that the quantity of surface impurities decreases with the increase of alkali concentration. Although the change in colour cannot be used as a reliable quantitative mean of evaluating the effectiveness of the alkali treatment, it is at least indicative of the impact of alkali treatment on the fibre texture. The discoloured kenaf mats acts a confirmation thereof and can be seen in Figure 3.11. It was found that the dark brown colour of the untreated mats becomes lighter with an increase in alkali concentration. Masud *et al* [24] confirmed the change in fibre surface texture due to alkali treatment and concluded that 5% NaOH was the optimal concentration for treatment of kenaf fibres. In this study, SEM examination showed that alkali treatments using 7% or 8% NaOH solution damage considerably the texture of kenaf fibres. Fibre degradation caused by excessive alkali is shown in Figure 3.10 (d). The degradation of the kenaf fibre textures due to high alkali concentration was also reported by early researchers [7].

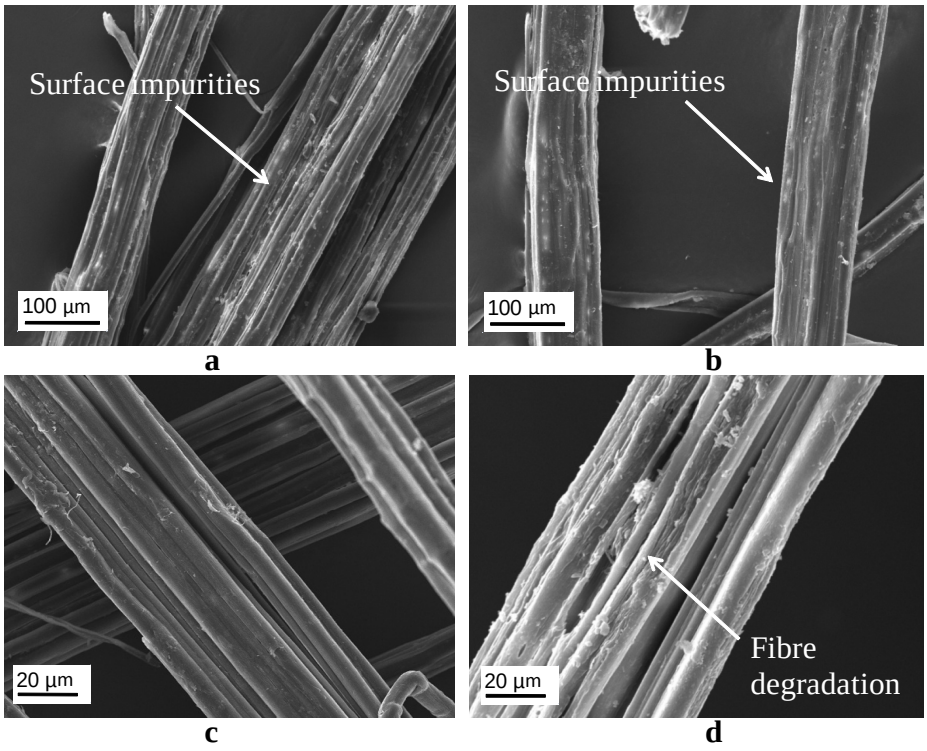


Figure 3.10: SEM of alkali treated kenaf fibres at: (a) 3%NaOH, (b) 4%NaOH, (c) 6%NaOH and (d) 8%NaOH



Figure 3.11: Alkali treated kenaf mats

3.2.2 Alkali-silane treatments

The objective of the silane treatment is to attach silano radical groups onto the kenaf fibres through the reaction between the hydroxyl groups and silanols. In the treatment process, kenaf mats were treated with a solution of NaOH followed by a

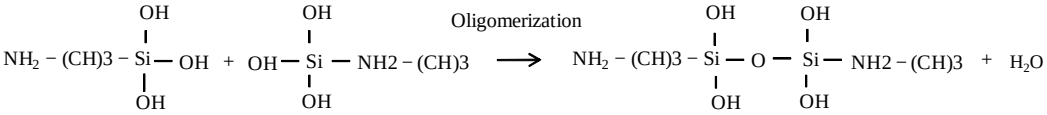
silane solution. The silane solution was made of 5% of three aminopropyltriethoxysilane (weight of silane relative to the weight of kenaf mat) diluted in a 50% aqueous solution of methanol in order to hydrolyze the silane and bring it into its active state. The formulation in alcohol (methanol) helps preventing excessive poly-condensation of the silanols ($NH_2-(CH)3-Si(OH)_3$). The pH of the silane solution was kept at a minimum of 4 in order to slow down the condensation process of the hydrolyzed silane molecules.

The mechanism of the silane treatment can be explained as follow: The dilution of three-aminopropyltriethoxysilane in water produces silanol molecules because of the hydrolization of the ethoxy groups. These silanols also lead to the formation oligomers through the process of condensation. When the kenaf fibre comes into contact with the silanol molecule, stable covalent bonds are formed between it and the newly added hydroxyl groups [7]. The silano radical groups attached onto the kenaf fibres are then intended to act bonding sites to enhance the fibre-matrix bonding strength by ensuring strong cross-linkages and interlocking between the fibre and polymer chains of the matrix. The expected reaction mechanism governing the treatment process is summarized in Figure 3.12 and the optimum alkali and alkali-silane treatment parameters are shown in Table 3.7. Li *et al* [13] reported a similar reaction mechanism during their investigating into the chemical treatment of natural fibres.

Hydrolisis of the three-aminopropyltriethoxysilane leading to the formation of silanol



Condensation of silanol molecules leading to the formation of oligomers



Attachment of silanols and oligomers onto kenaf fibre

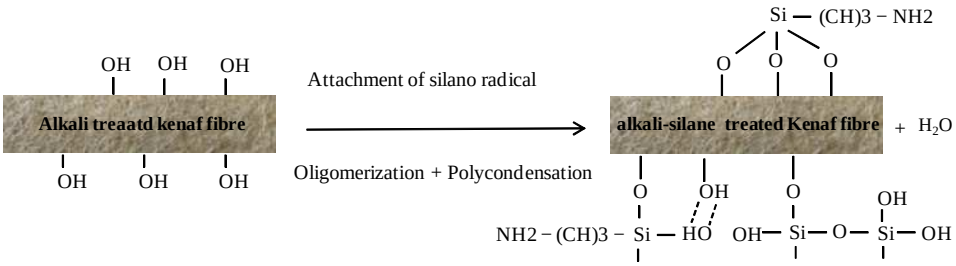


Figure 3.12: Alkali-silane treatment mechanism of kenaf fibre

Table 3.7: Alkali and silane treatment parameters

Parameters	Alkali treatment	Silane treatment
Immersion time (Hours)	24	4
Immersion temperature (°C)	45	28
pH	Greater than 10	4 to 5
Drying time (Hours)	12	12
Drying temperature (°C)	45	45

3.3 Chemical treatments of MWCNTs

Surface treatment is essential for the improvement of the nanotube dispersion and enhancement of the interfacial bonging between the nanotubes and the polymer matrix. In this study, the treatment is aimed to improve the dispersion of the nanoparticles and to attach silano functional groups onto MWCNTs. These functional groups are then intended to provide sites for interlocking bonds, which

will enhance the nanotube-matrix and nanotube-kenaf fibre compatibility. The surface treatment of the MWCNTs consisted of three main stapes, namely ultrasonic, acid and silane treatment. The process was designed in such a way that the grapheme sheets of the functionalized CNTs are not significantly altered and damaged to such extend that the CNT aspect ratio are not reduced - undesired attributes for reinforcing materials intended for use in polymeric composites. The aim of the ultrasonic treatment is to eliminate bundling and to break down the aggregates. The objective of the acid treatments (oxidation and reduction) is to attach active sites (–OH groups) onto the MWCNTs intended to react with silanols in order to attach the silano radicals groups onto the carbon nanoparticles [66] during silane treatment. The treatment of the MWCNTs was conducted in a controlled atmospheric chamber (Frontier, Model: EFA – 4UDRVW-8 Serial: 2011 - 60074) to prevent subsequent condensation of active silane molecules. The apparatus was made available by the RP/Composites Facility Laboratory of the University of the Witwatersrand, Johannesburg. See Figure 3.13.

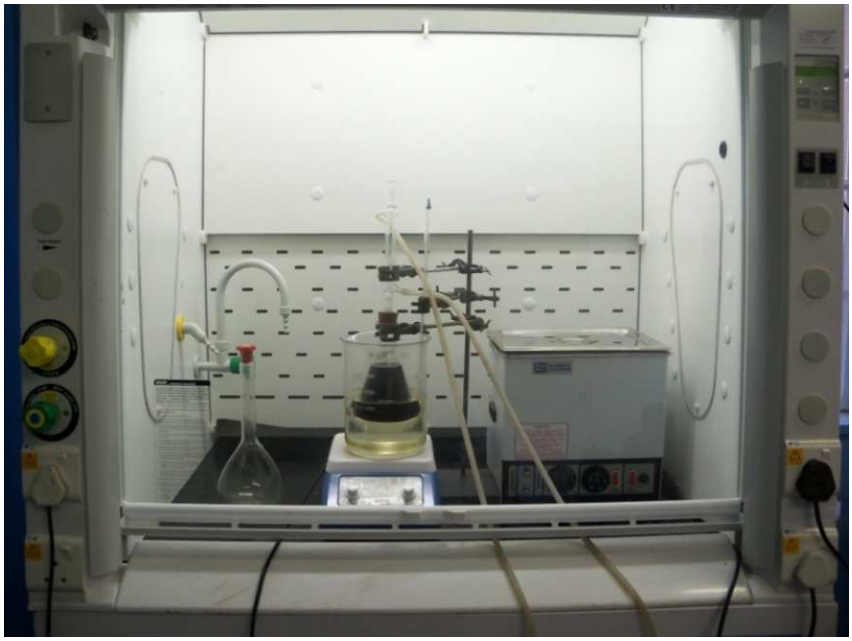


Figure 3.13: Silane treatments of MWCNTs

Analytical examinations, including Field Emission Analytical Transmission Electron Microscopy (TEM), Fourier Transform Infrared spectrometry (FTIR)

and Raman spectroscopy (RAMAN) were conducted at each step of the treatment to evaluate the process effectiveness [16, 66, 68]. The visual examination along with the TEM and RAMAN results confirmed the improvement of the MWCNT dispersion and the attachment of the functional groups (silanols and oligomers) onto the MWCNTs. TEM results showed that the CNT dispersion (Figure 3.18) and the suspension stability (Figure 3.19) improved substantially, especially after the silane treatment. TEM results in combination with the RAMAN results (Figure 3.21) showed that acid and subsequent silane treatment did not significantly damage the grapheme layers of the MWCNTs or alter the CNT length. This implies that the ultrasonic and acid treatments did not affect the aspect ratio the carbon nanotubes. FTIR identified –OH and Si–O–Si groups attached onto the MWCNTs suggesting that the functionalization process of the MWCNTs was successful (Figure 3.22).

Because of the incorporation of functionlaized MWCNTs into the PP matrix by using the melt-mixing process, concerns regarding the thermal stability of the functional groups (silano groups and oligomers) have to be addressed and the effects of temperature were therefore investigated. RAMAN results suggested that the heat treatment, at temperatures below 180°C, did not alter the grapheme layers and the functional groups attached to the carbon MWCNTs. Visual examinations also suggested that the suspension stability of functionalized MWCNTs were not altered.

Reagents

The three-aminopropyltriethoxysilane, $NH2{-}(CH_2)3{-}Si(OCH_2\ CH_3)_3$, was donated by Southern Chemicals (PTY) LTD. The commercial name of the three-aminopropyltriethoxysilane is Silquest A-1100. The three-aminopropyltriethoxysilane was received in a liquid form and used without any further treatments. Organofunctional silanes are highly reactive materials and may pose safety issues and hazards, requiring special precaution during storage and handling. Therefore, guideline for handling provided the supplier was used. The methanol - silane solution, used for silane treatment, was prepared in accordance

with the supplier's user guide. The physical properties of the reagents presented in Table 3.8 are as indicated on their respective datasheets.

Table 3.8: Typical physical properties of silane

Properties	Unit	Value
Physical form		Liquid
Colour		Clear, colourless
Density at 25°C	(g/ml)	0.9500
Boiling Point at 760 mm Hg,	°C	220
Refractive Index, $_n$ D25°C		1.420
Flash Point, Pensky-Martens Closed Cup	°C	96

The reagents listed in Table 3.9 were supplied by the School of Chemistry of the University of the Witwatersrand, Johannesburg and were used without any further purification:

Table 3.9: Characteristics of reagents

	Methanol	Toluene	Sulphuric acid	Nitric acid
Physical form	Liquid	Liquid	Liquid	Liquid
Density (g/ml)		0.87	1.84	1.34
Concentration	99% (Promak)	99% (ace)	98% (uniLAB)	55% (ace)

3.3.1 Treatments

3.3.1.1 Ultrasonic treatments

The MWCNTs were supplied in a powdered form and it was therefore important to conduct the ultrasonic treatment in order to eliminate the bundles and to break down the clusters. In order to achieve this, every batch of MWCNTs, weighing approximately 100 grams, was transferred to a beaker and dispersed in 1000 ml of 95wt% aqueous methanol. The ultrasonic treatment was conducted at 25°C for 25

minutes using an Integral Systems UD 80SH-2L Digital Sonifier, Figure 3.14 (a). After the treatment, the suspension was allowed to deposit for 3 hours and then filtered through a paper filter with a pore size of less than 1.0 µm, Figure 3.14 (b). Thereafter, the MWCNTs were placed into an oven at 90°C for 4 hours to dry.



a **b**

Figure 3.14: Ultrasonic treatment of MWCNTs

3.3.1.2 Acid treatment of MWCNTs

The dried MWCNTs were transferred into a 1000 ml Erlenmeyer flask containing an acid solution. The acid solution was made of 45% nitric acid (HNO_3) and 45% sulphuric acid (H_2SO_4) in a ratio of 1 to 3. The mixture (MWCNT and acid solution) was then homogeneously mixed at 45°C for 45 minutes using a combined hot-plate magnetic stirrer device. The acid treatment was also conducted in the atmospheric controlled chamber, Figure 3.13. The mixture was again ultrasonically treated for 25 minutes at ambient temperature to ensure a uniform dispersion of the MWCNTs and prevent phase separation. The acid treated MWCNTs were filtered and washed 4 times with deionised to remove excess of acid neutralise the solution. The wet MWCNTs were then dried for 24 hours in an oven at 90°C.

Preliminary tests revealed that acid treatment using concentrated acid solutions (more than 65% HNO_3 and 65% H_2SO_4) damaged the nanoparticles. TEM images showing broken MWCNTs due to high acid concentration can be seen in Figure 3.15. The roughness of the outer layer suggests possible damage to the outer

structural layer of the carbon nanotubes. TEM conducted on MWCNTs treated with acid solutions of different concentrations revealed that a solution made of 45% nitric acid (HNO_3) and 45% sulphuric acid (H_2SO_4) in a ratio of 1 to 3 was the optimal concentration.

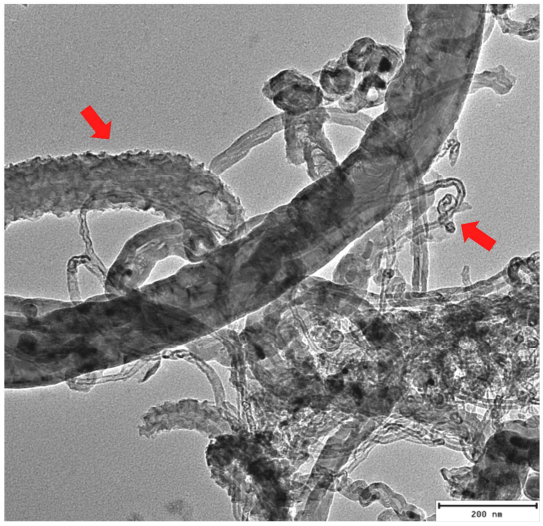


Figure 3.15: Damaged acid treated MWCNTs

3.3.1.3 Silane treatment of acid treated MWCNTs

The acid treated MWCNT powder was dispersed in 950 ml of a methanol - silane solution. The solution was made by adding 5% of three-aminopropyltriethoxysilane (by weight) to an aqueous solution of 90% methanol. The methanol solution was made with a limited amount of water (10% by weight) in order to minimize the poly-condensation of the silanols (NH_2−(CH)3−$Si(OH)_3$) during the silane treatment. The mixture was stirred at room temperature for 48 hours to allow the hydrolysis of the three-aminopropyltriethoxysilane to silanol; and to facilitate the reaction between the active sites (–OH groups) of the MWCNTs and the NH_2−(CH)3−$Si(OH)_3$. Not only silano-groups were expected to attach to the MWCNTs, but oligomers resulting from the polycondensation of the silanol molecules were also expected to bond to the MWCNTs. This phenomenon was also observed by Ma *et al* [66]. Thereafter, the solution was filtered and using methanol, washed three times to remove the remaining silane.

The filtrate (Figure 3.16) was again ultrasonically treated for 10 minutes at ambient temperature to ensure a homogeneous dispersion and to prevent any possible damage to the functional groups attached onto the MWCNTs. Finally, the silane treated MWCNTs were filtered and placed into an oven at 90°C for 24 hours to dry.

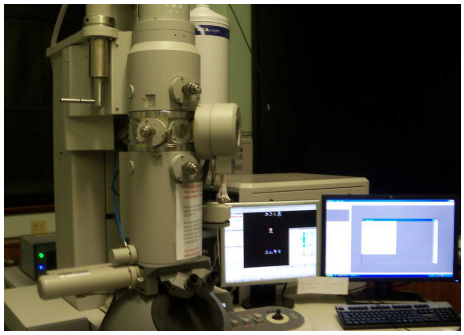


Figure 3.16: Filtrate of acid-silane treated MWCNTs

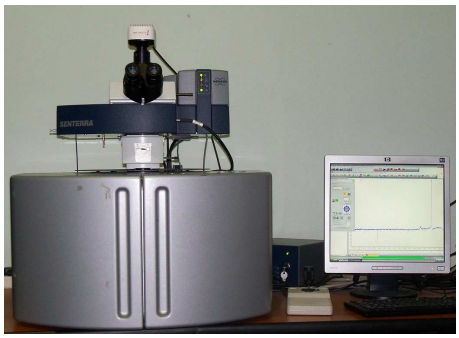
3.3.2 Characterization of MWCNTs

Analytical examination, including Field Emission Analytical Transmission Electron microscopy (TEM), Raman spectroscopy (RAMAN) and Fourier Transform Infrared spectrometry (FTIR) were conducted at each step of the treatment process. TEM microscopy was conducted to evaluate the change in the surface morphology of the MWCNTs caused by the acid treatment. It also allowed evaluating the dispersion of the MWNTs in a methanol solution, at each step of the process. A FEI Spirit 120 kV Transmission Electron microscope was used for TEM, Figure 3.17 (a). RAMAN analysis was conducted to evaluate the changes that might occur on the graphemes structures during the treatment by comparing the Raman spectrums of the MWCNTs at different steps of the treatment. A SENTERA Raman spectroscope, Figure 3.17 (b), was used for the analysis. FTIR was conducted to indentify the functional groups of interest attached to the MWCNTs. TENSOR 27 Infrared spectrometer, Figure 3.17 (c), was used to conduct the FTIR. The TEM, RAMAN and FTIR equipment were

made available by the School of Chemistry of the University of the Witwatersrand, Johannesburg.



a



b



c

Figure 3.17: Microanalysis equipment: (a) FEI Spirit 120 kV Transmission Electron microscope (b) SENTERA Raman spectroscope, (c) TENSOR 27 Infrared spectrometer

3.3.2.1 Dispersion and surface morphology of the MWCNTs

Evaluation of the MWCNT dispersion and suspension stability

Figure 3.18 shows the TEM results of the MWCNTs at different processing steps. Figure 3.18 (a) shows the aggregates of the raw MWCNTs and are probably caused by the Van der Waals interactions [16, 68]. It is also believed that the moisture absorbed during handling, could have contributed to the formation of these aggregates. Figure 3.18 (b) shows the dispersion of the raw MWCNTs subjected to ultrasonic treatment in 95 wt% aqueous methanol; it can be seen that the sizes of the aggregates are slightly reduced. In Figure 3.18 (c), the TEM image shows a substantial improvement of the MWCNT dispersion. Further improvement in the dispersion of the acid-silane treated MWCNTs can be seen in

Figure 3.18 (d). This improvement could be an indication of the presence of active functional groups attached to the carbon nanotubes, preventing the agglomeration.

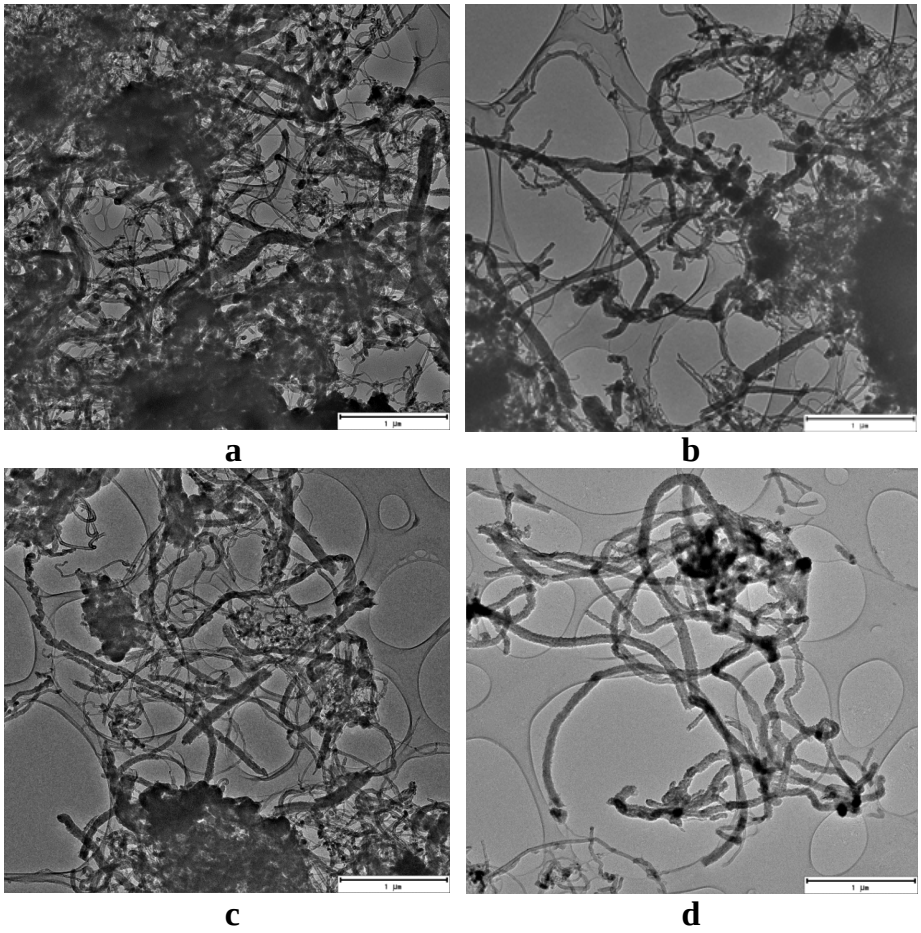


Figure 3.18: Dispersion of MWCNTs: (a) Untreated MWCNTs, (b) Sonicated MWCNTs, (c) Acid treated MWCNTs and (d) Acid-silane treated MWCNTs)

With time, carbon nanotubes generally tend to re-agglomerate into clusters, if left in an unstable solution. This phenomenon can be used as a practical indicator to evaluate the quality and stability of the dispersion of the nanoparticles. In this study, the suspension stability of the MWCNTs at different processing steps was compared in order to evaluate the effectiveness of the surface treatment on the dispersion of the MWCNTs in 95wt% aqueous methanol (Figure 3.19). Although this method cannot quantify the dispersion quality, it can, however, provide useful information for comparative studies [66]. Four specimens were prepared, diluted in methanol with a concentration of 0.5 mg/ml of MWCNTs obtained at different processing steps. All four specimens were treated ultrasonically for 1 hour at

ambient temperature and left to rest for three hours. Methanol was used in order to prevent further condensation of the silano radicals deposited on the surface of the nanoparticles. Visual examination showed that the raw and untreated MWCNTs completely settled after 2 hours leaving the upper portion of the solution transparent. Acid treated MWCNTs settled after 4 hours; whereas visible phase separation in silane treated MWCNTs could only be observed after 24 hours. These observations are again a clear indication of the improvement on the dispersion and suspension stability provided by the functional groups attached onto the surface of the nanoparticles and are in agreement with the observations confirmed by Ma *et al* [66] and the TEM results, which suggests that the chemical treatment improve the dispersion of MWCNTs.

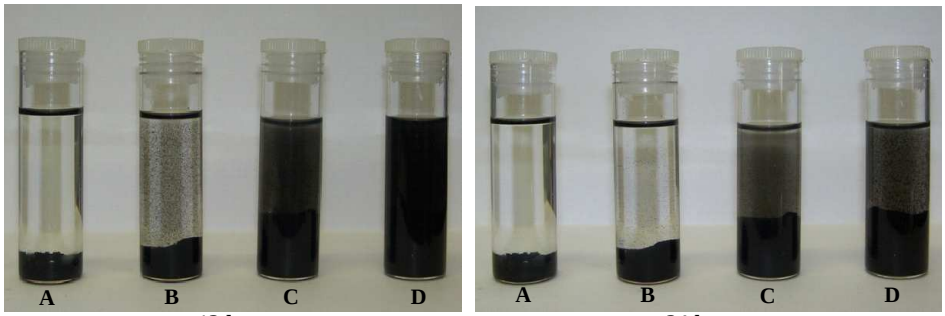


Figure 3.19: Suspension stability (A: Raw and untreated MWCNTs, B: Untreated MWCNTs, C: Acid treated MWCNTs, D: Acid-silane treated MWCNTs)

Evaluation of MWCNT surface morphology

The alteration of the structural wall (grapheme layers) of the MWCNTs, imparted by the chemical treatment was investigated. It was found that the structural layers of the individual MWCNTs do not have significant signs of damage after the silane treatment. TEM microscopy revealed that the outer layers of the acid treated and acid-silane treated MWCNTs are smooth and exhibit a flawless surface regularity. This suggests that the grapheme layers of the MWCNTs largely remained intact and that the length of the individual MWCNTs did not change significantly, implying that the ultrasonic and acid treatment did not damage the carbon nanotubes, Figure 3.20 (a) and (b).

Opened tips suggest that some of the CNTs were damaged by intensive ultrasonic treatment. Figure 3.20 (c) shows a high magnification micrograph of a possible open ended tip (red arrow) after 12 hours of ultrasonic treatment. Based on these observations, 1 hour was determined to be the upper limit for ultrasonic treatment in order to prevent significant damage. Defects caused by mechanical treatment were also reported by Ma *et al* [66], claiming that the open ended tips found on MWCNTs, after ball milling and ultrasonic treatment, were an indication of broken carbon bonds along the grapheme layers of the co-axial tubes.

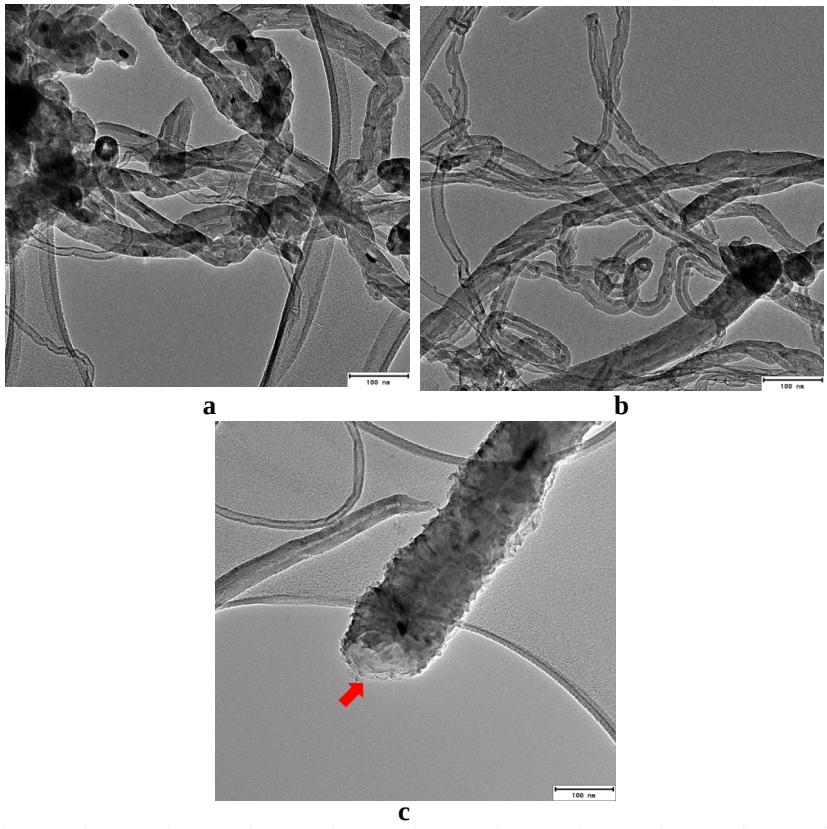


Figure 3.20: Surface morphology of MWCNTs: (a) Acid treated MWCNTs and (b) Acid-silane treated MWCNTs and (c) Acid-silane treated MWCNTs after 12 hours of ultrasonic treatment

Comparing the RAMAN spectrums of untreated MWCNTs with that of acid treated MWCNTs and acid-silane treated MWCNTs in Figure 3.21, the following can be suggested: the intensities of G and D bands of the untreated nanotubes are greater than those of the acid treated and acid-silane treated MWCNTs. However,

the differences are minor. This suggests that the structure of the untreated MWCNTs was slightly altered after acid treatment. This modification could be an indication of the functionalization of the MWCNTs (attachment of –COOH and –OH groups on the MWCNTs) due to acid treatment. Figure 3.21 also shows that the G and D bands of the acid treated and acid-silane treated MWCNTs are similar. This suggests that acid treatment and silane treatment did not alter additionally the grapheme layers of the carbon-nanoparticles.

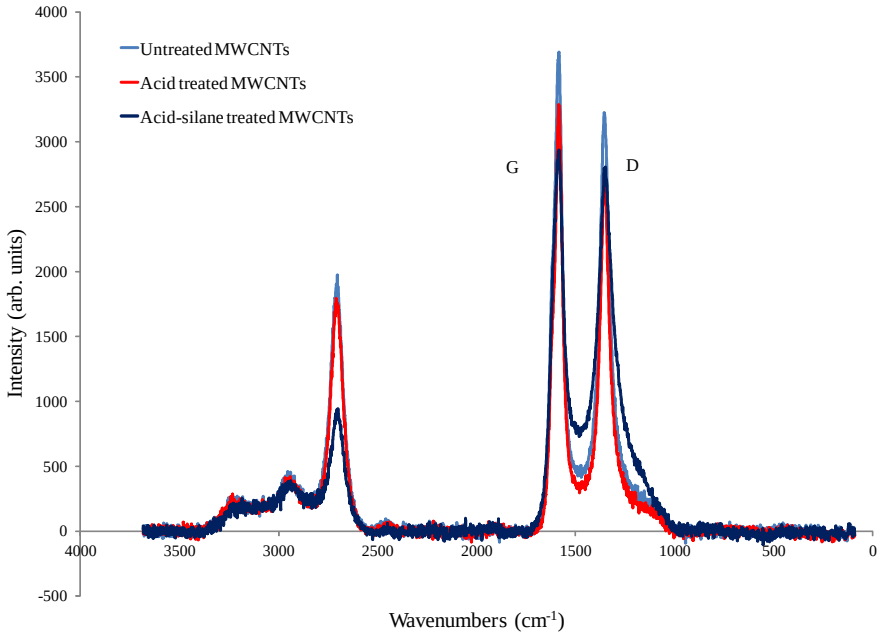


Figure 3.21: RAMAN spectrums of untreated and treated MWCNTs

3.3.2.2 Characterization of the functional groups

FTIR microscopy was used to identify the functional groups such as –OH and Si–O–Si that were attached onto the carbon-nanoparticles. It was significant to conduct the FTIR microscopy test because of its ability to detect the stretching of unsymmetrical bonds such as the kind found in these functional groups [71]. Figure 3.22 shows the FTIR results of the untreated, acid treated and acid-silane treated MWCNTs. The broad peak at 3420 cm^{-1} on the acid treated MWCNT curve is attributed to the presence of hydroxyl groups (–OH) attached to the surface of the MWCNTs [16, 66, 71]. The absence of such a band on the untreated MWCNT curve

also supports the proposal that these hydroxyl groups have been attached during the acid treatment process. On the acid-silane treated MWCNT curve, the peak at 3420 cm^{-1} substantially flattens. This confirms the reduction of the quantity of –OH groups on the MWCNTs suggesting that there is a reaction between it and the NH_2−(CH)3−$Si(OH)_3$ groups, which subsequently leads to the attachment of silano groups as indicated in the reaction mechanism in Figure 3.23. Concurrently, the characteristic peak absorption of Si–O–Si bonds appears at 1080 cm^{-1}. This also confirms the attachment of the silano groups and oligomers. These observations, along with TEM and RAMAN results, confirm the functionalization reaction mechanisms of the MWCNTs including: hydrolysis of the three-aminopropyltriethoxysilane, the condensation of the three-aminopropyltriethoxysilane to oligomers and the attachment of the silano groups and oligomers to the surface of the MWCNTs through hydrogen bonds and covalent links.

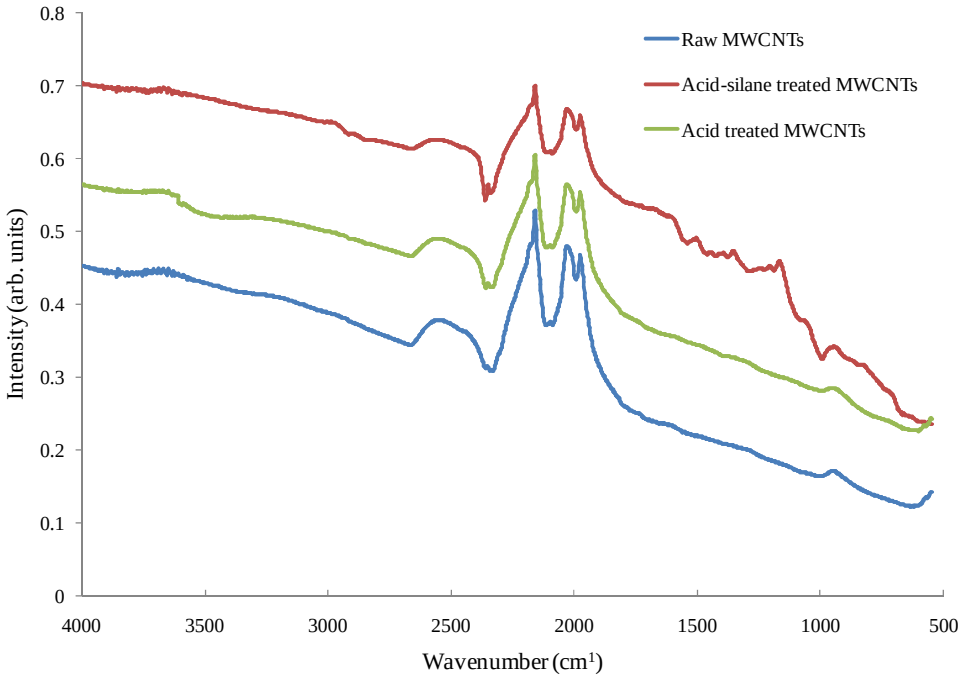


Figure 3.22: FTIR results of untreated MWCNTs, acid treated MWCNTs and acid-silane treated MWCNTs

3.3.3 Reaction mechanism of surface treatments

The predicted reaction mechanism of the surface treatment process is summarized in Figure 3.23. The TEM, FTIR and RAM results along with visual examination were found to be in agreement with the prediction.

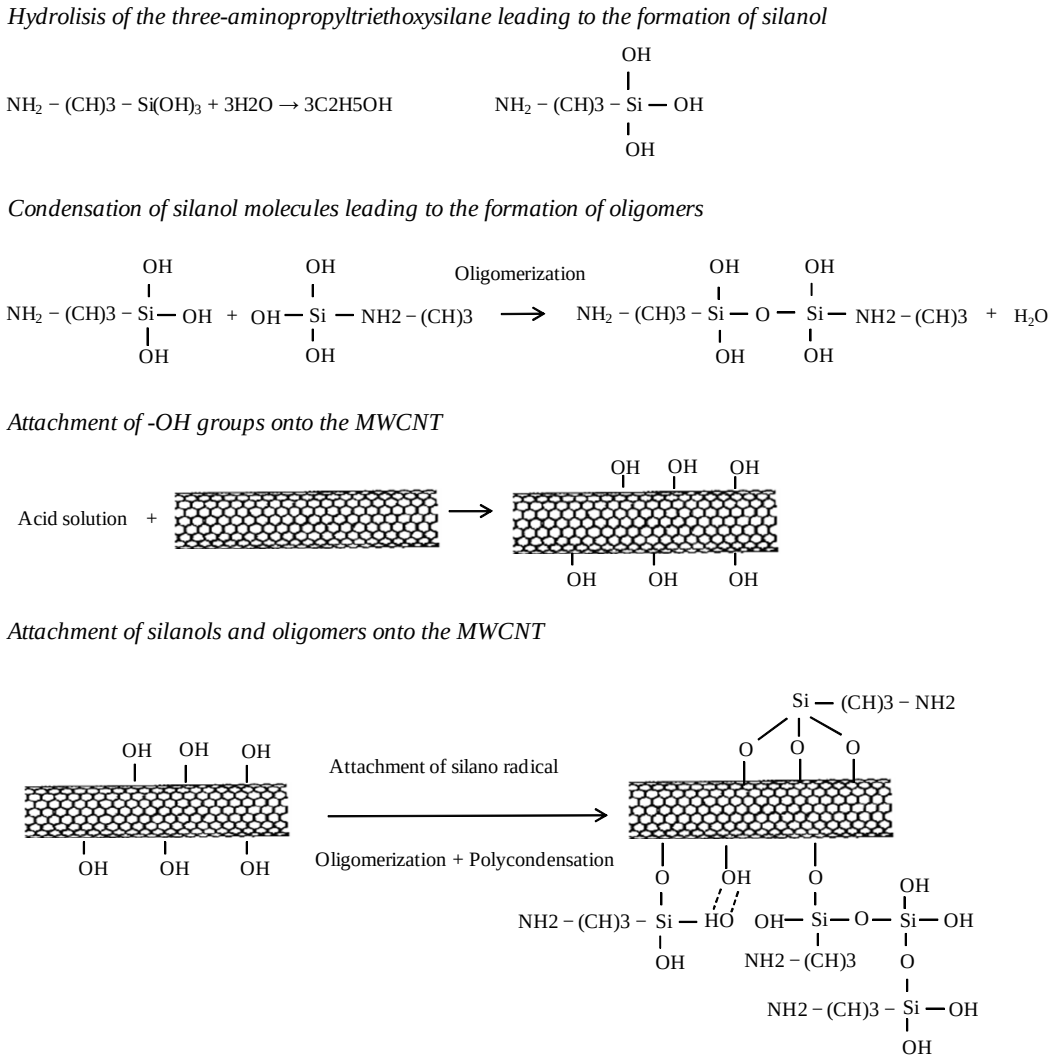


Figure 3.23: Functionalization of a MWCNT

3.3.4 Thermal stability of functionalized MWCNTs

Due to the incorporation of functionlaized MWCNTs into the PP matrix by using the melt-mixing process, concerns regarding the thermal stability of the functional groups (silano groups and oligomers) have to be addressed and the effects of

temperature were therefore investigated. The functionalized MWCNTs were heat-treated at 220ºC for 1 hour (greater than the operating temperature of the rheo-mixer) in an oven and then cooled down to ambient temperature (28ºC) for analysis. Firstly, the suspension stability of the heat-treated MWCNTs was compared to that of raw MWCNTs. The procedure used for this is similar to that specified in point 3.3.2.1 Secondly the RAMAN results of the heat-treated MWCNTs and those of the non-functionalized MWCNTs were compared. Visual examination showed that the two suspensions had similar settlement behaviours. Clear phase separation was only observed after 36 hours (Figure 3.24) confirming that the suspension stability has not been compromised.

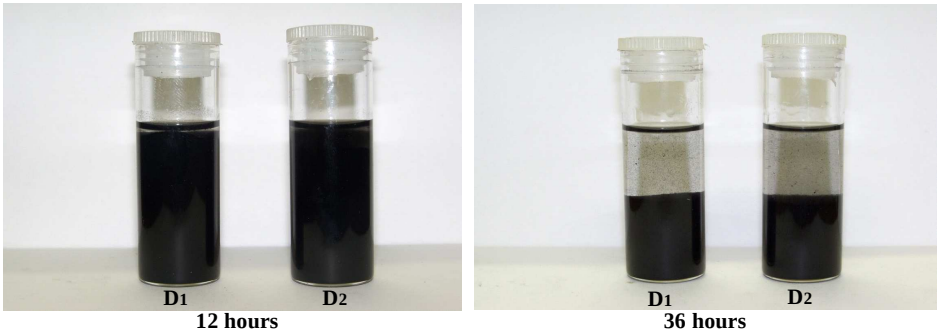


Figure 3.24: Suspension stability (D1: Heat-treated functionalized MWCNTs and D2: Non heat-treated functionalized MWCNTs)

Figure 3.25 show the RAMAN results of heat-treated functionalized MWCNTs and those of non heat-treated functionalized MWCNTs. It can be seen that the spectrums of the heat-treated functionalized MWCNTs are similar to those of non-heat-treated functionalized MWCNTs. These observations suggest that the heat treatment did not alter the grapheme layers and the functional groups attached to the carbon MWCNTs. These findings were expected. The silane (Silquest A-1100) used in this study is generally used for improvement of the thermal stability of filler materials, such as colorants, designed to operate at elevated temperatures in industrial applications.

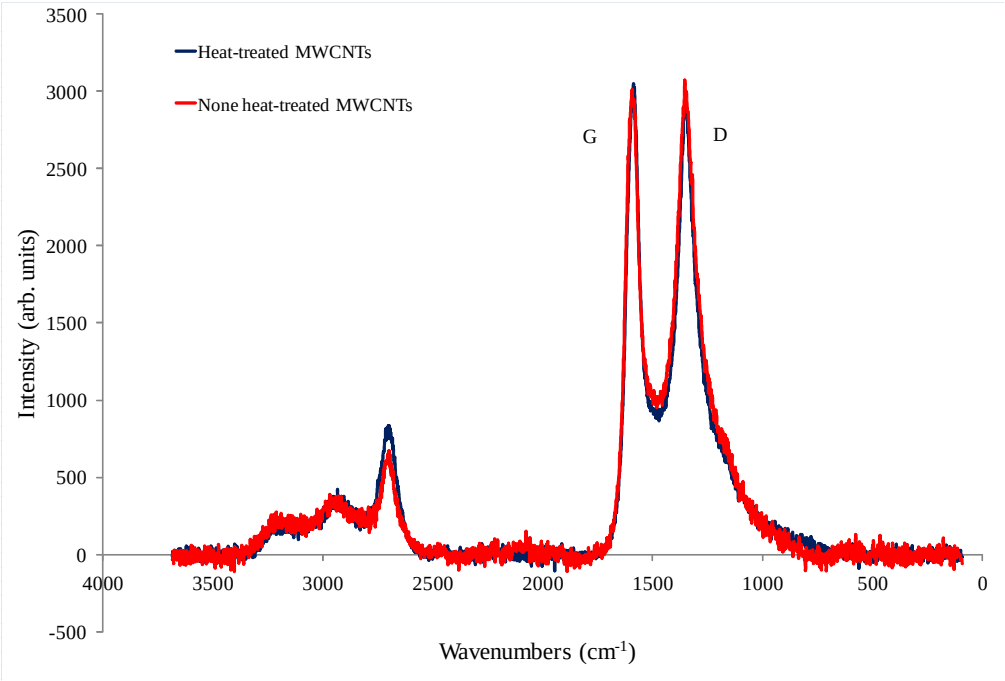


Figure 3.25: RAMAN spectrums of heat-treated functionalized MWCNTs and none heat-treated functionalized MWCNTs

3.4 Fabrication of kenaf and glass fibre reinforced PP composites

The CMFST manufacturing process used for the fabrication of composite plates, as well as the advantages and limitations thereof, is presented. The process comprises five stages namely, initial compaction, fibre impregnation, compression, release of the compaction load and cooling. Detailed view of the mould assembly is shown in Figure 3.26 and the manufacturing arrangement is illustrated in Figure 3.27. The optimum manufacturing parameters are shown in Table 3.10 and illustrated in Figure 3.35. The mould (Figure 3.28) and oven (Figure 3.29) were constructed at the RP/Composites Facility of the University of the Witwatersrand, Johannesburg.

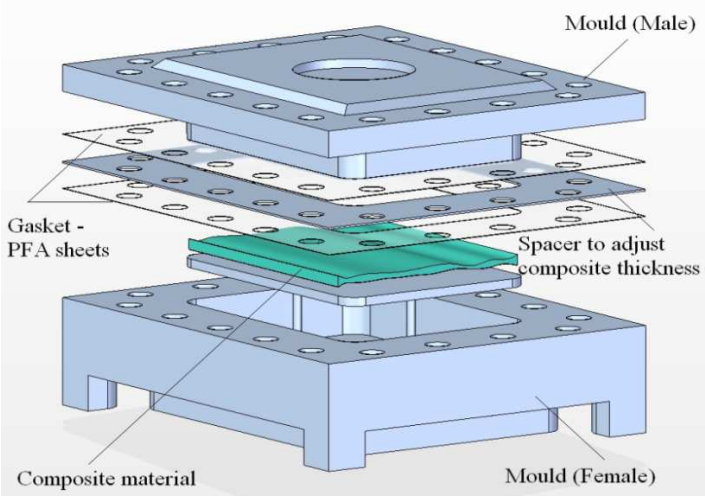


Figure 3.26: Detailed view of the mould assembly

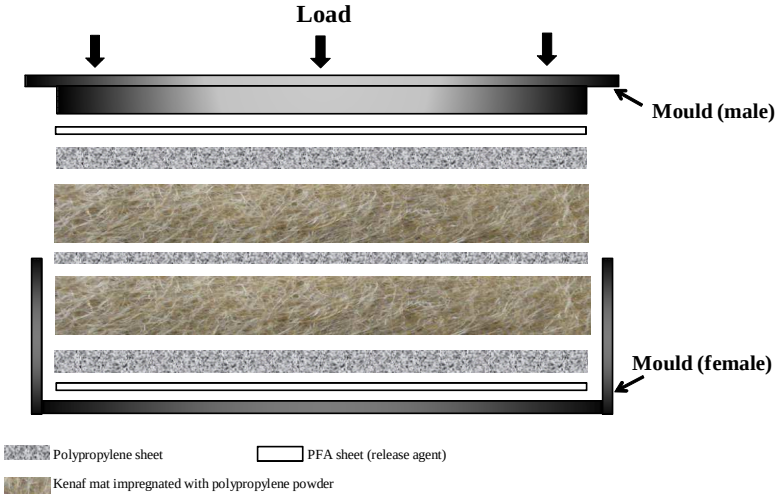


Figure 3.27: Manufacturing arrangement

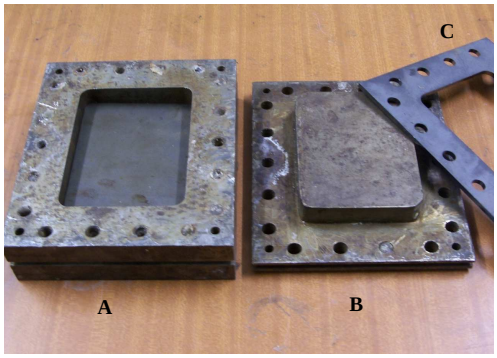


Figure 3.28: Carbon steel mould (A: Female, B: Male, C: Spacer) and laminate arrangement

Seven different configurations of composite plates were manufactured:

- Unreinforced PP
- PP reinforced with untreated kenaf fibre
- PP reinforced with alkali treated kenaf fibre
- PP reinforced with alkali–silane treated kenaf fibre
- PP reinforced with glass fibre
- PP reinforced with MWCNTs
- PP reinforced with alkali-silane treated kenaf fibres and MWCNTs

Fibre contents ranging from 20% to 35% (by mass) in interval of 5% were considered for both kenaf and glass fibre reinforced plates. The CNT concentrations range from 0.1% to 1.25% (by mass). The fabricated composite plates were rectangular (90mm x 150mm). Depending on the fibre content, the laminate thicknesses ranged between 3.5 mm and 4.2 mm. The material formulations of the different material configurations are detailed in Table 3.11, 3.12 and 3.13.

Initial compaction

Kenaf fibre reinforced PP composite plates (kenaf/PP composites) are made by sandwiching layers of unreinforced PP sheets and kenaf mats impregnated with PP powder. Whereas kenaf fibre reinforced MWCNT-PP composite plates (kenaf/PP-MWCNT composites) are fabricated by sandwiching layers of MWCNT-PP sheets and kenaf mats impregnated with small pallets of MWCNT-PP. The average size of the MWCNT pallets range between 0.3 and 1 mm. PerFluoroAlkoxy sheets (PFA) 0.2 mm thick were used as a release agent to prevent the fabricated laminates from sticking to the mould surface and to ensure smooth surface finish of the final product. The use of PFA sheets is justified by the fact that the melting temperature of the PFA (305 °C) is substantially higher than that of polypropylene (164ºC). The weights of the matrix system (e.g. PP sheets and PP powder) and kenaf fibres were determined prior to the fabrication in order to calculate the fibre contents in each fabricated composite plate. From these values the fibre content, M_f, was calculated using the equation below:

$$M_f = \frac{m_{Kenaf\ mat}}{m_{PP\ sheet} + m_{PP\ powder}} * 100 \quad (3.1)$$

Where m_{kenaf} represents the mass of the kenaf mat, $m_{PP\ sheet}$ the PP sheet weight and $m_{PP\ sheet}$ the PP powder weight.

Spacers were used to adjust the thickness of the composite plate. PP powder and MWCNT-PP pellets (Figure 3.1) were used to facilitate improved matrix penetration within the fibre dominated regions of the composites and to reduce the processing time and temperature which could result in thermal degradation of the kenaf fibres and functional groups [82].

After the material charge was packed, the mould was closed and loaded in to the oven at ambient temperature. The compaction load was applied to ensure proper contact between the matrix and the fibres. The oven (Figure 3.29) was allowed to heat up gradually to 220ºC for five minutes; and then the temperature was increased to 250ºC within 5 minutes. This resulted in the composite temperature rising to 105ºC. The compaction load was maintained at 75 bar and the duration of the compaction phase was 15 minutes.



Figure 3.29: Ovens

Fibre impregnation

The temperature of the oven was maintained at 250ºC to keep the viscosity of the molten thermoplastic matrix at an adequate level, thereby allowing sufficient penetration of the matrix into the mat. Afterwards, the compaction load was reduced from 70 bar to 50 bar within 5 minutes to prevent excessive leakage and flashing of the matrix, which could lead to uneven fibre distribution and distortion of the shape of the final product, Figure 3.30. At this stage, the temperature of the mould increased to about 150ºC, whereas that of the composite increased to 110ºC.

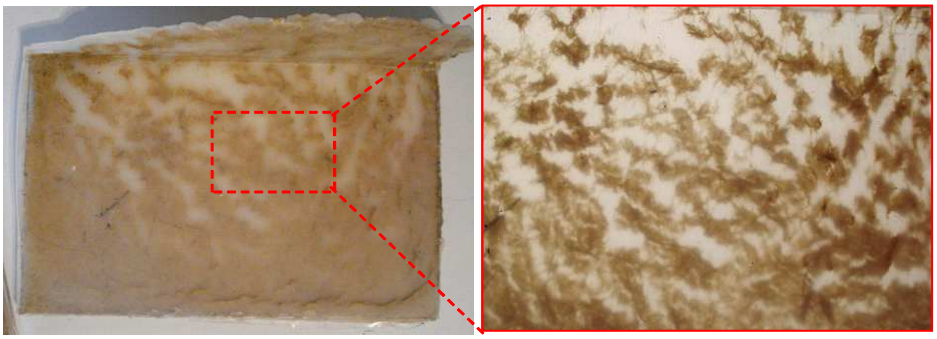
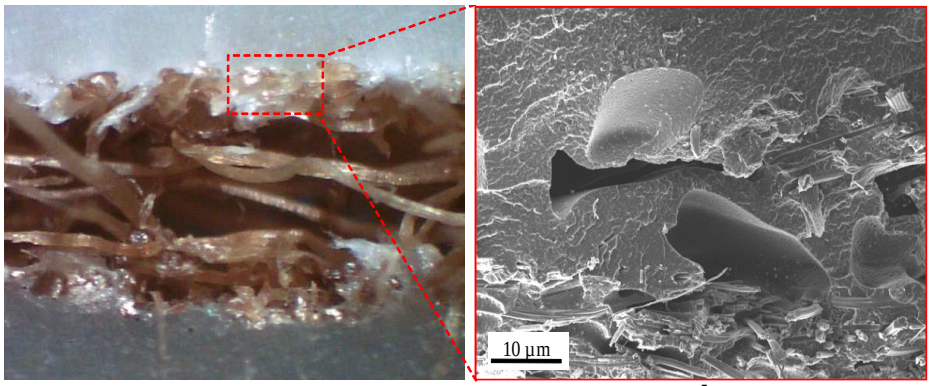


Figure 3.30: Uneven kenaf fibre distribution caused by excessive compaction load during impregnation phase

Compression

During the compression step, the temperature of the mould and composite increased from 150ºC to 180ºC and from 110ºC to 120ºC respectively. The slight increase of the temperature of the composite (from 121.2 to 122.5ºC) for a period of 5 minutes indicated the melting of the matrix. The compaction load was still maintained at 50 bar to cause the matrix to flow through the mat in order to achieve a proper contact between the matrix and fibres. The compaction load was monitored and maintained at 50 bar to prevent poor fibre impregnation especially in composite plates with high fibre content. Manufacturing defects, (e.g. poor fibre impregnation and voids) caused by low compaction load in composite with 30% fibre content can be seen in Figure 3.31.

The measurement of the inside temperature of the specimen at the impregnation step was achieved by embedding a thermocouple into the specimen as shown in Figure 3.32. The temperature measurement of the inside the mould was done during the preliminary tests. The temperature readings showed that the matrix melt at temperature relatively lower (122.5ºC) than the typical melting temperature of the matrix (164ºC). These observations sustain the proposal that the use of polypropylene powder was essential to reduce the processing time and the melting temperature of the fabricated composite below the typical melting temperature of the polypropylene [82].



a **b**

Figure 3.31: Manufacturing defects kenaf/PP composite plate: (a) Poor fibre impregnation, (b) Voids in matrix and fibre dominated regions

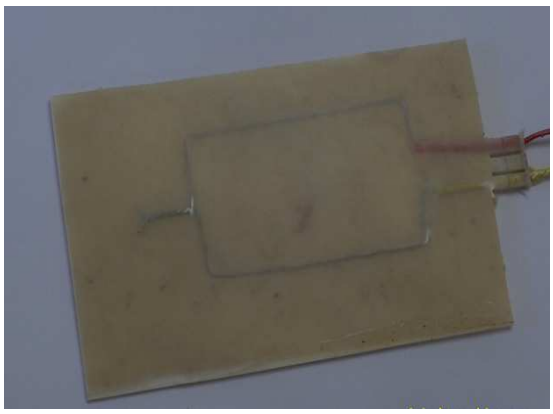
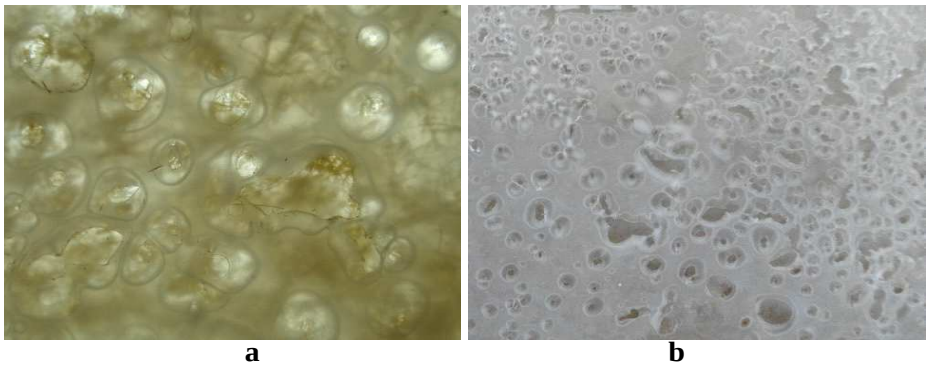


Figure 3.32: Embedded thermocouple in kenaf/PP composite plate

Release of the compaction load

The compaction load was gradually decreased from 50 bar to approximately 5 bar within 5 minutes to prevent the formation of voids and cavities (Figure 3.33) caused by the instantaneous pressure drop inside the mould.



a **b**

Figure 3.33: Voids and cavities: (a) kenaf fibre reinforced PP composite, (b) PP plate

Cooling and release of the fabricated composites

The mould was removed from the oven and exposed to running tap water to allow the temperature to drop to ambient temperature, resulting in a gradual reduction of the fabricated laminate inside the mould. The mould was kept closed in order to prevent the geometric distortion of the composite plate during shrinkage. The fabricated composite plate (Figure 3.24) was then released from the mould once ambient temperatures were reached.



Figure 3.34: Kenaf/PP composite plates

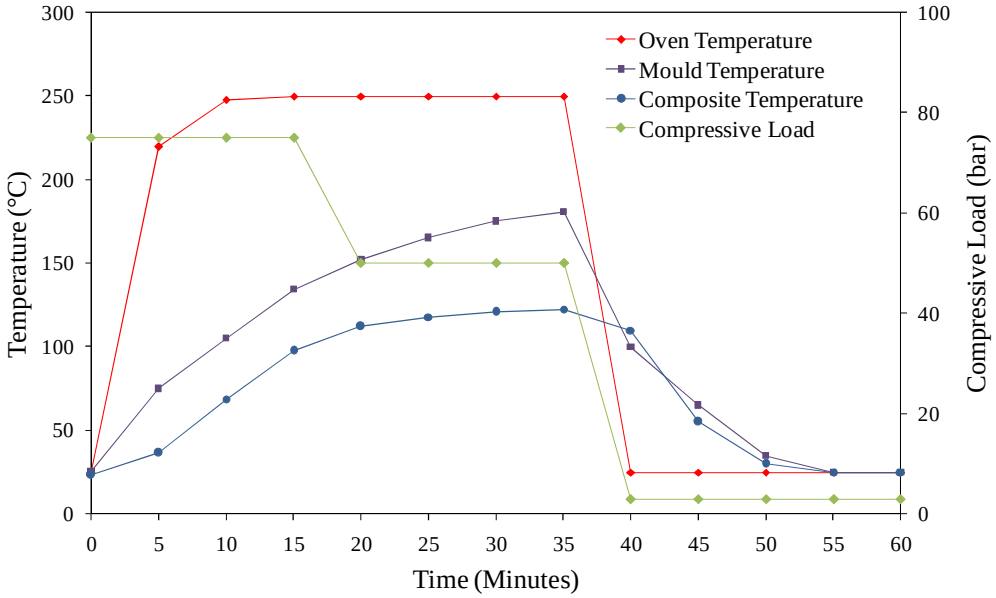


Figure 3.35: Optimum manufacturing parameters

Table 3.10: Optimum manufacturing parameters

Steps	Time (Minute)	Temperature (Deg C)			Load (bar)
		Oven	Mould	Sample	
		Oven	Mould	Sample	
1-Initial compaction	15	25 to 250	25 to 135	25 to 98	75
2-Impregnation of fibres	5	250	135 to 150	98 to 110	75 to 50
3-Compaction of the charge	15	250	150 to 180	110 to 120	50
4-Release of the compaction load	5	250 to 25	180 to 100	120 to 110	50 to 5
5-Cooling	20	……	100 to 25	110 to 25	$\leq$ 3

3.5 Fabrication of polypropylene reinforced MWCNT plates

Homogenous dispersion of the carbon nanotubes within the matrix system is required for effective exploitation of their exceptional mechanical properties in polymeric composites. A homogeneous distribution is generally prevented by the intermolecular interaction (e.g. Van der Waals forces) between the nanotubes, which cause the nanoparticles to form clusters. Mechanical treatment (including melt-mixing, ball milling and mechanical stirring) can be used to achieve the required dispersal [16, 66, 67]. The melt-mixing process (shear mixing process) is the most practical and preferred method of incorporating nanoparticles into thermoplastic materials. The technique is wildly considered as a successful method of achieving sufficient dispersion at high CNT concentration [83, 92]. The shear-mixing consists of mixing the nanoparticles and the matrix thermoplastics at an elevated temperature, generally greater than the melting temperature of the matrix.

In principle the shear-mixer works as follows: the thermoplastic matrix is introduced into a pre-heated shear mixer (Rheo-mixer) set to temperatures above the melting point of the thermoplastic in order to improve the fluidity of the charge [92]. The operating temperature is, for example, generally set to 10°C to 20°C above the melting temperature of the polypropylene (164°C) to allow complete melting while retaining the cristalinity of the material [35, 36]. The shear-mixer comprises a set of double screws which create shear stresses within the molten matrix by causing two adjacent flow lines to travel at different velocities, causing the nanoparticles to disperse within the bulk of the material.

There are two types of shear-mixing processes, namely the master-batch and the direct incorporation method. The two processes differ fundamentally in the material loading sequence [83, 92]. In the master-batch method, commercially available master batches of carbon nanotube reinforced polymer composites are used for the initial loading, which are subsequently mixed with unreinforced polymer during fabrication. One advantage thereof is that the process is practical for use in small to medium production scales. On the other hand the direct incorporation method is more appropriate for research purposes since it is more flexible and allows easy customization of the final product. The direct incorporation consists in progressively mixing the nanoparticles in a powder form with the polymer matrix (e.g. molten polypropylene) at elevated temperatures. Generally this type of mixing method yields reinforced polymers with good dispersion. In an effort to optimize the dispersion process whilst achieving a high CNT concentration, the direct incorporation method was selected. The Rheo-mixer apparatus (Figure 3.36) comprises of three units: the driver (Haake PolyLab OS), the Rheo-mixer (Rheomex) and the extruder (Rheomex). A close-up view of the double screws and extrusion die can be seen in Figure 3.37. The Haake PolyLab OS is an automated Rheo-mixer programmed for various predetermined setups. The fabrication process is summarized in Figure 3.38 and the optimum manufacturing parameters of the shear-mixing process are presented in Table 3.11.

The blending of the PP matrix was achieved as follows:

- The controller is switched on and the shear-mixer is pre-heated to 100°C. The rotation speed of the screws is set to 60 rpm.
- The safety lock is opened and the shear mixer is gradually loaded with the PP pellets and MWCNTs. The total mass of each batch was set to 42 grams as the shear-mixer can only handle 50 grams per batch.
- After the loading, the safety lock of the shear-mixer is closed and the shear-mixer is allowed to operate for 30 minutes.
- The Rheo-mixer is stopped and the MWCNT-PP is removed.

The operating variables (temperature and torque) for six different specimens were recorded in situ and shown in Figure 3.39. It can be seen that an average operating temperature of 180°C was maintained during the process and the torques developed are similar and constant for all the specimens. The high torque values during the initial stages of fabrication indicate that the PP matrix is in a solid state, as the temperature of the shear-mixer is still below the melting temperature (164°C) of polypropylene. As the temperature increases, the applied torque decreases indicating that the matrix is melting. This graph shows that all the specimens were fabricated at the same process conditions.

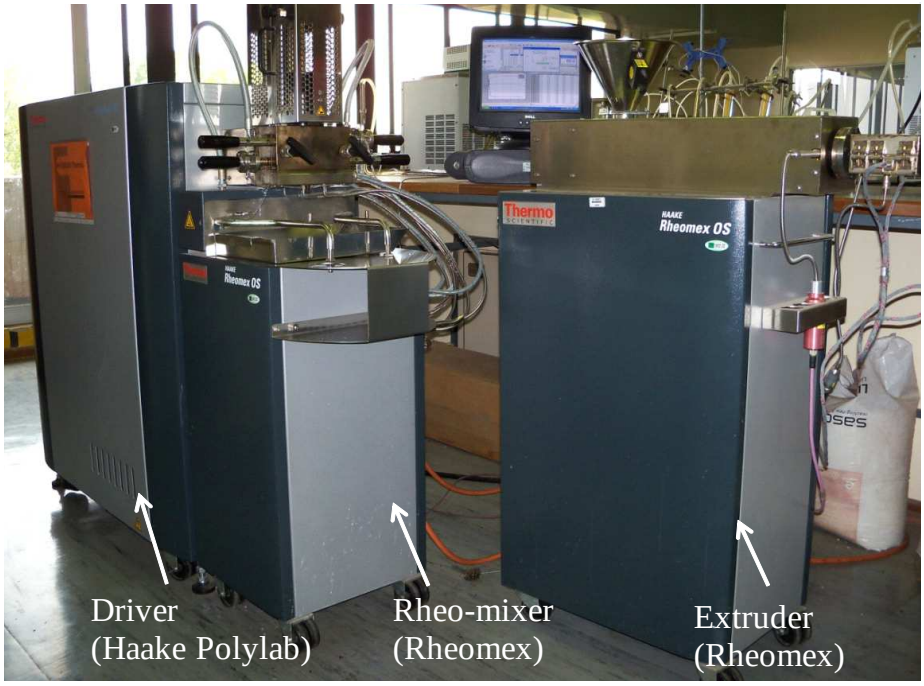


Figure 3.36: Haake PolyLab OS rheo-mixer

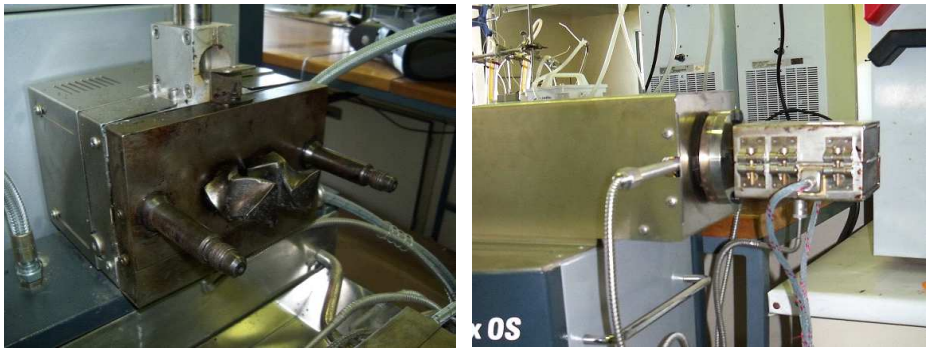


Figure 3.37: Double screws and extrusion die

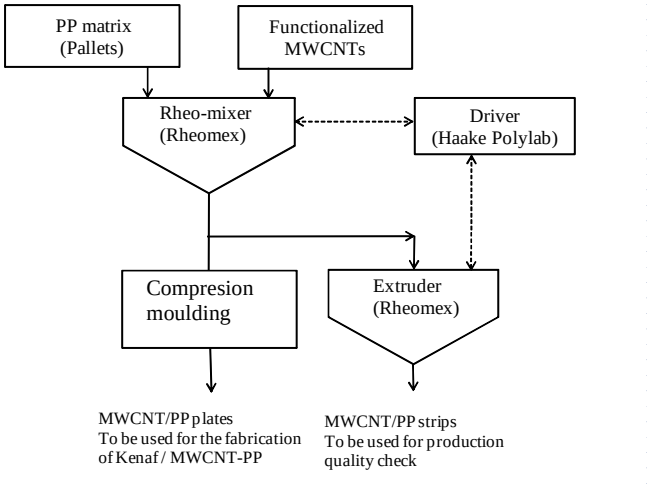


Figure 3.38: Flow process

Table 3.11: Optimum conditions of the shear-mixing process

Process	Time (Minute)	Temperature (ºC)	Shear loading (MPa)	Speed (rotation/min)
Conditioning	10	45	------	------
Rheo-mixing	30	180	35 - 37	60

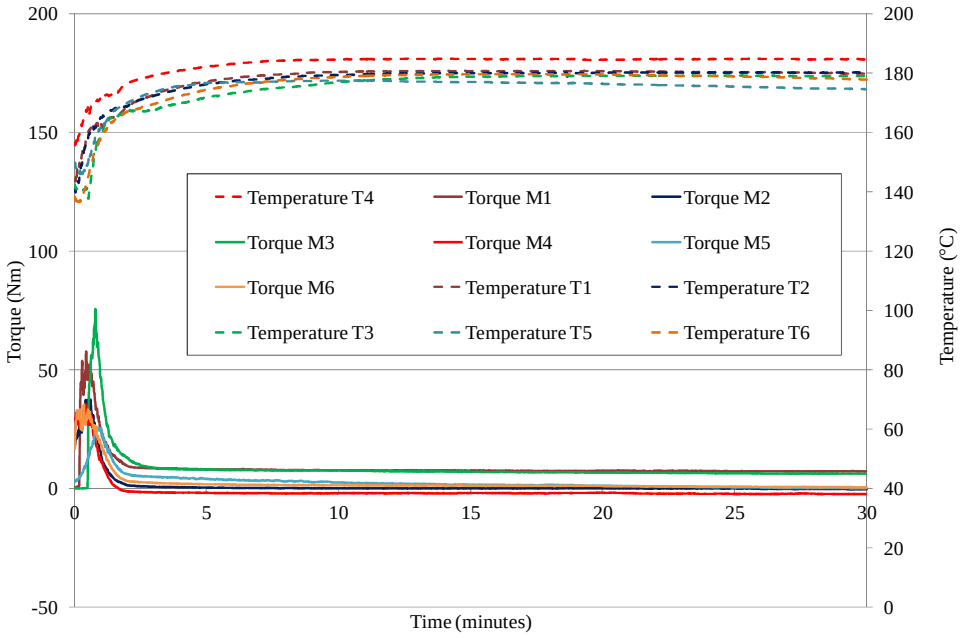
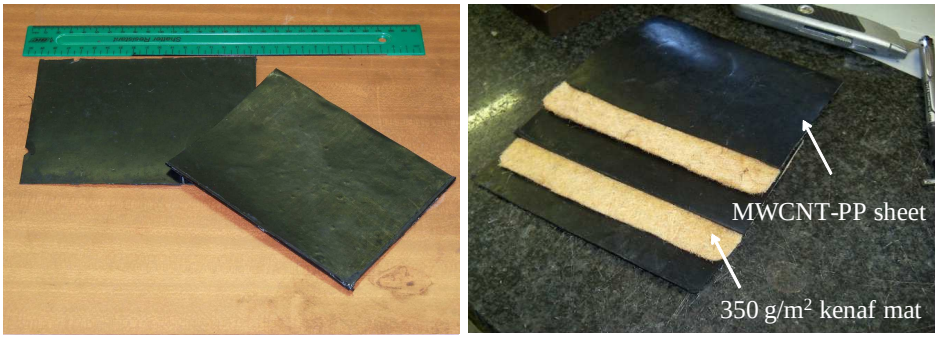


Figure 3.39: Recorded operating conditions of rheo-mixer

The MWCNT-PP retrieved from the shear-mixer was then used to fabricate the MWCNT-PP plates using the compression moulding process at the RP/Composites Facility of the University of the Witwatersrand, Johannesburg. The fabricated MWCNT-PP plates, Figure 3.40 (a), were used to fabricate the kenaf/PP-MWCNT composite plates based on procedure described in section 3.4. The packing arrangement is illustrated in Figure 3.40 (b).



a **b**

Figure 3.40: (a) MWCNT-PP plates with 0.75% CNT, (b) packing arrangement

The concentration of the MWCNTs in each specimen was determined by measuring the mass of the MWCNTs and unreinforced PP separately before fabrication. From these values the CNT concentration, M_{MWCNT}, was calculated using the equation below:

$$M_{MWCNT} = \frac{m_{MWCNT}}{m_{PP}} * 100 \qquad (3.2)$$

Where, m_{MWCNT}, denotes the mass the CNT and m_{PP} the mass of polypropylene.

As mentioned in section 3.1 the range of the CNT concentration (0.1% to 1.25%) used in this study was based on preliminary mechanical tests conducted to optimize the fabrication process. In order to optimize the quality of the product, it was imperative to ensure a homogeneous dispersion of the MWCNTs within the PP matrix and achieve a high CNT concentration. Previous researchers reported that the main disadvantage of the shear mixing process is that the shear forces developed during fabrication tend to sever the carbon nanotubes, thereby reducing the aspect ratio [68, 83, 92]. More importantly, the processing time also tends to

increase significantly as the nanoparticle concentration increases, thereby increasing the exposure time of the nanoparticles to excessive heat. In addition, exposure of thermoplastics to high temperature tends also to alter the cristalinity of the bulk of the material [36, 35] and therefore in this study, the processing time had to be minimized. The optimum manufacturing parameters of the compression moulding process used to fabricate the MWCNT-PP plates are shown in Table 3.12 and illustrated in Figure 3.41.

Table 3.12: Optimum manufacturing parameters of MWCNT-PP plates

Steps	Time (Minute)	Temperature (Deg C)		Load (bar)
		Oven	Mould	
1-Initial compaction	15	25 to 250	25 to 135	50
2-Compaction of the charge	20	250	135 to 160	50
3-Release of the compaction load	5	250 to 25	160 to 105	50 to 5
4-Cooling	20	……	100 to 25	≤ 3

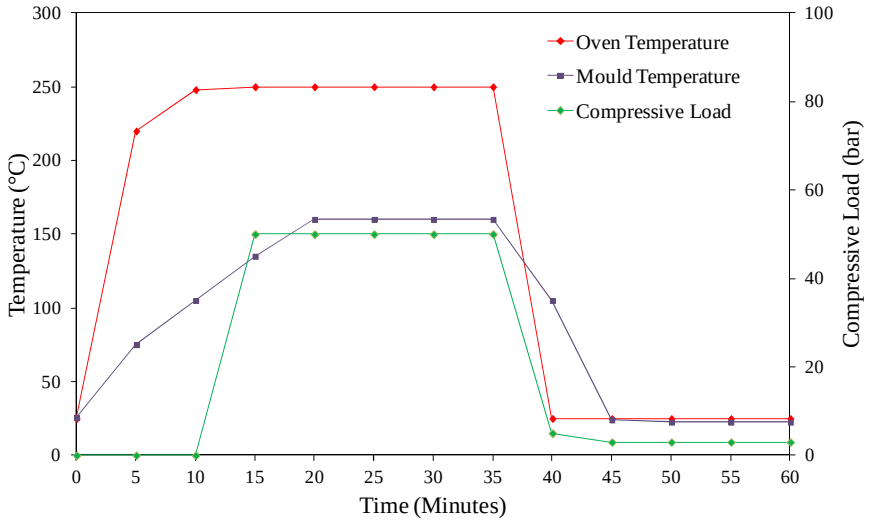


Figure 3.41: Optimum manufacturing parameters of the MWCNT-PP plate

3.6 Material formulation

The nomenclatures identifying each composite plate are shown in Table 3.13, 3.14 and 3.15. Two sets of characters are used for material identification of treated kenaf/PP composites (Table 3.13 and 3.14). The first characters specify the concentration of the alkali solution used for fibre treatment and the type of chemical treatment. (e.g. 5A indicates a 5% NaOH and 1AS indicates a 1% NaOH alkali-silane treatment). The second set indicates the type of fibre and the fibre content of the composites (e.g. KF/20PP indicates kenaf fibre at 20% fibre content whereas GF/30PP specifies glass fibre and 30% fibre content). For untreated kenaf/PP composites, the first set UT specifies the untreated condition, with the second similar to that of treated kenaf/PP composites. For kenaf reinforced MWCNT-PP (Table 3.15), three sets of characters are used. The first set indicates the concentration of the alkali solution and the type of treatment (e.g. 6AS), the second set indicates the type of fibre and the fibre content. The third set indicates the CNT concentration (e.g. 0.25MWCNT means 0.25% carbon nanotube).

Table 3.13: Material formulation of alkali treated kenaf reinforced PP

	Material formulation			
	20% fibre content	25% fibre content	30% fibre content	35% fibre content
1% NaOH treated kenaf	1A-KF/20PP	1A-KF/25PP	1A-KF/30PP	1A-KF/35PP
2% NaOH treated kenaf	2A-KF/20PP	2A-KF/25PP	2A-KF/30PP	2A-KF/35PP
3% NaOH treated kenaf	3A-KF/20PP	3A-KF/25PP	3A-KF/30PP	3A-KF/35PP
4% NaOH treated kenaf	4A-KF/20PP	4A-KF/25PP	4A-KF/30PP	4A-KF/35PP
5% NaOH treated kenaf	5A-KF/20PP	5A-KF/25PP	5A-KF/30PP	5A-KF/35PP
6% NaOH treated kenaf	6A-KF/20PP	6A-KF/25PP	6A-KF/30PP	6A-KF/35PP
7% NaOH treated kenaf	7A-KF/20PP	7A-KF/25PP	7A-KF/30PP	7A-KF/35PP
8% NaOH treated kenaf	8A-KF/20PP	8A-KF/25PP	8A-KF/30PP	8A-KF/35PP
Untreated kenaf	UT-KF/20PP	UT-KF/25PP	UT-KF/30PP	UT-KF/35PP
Glass fibre/PP	GF/20PP	GF/25PP	GF/30PP	GF/35PP

Table 3.14: Material formulation of alkali-silane treated kenaf reinforced PP

	Material formulation			
	20% fibre content	25% fibre content	30% fibre content	35% fibre content
1% NaOH-silane treated kenaf	1AS-KF/20PP	1AS-KF/25PP	1AS-KF/30PP	1AS-KF/35PP
2% NaOH-silane treated kenaf	2AS-KF/20PP	2AS-KF/25PP	2AS-KF/30PP	2AS-KF/35PP
3% NaOH-silane treated kenaf	3AS-KF/20PP	3T-KF/25PP	3AS-KF/30PP	3AS-KF/35PP
4% NaOH-silane treated kenaf	4AS-KF/20PP	4AS-KF/25PP	4AS-KF/30PP	4AS-KF/35PP
5% NaOH-silane treated kenaf	5AS-KF/20PP	5AS-KF/25PP	5AS-KF/30PP	5AS-KF/35PP
6% NaOH-silane treated kenaf	6AS-KF/20PP	6AS-KF/25PP	6AS-KF/30PP	6AS-KF/35PP
7% NaOH-silane treated kenaf	7AS-KF/20PP	7AS-KF/25PP	7AS-KF/30PP	7AS-KF/35PP
8% NaOH-silane treated kenaf	8AS-KF/20PP	8AS-KF/25PP	8AS-KF/30PP	8AS-KF/35PP

Table 3.15: Material formulation of kenaf reinforced MWCNT-PP

	Material formulation				
	0.25%CNT	0.5%CNT	0.75%CNT	1.0%CNT	1.25%CNT
6% NaOH-silane treated kenaf	6AS-KF/30PP-025MWCNT	6AS-KF/30PP-0.5MWCNT	6AS-KF/30PP-0.75CMWNT	6AS-KF/30PP-1.0MWCNT	6AS-KF/30PP-1.25MWCNT

4 EXPERIMENTAL EVALUATION OF THE MECHANICAL AND MOISTURE PROPERTIES

The following chapter discusses the test parameters and setup used to investigate the mechanical and moisture absorption properties of the composites and is divided into three sections. Section 4.1 describes the mechanical tests (tensile tests, flexural test, stress-controlled tension-tension fatigue test and Izod notched impact test) as well as the technical considerations influencing the implementation thereof. Section 4.2 focuses on the moisture absorption tests whilst Section 4.3 describes the types of microscopic examinations (e.g. scanning electron microscopy and optical microscopy) conducted in this study.

4.1 Mechanical testing

4.1.1 Tensile tests

The tensile tests were conducted to determine the tensile properties of the composites, the tensile strength and tensile modulus in particular. The test protocols of both tests were developed in accordance with the requirements of ISO 527 [75] and ASTM D3039/ D3039 M standards [76]. These standards were used because they address the necessity for determining the residual strength of the specimens during the fatigue test. A Lloyd MX 100 universal testing machine, equipped with a 5kN load cell was used for testing purposes; the test set can be seen in Figure 4.1. Mandatory specimen dimensions (thickness, width and length) are specified by ASTM D3039/ D3039 M.



Figure 4.1: Tensile test set up

4.1.2 Flexural test

The flexural strength of the composite was determined in accordance with the requirements of ISO 178 and ASTM D790 [77, 78]. The Lloyd MX100 instrument equipped with a 5KN load cell was once again utilized. The requirements for the sizes of the specimens, including the thickness, width and length are also described in ISO 178 standard. The flexural test set up on the Lloyd MX100 machine can be seen below in Figure 4.2.



Figure 4.2: Flexural test set up on Lloyd MX100

4.1.3 Fatigue test

The stress-controlled tension-tension fatigue test was designed in accordance with the requirements of BS ISO 13003 and ASTM D 3479/D 3479M-09 [84–87]. These two standards were selected since they specify the requirements that allow easy characterization of the fatigue damage in polymer reinforced composites (e.g. initiation and development of microcracks, delamination and fibre fractures).

In contrast to isotropic materials, fibre reinforced thermoplastic composites exhibit complex failure mechanisms under fatigue loadings. In general, the material damage is characterised by gradual loss of stiffness, resulting in increased strain before the onset of any visible damage. Depending on the stress level and material configuration (e.g. fibre direction, fibre contents), damage may grow in size in a progressive manner until failure ultimately occurs. Visible damage may occur in the form of cracks, matrix yielding, delamination, debonding along the fibre-matrix interfaces and fibre breakage. Trial tests were therefore conducted to evaluate systematically the effects of the test control parameters (e.g. stress ratio, load frequency and stress level) on the fatigue behaviours of the specimens and the reliability of the results facilitating a satisfactory level of confidence of the results. Focus was placed on the characterization of the material failure modes (e.g. cracks, delamination and fibre fractures occurring during the testing) and hysteretic heating because they are important factors playing a vital role in the comprehension of the fatigue behaviours and performances of the material [43]. Based on the preliminary test results, the stress-controlled tension-tension fatigue test was conducted at 1 Hz with a stress ratio of 0.1 (R = 0.1), resulting in minimal hysteretic heating, and local instability (buckling). The fatigue characteristics were investigated at three stress levels: 30%, 45% and 60% of the initial ultimate tensile strength (UTS) of the specimen. Because of inconsistency in the failure modes of most of test specimens, visual characterization of failure was ineffective; failure was subsequently defined as 10% of the initial stiffness. At this cut-off value, the residual stiffness could experimentally still be determined, within an acceptable level of confidence by subjecting the specimen to a quasi-static tensile test at

selected intervals. Residual tensile modulus was therefore determined in accordance with the requirements of ASTM D3039/ D3039 M standards [76], because of the implementation of the fatigue test in accordance with BS ISO 13003 and ASTM D 3479/D 3479M-09 [84, 85]. The INSTRON 8872 servo-hydraulic fatigue testing machine, equipped with a 10kN load cell, was used. The requirements for the sizes of the specimens (e.g. geometry, dimensions, preparation, and tabbing) are in accordance with ASTM D3479/D 3479M-09.

The quantity of specimens to be tested at each stress level generally depends on the intent of the test and on the confidence level of the expected results [85]. Seven specimens were therefore, in view of material availability, made from each particular type of composite of which the results of only five samples were presented because of scattering. The schematic diagram of the computer-controlled closed-loop fatigue testing machine is shown in Figure 4.3.

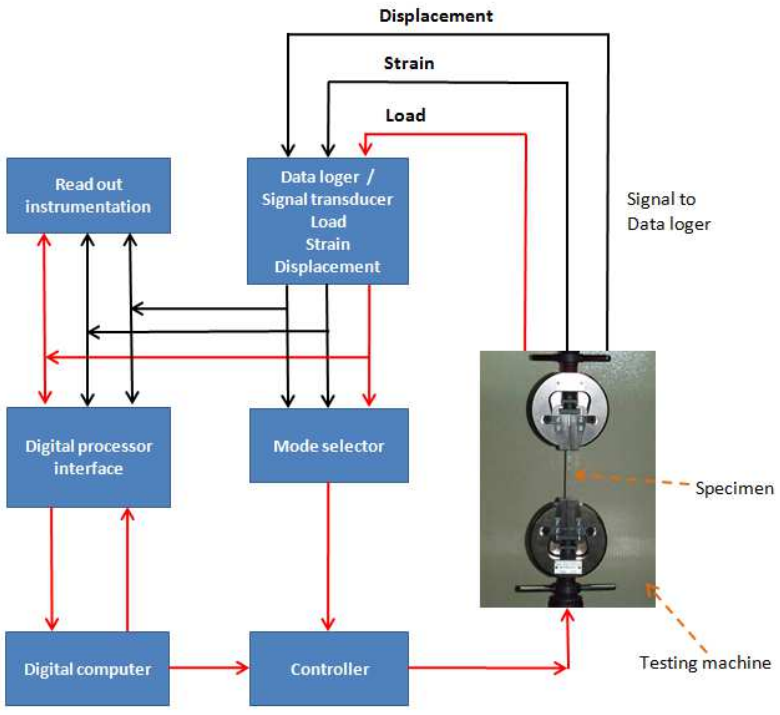


Figure 4.3: Schematic diagram of the computer-controlled closed-loop fatigue testing

4.1.3.1 Test control parameters

Preliminary fatigue tests that were conducted to determine the optimum test control parameters, including the stress ratio, load frequency and stress level are described and discussed below:

Stress ratio

Trial fatigue tests were conducted at different stress ratio, (R = 0.1, 0.5 and 1) in order to determine a suitable value of R. For the purposes of these preliminary tests, a frequency of 1Hz was considered. A stress ratio is defined as the ratio between the minimum and the maximum stress applied during fatigue loading; and can be expressed as follow [93]:

$$R = \frac{\sigma_{min}}{\sigma_{max}} \tag{4.1}$$

Where, R represents the stress ratio, σ_{min} the minimum stress and σ_{max} the maximum stress.

Test results indicated that for a stress ratio greater than 0.1 (e.g. R = 1), the specimens exhibited incoherent fatigue behaviours and complex failure modes that could not be interpreted in a consistent manner; and for which the main causes could not clearly be determined. Premature failure, possibly caused by local instability (buckling) was observed. Most of the specimens (about 56% of tested samples) exhibited signs of delamination in the laminate code at low stress levels (e.g. less than 60% of the UTS). Delamination along the mid-plane was followed by splitting in both kenaf/PP and glass/PP laminates with 35% fibre contents. This is mainly attributed to improper matrix penetration of the laminate core. Figure 4.4 shows the delamination of fibre dominated region of a 5A-KF/25PP specimen subjected to tension-tension at R = 1.

As the stress was increased to 75% of the UTS, matrix cracking, caused by tensile stresses, was the prevalent failure mode in the resin dominated regions of the composites (Figure 4.5). It was found that the development and propagation of

cracks was more substantial at the final stage of the fatigue life of the laminates. Microscopic examination, seen in Figure 4.6, also revealed matrix yielding within the crack. In most cases, the failures of untreated and treated kenaf/PP composites, with 35% fibre content, were characterised by axial splitting prior to ultimate failure. Delamination caused by local instability, is shown in Figure 4.7. These observations suggest that reversing stress cycles could be the main contributing factor to premature failure.

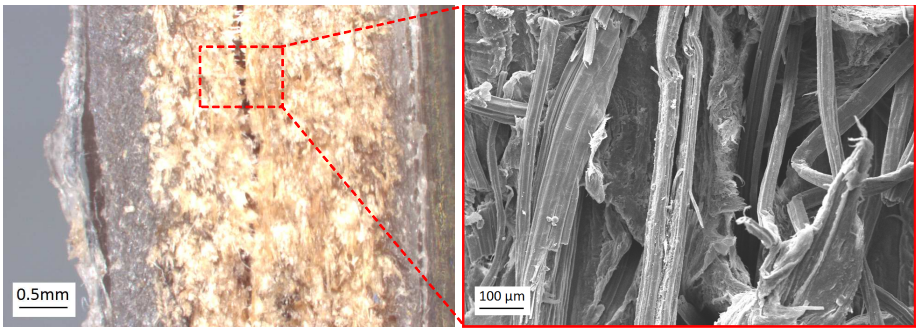


Figure 4.4: Mid-plane delamination in fibre-dominated region of a 5A-KF/25PP composite

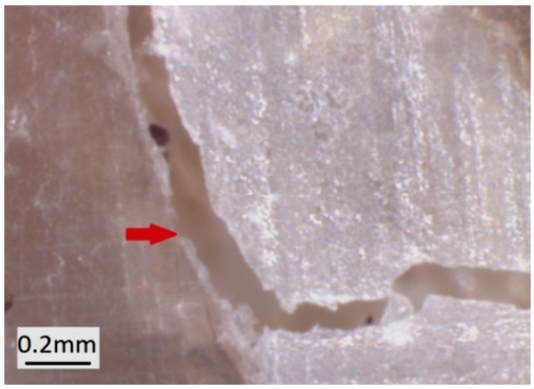


Figure 4.5: Crack in matrix dominated region of 6AS-KF/25PP composite at 410321 cycles

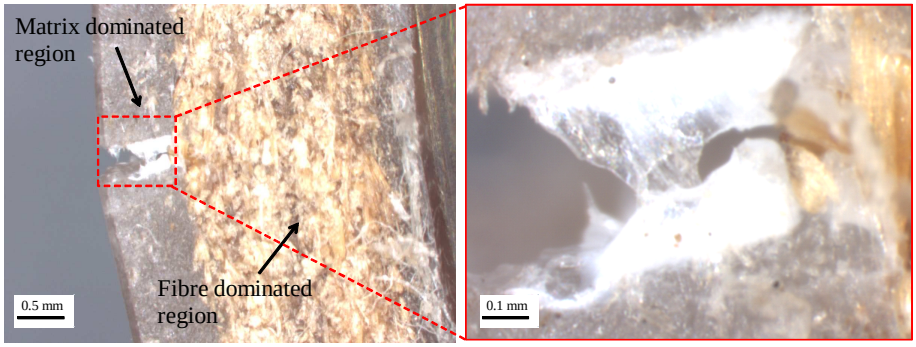


Figure 4.6: Crack and matrix yield in matrix dominated region in 6AS-KF/25PP composite

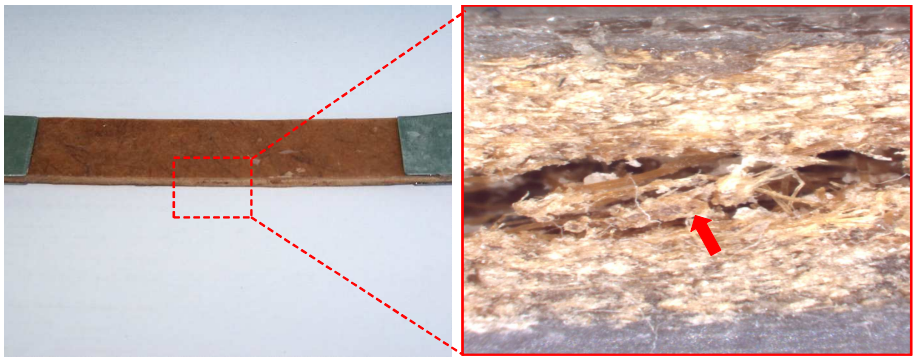


Figure 4.7: Splitting of UT-KF/35PP composite caused by local instability

The failure of unreinforced specimens was characterized by random cracks developing perpendicular to the loading direction. The majority of micro-cracks were located mid-span in the test samples. Microscopic examination showed that the micro-cracks develop into macro scale cracks, spreading into the bulk of the material over time, ultimately leading to material failure. At lower stress levels (e.g. 30% of the UTS), yielding of the polypropylene was observed. Besides the ambiguity of the fatigue behaviour, preliminary test results at R = 1, showed considerable inconsistencies (e.g. number of cycles to failure for a specific stress level) which did not allow the prediction of statistical life in a manner consistent with Procedure A of ASTM D 3479/D 3479M-09. Tow and Ansel [46] reported similar complexity in the fatigue behaviour of sisal reinforced thermoset composites. They suggested that 0.1 was the appropriate stress ratio guaranteeing

non-reversing stress cycles, thereby preventing buckling. Based on these findings, 0.1 was selected as the suitable stress ratio in this study.

Load frequency

The low thermal conductivity and poor heat dissipation characteristics of fibre reinforced thermoplastic materials generally result in these materials retaining a considerable amount of heat. Previous studies [36] investigated the fatigue behaviour of fibre reinforced polymer composites and showed that the thermal characteristics are responsible of premature fatigue failure due to heat retention when loaded at higher frequencies. On the other hand, low frequencies also affect the accuracy of the test results negatively, since they cause internal abrasion and promote degradation of the surrounding material. Mallick [10] reported that the build-up of heat in polymers, which largely depends on the loading frequency, contributed to poor fatigue properties. This clearly suggests that the frequency of the cycling load is a crucial variable for prevention of excessive temperatures. Thus, trial fatigue tests were conducted to determine this crucial frequency that will minimize heating of the specimens and prevent abrasion during testing. The load frequency that was considered ranged between 1-9Hz, increasing in intervals of 3Hz. The stress ratio was 0.1.

The decrease in tensile modulus and the increase of specimen temperature was used indicatively to evaluate the effect of the frequency on the fatigue behaviour of the material. In order to ensure consistent interpretation of the results, the specimens were subjected to 210 000 cycles. Figure 4.8 shows the drop of the tensile modulus in terms of the load frequency at 30% of the material UTS. For simplicity of the illustration, the test results of composites with 30% fibre content are considered. It can be seen that the reduction in the tensile modulus of kenaf/PP and glass /PP composites as the frequency increases from 1Hz to 3Hz, is insignificant (about 10%). Substantial reduction (30%) occurs as the frequency increases to 6Hz. It can be seen that the reduction in the tensile strength of kenaf/PP composites is more prominent than those of glass /PP. For example, the initial tensile modulus of 6AS-KF/30PP composite drops by 32%, whereas that of

GF/30PP composite drops by 38%. As the frequency approaches 9Hz, the decrease in the tensile modulus of all the test specimens is more than 60%. The specimen temperature increase in terms of the load frequency is illustrated in Figure 4.9. It can be seen that the temperatures of all the test specimens increase slightly from 1Hz to 3Hz. As the frequency rises above 3Hz, the temperature noticeably increases. Creed [94] suggested that reducing the specimen size to allow rapid heat dissipation during fatigue testing of glass fibre reinforced was an appropriate way of minimizing the effect of hysteretic heating that caused an increase in temperature at high frequency fatigue load (100 Hz) beyond 10^8 cycles.

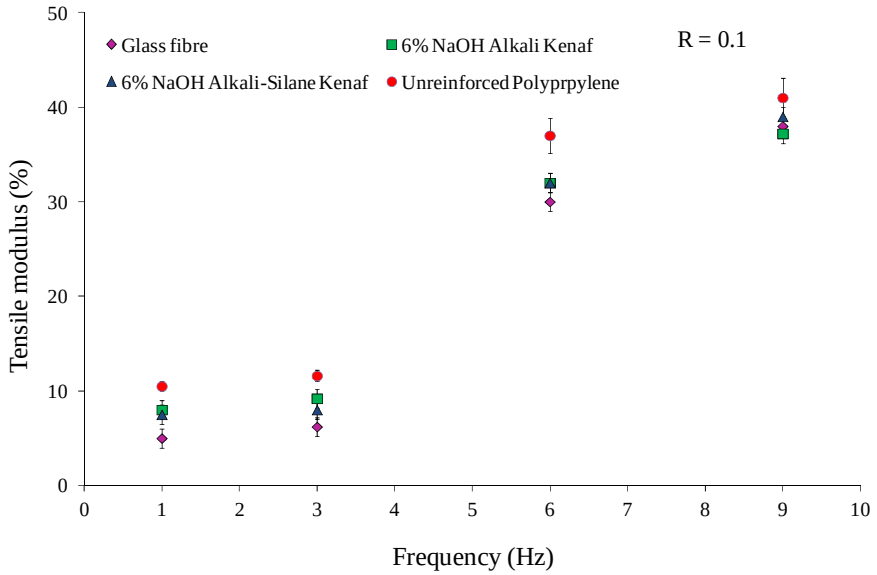


Figure 4.8: Tensile modulus in terms of the load frequency at 30%UTS

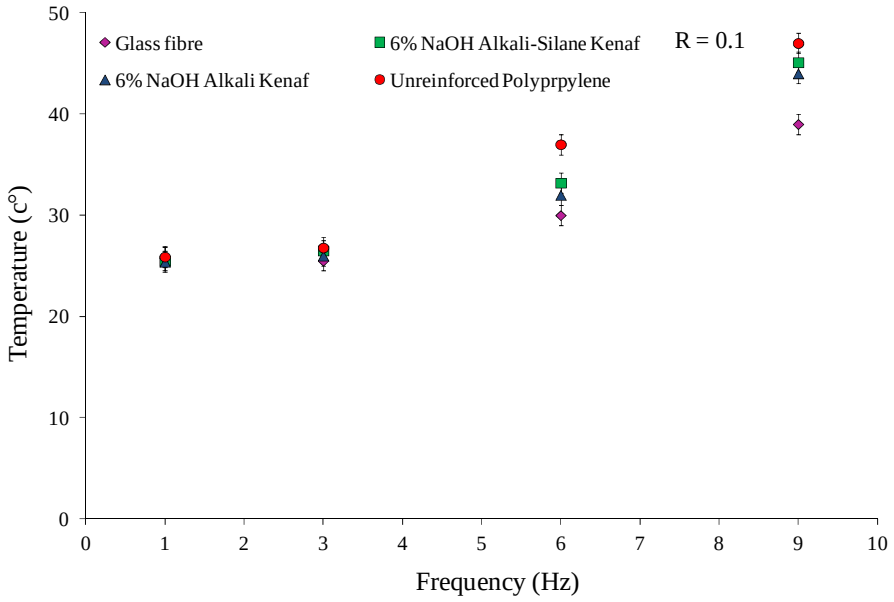


Figure 4.9: Temperature increase in terms of the load frequency

Figure 4.10 shows a close-up view of yielding in the matrix dominated region of a 2AS-KF/20PP specimen. It was found that poor fibre-matrix adhesion, probably caused by resin softening, was the main cause of excessive fibre pull-outs. Microscopic examinations showed that failures of kenaf/PP and glass /PP composites were mainly characterized by excessive yielding in matrix dominated region and by fibre pull-out in the fibre dominated region. In Figure 4.11, a SEM image of an unreinforced PP specimen that was subjected to high frequency (6 Hz), high stress level (90% of the UTS of PP) of the fatigue loading reveals an unusual surface configuration (ridges) after 430 451 cycles. These patterns imply material softening prior to creep failure. Short splinters on the fracture surface are a clear indication of a high load frequency, which restricts the stretching of material prior to failure. These findings clearly indicate that lower load frequencies (ranging between 1Hz and 3Hz) would prevent a considerable increase in the material temperature. Consequently, 1Hz was selected as the load frequency for this study.

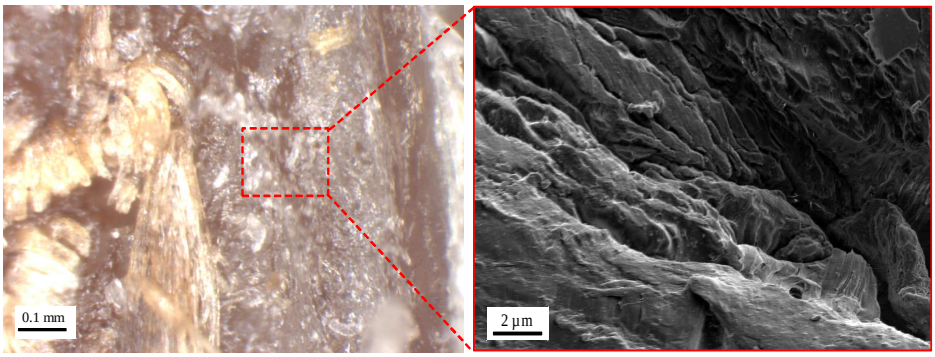


Figure 4.10: Matrix yielding in matrix dominated region of a 2AS-KF/20PP specimen

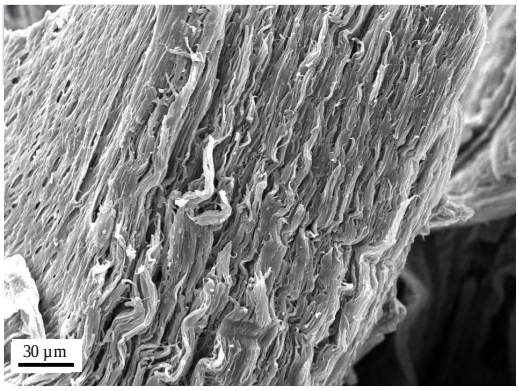


Figure 4.11: Unreinforced PP specimen at 6Hz and 95% UTS

The ASTM D 3479/D 3479M-09 standard requires the temperature recording device to be attached to the specimen in such a way that the dynamic response of the specimen is not affected. The use of a digital thermometer with thermocouple glued onto the test specimen is the preferred technique to monitor the temperature since the thermocouple is in direct contact with the test sample [85]. However, trial tests showed that attaching a thermocouple using glue leads to inconsistent results. Therefore, an infrared thermometer was used to monitor the surface temperature of the test samples. The impact of the loading rate (ratio of the maximum load and the required time to reach the maximum load) on the fatigue behaviour of the specimens was minimized by ensuring that the loading rate is kept constant.

Stress level

It well known that the fatigue behaviour of polymers is highly affected by the stress level of the applied load [36]. Depending on the molecular weight and structure of the material, an increase or a decrease in the crack propagation rate can be expected. The increase of the propagation rate in terms of the mean stress in polymers (e.g. e.g. epoxy resin, high density polyethylene copolymers and PVC) is in the literature [36]. It also has been reported that polymers prone to this increase are mostly affected by monotonic fracture associated with the maxima of the fatigue cycle as it approaches a critical stress intensity level. Polymers, such as low density polyethylene, exhibit improved crack propagation resistance as the mean stress increases. Research carried out by Hertzberg and Manson and reported in *ASM International* [36] suggests that the effects of mean stress on the resistance of polymers to fatigue crack propagation directly depend on the hysteresis ratio. The researchers concluded that polymers that have molecular structures, which are susceptible to hysteretic losses or able to be reorganized structurally, will likely exhibit greater resistance to fatigue crack propagation as the mean stress increases.

Thus, the effects of the number of cycles to failure (N) on the stress level of unreinforced PP material, glass/PP and kenaf/PP composites have been investigated. In order to represent the results simplistically, only specimens with 30% fibre content are illustrated in Figure 4.12. Test results revealed that the stress level dictates the failure mode of the specimens and significantly affects the accuracy and the confidence level of the test results. Figure 4.12 shows that between 15% and 30% of the UTS, the change in the fatigue life is insignificant. For example, a reduction of less than 10% can be observed for 6AS-KF/30PP and 6A-KF/30PP composites. However, in some cases, the fatigue life of the composite increased within the mentioned range. Clear evidence of defects could not be observed below 10^5 cycles; therefore, microscopic examination was used to monitor the damage. SEM revealed noticeable inconsistencies in the failure mode at stress levels below 15% of the UTS. For example, failures characterised by abrasion were prevalent, mostly in specimens with fibre content greater than 20%.

A combination of tearing, plastic flow, necking and shear (Figure 4.13) could also be noticed. Between 30% and 60% of the UTS, reasonable consistency in the accuracy of the test results was noticed. Clear defects and distinct failure modes were noticed during the early stages of the fatigue life (1000 cycles), although plastic flow and necking were visible in some cases. As the stress increased to above 75% of the UTS, the reduction in becomes obvious. For example, a reduction of more than 50% can be observed for most of the specimens. Based on these findings, three different stress levels, (30%, 45% and 60% of the UTS), were selected in this study.

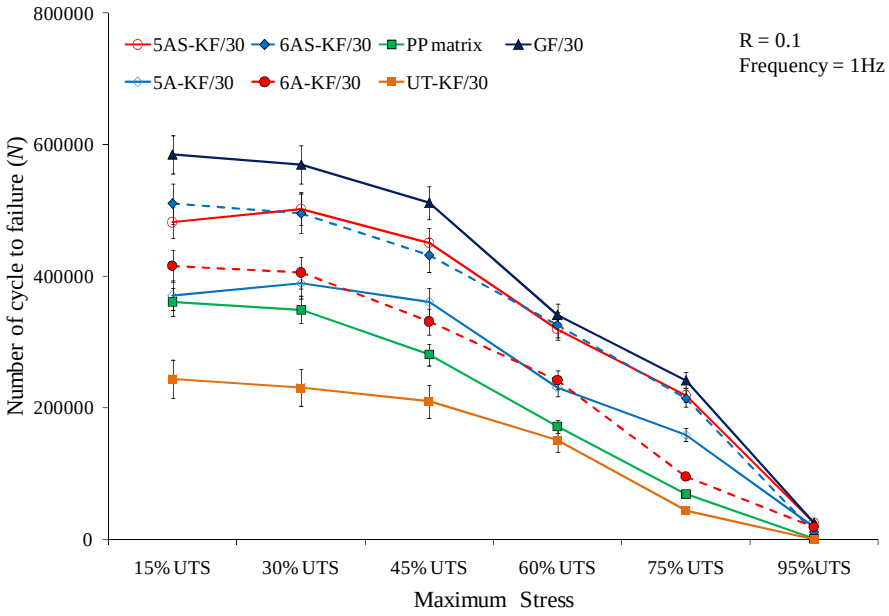


Figure 4.12: Figure E 1 Fatigue life of kenaf and glass /PP composites at different stress levels

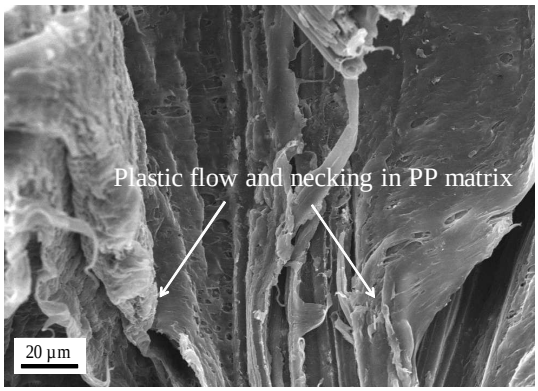


Figure 4.13: Failure in matrix-dominated region of UT-KF/25PP at 15% UTS

4.1.3.2 Test specimen characteristics and equipment

As indicated previously, the characteristics of the specimens (e.g. geometry, dimensions, preparation, and tabbing) are in accordance with ASTM D3479/D 3479M-09, Figure 4.14. It is evident that poor material fabrication, such as significant geometric inconsistencies (edge irregularities) and damage resulting from machining, generally leads to noticeable discrepancies in the test results. It is imperative that the characteristics of the test specimens were consistent, in order to ensure results of an acceptable confidence level. Manufacturing defects, such as voids, also affect the failure mode and performance during mechanical testing. Therefore, an optical microscope was used to assess different test specimens by evaluating and comparing the level of material irregularity. The intent of such an approach was to ensure consistent test results and reduction of the effects of flaws, which contribute to premature failure more often, by acting as stress raisers in the material.

Based on the results of these three sets of preliminary tests, it was concluded that reliable data could be obtained by conducting the fatigue test at 1 Hz with a stress ratio of 0.1 and by considering three stress levels: 30%, 45% and 60% of the initial UTS of the material.

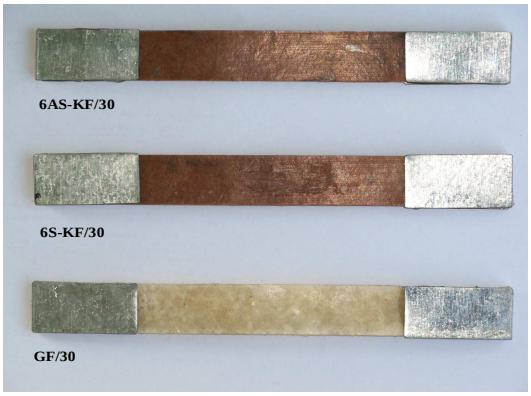


Figure 4.14: Kenaf and glass/PP specimens

4.1.4 Izod notched impact test

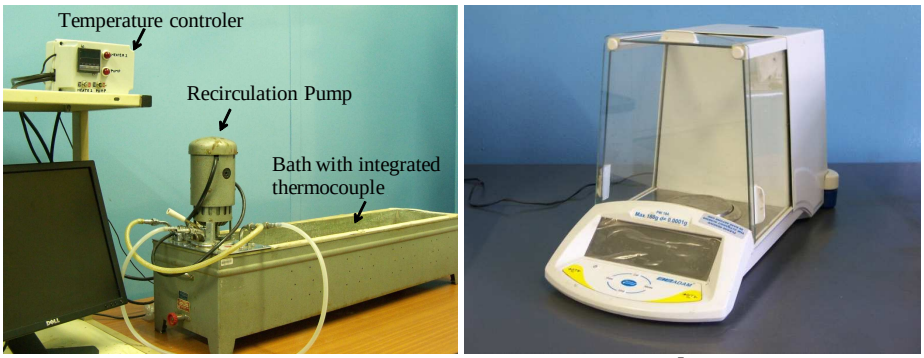
The Izod notched-beam test (Figure 4.15) was conducted in accordance with the requirements of Test Method C as described in ASTM D 256-10 [48]. This standard was selected as a guideline because it provides direction of how to generate data that can effectively be used as quality control tools for the fabricated composites. It also permits the evaluation of the effects of the manufacturing variables (e.g. fibre treatments and fibre contents) on the mechanical properties of the material. The most important test control parameters of the Izod notched-beam impact test are the notch dimensions (notch angle, notch depth and notch tip radius), the position of the test specimen (e.g. depth of the beam), the specimen size (e.g. width of the beam) and the pendulum impact velocity. Precautions were therefore taken to ensure consistent specimen geometry (e.g. notch edge irregularities) in order to ensure failure mode consistency and to lessen discrepancies of the test results (e.g. energy break) by maintaining a consistent pendulum impact velocity. Preliminary test results showed consistency in the failure mode (e.g. brittle fracture) and an acceptable level of confidence (e.g. lower standard deviation). An AVERY non-instrumented Izod test machine capable of yielding 4.2 Joules at 2.44 m/sec was used. Six specimens were made from each particular type of composite plate. Only test results of five samples, showing appreciable consistency, were considered.



Figure 4.15: Kenaf/PP specimen under impact load

4.2 Moisture absorption test

The moisture absorption test was designed in accordance with the requirements of ISO 62 and ASTM D5229/ D5229M standards [88, 89]. These two standards were selected since they provide guidelines to generate data that can effectively be utilized to evaluate the moisture absorption characteristics of polymer reinforced composites. The sample preparation was completed as follows: The test specimens were first cleaned with acetone to remove surface contaminants and dried in an oven at 35°C for 24 hours and cooled to room temperature (25°C) in a desiccator. Afterwards, the weight of the dry specimen was determined using an AE ADAM PW 184 electronic scale accurate to 0.001 mg. The test specimens were subsequently immersed into distilled water at (27.0 ± 1)°C whilst maintaining the temperature, Figure 4.16. A centrifugal pump was used to circulate water and create turbulence in order to ensure a uniform temperature distribution within the water bath. The test specimens (Figure 4.17) were at regular intervals, dried with tissue paper and then weighed to determine the change in mass. In the initial stages of the test (5 days), the measuring interval was 5 hours to ensure accuracy of the weight results.



a **b**

Figure 4.16: Moisture diffusion test set up and AE ADAM PW 184 scale

The lateral edges of the test specimens were sealed with silicon to prevent water molecules from diffusing into the test specimens through their edges and to minimize the extraction of water-soluble components from the specimens during the test. The extraction of water-soluble components is detrimental as it would compromise the validity of the results. The seal also ensured that the diffusion process was one-dimensional [88, 90, 91]. The moisture content was calculated using equation 4.1 [88, 89].

$$Weight\ gain\ (\%) = \frac{M_t - M_0}{M_0} \times 100 \qquad (4.1)$$

Where, *Mt* denotes the mass of the specimen at a specified time, whereas *Mo* represents the initial mass of the specimen.



a **b**

Figure 4.17: Test specimens: kenaf/PP and glass/PP composites

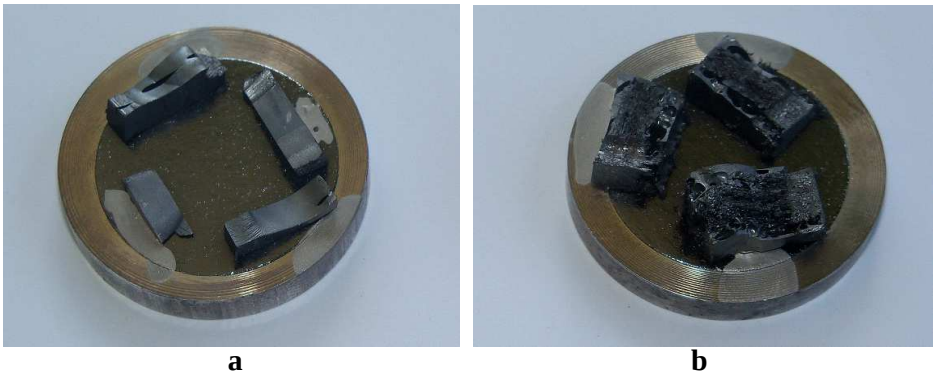
4.3 Microscopic examination

For decades, microscopic examination has been one of the scientist's most powerful tools for material characterization and failure mode analysis. Scanning electron microscopy (SEM) is an indispensable tool in this field, due the high resolution and magnification. In the present study, SEM was extensively used to characterise the material damage mechanism by analysing the fibre and matrix structures (e.g. matrix cracks, fibre surface morphology and fibre breakage). This was essential since it plays an important role in comprehending the mechanical behaviours of the material. SEM examinations of specimens subjected to moisture absorption were carried out on a FEI Nova 600 Nanolab FIB, Figure 4.18 (a) and a EMITECH K950X apparatus was used for sample preparation, Figure 4.18 (b). The SEM specimens (Figure 4.19) were coated with carbon at 10nm followed by gold palladium at 15nm. BX63 FM and Motic Images plus 2.0 ML microscopes were used to evaluate the surface morphologies of kenaf fibres as well as the failures of kenaf/PP composites, Figure 4.20 (a) and (b). The FEI Nanolab FIB, EMITECH K950X and BX63 FM apparatus were made available by the Microscopy and Microanalysis Unit of the University of the Witwatersrand, Johannesburg (MMU). A Zeiss ULTRA 55 scanning electron microscope equipped with a field emission tungsten hairpin filament and a ZrO reserve (electron source) was used for microscopic examination of specimens subjected to the mechanical testing.



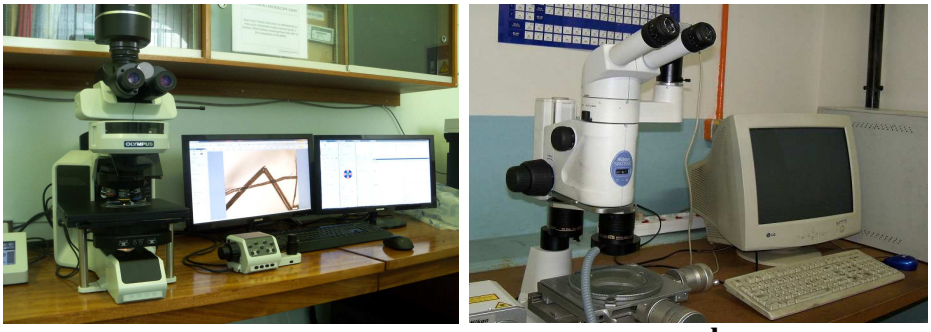
a **b**

Figure 4.18: (a) FEI NOVA 600 Nanolab FBI and (b) EMITECH *K950X*



a **b**

Figure 4.19: (a) MWCNT-PP and (b) Kenaf/PP-MWCNT specimens



a **b**

Figure 4.20: (a) BX63 FM microscope and (b) Motic Images plus 2.0 ML

5 DISCUSSION

The results of the mechanical and the moisture absorption tests conducted on kenaf/PP, and kenaf/PP-MWCNT and glass/PP composites are presented and discussed below. The discussion also refers to the images of the microscopic examinations for clarity. This chapter comprises 4 sections. In Section 5.1 the effects of fibre treatment on the improvement on the mechanical properties are evaluated (e.g. tensile, flexural, fatigue and impact properties). Section 5.2 discuses the effects of fibre treatment on the resistance to moisture absorption. The influence of the filler material (e.g. multi-wall carbon nanotubes) concentration on the mechanical properties of MWCNT-PP and kenaf/PP-MWCNT composites, fabricated using an optimal alkali concentration and fibre content (6% NaOH and 30 wt%, respectively), are discussed in Section 5.3. Section 5.4 discusses the influence of the variations in the CNT concentration on the resistance to moisture absorption of kenaf/PP- MWCNT composites. For clarity, the findings of each section are summarized at the end of the section.

5.1 Effect of fibre treatment on the mechanical properties

The discussion is presented in the following way: The improvement[ii] of the mechanical properties of kenaf/PP composites, due to the enhancement of the fibre-matrix adhesion, is evaluated and discussed first. Then, the failure characteristics of kenaf/PP composites are discussed based on the results of the microscopic examinations. The influence of changing the fibre content on the mechanical properties is also evaluated. Finally, the improvement on the tensile properties of kenaf/PP composites is compared to that of glass/PP composites.

[ii] For the purpose of this study, “Mechanical improvement” of a particular material refers to the changes in the mechanical properties (e.g. tensile, flexural, fatigue and impact strengths) of the material in comparison to that of unreinforced polypropylene. The average values are used to plot the graphs, error bars are omitted for the sake of clarity.

5.1.1 Tensile strength and tensile modulus of kenaf/PP composites

The effect of the fibre-matrix interfacial bonding on the tensile strength and tensile modulus of kenaf/PP, at various alkali concentrations, is evaluated by comparing the stresses required for composite failure to that of unreinforced PP plates, using equation 5.1[ii]. See Figures 5.3, 5.4, 5.7 and 5.8 for clarity. In these figures, zero percent refers to the tensile strength/modulus of unreinforced polypropylene, which is the reference point for comparison purposes.

$$TS = \left(\frac{TS_{composite} - TS_{unreinforced\ PP}}{TS_{unreinforced\ PP}} \right) * 100 \qquad (5.1)$$

5.1.1.1 Effect of alkali treatment on the tensile properties of kenaf/PP composites

From Figures 5.1 and 5.2, it is evident that the tensile strength and tensile modulus vary as a function of the alkali concentration. It can be noted that the tensile properties of alkali treated kenaf/PP composites are slightly better than those of untreated kenaf/PP composites. Below a concentration of 4% NaOH, the improvement is negligible (less than 5%). This is attributed to kenaf surface impurities (Figure 3.10) causing poor fibre-matrix adhesion, which in turns prevents proper load transfer between the fibre and matrix. Maximum values of the tensile strength and tensile modulus are observed at 5% and 6% NaOH. The improvement on the tensile properties of alkali treated kenaf/PP composites over those of untreated kenaf/PP composites, especially at 5% and 6% NaOH, indicate that the alkali treatment contributes to the enhancement of the tensile properties, suggesting that there are the optimal concentrations. The improvement is, however, limited; the tensile strength and tensile modulus for the 5A-KF/30PP composite is only 40.7% and 36%, respectively (Figures 5.3 and 5.4). These observations agree well with the results reported by Edeerozey *et al* [(40)]. The researchers investigated the morphological and structural changes of kenaf fibres subjected to alkali treatments and reported that 6% NaOH was the optimum concentration for alkali treatments. Based on the microscopic examination, they

indicated that 6% NaOH adequately cleans the fibre, chemically modifies the fibre surface, increases the surface roughness and improves the mechanical properties of the kenaf fibre. If the alkali concentration is increased above 6%, the tensile strength and tensile modulus drop, regardless of the fibre content. The cause of the reduction was found to be the degradation of kenaf fibre (Figure 3.10). Composite failures are mainly characterized by fibre pull–out and matrix yielding; breakages were not noticed. Fibre pulling out of the matrix is clear evidence of ineffective load transfer between the matrix and fibre. Fibre pull-out caused by poor fibre-matrix bonding is shown in Figure 5.12.

Considering the effects of the fibre content on the tensile properties (Figures 5.3 to 5.4), it can be seen that the tensile strength and tensile modulus increase with the increase in the fibre content. The maximum tensile strength occurs at 25% and 30 wt%, whereas the tensile modulus exhibits a noticeable improvement at 30 wt%. These discrepancies are probably due to the versatility of the microstructure configuration of individual kenaf fibres [4, 19]. This suggests that 25% and 30 wt% are the optimum fibre contents. The drop of the tensile properties at 35 wt% was found to be caused by poor fibre impregnation (Figure 3.31). It can also be seen that the mechanical properties of glass/PP composites are in general significantly greater than those of kenaf/PP composites. For example, the improvement of GF/30PP is 130% whereas the improvement of A5-KF/30PP is 45%. This can be attributed to the exceptional tensile properties of glass fibre as compared to those of kenaf fibre (See Table 3.3).

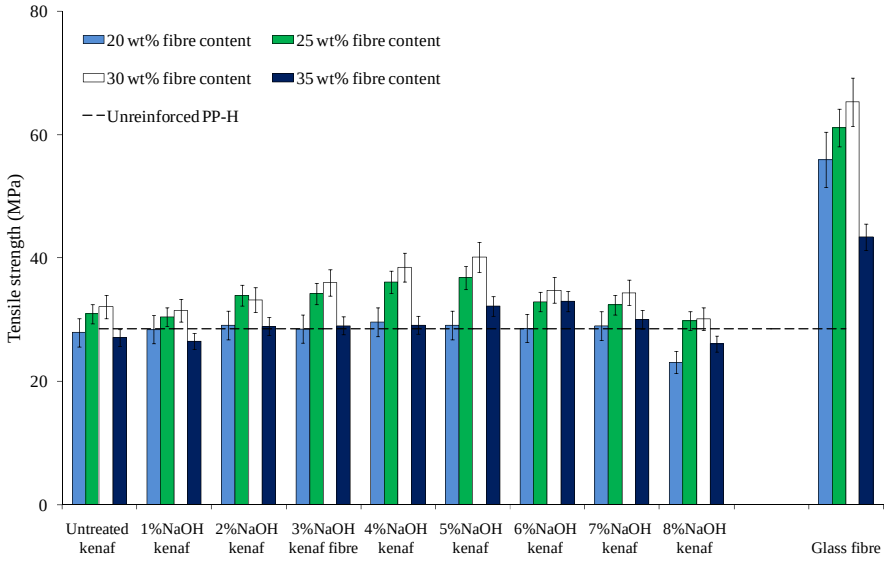


Figure 5.1: Tensile strength of alkali treated kenaf/PP and glass/PP composites

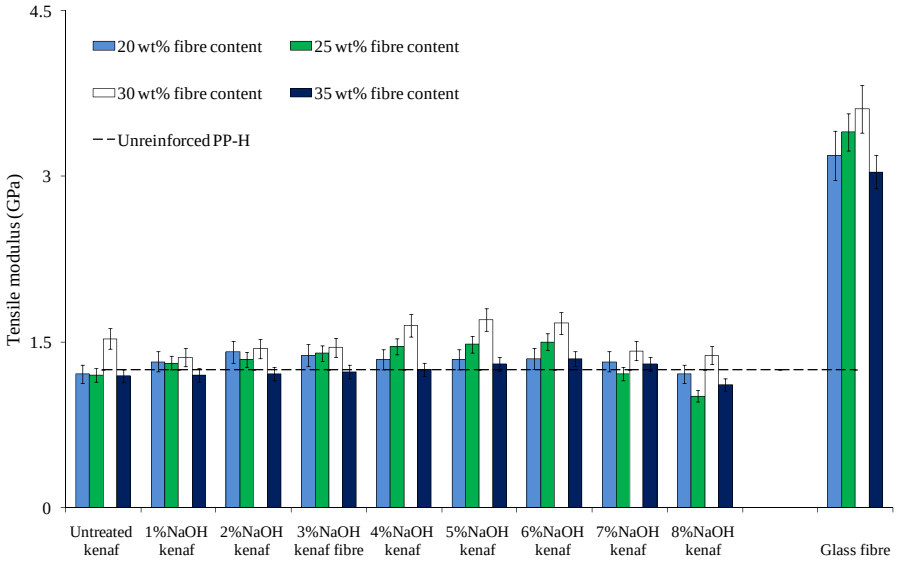


Figure 5.2: Tensile modulus of alkali treated kenaf/PP and glass/PP composites

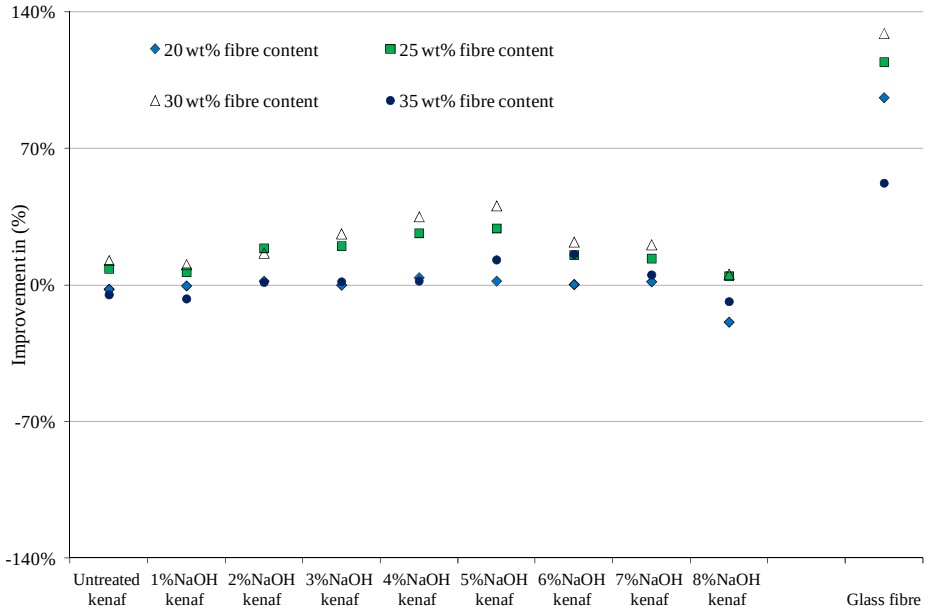


Figure 5.3: Improvement in the tensile strength of alkali treated kenaf/PP and glass/PP composites

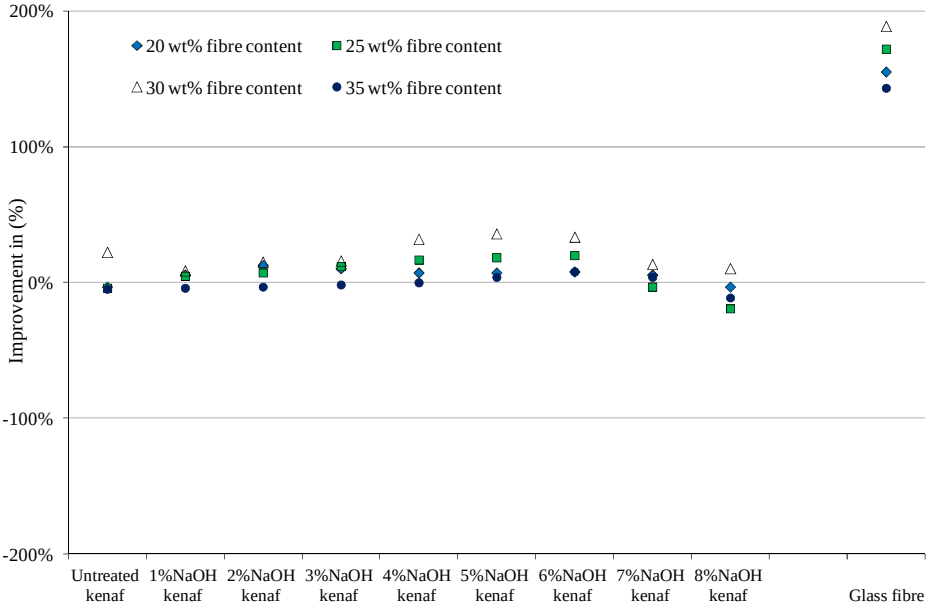


Figure 5.4: Improvement in the tensile modulus of alkali treated kenaf /PP and glass/PP composites

5.1.1.2 Effect of alkali-silane treatment on the tensile properties of kenaf/PP composites

Figures 5.5 and 5.6 show that the tensile properties of alkali–silane treated/PP composites improve significantly over those of untreated kenaf/PP composites and PP matrix, respectively, increasing from alkali concentrations greater than 3% NaOH. The tensile strengths and modulus exhibit maximum values at 5% and 6% NaOH [60]. Clear differences in the surface morphologies of untreated kenaf and alkali-silane treated kenaf fibres indicating the effects of the combined alkali-silane treatment can be seen in Figure 5.9. It can be noted that surface impurities that cause poor fibre-matrix adhesion are completely removed from the alka-silane treated kenaf fibres.

Scanning electron microscopy revealed that the failures of alkali–silane treated composites with 30% fibre content, treated with 6% NaOH, are predominately characterized by fibre dominated failure. Fibre breakage in alkali-silane treated kenaf/PP composites are shown in Figure 5.10. Such failure modes suggest that kenaf fibres carry a significant percentage of the load because of stronger fibre–matrix interfacial bonding. The improvement of the fibre–matrix interfacial bonding is attributed to the silane treatment which creates strong links between the fibre and the polymer matrix. A detailed description of the alkali and alkali-silane treatment mechanism can be found in Chapter 3, figures 3.9 and 3.12. These observations agree well with the findings reported in literature. Mohanty *et al* [96] emphasized that a suitable coupling agent could be used to overcome the chemical incompatibility between the polar nature of lignocellulosic fibres and the non–polar nature of thermoplastics in order to improve the fibre–matrix interfacial bond. Masud *et al* [42] also argued that the use of 5 wt% silane as coupling agent improves the fibre's wettability and flexural properties of the composites.

The adherence of polypropylene to the surface of kenaf fibres extracted from test specimens subject to failure confirmed strong fibre–matrix interfacial bonding caused by silane treatment. Figure 5.11 shows the attachment of a larger quantity of polypropylene to a broken fibre of 6AS-KF/30PP when compared to a 4AS-KF/30PP specimen subjected to tensile testing. This confirms the notion that the

effectiveness of silane treatment depends on the cleanliness of the fibre achieved through alkali treatment.

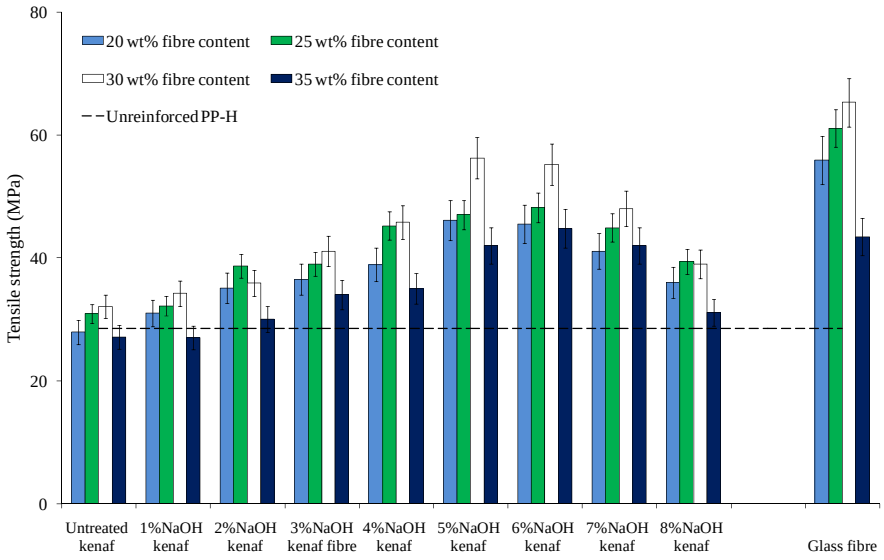


Figure 5.5: Tensile strength of alkali-silane treated kenaf/PP and glass/PP composites

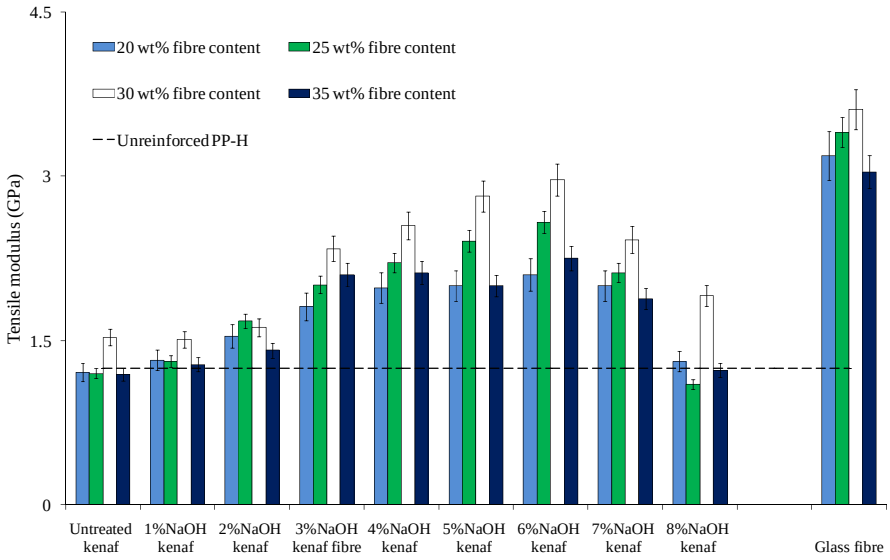


Figure 5.6: Tensile modulus of alkali-silane treated kenaf/PP and glass/PP composites

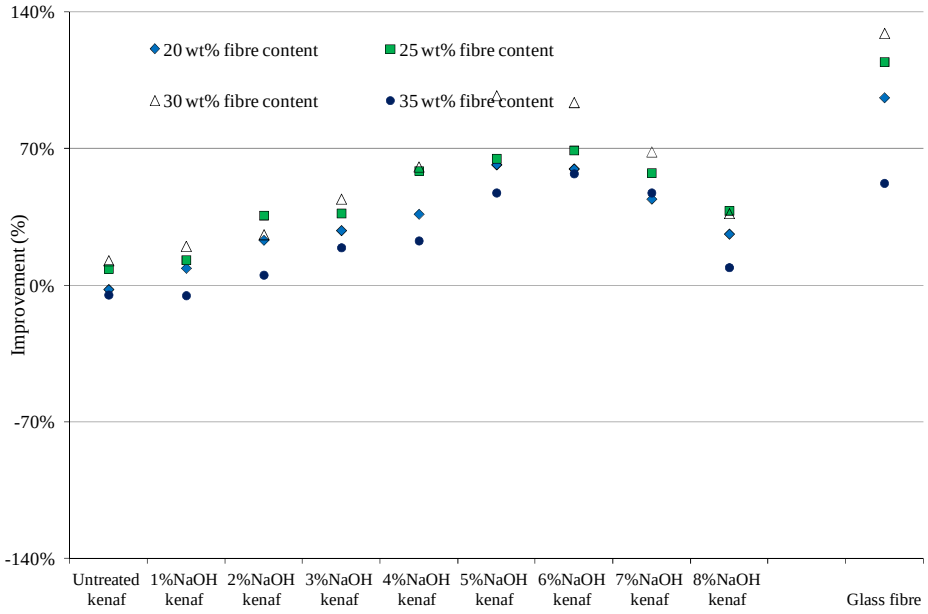


Figure 5.7: Improvement in the tensile strength of alkali-silane treated kenaf/PP and glass/PP composites

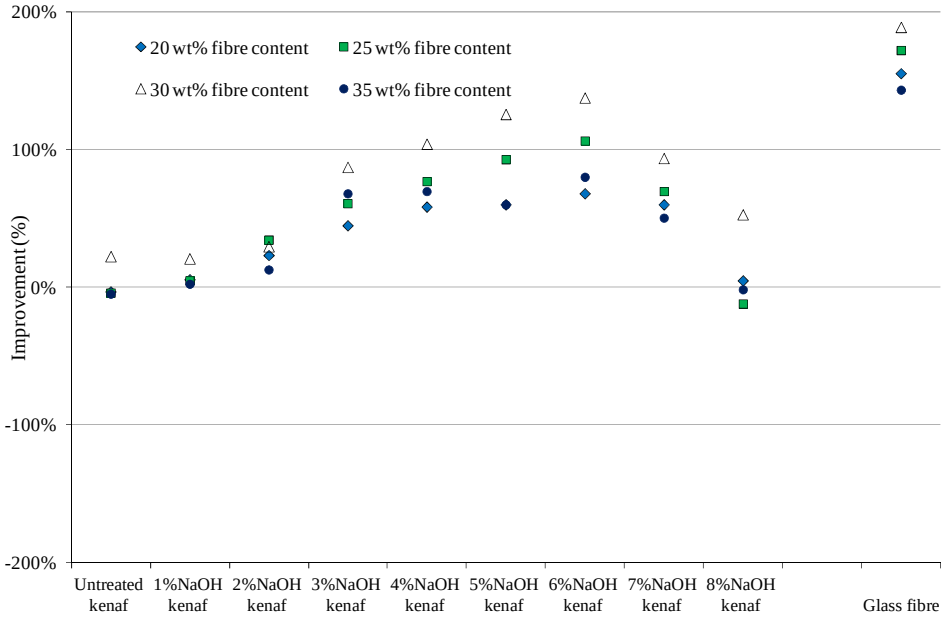
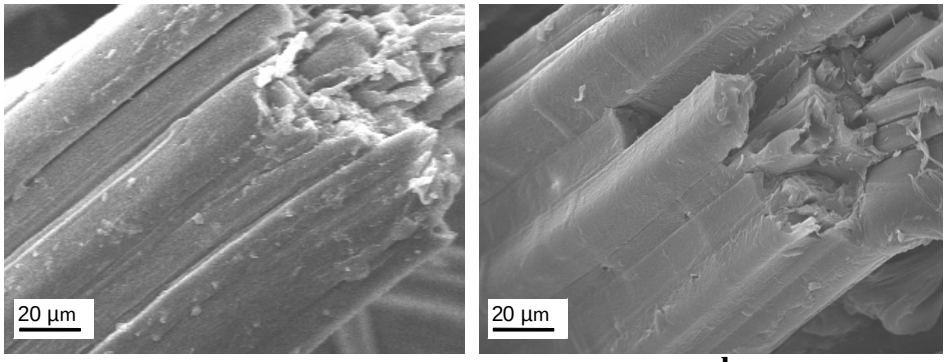
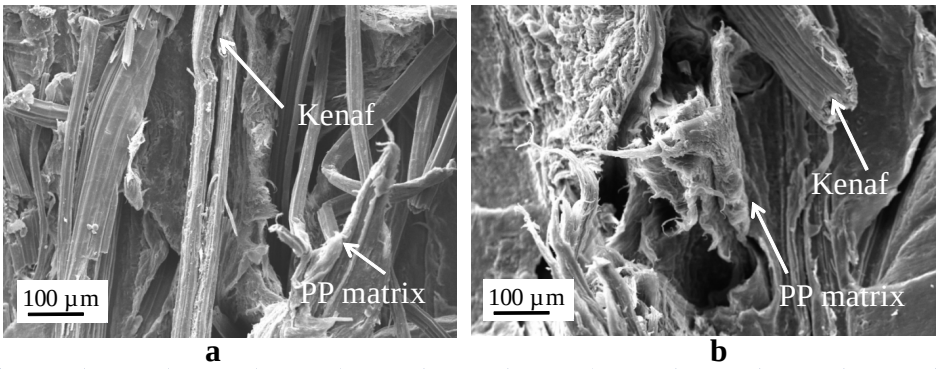


Figure 5.8: Improvement of the tensile modulus of alkali-silane treated kenaf/PP and glass/PP composites



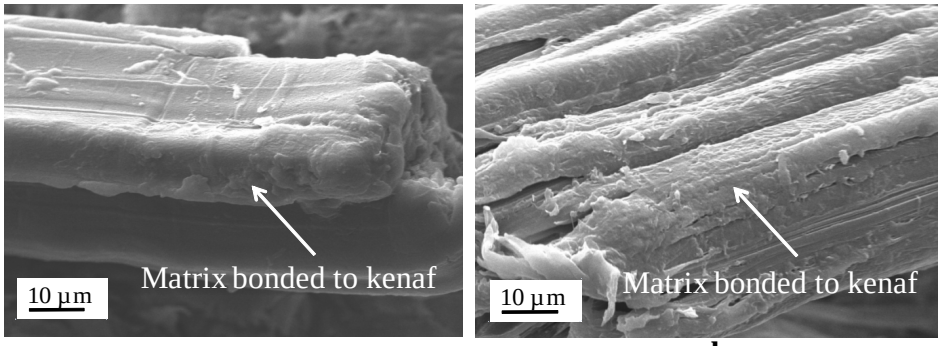
a **b**

Figure 5.9: Alkali-silane treated kenaf fibres: (a) Untreated kenaf, (b) 6%NaOH treated kenaf



a **b**

Figure 5.10: Fibre dominated failure: (a) 5AS-KF/30PP, (b) 6AS-KF/30PP



a **b**

Figure 5.11: PP matrix adhering to kenaf: (a) 4AS-KF/30PP, (b) 6AS-KF/30PP

Tensile test results (Figures 5.7 and 5.8) also show that alkali–silane treatments, using alkali solutions with concentration less than 3% NaOH, do not contribute effectively to the improvement of the mechanical properties of the composites. This was expected: SEM revealed that kenaf fibre treated with 3% NaOH still has

a considerable quantity of surface impurities, which causes poor fibre–matrix interfacial bonding. Edeerozey *et al* [40] also reported that 3% NaOH was not the appropriate concentration for alkali treatment of kenaf fibres because the surface impurities reduce the interfacial contact area between the matrix and fibre leading to an ineffective load transfer between the matrix and fibre. It was confirmed, using microscopic examination, that composites treated with alkali solutions of concentrations less than 3%, exhibited poor matrix interfacial bonding. SEM revealed that the failures of 2% NaOH alkali–silane treated composites with 30% fibre content (e.g. 2A-KF/30PP) are mainly characterized by fibre disbondement and pull–out followed by matrix yielding; fibre breakage was not evident, Figure 5.12. These failure modes are clear evidence of ineffective load transfer between the matrix and fibre, resulting in the matrix carrying the majority of the load. The absence of matrix bonding to the fibres also suggests that the matrix–fibre interfacial bonding is not strong enough to retain the matrix. These observations, once again, substantiate the notion that the alkali–silane treatment of kenaf fibres can be effective only if the surface impurities are removed.

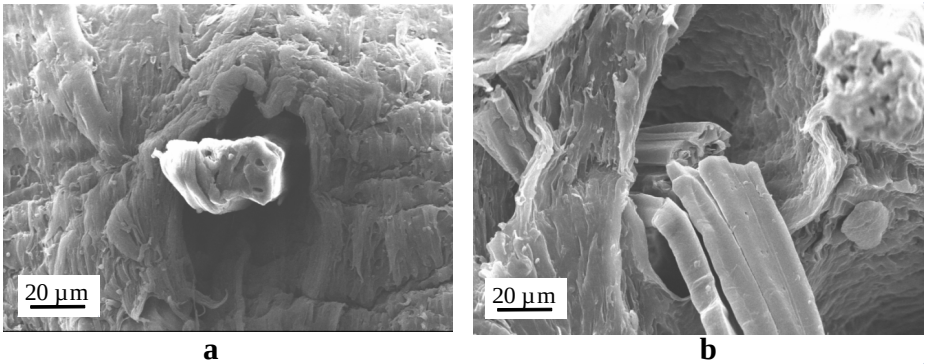


Figure 5.12: Fibre pull-out followed by matrix yielding failure

Figures 5.5 and 5.6 also show that the treatment of fibres with higher alkali concentrations (8% NaOH) drastically compromise the mechanical properties of the composites. The reduction in the tensile and flexural properties is attributed to the degradation of the mechanical integrity of the fibres, also shown in Figure 3.10 in Chapter 3. Edeerozey *et al* [40] reported similar observations at 9% NaOH.

Considering the effect of fibre content, it can be seen that the tensile properties increase with an increase in the amount of the reinforcing material in the composites. Figures 5.7 and 5.8 show that irrespective of the type of reinforcement, the tensile properties of the composites improve with an increase in fibre content. Below 30 wt%, the composites exhibit poor tensile properties. Poor tensile properties were confirmed by microscopic examinations, which revealed matrix dominated failure as the prevalent failure mode in composites with less than 30 wt% [96]. The improvement of the tensile strength and tensile modulus reached a maximum at 30 wt%. SEM revealed fibre dominated failure as the prevalent failure mode in composites with 30% fibre content, especially in alkali-silane treated composites (e.g. 6AS-KF/30PP composite). Similar failure modes were observed in glass fibre reinforced composites. As the fibre content rises above 30%, the tensile properties of the composites drastically drop. SEM showed that the drop in tensile strength and modulus is attributed to poor fibre impregnation and excessive voids (Figure 5.13) within the fibre dominated regions of the fabricated composites. Poor fibre impregnation and voids are also shown in Figure 3.31 in Chapter 3. These observations clearly indicate that 30% is the optimum fibre content for both kenaf and glass fibre reinforced polypropylene composites.

Comparing the results of tensile tests of glass/PP to those of kenaf/PP composites, it is noted that the tensile properties of glass/PP composites are greater, regardless of the alkali concentration and fibre content. This is attributed to the exceptional tensile properties of glass fibres, as discussed previously.

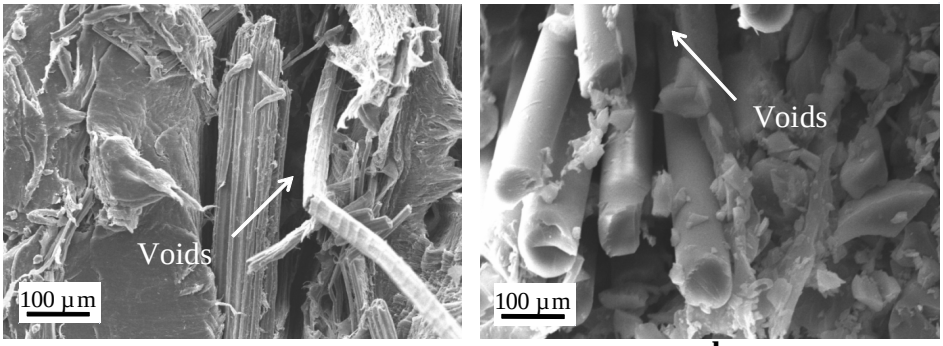


Figure 5.13: Poor fibre impregnation and excessive voids: (a) 6AS-KF/35PP, (b) GF/30PP composites

5.1.2 Flexural strength of kena/PP composites

The variations in the flexural strength of alkali and alkali-silane treated kenaf/PP composites are presented in Figures 5.14 and 5.16 respectively, in terms of the alkali concentration. For comparison purposes, the improvement[ii] of the flexural strength of kenaf/PP and glass/PP composites (Figures 5.15 and 5.17) were also plotted, using equation 5.1.

5.1.2.1 Effect of alkali treatment on the flexural properties of of kenaf/PP composites

From Figure 5.14 it can be seen that the trends in the flexural strength are similar to those observed in the tensile properties. There is little improvement in the flexural strength below 4% NaOH, with maximum values observed at 5% and 6% NaOH. This suggests that 5% and 6% NaOH are the optimums alkali concentration for improvement of the flexural strength of kenaf/PP composites. Similar observations were made by Edeerozey *et al* [(40)] and Li *et al* [(13)]. From Figure 5.15 it is also noticed that the flexural properties of both kenaf/PP and glass/PP composites increase with the increase in the amount of the reinforcing material. Maximum values of the flexural strength are observed at 30% fibre content, suggesting that it is the optimal percentage.

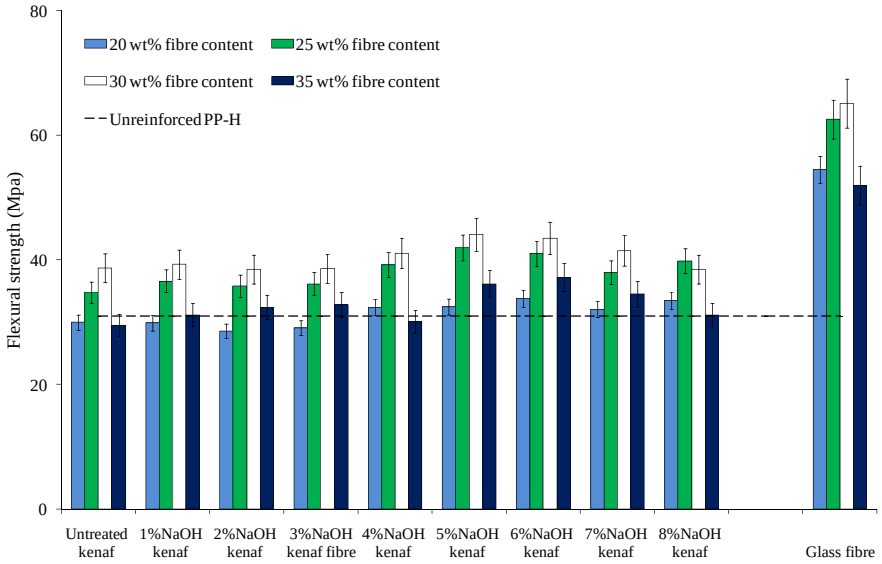


Figure 5.14: Flexural strength of alkali treated kenaf /PP and glass/PP composites

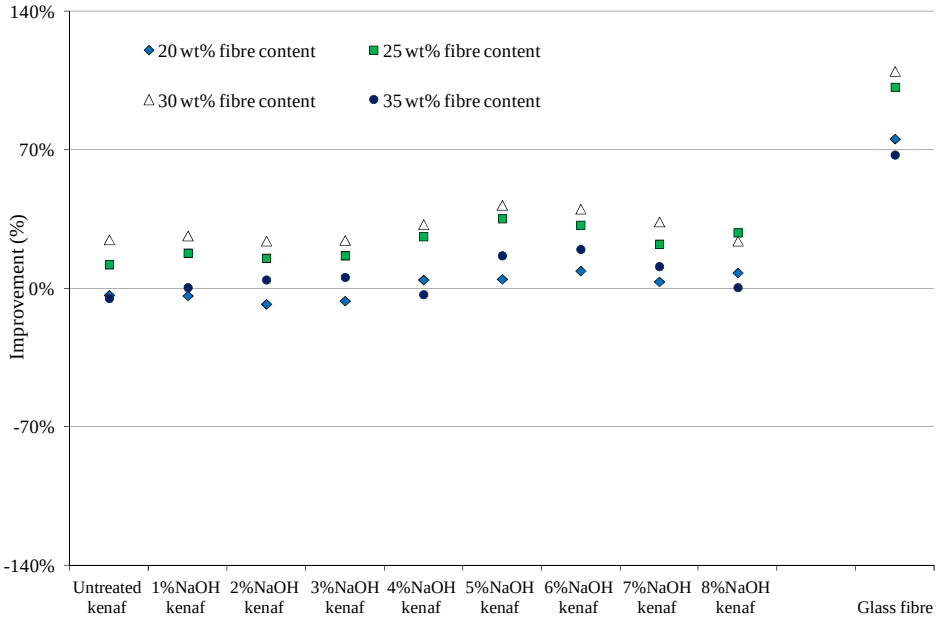


Figure 5.15: Improvement in the flexural strength of alkali treated kenaf/PP and glass/PP composites

5.1.2.2 Effect of alkali-silane treatment on the flexural properties of kenaf/PP composites

Comparing Figures 5.14 and 5.16 it can be seen that alkali treated composites do not perform as well as alkali-silane treated composites. Below 3% NaOH, the improvement is insignificant. Significant improvement of the flexural strength due to the silane treatment is noticeable at 5% and 6% NaOH. Masud *et al* [(42)] also reported that the use of silane as coupling agent improved noticeably the flexural properties of the composites.

When observing the effect of fibre content, it can be seen that the flexural strengths exhibit maximum values at 30%, suggesting that it is the optimal point. Figures 5.17 also show that the improvement in the flexural strength of glass/PP composites is greater than those of kenaf/PP composites, as expected.

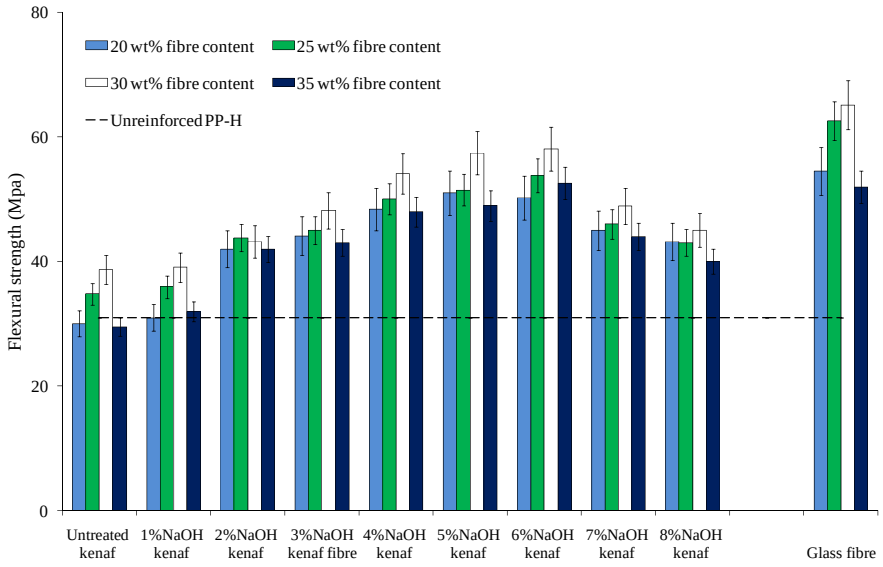


Figure 5.16: Flexural strength of alkali-silane treated kenaf/PP and glass/PP composites

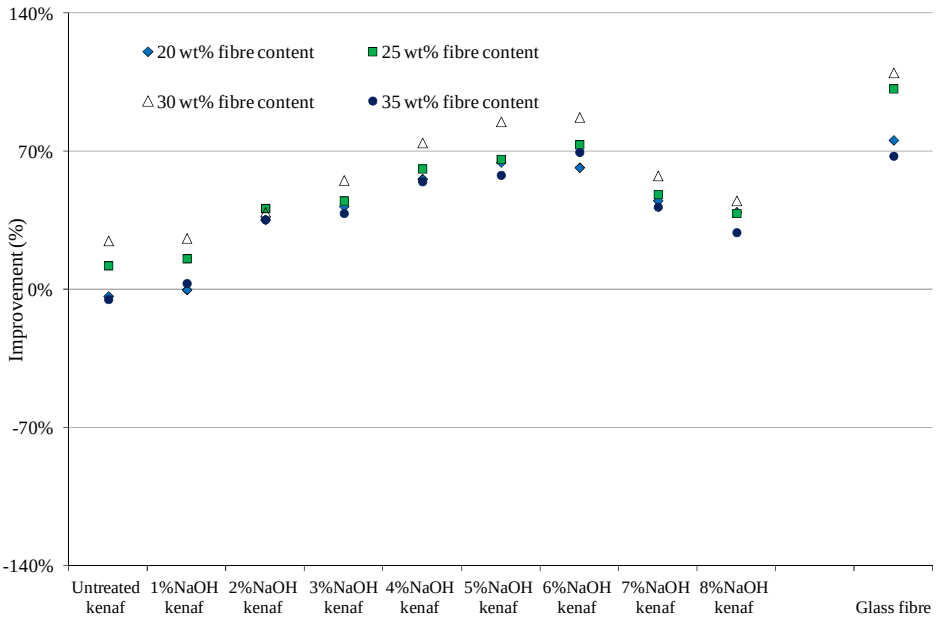


Figure 5.17: improvement in the flexural strength improvement of alkali-silane treated kena/PP and glass/PP composites.

5.1.3 Fatigue strength of kenaf/PP composites

The fatigue behaviour and fatigue life (number of cycles to failure) of alkali and alkali-silane treated kenaf/PP composites (Figures 5.18 through 5.20) are discussed. The fatigue performance[ii] of kenaf/PP composites are evaluated by considering the effects of the fibre treatment, fibre content and stress level. The failure mechanisms of kenaf/PP and glass/PP composites are also discussed. Similar to the approach used for the evaluation of the tensile test results, equation 5.2 is used to plot the graphs depicted in Figures 5.21 through 5.23.

$$FP = \left(\frac{N_{composite} - N_{unreinforc\ ed\ PP}}{N_{unreinforc\ ed\ PP}} \right) * 100 \qquad (5.2)$$

5.1.3.1 Effect of alkali treatment on the fatigue properties of kenaf/PP composites

The influence of the alkali concentration on the fatigue life of untreated kenaf/PP, alkali treated kenaf/PP and glass fibre/PP composites at different stress levels are

illustrated in Figures 5.18 through 5.20. A general observation can be made when viewing these figures: it is seen that the fatigue life increases as the alkali concentration increases. Poor fatigue properties of untreated kenaf/PP and alkali treated kenaf/PP composites, at an alkali concentration less than 3% NaOH, is noticed at all the stress levels. Although alkali treated kenaf/PP composites exhibit a slight improvement over untreated kenaf/PP composites, the results are poor when compared to unreinforced polypropylene specimens. The main reason for the poor performance was found to be ineffective fibre-matrix bonding. As indicated in section 5.1, solutions with a concentration of NaOH less than 3% do not successfully remove the fibre surface impurities that prevent effective fibre-matrix adherence - an essential attribute for effective load transfer between the fibre and matrix. This leads to the conclusion that kenaf fibres treated with alkali solutions with concentrations less than 3% are not effective reinforcing material, but compromise the fatigue performance of the composites [(94)]. As the alkali concentration rises above 3% NaOH, the fatigue life increases and reaches a maximum at 5% and 6% NaOH, giving a clear indication of the contribution of the alkali treatment to the interfacial bonding. These observations agree well with the results reported by Tow and Ansel [(46)]. The researchers argued that the strong fibre-matrix bonding resulting from the alkali treatment was the main cause of the improvement of the fatigue characteristics of sisal reinforced thermoset composites. As the alkali concentration rises above 6% NaOH, the fatigue life unexpectedly drops to values below the fatigue life of untreated kenaf/PP composites. As an example, the number of cycles to failure of 8A-KF/30PP is less than to that of UT-KF/30PP and 1A-KF/30PP when tested at 45% and 60% UTS. The reduction in fatigue life was also attributed to excessive alkali concentrations; treatment with a solution of 8% NaOH damaging the fibres to the extent that they become weaker than untreated fibres, thereby increasing the quantity of weak points in the bulk of the material where cracks can easily initiate. This suggests that the mechanical integrity of kenaf fibre is an essential attribute for the achievement of high fatigue performance in kenaf/PP composites. SEM of a degraded fibre, caused by alkali treatment with an 8% NaOH solution, can be seen in Figure 3.10.

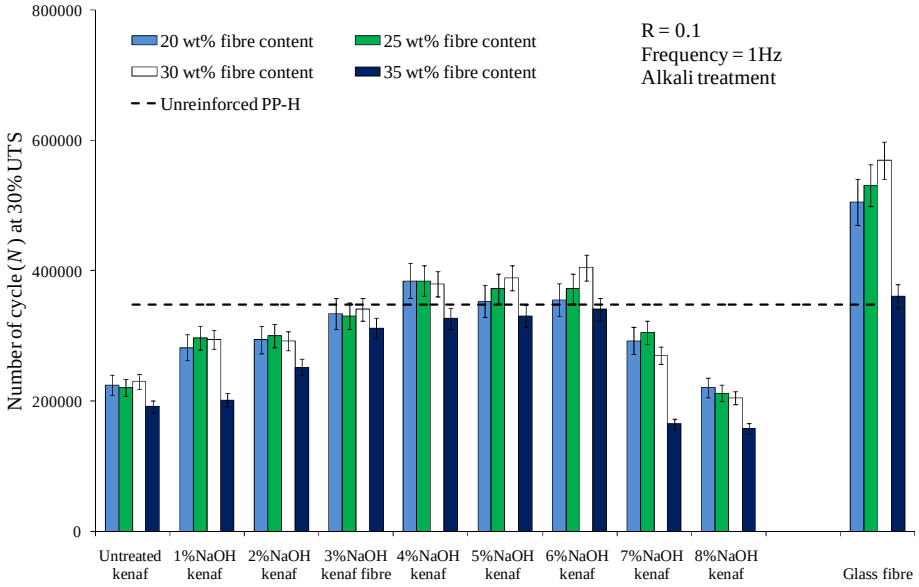


Figure 5.18: Fatigue life of alkali treated kenaf/PP and glass/PP composites at 30% of UTS

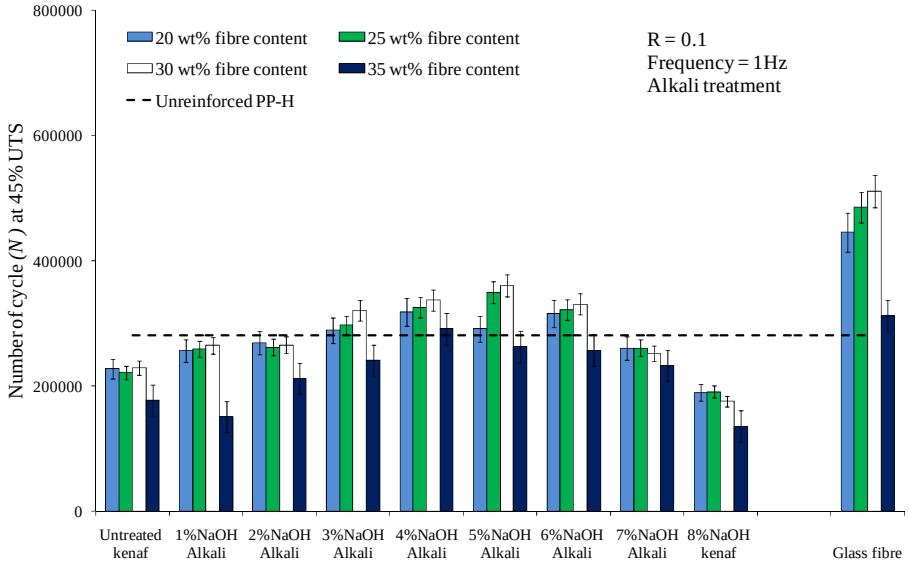


Figure 5.19: Fatigue life of alkali treated kenaf/PP and glass/PP composites at 45**%** UTS

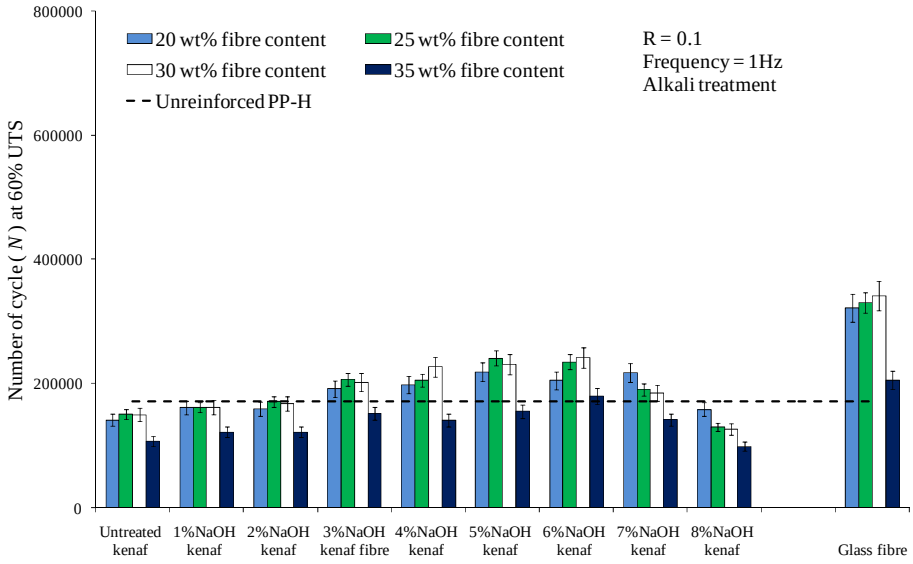


Figure 5.20: Fatigue life of alkali treated kenaf/PP and glass/PP composites at 60% UTS

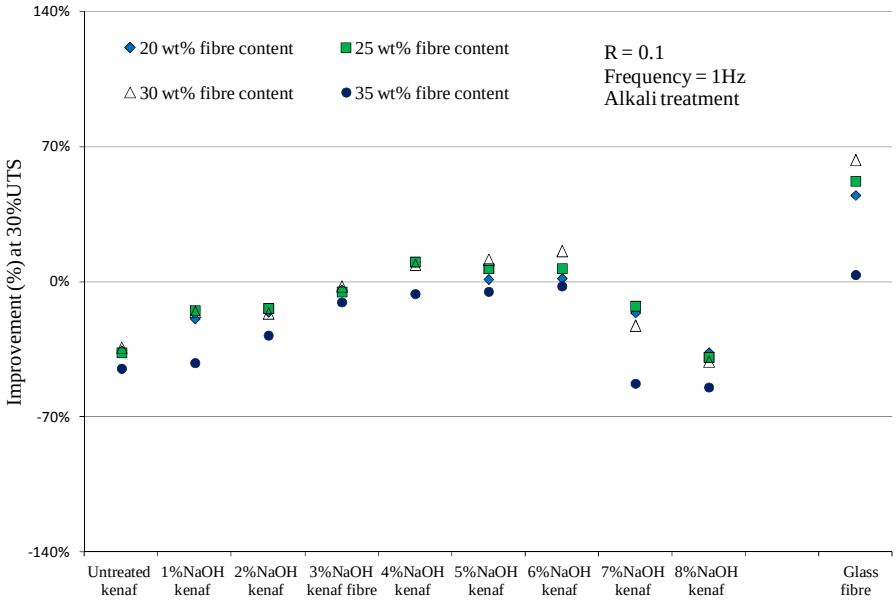


Figure 5.21: Fatigue performances of alkali treated kenaf/PP and glass/PP composites at 30% UTS

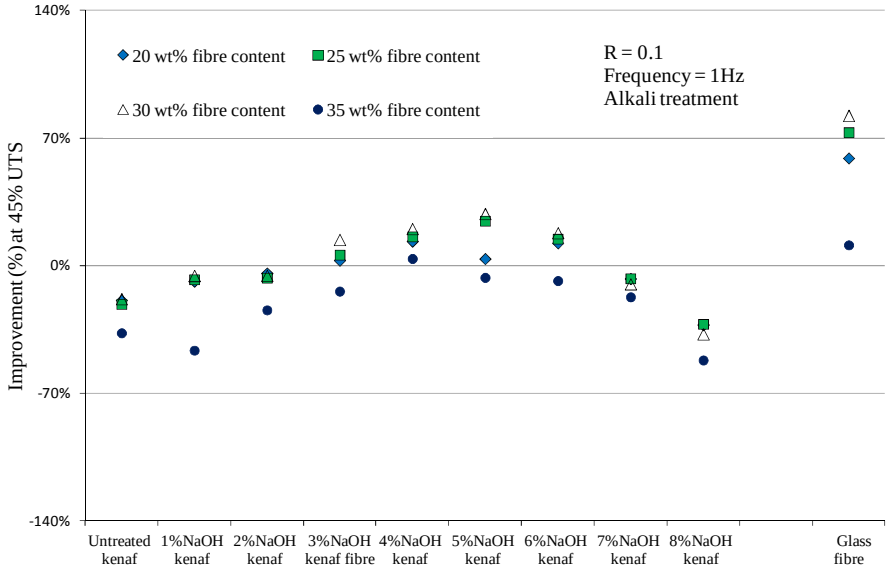


Figure 5.22: Fatigue performances of alkali treated kenaf/PP and glass/PP composites at 45% of UTS

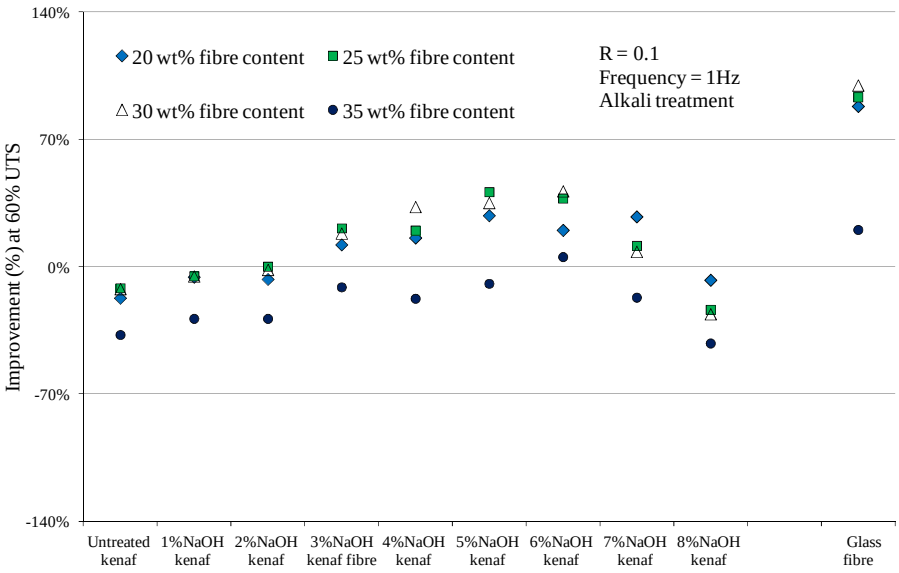


Figure 5.23: Fatigue performances of alkali treated kenaf/PP and glass/PP composites at 60% UTS

Failure mechanisms in alkali treated kenaf/PP composites

Previous studies reported that the failure mechanism in fibre reinforced polymer composites under fatigue loading is generally characterised by three main stages: crack initiation, crack propagation and ultimate failure [10, 46]. In the present study, microscopic examinations, conducted at specific cycle intervals, revealed that the failure mechanism of alkali treated kenaf/PP composites is characterised by two main stages, namely: crack propagation followed by ultimate failure. The crack initiation phase, as indicated in the literature, could not be distinctively characterized because the fibre-matrix disbondement behaves like a pre-existing crack, from which cracks propagate through the bulk of the material. SEM revealed that the crack density increases with the increase in the fibre content [10]. As an example, 6A-KF/30PP composites had greater fibre-matrix disbondement than 6A-KF/20PP. This is obvious since one could argue that the increase in the amount of fibres in the composite would increase the availability of fibre-matrix interfacial sites in the material.

Crack propagation phase

Crack propagation is characterised by the development of the disbondement fibre-matrix into macrocracks as the number of cycles increase. Microscopic examination revealed that the crack density and crack length is affected by the fibre content, fibre distribution and the stress levels. As reported by Creed [94], elongated cracks will develop in the matrix-dominated regions and shorter cracks in the fibre-dominated regions. This is not the case in the present study, since it was found that elongated matrix cracks develop in both matrix and fibre-dominated regions. Elongated cracks found in the fibre-dominated regions are caused by close proximity of adjacent fibres, which facilitates the coalescence of adjacent cracks [36, 43]. Mallick [10] also reported similar findings. Although fibre-matrix disbondement was found to be the main driver for crack development, SEM also revealed that cracks in the matrix-dominated regions emanate from the surface of the specimen. Test results showed that 25 percent of 5% and 6% NaOH alkali treated kenaf/PP composites, with fibre content ranging between 20% and 30 wt%, exhibited such cracks. These cracks were noticeable only at a later stage

of the crack initiation phase, especially for specimens loaded at 60% of UTS. Figure 5.24 shows cracks emanating from the surface of a 6A-KF/30PP specimen. The mechanism found to be responsible for these failures was the improved fibre-matrix interfacial adhesion. Tensile tests conducted at selected intervals, intended to determine the residual stiffness of the test specimen, showed that damage occurring at an early stage of the loading history substantially compromises the overall strength of the specimens, especially at 45% and 60% UTS. As an example, the fatigue resistance of a 6A-KF/30PP composite dropped by 30% after 25840 cycles at 60% UTS.

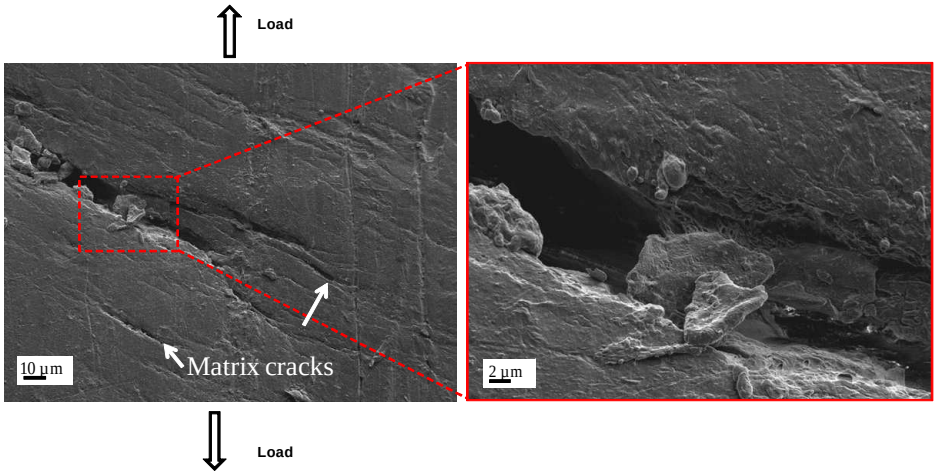


Figure 5.24: Cracks initiating in the matrix-dominated region of 6A-KF/30PP composite loaded at 60% UTS

Ultimate failure phase

During the failure phase, the amount of damage (cracks along the fibre-matrix interfacial regions) accumulated within the fibre and matrix-dominated regions increases to the extent that the residual stiffness of the composite drastically drops. As a result, elongated cracks spread rapidly into the bulk of the material, subsequently leading to material failure. Failure in both kenaf/PP and glass/PP composites is characterized by a combination of brittle and ductile failure, predominantly in the matrix-dominated regions. Ductile failure, characterized by plastic flow and necking, was found to be the prevailing failure in the matrix-dominated regions at 30% UTS. At 30% UTS, no evidence of beach marks in the

matrix-dominated regions could be found, but it was visible, along with slight gross plastic flow, at 45% and 60% UTS. Fibre pull-out was found to be the predominant failure mode in matrix-dominated regions, regardless the stress level.

Comparing Figures 5.21, 5.22 and 5.23, it is clear that the fatigue performance increases with the increase in fibre content, regardless of the stress level. In general, composites with 25% and 30% fibre have the highest fatigue performance, especially at 5% and 6% NaOH. This suggests that 25% and 30% fibre content are the optimums fibre contents for improvement of the fatigue properties of alkali treated kenaf/PP composites. Composites with 35% fibre content exhibit poor fatigue performance. Microscopic examinations revealed that poor fatigue properties originate because of excessive voids (Figure 3.31) caused by a matrix deficiency within the core of the composite plate.

Comparing the fatigue performance of glass/PP to those of kenaf/PP composites, it is noticed that the fatigue properties of glass/PP composites are better than those of kenaf/PP composites, in general. The exceptional mechanical properties were, once again, the cause for such behaviour. Geometric irregularities in the peripheral cells of the kenaf fibres (Figure 5.25) were also found to contribute to the weakening of the kenaf/PP composites by acting as weak points, causing disadvantageous localized stress concentrations in the surrounding matrix.

When considering the effects of stress levels on the fatigue performance of kenaf/PP composites, it is noticed that the composites have better fatigue properties at 45% and 60% UTS than at 30% UTS (see Figures 5.21, 5.22 and 5.23). For example, the improvement of 6A-KF/30PP is 16.1% greater than that of unreinforced PP at 30% UTS, whereas at 60% UTS, the improvement increases to 41.5%. Glass/PP composites also showed similar trends. From the figures, it can be seen that the improvement of GP/30PP is 63% and 99.6% greater than that of unreinforced PP at 30% UTS and 60% UTS, respectively. These observations suggest that, although the fatigue life of both reinforced and unreinforced PP composites have decreased with the increase of the stress level, the life of reinforced PP did not significantly decrease due to the addition of reinforcing material.

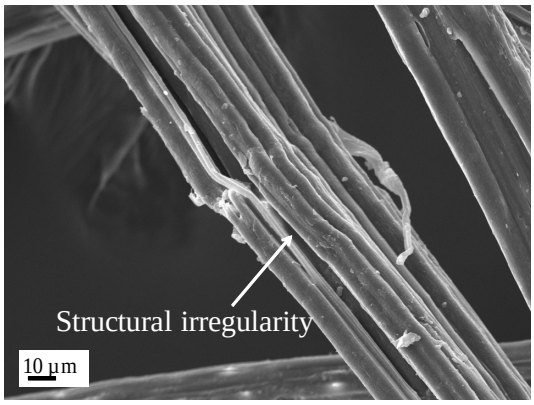


Figure 5.25: Localized structural irregularities on 5% NaOH treated kenaf

5.1.3.2 Effect of alkali-silane treatment on the fatigue properties of kenaf/PP composites

The influence of the alkali concentration on the fatigue life of untreated kenaf/PP, alkali-silane treated kenaf/PP and glass/PP composites at different stress levels is illustrated in Figures 5.26 through 5.29. Similar to the fatigue behaviour of alkali treated kenaf/PP composites, the results indicate that the fatigue life of alkali-silane treated kenaf/PP composites increases with the increase in the alkali concentration. Poor fatigue life is observed for composites treated with alkali concentrations smaller than 2% NaOH. At 3% NaOH, alkali-silane treated kenaf/PP composites exhibit noticeable improvements over unreinforced polypropylene specimens, especially at 45% and 60% UTS. The cause of the poor fatigue performance is the ineffective fibre-matrix interfacial adhesion, as mentioned in section 5.1.3.1. These fatigue behaviour leads to the conclusion that additional silane treatment can effectively contribute to the improvement of the fatigue resistance of kenaf /PP composites, provided that surface impurities preventing effective fibre-matrix interfacial bonding are completely removed by the alkali treatment. As the alkali concentration rises above 3% NaOH, the fatigue performance drastically improves and reaches a maximum value at 5% and 6 % NaOH. Comparing to Figures 5.21 through 5.23 and to 5.29 through 5.31, it can be seen that the fatigue performance of alkali-silane treated kenaf/PP composites are noticeably superior than those of alkali treated kenaf/PP composites. Comparing the performance of 5AS-KF/30PP and 6AS-KF/30PP, it is shown that

the fatigue properties of 5A-KF/30PP and 6A-KF/30PP differ by 27.27% and 38.10% at 30% UTS, respectively.

Microscopic examination revealed that material failure of 5AS-KF/30PP and 6AS-KF/30PP are predominately characterized by fibre breakage. The adherence of polypropylene to the kenaf fibres subsequent to fatigue failure, as well as matrix cracks originating from the matrix rich regions, far removed from the fibre-matrix interface, suggest strong bonds between the PP matrix and alkali-silane treated kenaf fibres, Figure 5.32. As the alkali concentration rises above 6% NaOH, the fatigue life decreases, indicating that kenaf fibres have been damaged. The reduction in the fatigue performance is, however, not as significant as that of alkali treated kenaf /PP composites. This affirms the contribution of additional silane treatment on the improvement of the fibre-matrix adhesion, in turn improving the fatigue resistance of alkali treated kenaf/PP composites.

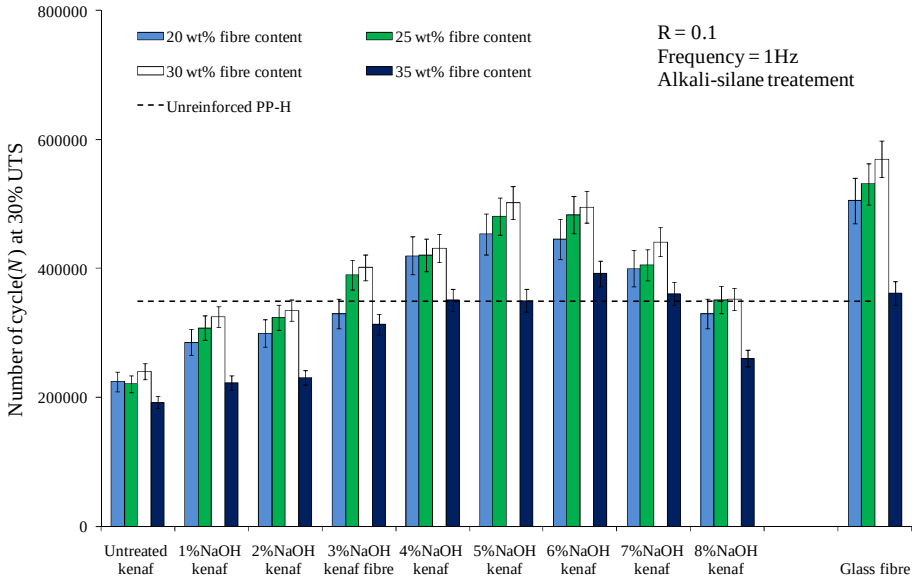


Figure 5.26: Fatigue life of alkali-silane treated kenaf/PP and glass/PP composites at 30% of UTS

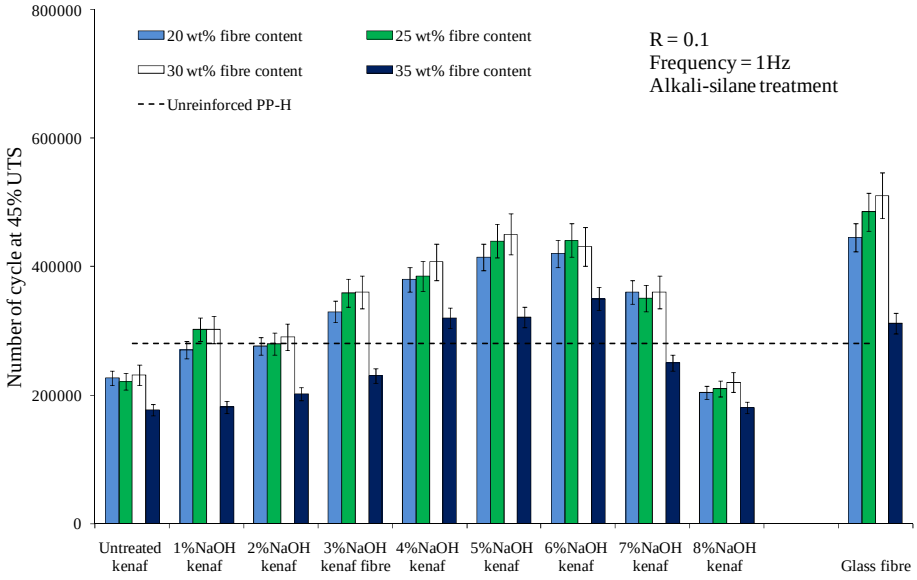


Figure 5.27: Fatigue life of alkali-silane treated kenaf/PP and glass/PP composites at 45**%** UTS

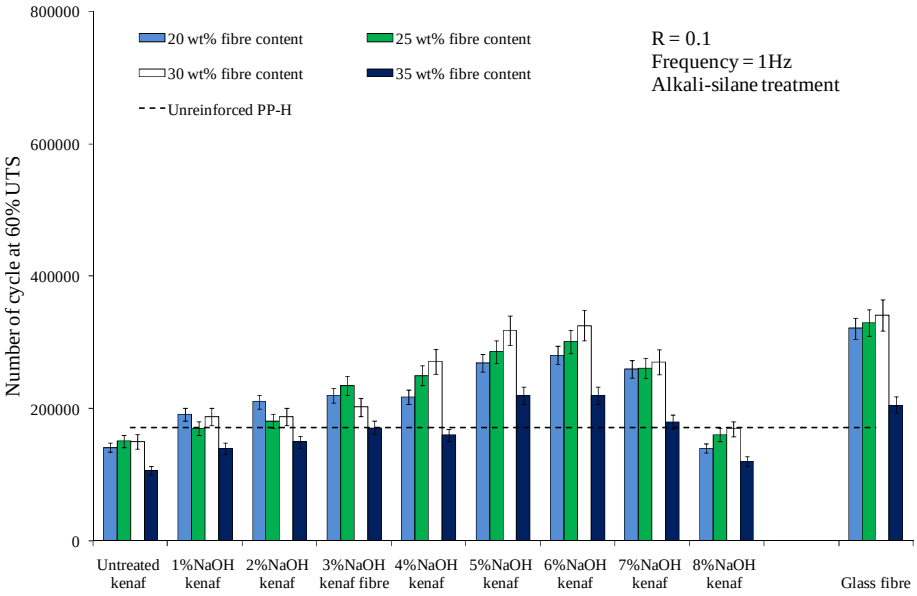


Figure 5.28: Fatigue life of alkali-silane treated kenaf/PP and glass/PP composites at 60% UTS

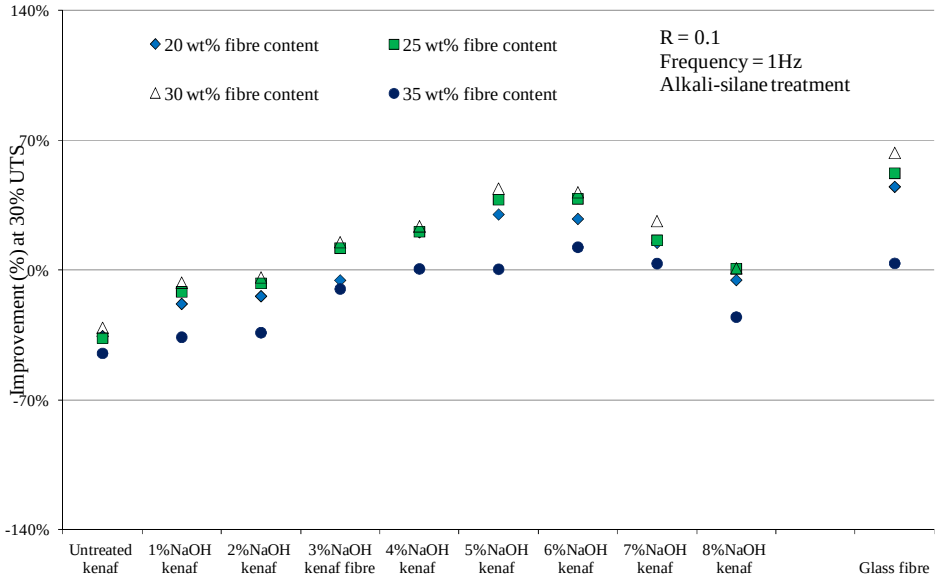


Figure 5.29: Fatigue performances of alkali-silane treated kenaf/PP and glass/PP composites at 30% UTS

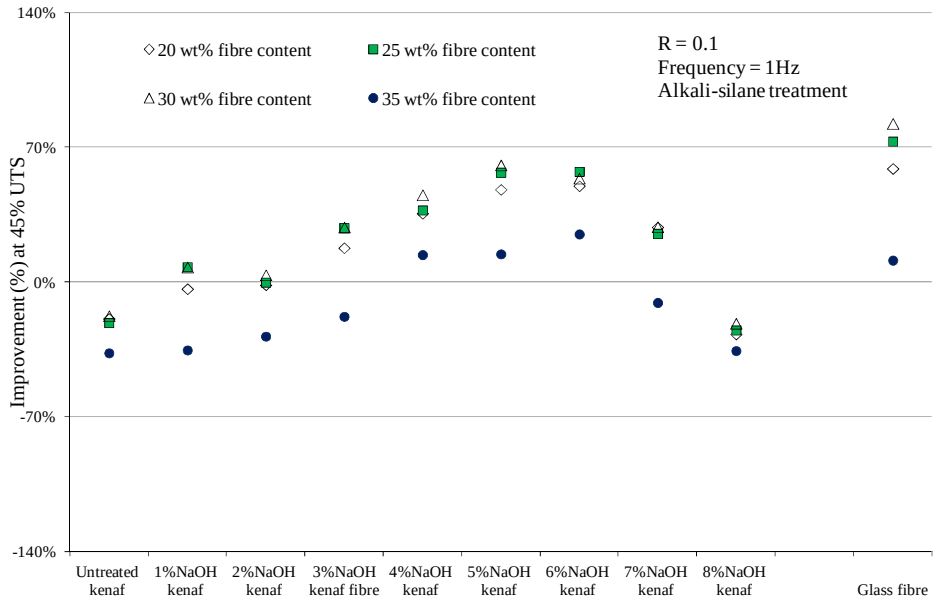


Figure 5.30: Fatigue performances of alkali-silane treated kenaf/PP and glass/PP composites at 45% UTS

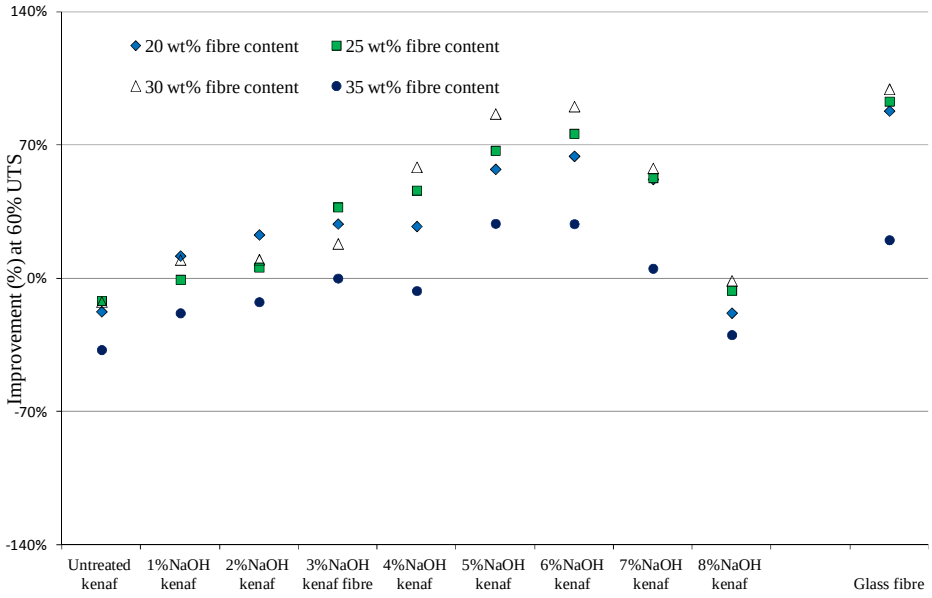


Figure 5.31: Fatigue performances of Alkali-silane treated kenaf/PP and glass/PP composites at 60% UTS

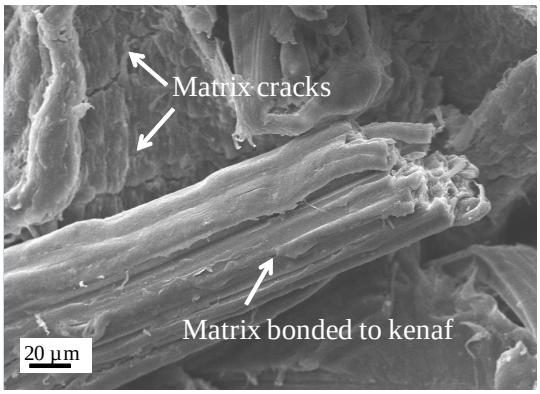


Figure 5.32: PP matrix adhering to kenaf of a 6AS-KF/30PP specimen (45%UTS)

Failure mechanism in alkali-silane treated kenaf/PP composites

Matrix cracks and fibre breakages were found to be the predominant failure modes in alkali-silane treated kenaf/PP composites. Microscopic examinations conducted at selected intervals revealed that the damage mechanism of alkali-silane treated kenaf/PP composites consists of three main stages: crack initiation, crack propagation and failure. However, the duration of each phase varies in terms of the fibre content and the stress levels [(10)].

Crack initiation phase

The crack initiation phase is characterized by a fibre-matrix disbondement and the initiation of microcracks within the matrix-dominated regions. SEM revealed that several factors, including fibre content, fibre orientation and stress levels, affect the crack density and crack patterns. For example, most of the cracks originated along the fibre-matrix interfaces and are oriented in a direction transverse to the applied load. Elongated cracks were found in both matrix-dominated and fibre-dominated regions. Cracks occurring within the fibre-dominated regions are caused by the close proximity of fibres, as discussed in point 5.1.3.1. However, in composites with 35% fibre content, SEM showed that the majority of the elongated cracks within the fibre-dominated regions are caused by the growing voids acting as pre-existing cracks [(10)]. Glass/PP composites showed similar failure characteristics during the crack initiation stage. Elongated microcracks within the matrix-dominated region of a GF/30PP specimen are shown in Figure 5.33.

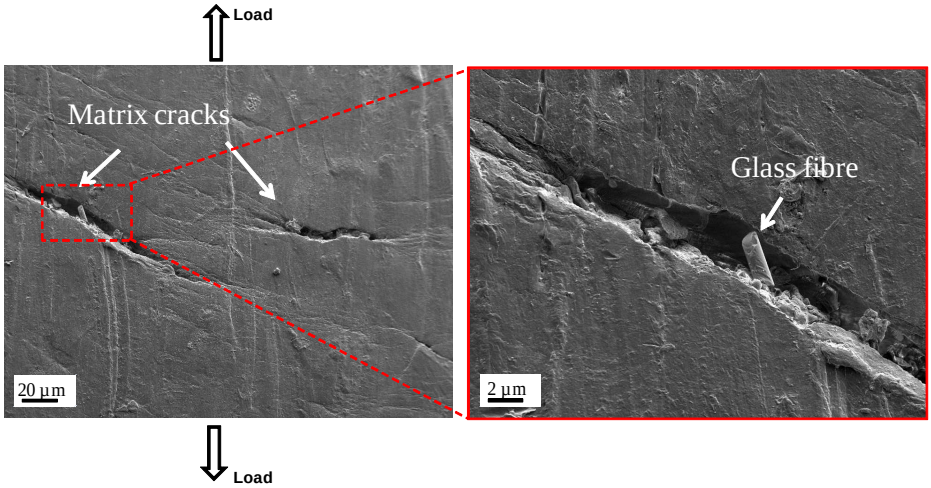


Figure 5.33: Cracks originating from the matrix-dominated layer of GF/30 composite loaded at 60% UTS

Crack propagation phase

The propagation stage is characterized by the increase in size and density of the microcracks. Microscopic examination revealed that macrocracks developing in the bulk of the material depends on the stress level and material configuration. Composites with a fibre content greater than 25% exhibit high crack density within the fibre-dominated regions because of the proximity of sites prone to disbondement. It was also found that microcracks developing in the fibre and matrix-dominated regions compromise the overall load bearing ability of the specimens; evident at 45% and 60% of UTS where rapid crack development was observed. For example, the fatigue resistance of 6AS-KF/30PP composite dropped by more than 24% after 36190 cycles at 60% UTS.

Ultimate failure phase

The failure mechanism of alkali-silane treated kenaf/PP composites was found to be similar to that of the alkali treated kenaf/PP composites. At an advanced stage of crack propagation, microscopic examination showed that damage accumulated in both fibre and matrix-dominated regions of the composite increase significantly. This leads to cracks rapidly spreading into the bulk of the material, subsequently leading to failure. Ductile failure, characterized by the matrix tearing, was found to be the prevalent failure mode in the matrix-dominated regions at low stress levels (30% UTS). Yielding of the matrix, characterized by tearing and necking of a 6AS-KF/25PP composite, is shown in Figure 5.34 (a). Beach marks and a slight gross plastic flow was noticeable in the matrix-dominated regions at 45% and 60% UTS. Figure 5.34 (b) shows fibre breakage and beach marks in a 6AS-KF/30PP composite, respectively. The beach marks are clear evidence of failure by fatigue loading. SEM revealed that the majority of kenaf fibres pulling out of the matrix during failure are coated with polypropylene, shown in Figure 5.32. This also suggests strong fibre-matrix adhesion. In glass/PP composites the failure is characterized by a cracking matrix and fibre breakage, for composite with a fibre content less than 35%. Cracks

developing at the fibre-matrix interface and fibre breakages in glass/PP composites are shown in Figure 5.35.

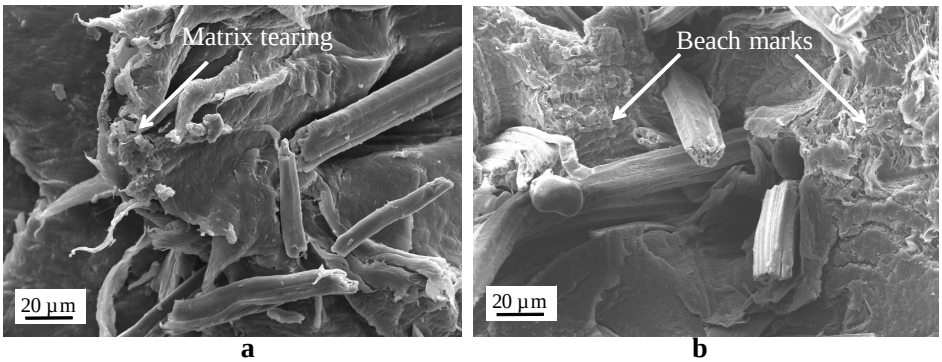


Figure 5.34: Failure of 6AS-KF/30PP: (a) 30% UTS, (b) 60% UTS

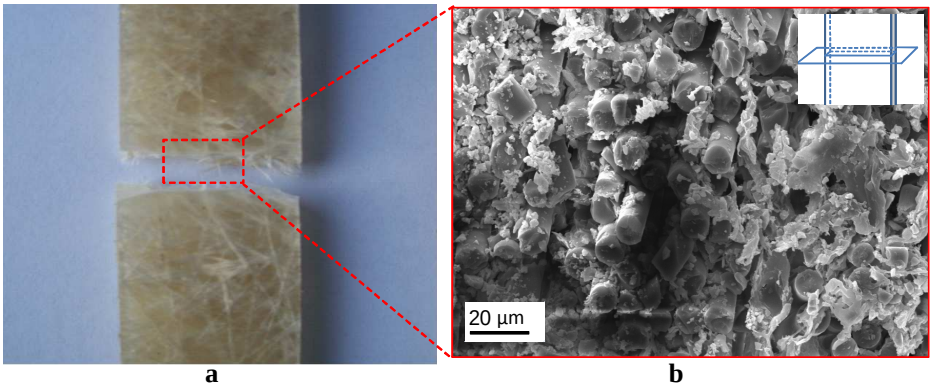


Figure 5.35: Fibre-matrix splits and fibre breakage in GF/30PP composite loaded at 60% UTS

From Figures 5.29 through 5.31 it is observed that the fatigue performance increases with an increase in the fibre content. Composites with 30% fibre content have the highest fatigue performance values, suggesting that a fibre content of 30% is the optimal concentration for improvement of the fatigue properties of alkali-silane treated kenaf /PP composites.

The figures also show that the improvement in fatigue performance of glass/PP composites is greater than that of kenaf /PP composites, in general. However, the fatigue performance of GF/30PP compares relatively well with that of glass/PP composites at 45% and 60% of UTS. For example, the fatigue performance of 6AS-KF/30PP composite is 11.8% less than that of GF/30PP composite at 60% of

UTS (Figure 5.31). The improvement is clear evidence of the effectiveness of the additional silane treatment on the fibre-matrix interfacial adherence. This also agrees with the observations discussed in section 5.1.1.2.

When evaluating the effect of the stress level on the fatigue performance, Figures 5.29 through 5.31 show that kenaf/PP composites have improved fatigue properties at higher stress levels (45% and 60% UTS). For example, the improvement of a 6AS-KF/30PP specimen is 41.9% at 30% of UTS, whereas the improvement of 6AS-KF/30PP at 60% of UTS is almost 90.5%. This also sustains the notion that the influence of the fibre-matrix interfacial adhesion on the fatigue strength of kenaf/PP composites becomes substantial at stress levels greater than 30% of UTS.

5.1.4 Izod notched impact strength of kenaf/PP composites

The impact properties of untreated kenaf/PP, alkali treated kenaf/PP, alkali-silane treated kenaf/PP and glass/PP composites are discussed below. Equation 5.3 was used to plot the graphs that illustrate the improvement of the composites[ii]; see Figures 5.36 and 5.40. The impact properties of kenaf/PP composites are evaluated by considering the influence of the fibre treatment and fibre content. The failure mechanisms of kenaf/PP and glass/PP composites are also discussed.

$$IR = \left(\frac{IE_{composite} - IE_{unreinforced\ PP}}{IE_{unreinforced\ PP}} \right) * 100 \qquad (5.3)$$

5.1.4.1 Effect of alkali treatment on the impact properties of kenaf/PP composites

The impact strength of untreated and alkali treated kenaf/PP and glass fibre/PP composites at different alkali concentrations are illustrated in Figures 5.36. It is seen that the impact strength increases with an increase in the alkali concentration. Untreated and alkali treated kenaf/PP composites exhibit poor impact resistance when compared to unreinforced PP specimens, at alkali concentrations less than 4% NaOH, regardless of the fibre content. The main cause of poor impact

properties was found to be poor fibre-matrix interfacial adhesion, resulting in the matrix absorbing the majority of the impact energy due to improper energy transfer between the fibre and matrix. In the fibre dominated region, failure is predominantly characterized by a fibre-matrix disbondement and fibre pull-out although little fibre breakage was noticed. SEM images of untreated kenaf/PP composites, revealing fibres pulling out of the matrix due to poor fibre-matrix interfacial bonding, can be seen in Figure 5.38 (a). A clean kenaf fibre pulling out of the matrix with a smooth internal cavity surface, illustrated in Figure 5.38 (b), is clear evidence of poor fibre-matrix adhesion. Brittle failure was found to be the predominant failure mode within the matrix-dominated regions. Scattered fragments on an A-KF/25PP specimen (red arrows in Figure 5.39) are clear indications thereof. These findings suggest that below 4% NaOH, the impact strength of alkali treated kenaf/PP composites are mainly governed by the effectiveness of the fibre-matrix adhesion, whereas the fibre content has little influence.

As the alkali concentration rises above 4% NaOH, the impact strength increases and a maximum value is achieved at 5% and 6% NaOH. The impact strength of 5A-KF/30PP increased by 96.5%, whereas that of 6A-KF/30PP increased by 89.7% in comparison to that of unreinforced PP (Figure 5.37). The increase in the impact strength indicates that proper cleaning of kenaf fibres can improve the capacity of kenaf/PP composites to absorb impact energy. It also suggests that 5% and 6% NaOH are the optimum alkali concentrations for the improvement of the impact strength of alkali treated kenaf/PP composites [(42)]. The improvement of the impact strength due to strong fibre-matrix adhesion was also reported by Ramires and Frollini [(11)]. The researchers indicated that the improvement of the impact strength was attributed to improved fibre-matrix adhesion.

At 7% NaOH the impact strength slightly decreases. But it drops to below the impact strength of unreinforced PP at 8% NaOH. For example, the impact strength of a 7A-KF/30PP specimen drops, but remains at 41.4% above that of unreinforced PP, whereas that of 8A-KF/30PP drops to 27,6% below the impact

strength of unreinforced PP (Figure 5.37). As mentioned in section 5.1.3, damaged fibres is a possible cause of such behaviour, especially at 8% NaOH.

From Figure 5.37 it is obvious that the impact strength increases with an increase in the fibre content. The maximum improvement occurs at 30% fibre content. Kenaf/PP composites with 35% fibre content exhibit poor impact performance, regardless of the alkali concentration. In all cases the impact strength is less than that of unreinforced PP by more than 41%. Microscopic examinations revealed that the poor impact performance is attributed to improper fibre impregnation leading to poor fibre-matrix adhesion.

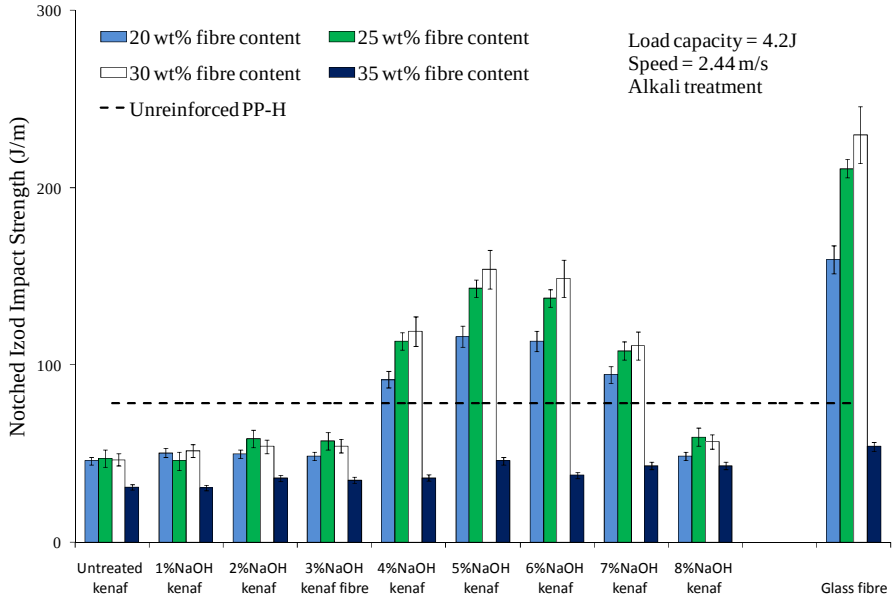


Figure 5.36: Impact resistance of alkali treated kenaf/PP and glass/PP composites

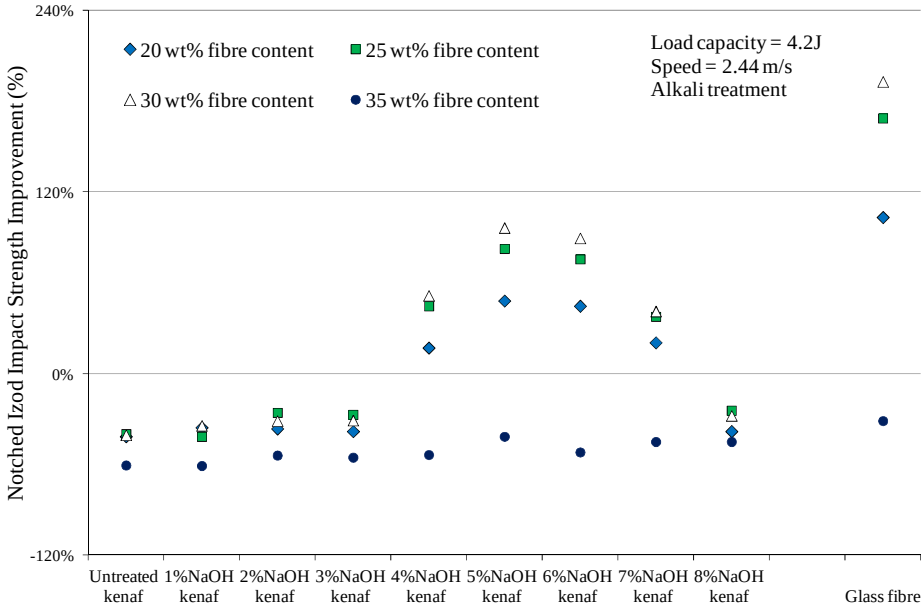


Figure 5.37: Impact performances of alkali treated kenaf/PP and glass/PP composites

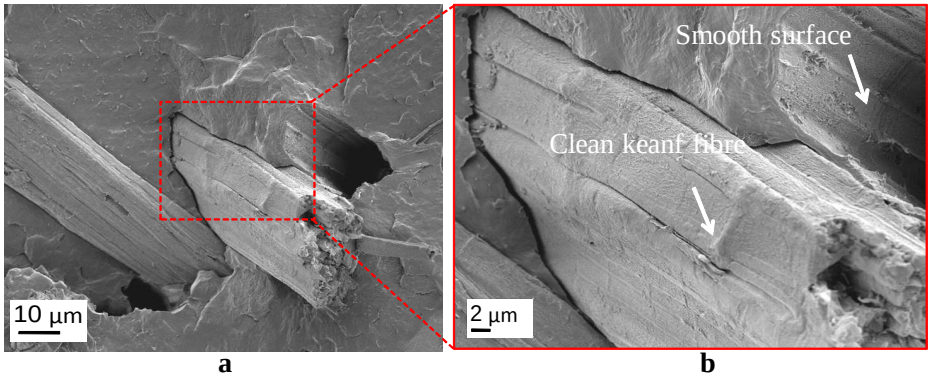


Figure 5.38: UT-KF/30PP composite: (a) kenaf fibres pulling out (b) smooth surface of the cavity

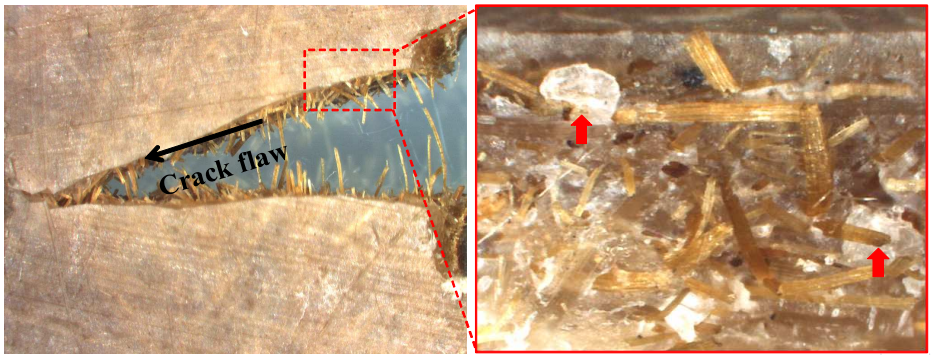


Figure 5.39: Matrix fragments emanating from PP matrix

5.1.4.2 Effect of alkali-silane treatment on the impact properties of kenaf/PP composites

The influence of the alkali concentration on the impact strength of untreated and alkali-silane treated kenaf/PP and glass/PP composites are illustrated in Figure 5.40. The results indicate that the impact resistance of alkali-silane treated kenaf/PP composites increases with an increase in the alkali concentration. Similar to alkali treated kenaf/PP composites, the poor impact strength of alkali-silane treated kenaf/PP composites at alkali concentration less than 3% NaOH is noticed. For example, the impact strength of an AS1-KF/30PP and an AS2-KF/30PP composite is 32.8% and 31.0%, respectively; less than that of unreinforced PP, although a slight improvement is demonstrated (less than 5% in average) over that of untreated kenaf/PP composites. These findings indicate that additional silane treatments of alkali treated kenaf fibres enhance the impact properties of kenaf/PP composites. Fibres pulling out of the matrix of a 2AS-KF/30PP composite (Figure 5.42) is a clear result of poor fibre-matrix adhesion, caused by an ineffective alkali treatment. Above 3% NaOH, the impact strength improves noticeably and reaches a maximum value at 5% and 6% NaOH, suggesting that these two concentrations are the optimum for the improvement of the impact strength of alkali-silane treated kenaf/PP composites.

Microscopic examination revealed that the failure of a 5AS-KF/30PP and 6AS-KF/30PP specimen is predominately characterized by fibre breakage and fibre splitting, although few fibres pulling –out of the matrix was observed (Figure 5.43). In matrix dominated regions, brittle fracture was found to be the main failure mode.

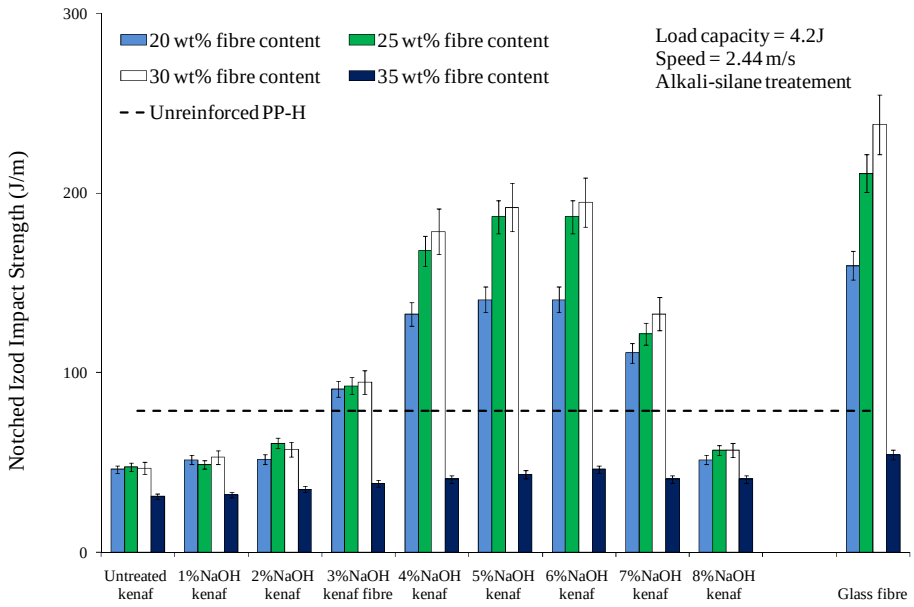


Figure 5.40: Impact resistance of alkali-silane treated kenaf/PP and glass/PP composites

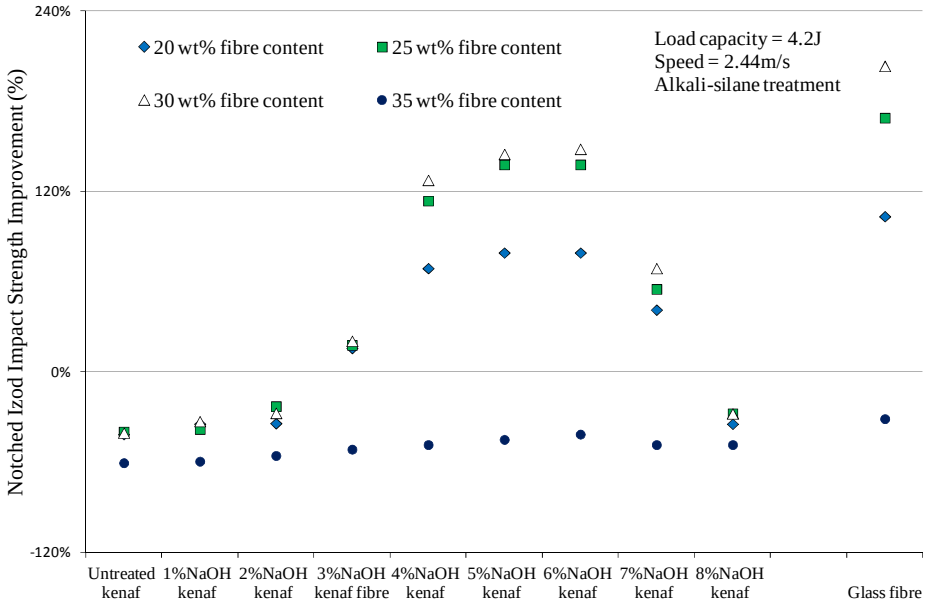


Figure 5.41: Impact performances of alkali-silane treated kenaf/PP and glass/PP composites

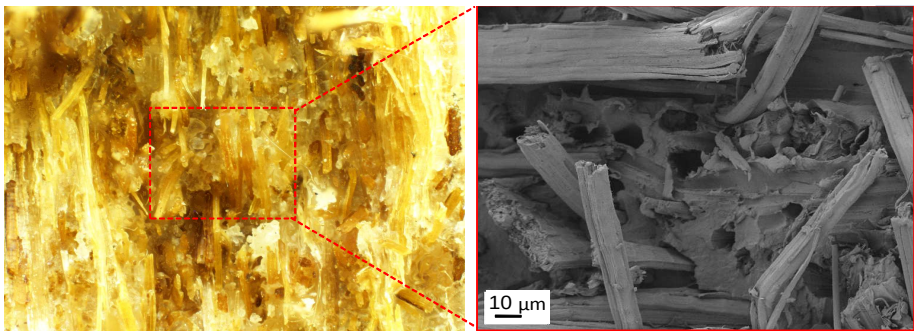


Figure 5.42: Fibre pull out and fibre breakage in 2AS-KF/30PP

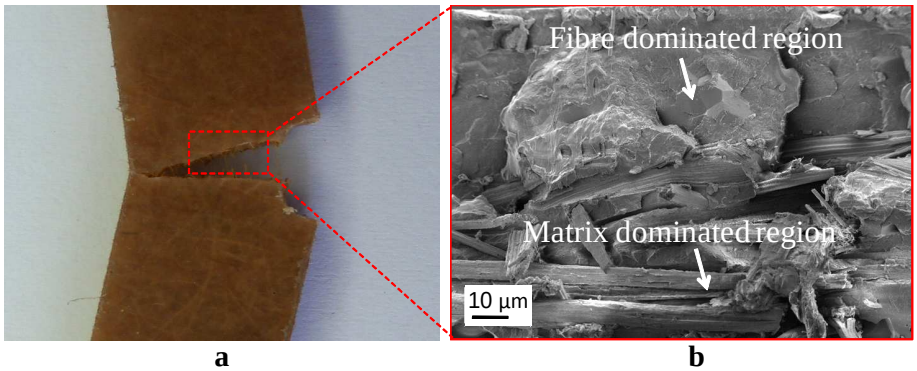


Figure 5.43: Matrix crack and fibre breakage in AS6-KF/30PP composite

The changes in colour (crazing effects) surrounding broken fibres within the matrix region indicates that, due to the additional silane treatment, the fibre-matrix adhesion was improved. The crazing effects (Figure 5.44) are explained as follows [36]: as the impact load is transferred from the fibres to the matrix, a substantial amount of energy is dissipated at the interfacial region. If the matrix critical strain is exceeded, a localized cavitational phenomenon, called “crazing”, appears as whitening of the matrix. The phenomenon is generally characterized by microcracks in the matrix surrounding the fibres. Depending on the magnitude of the impact load and impact strength of the matrix, the microcracks may develop into macrocracks and eventually lead to fracture. Optical microscopy shows the crazing effect in Figure 5.44 (a) and induced microcracks in Figure 5.44 (b). Microscopic examinations also revealed that the crazing effects occurred mostly around fibres oriented transverse to the direction of the crack path. Failure of the fibres oriented parallel to the direction of the crack path was characterized by splitting fibres.

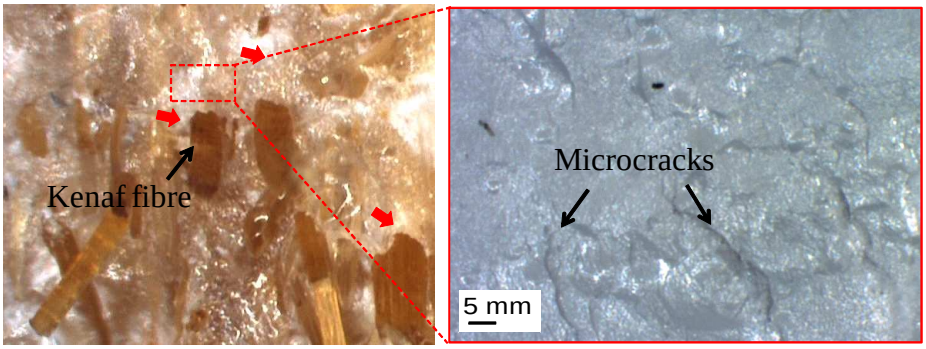


Figure 5.44: Crazing effect on 6AS-KF/30PP composites (a) Crazing effects, (b) Microcracks

Similar to Figure 5.37, Figure 5.41 indicates that the impact strength increases and reaches a maximum value at 30%. This indicates that the impact energy is effectively absorbed by the kenaf/PP composites as the fibre content increases. Based on these observations, one can conclude that a fibre content of 30% is optimal for the improvement of the impact resistance of alkali-silane treated kenaf /PP composites at 5% and 6% NaOH.

Comparing the impact performance of kenaf/PP composites to that of glass/PP composites, Figures 5.37 and 5.41 indicate that the impact strength of glass/PP composites are greater than that of alkali-silane treated kenaf/PP composites, except for composites with a fibre content less than 35%. As mentioned in section 5.1.1.2, the differences in impact performance are attributed to the exceptional tensile properties of glass fibre. Although bridging effects found on the majority of the GF/30PP specimens are clear evidence of the high tensile properties of glass fibre, no substantial bridging effects were noticed on failed alkali-silane treated/PP composites.

The results from the mechanical test and microscopic examination results presented in Section 5.1 allow the following conclusions to be drawn:

- Alkali treatments improve the mechanical properties (e.g. tensile, flexural, fatigue and impact properties) of kenaf/PP composites. However, the improvement due to alkali-silane treatments is more significant because of the additional silane treatment which enhances the fibre-matrix interfacial bonding strength. Alkali concentrations of 5% and 6% NaOH are the optimal concentrations to clean the fibre and improve the bonding strength between the kenaf fibres and the polypropylene matrix.

- Material failures in untreated kenaf/PP composites and alkali treated kenaf/PP composites are mainly characterized by fibre pull-outs, whereas fibre breakages are observed in alkali-silane treated kenaf/PP composites.

- The mechanical properties of glass/PP composites are generally greater than those of kenaf/PP composites. This is attributed to the exceptional tensile properties of glass fibre in comparison to those of kenaf fibre.

- Fibre content of 30% is optimal for the improvement of the mechanical properties (e.g. tensile, flexural, impact and fatigue strengths) of alkali-silane treated kenaf /PP composites at 5% and 6% NaOH.

5.2 Effects of fibre treatments on the resistance to moisture absorption

As discussed in Chapter 4, the saturated moisture content is calculated by using equation 4.1. For the purpose of this study, the saturation phase has been reached if the differential weight gain of a particular specimen is less than 5%. The moisture contents at saturation, $M_{S,}$ of treated and untreated kenaf/PP composites at different alkali concentrations are plotted in Figures 5.45 and 5.46 and presented in Tables 5.1 and 5.2. For a better understanding of the moisture behaviour of kenaf/PP composites, the moisture content at saturation is evaluated by considering the influence of fibre treatment and fibre content.

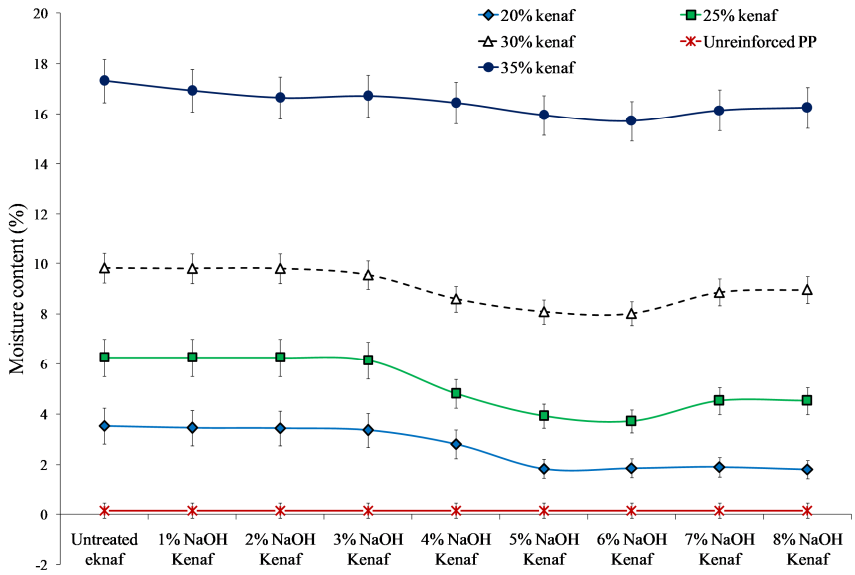


Figure 5.45: Moisture content of alkali treated kenaf/PP composites at saturation

[iii] For reference purposes the minimum saturation time, which corresponds to that of UT-KF/35PP specimen, was 72 Days.

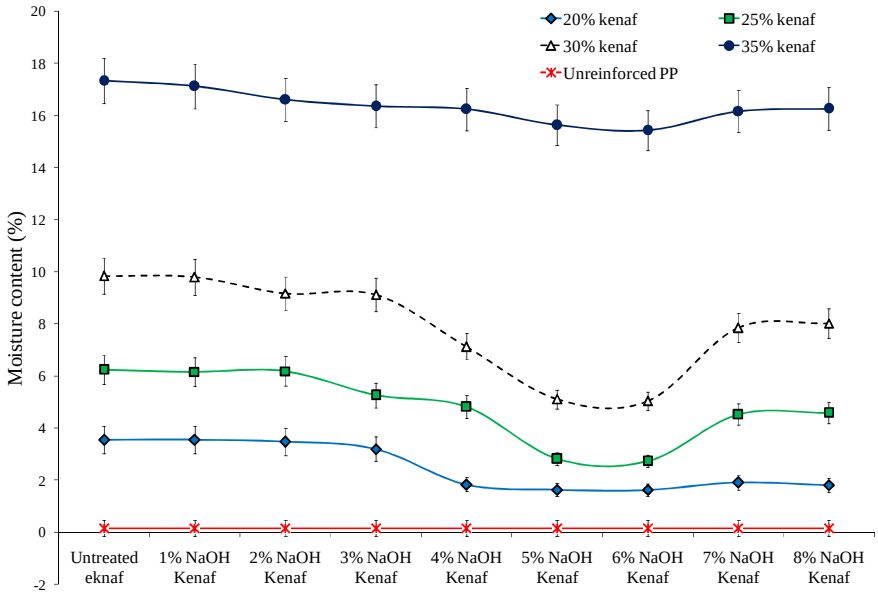


Figure 5.46: Moisture content of alkali-silane treated kenaf/PP composites at saturation

Evaluating the influence of the fibre treatment on the moisture content at saturation, Figures 5.45 and 5.46 show that M_S vary as a function of the alkali concentration. It is seen that untreated kenaf/PP, alkali treated kenaf/PP and alkali-silane treated kenaf/PP composites, treated with solutions less than and including 4% NaOH, have high values of M_S. This implies that they absorb more water than composites made of fibres treated with caustic solutions of concentrations greater than 4% NaOH. Such behaviour is attributed to an ineffective alkali treatment that is unable to remove the surface impurities of kenaf fibres [7]. As indicated in section 5.1, these surface impurities contribute to poor fibre-matrix interfacial adhesion, which in turn leads to voids and microcracks along the fibres acting as additional reservoirs and paths for penetrating water molecules. Kamal *et al* [51] argued that poor interfacial adhesion caused by surface impurities, increased the moisture absorption in hot-press moulded composites made of sawdust (Pinus radiata) reinforced polymers.

As the alkali concentration rises above 4% NaOH, the moisture content at saturation decreases and reaches a minimum value at 5% and 6% NaOH. As an example, the M_S of kenaf/PP composites with 30% fibre content drops by 45% as

the alkali concentration increases from 3% to 6% NaOH. This is a clear indication of an increase in the moisture resistance of kenaf/PP composites resulting from the improved fibre-matrix bonding.

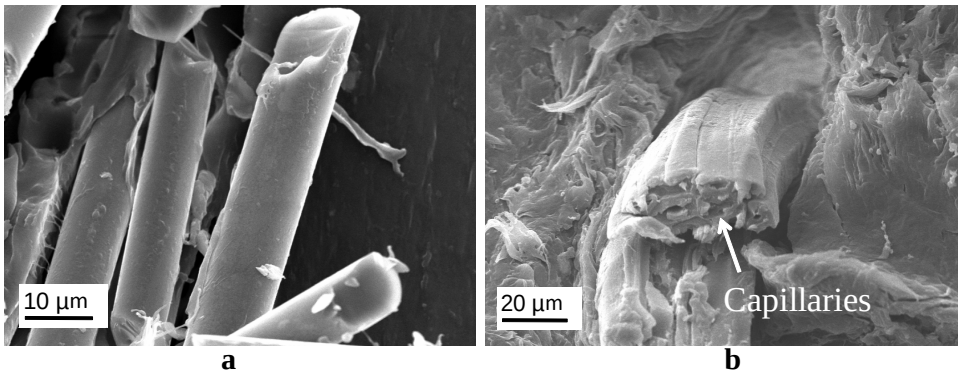
As the alkali concentration rises above 6% NaOH, the moisture content increases. This suggests that alkali treated and alkali-silane treated kenaf/PP composites, treated with 5% and 6% NaOH solutions absorb less moisture than kenaf/PP composites made of fibres treated with 7% and 8% NaOH solutions. However, the moisture contents at saturation at 7% and 8% NaOH are still smaller than those of composites treated with caustic solutions of 4% NaOH and less. This suggests that alkali treated and alkali-silane treated kenaf/PP composites made of fibres treated with 7% and 8% NaOH solutions absorb less moisture than kenaf/PP composites made of fibres treated with less than 4% NaOH solution. The raison of such behaviour is that sufficient NaOH is required to guaranty proper cleaning in order to achieve good fibre-matrix bonding. However, excessive NaOH tends to damage the fibre, thereby providing additional cavities for water molecules to penetrate into the material.

Comparing Figures 5.45 and 5.46, it is evident that that the resistance to moisture of alkali and alkali-silane treated composites considerably improve over those of untreated composites. However, the improvements of alkali-silane treated kenaf/PP composites are greater than those of alkali treated kenaf/PP composites. As an example, 6A-KF/30PP composites reached 8.01% mass gain over a period of 2500 hours, whereas 6AS-KF/30PP reached 5.03% over a period of 3600 hours. This is an expected result as the additional silane treatment reduced the amount of cavities along the interfacial regions by improves fibre-matrix interfacial adhesion in alkali-silane treated kenaf/PP.

From Table 5.1 and 5.2, it is observed that the moisture content at saturation, M_S, of both kenaf/PP and glass fibre/PP composites increases with an increase in the fibre content. As an example, the M_S of a 6AS-KF/20PP, 6AS-KF/30PP and 6AS-KF/35PP specimens are 1.62%, 5.03% and 15.42% respectively. This is due to the fact that the amount of uncovered kenaf fibres being exposed to water increases with the increase in fibre content. Paiken [(99)] also mentioned the influences of the

laminate configuration on the moisture absorption rate of hemp fibre reinforced polypropylene composite plates fabricated by compression moulding. The author reported that hemp fibres sticking out of the surface of the composites create additional pathways for water molecules to penetrate into the material, thereby leading to a higher moisture absorption rate and a higher saturation value. This tendency was more evident with an increase in fibre weight fraction.

Comparing the M_S of kenaf/PP to those of glass/PP composites it can be noted that the moisture contents at saturation of kenaf/PP composites are smaller than those of glass/PP composites in general. High moisture content at saturation in kenaf/PP composites could be attributed to several factors, including the availability of hydroxyl groups attached to the fibres, the amount of voids along the fibre-matrix interface and the presence of capillaries in kenaf fibres, which provide additional cavities for water molecules. Capillaries in kenaf fibre are illustrated in Figure 5.47. Sgriccia *et al* [60] also reported similar findings. The authors argued that natural fibre composites absorb more water than glass fibre composites because they absorb water through several pathways including fibres and matrix. SEM images revealed that glass fibres do not have capillaries that can act as reservoirs for water molecules, Figure 5.47 (a). Therefore, gaps and voids along the interfacial regions were identified as the main cause of the increase of M_S with the increase in the fibre content given the hydrophobic nature of glass fibre.



a **b**

Figure 5.47: Morphological configuration of glass and kenaf fibre

The saturation time, T_S, as determined in the present study, is significantly greater than those reported in literature [52]. For example, alkali treated kenaf/PP composites had an 8.01% mass increase at saturation over a period of 100 days, whereas alkali-silane treated kenaf/PP composites had a 5.03% increase over a period of 150 days. Microscopic examination in conjunction with the test results showed that the manufacturing technique, which enables the manufacturing of composite plates with layers of different moisture diffusion resistances, had a significant influence on the resistance of kenaf/PP composites. Prior to compaction, PP sheets and kenaf mats are arranged in such a way that kenaf mats are sandwiched between layers of PP sheets, Figure 3.40 (b). During the compression phase, conducted at 250ºC, the molten PP matrix diffuses into the mats and encapsulates them, forming a matrix rich layer on both outer surfaces of the laminate. This results in the top and bottom layers (hydrophobic layers) of the fabricated composite having a reduced fibre content in comparison to the core (fibre-dominated region). The change in fibre content through the thickness results in a variation of the diffusion rate since the diffusion coefficient tends to increase towards the core of the laminate. Therefore, the outer hydrophobic layers act as barriers against water molecules, thereby reducing the kinetic of the fluid front penetrating into the core of the composite. A cross section view of a 6AS-KF/20PP composite (Figure 5.48) shows the variation of fibre content through the laminate. The present configuration cannot be achieved by other fabrication methods such as injection moulding, extrusion and resin transfer moulding techniques. For example, not all of the fibres located on the surface of composite plates fabricated by injection moulding are covered with matrix. When a composite plate (fabricated by the extrusion method) is exposed to moisture, uncovered edges of the fibres will therefore constitute preferential paths for water molecules, given the hydrophilic nature of natural fibres. This suggests that kenaf/PP composites fabricated by CMFST are expected to have an extended service life since the kinetic of the diffusion process causing material degradation (swelling, leaching, bio-degradation) is significantly reduced. It is therefore obvious that the practical advantage the compression moulding is the ability to

fabricate kenaf/PP composite plates with lower moisture content at saturation and extended saturation time.

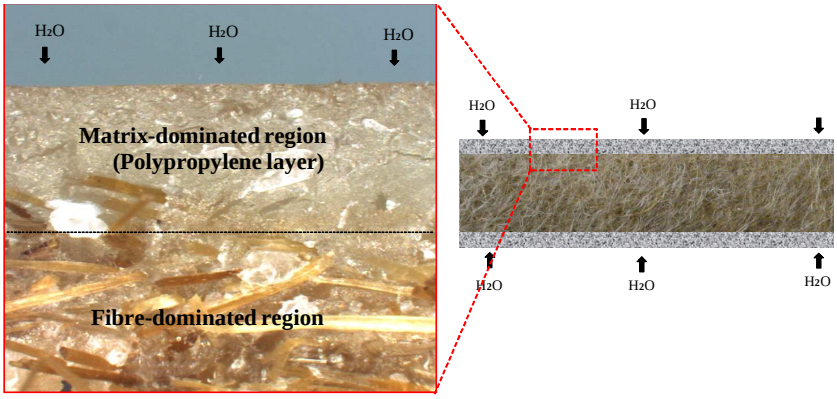


Figure 5.48: Fibre and matrix dominated regions of 6AS-KF/20PP composite

Table 5.1: Moisture contents at saturation of Alkali treated kenaf /PP composites

	Moisture content at saturation, M_S, (%)			
Composites	20% fibre content	25% fibre content	30% fibre content	35% fibre content
Untreated kenaf	3.54	6.24	9.83	17.32
1% NaOH treated kenaf	3.45	6.23	6.81	16.93
2% NaOH treated kenaf	3.44	6.24	9.80	16.65
3% NaOH treated kenaf	3.36	6.13	9.55	16.72
4% NaOH treated kenaf	2.81	4.81	8.59	16.45
5% NaOH treated kenaf	1.84	3.92	8.08	15.95
6% NaOH treated kenaf	1.86	3.72	8.01	15.72
7% NaOH treated kenaf	1.91	4.52	8.86	16.15
8% NaOH treated kenaf	1.81	4.52	8.96	16.25
Glass fibre/PP	0.92	2.32	4.25	13.52

Table 5.2: Moisture content at saturation of Alkali-silane treated kenaf/PP composites

	Moisture content at saturation, M_S, (%)			
Composites	20% fibre content	25% fibre content	30% fibre content	35% fibre content
1% NaOH-silane treated kenaf	3.55	6.15	9.79	17.11
2% NaOH-silane treated kenaf	3.47	6.18	9.16	16.60
3% NaOH-silane treated kenaf	3.19	5.26	9.11	16.35
4% NaOH-silane treated kenaf	1.83	4.81	7.12	16.23
5% NaOH-silane treated kenaf	1.63	2.81	5.10	15.62
6% NaOH-silane treated kenaf	1.62	2.73	5.03	15.42
7% NaOH-silane treated kenaf	1.91	4.52	7.84	16.15
8% NaOH-silane treated kenaf	1.81	4.58	8.01	16.25

The moisture absorption test results presented in Section 5.2 lead to the followings conclusions:

- Alkali treatments improve the resistance to moisture absorption of kenaf fibre/PP composites, 5% and 6% NaOH are found to the optimal concentrations.
- kenaf fibre/PP composites absorb more water than glass fibre/PP composites due to the hydrophilic nature of kenaf fibres. However, improved moisture resistance of alkali-silane treated specimens in comparison to those of untreated and alkali treated specimens is attributed to the additional silane treatment.
- The compression moulding using the film–stacking technique enables the manufacturing of kenaf/PP composite plates with matrix rich layers on both outer surfaces, contributing to the improvement of the moisture diffusion resistance.

5.3 Effect of the inclusion of MWCNTs on the mechanical properties

The influence of the CNT concentration on the mechanical properties of kenaf/PP-MWCNT composites are discussed below. However, the effects of including both the raw and functionalized MWCNTs on the mechanical properties (e.g. tensile, flexural and impact properties) of the polypropylene matrix, at various CNT concentrations, are initially discussed in order to obtain a better understanding. This also facilitates the evaluation of the effectiveness of the functionalization process. The impact of the CNT inclusion on the crystalinity of the polypropylene matrix is also investigated by evaluating the brittleness of the MWCNT-PP specimens by examining the failure modes under impact load.

The improvement of the mechanical properties of kenaf/PP-MWCNT composites (e.g. tensile, flexural, fatigue and Izod impact strengths) will be evaluated in relation to the CNT concentration. For comparison purposes, the mechanical properties of kenaf/PP-MWCNT composites are compared to that of unreinforced polypropylene, MWCNT-PP and 6AS-KF/30PP. A 6AS-KF/30PP composite plate was selected since it was fabricated using the optimal alkali concentration (e.g. 6% NaOH) and fibre content (e.g. 30% fibre content). The failure characteristics of kenaf/PP-MWCNT composites are discussed based on microscopic examination results. The improvement of the mechanical properties of kenaf/PP-MWCNT composites are also compared to that of glass/PP composites.

Mechanical properties of MWCNT-PP plates

The effects of CNT concentration on the mechanical properties of MWCNT-PP plates are presented in Figures 5.49 through 5.52. The tensile properties (tensile modulus and strength) were determined in accordance with BS ISO 527 and ASTM D 3039/D 3479M-96 [75, 76]. The flexural properties were determined in accordance with BS ISO 178 and ASTM D790-10 [77, 78]. The test results show that the mechanical properties of functionalized MWCNT-PP increase with an increase in the MWCNT concentration. There is no evidence of improvement in tensile strength, tensile modulus, flexural strength and Izod impact strength at

CNT concentration less than 0.25% (e.g. 0.1%). This suggests that the quantity of CNTs incorporated into the matrix at a concentration of 0.1% is inadequate to improve the strength of the material as the load is predominantly still carried by the matrix. The improvement slightly becomes noticeable at 0.25%, for example, the tensile modulus and tensile strength improve by about 12.8% and 3.5% respectively whereas the flexural strength and impact strength increase by 3.51% and 9.21% respectively. The tensile, flexural and impact strength reaches a maximum value at about 0.50% and 0.75%, indicating significant load transfer from the matrix to the CNTs [6, 8]. The tensile modulus and tensile strength improve by about 84.4% and 48% respectively at 0.50% CNT, while the flexural strength and impact strength increase by 37.4% and 57.2% respectively at 0.75% CNT. These improvements also imply that improved dispersion of the CNTs in the matrix and enhanced interfacial bonding between the CNTs and the PP matrix was achieved through the functionalization process. With further increase of the CNT concentration (e.g. beyond 0.75%), the tensile and flexural strength remain relatively constant whereas the tensile modulus (Figure 5.49) and Izod impact strength (Figure 5.52) drop by more than 10% and 25% respectively. Microscopic examination showed that at higher concentration, carbon nanotubes tend to form clusters in the matrix, which results in the formation of voids and material discontinuities acting as stress raisers. Previous studies also reported the decrease in the mechanical properties of functionalized MWCNT reinforced polypropylene as a result of an increased CNT concentration. Zhou *et al* [16] reported that 1% is the optimal CNT concentration required for sufficient dispersion of the MWCNTs. They indicated that a homogeneous dispersion of MWCNTs, using melt mixing, is difficult to achieve if additional MWCNTs are added. This is because the additional nanotubes act as material defects due to agglomeration, further decreasing the tensile strength of MWCNT reinforced PP composites. Prashantha *et al* [68] also reported similar findings. They argued that an increase in MWCNT concentration beyond 2% compromised the impact properties of PP-g-MA functionalized MWCNT reinforced PP.

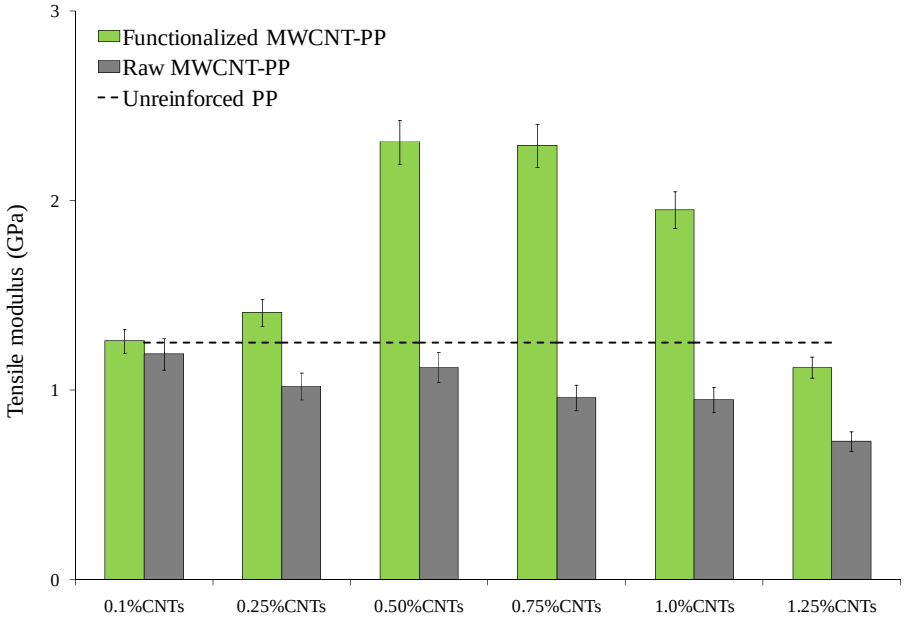


Figure 5.49: Tensile modulus of functionalized MWCNT-PP

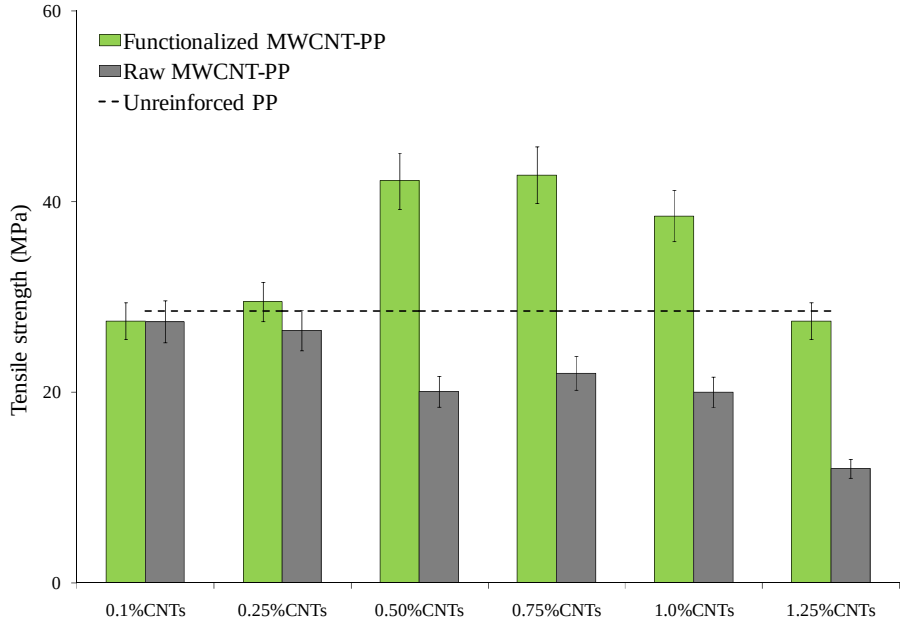


Figure 5.50: Tensile strength of functionalized MWCNT-PP

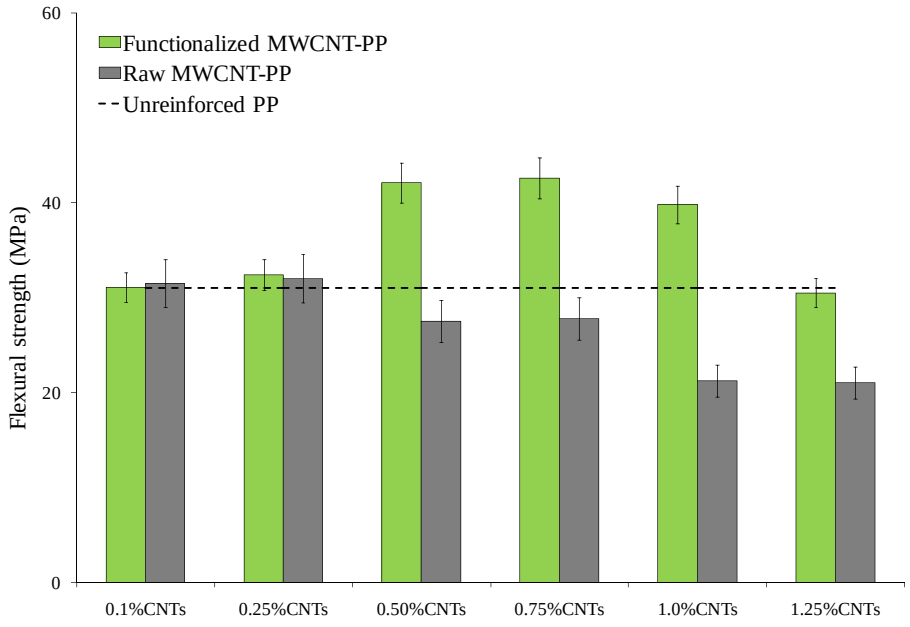


Figure 5.51: Flexural strength of functionalized MWCNT-PP

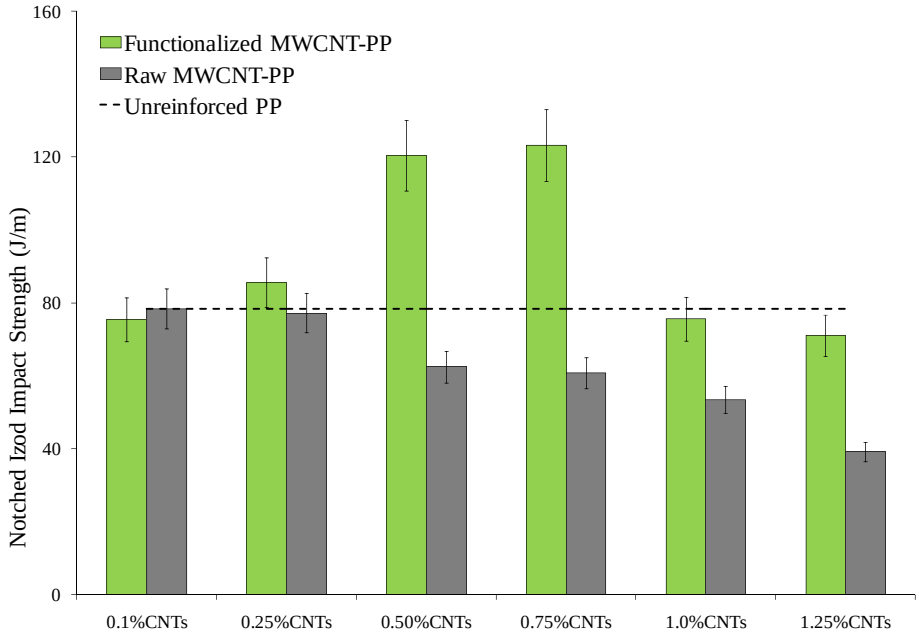


Figure 5.52: Izod impact strength of functionalized MWCNT-PP

Figures 5.49 through 5.52 also show that the mechanical properties of functionalized MWCNT-PP are greater than those of raw MWCNT-PP plates, regardless the CNT concentration. CNT clusters caused by inadequate CNT dispersion and acting as stress raisers were found to be the predominant factor that

negatively impacted the mechanical properties. It can be seen that the mechanical properties of the raw-MWCNT-PP specimens decrease with the increase in CNT concentration. The decrease is significant at CNT concentration greater than 0.25%. SEM showed that the quantity and size of the CNT clusters increase with the increase in CNT concentration. This suggests that CNT functionalization has definitely contributed in improving the mechanical properties of the polypropylene. These observations suggest that 0.5% and 0.75% are the optimum CNT concentrations for improving the mechanical properties of the MWCNT-PP plates.

The impact failure modes of the functionalized MWCNT-PP plates at various CNT concentrations were compared and the results were used to evaluate the change in the brittleness of the material (Figure 5.53). Similar damage characteristics are observed for all the specimens: the cracks propagate parallel to the direction of the applied force and there is no evidence of a particular failure mode to suggest the influence of the CNT concentration on the brittleness of the material.

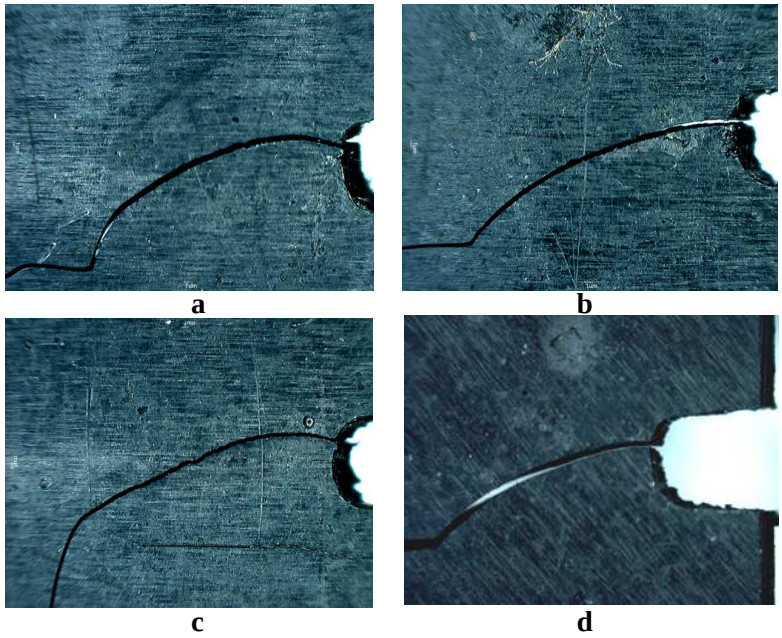


Figure 5.53: Typical fracture path of MWCNT-PP: (a) 0.25%, (b) 0.50%, (c) 0.75% and 1% MWCNT concentration

5.3.1 Tensile strength and tensile modulus of kenaf/PP-MWCNT composites

Figures 5.54 and 5.55 show that the tensile strength and tensile modulus of kenaf/PP-MWCNT composites increases with an increase in the CNT concentration. There is no evidence of improvement at CNT concentrations less than 0.25% (e.g. 0.1%). The tensile properties of kenaf/PP-MWCNT composites compare to those of 6AS-KF/30PP composites. This suggests that the quantity of CNTs incorporated into the matrix at a concentration of 0.1% is inadequate for further tensile strength improvement. The increase in the tensile strength and tensile modulus becomes noticeable at 0.25%. For example the tensile modulus and tensile strength improve by 12.8% and 3.5% respectively when compared to that of a 6AS-KF/30PP composite. The tensile properties reach a maximum value at 0.5% and 0.75% CNT. This suggests that 0.5% and 0.75% are the optimums functionalized CNT concentration required for improvement of the tensile properties of the kenaf/PP-MWCNT composites. The tensile strength and tensile modulus drop with an additional increase in the CNT concentration (e.g. at 1.0 and 1.25% CNT). At 1.25% CNT the tensile strength of a 6AS-KF/30PP-1.25MWCNT specimen is reduced to a value below that of unreinforced PP. The reduction is caused by excessive CNT aggregates which act as stress raisers in the bulk of the composites. Zhou *et al* [16] reported similar findings while investigating on the functionalization of MWCNTs with silane and its influences on the tensile properties of CNT reinforced PP composites. The authors argued that excessive CNT concentrations reduced the tensile strength of the MWCNT reinforced PP composites by acting as defects within the material. Although fibre breakage, Figure 5.56 (b), was found to be the prevalent failure mode, material failures mainly originated from the voids in both matrix and fibre dominated regions.

Figures 5.54 and 5.55 also show that the tensile strength and tensile modulus of kenaf/PP-MWCNT composites surpass those of a GF/30PP composite at 0.5% and 0.75% CNT. As an example, the tensile strength of 6AS-KF/30PP-0.5MWCNT and 6AS-KF/30PP-0.75MWCNT specimens are greater than that of

a GF/30PP composite by 15.6% and 13.5%, respectively. One can agree that the improvement of the tensile properties of kenaf/PP-MWCNT composites are most likely caused by a similar improvement in the matrix due to the incorporation of functionalized MWCNTs. Adherence of the matrix to the surface of kenaf fibres of a 6AS-KF/30PP-0.75MWCNT specimen subsequent to failure, Figure 5.56 (a), suggests strong fibre–matrix interfacial bonding resulting from the chemical treatment. This also indicates that the incorporation of the functionalized MWCNTs into the matrix does not compromise the interfacial bonding strength between the alkali silane treated fibres and the matrix, due to similar observations (matrix adhering to the kenaf fibres) being made on alkali-silane treated kenaf/PP composites, Figures 5.32 and 5.56 (a).

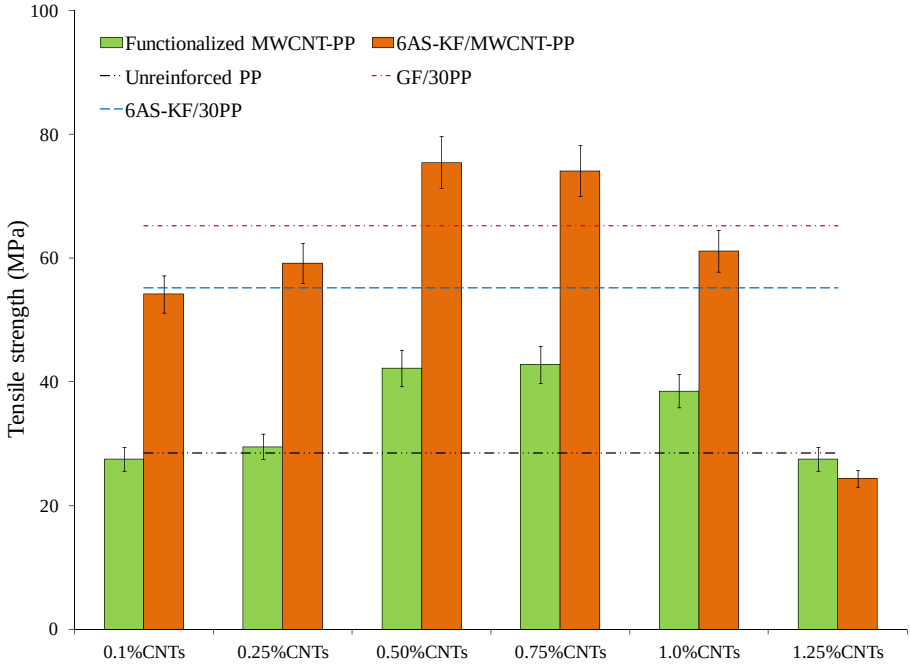


Figure 5.54: Tensile strength of kenaf/PP-MWCNT composites

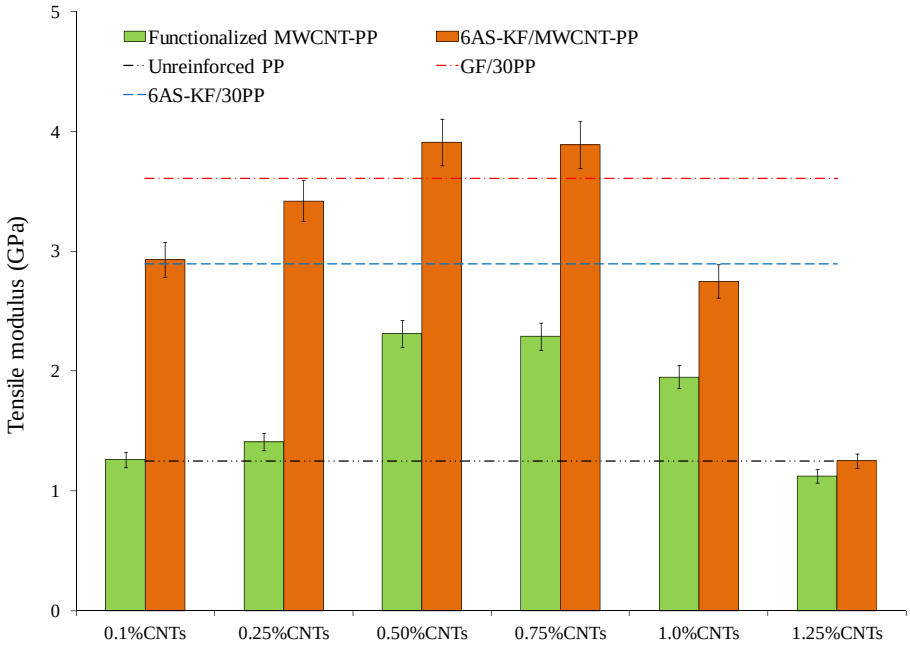
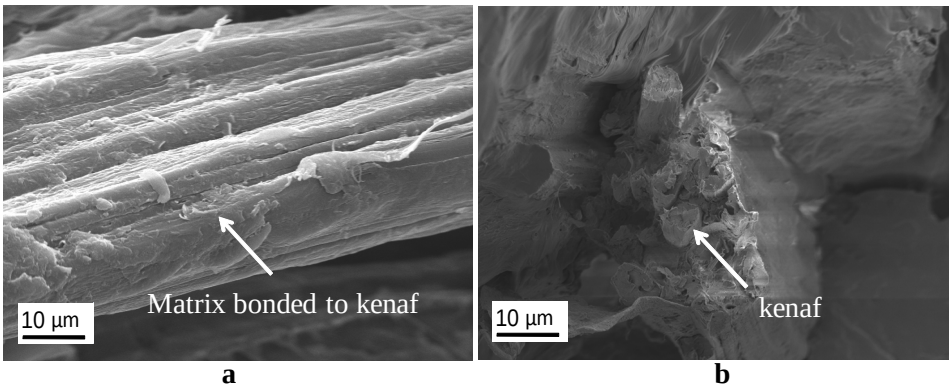


Figure 5.55: Tensile modulus of kenaf/PP-MWCNT composites



a **b**

Figure 5.56: Kenaf fibre: (a) Matrix adhering to the kenaf fibre and (b) fibre breakage

5.3.2 Flexural strength of kenaf/PP-MWCNT composites

Figure 5.57 shows the flexural strength of the kenaf/PP-MWCNT composites increasing with an increase in the CNT concentration. At a concentration of 0.1% and 0.25% CNT, the flexural strength compares well with that of a 6AS-KF/30PP specimen. The flexural strength reaches a maximum value at 0.5% and 0.75% CNT, suggesting that the two concentrations are optimal. The flexural strength

significantly drops with a further increase in concentration, most likely because of the formation of CNT agglomerates. As an example, it is drops below the value of unreinforced PP by 28%, at a concentration of 1.25% CNT. Although it was found that fibres tended to pull out of the matrix, breakages were the predominant failure mode in fibre dominated regions, regardless the CNT concentration, Figure 5.58 (a), whereas matrix cracks were the predominant failure mode in matrix dominated regions. However, a yielding matrix and a rough cavity surface, caused by the kenaf fibres pulling out of the matrix, imply that strong fibre-matrix adhesion was achieved Figure 5.58 (b).

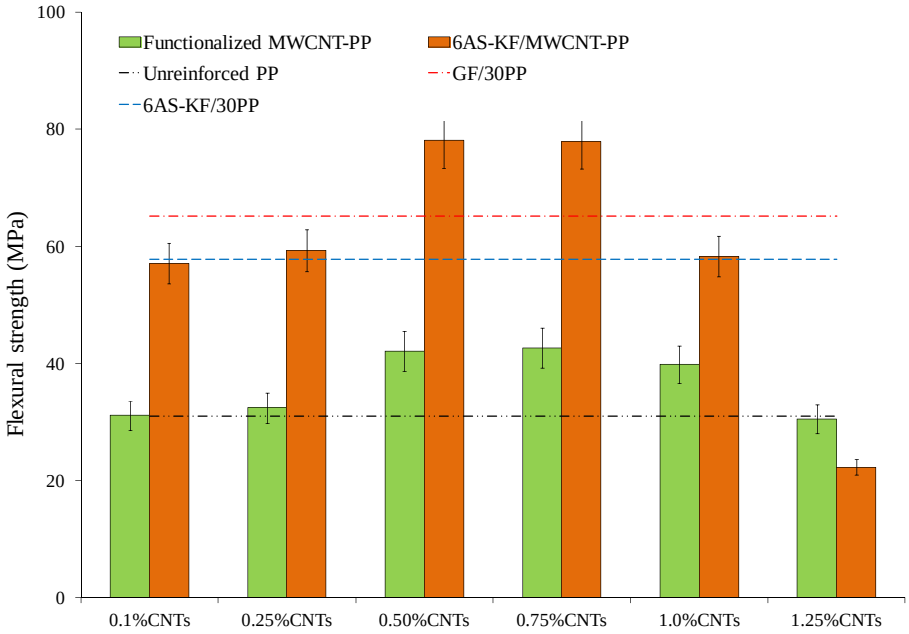


Figure 5.57: Flexural strength of kenaf/PP-MWCNT composites

The improvement in the flexural strength of the kenaf/PP-MWCNT composites, when compared to that of glass/PP composites, demonstrates the positive contribution of the functionalized CNTs, for instance, the flexural strength of a 6AS-KF/30PP-0.75MWCNT specimen is 20% greater than that of GF/30PP.

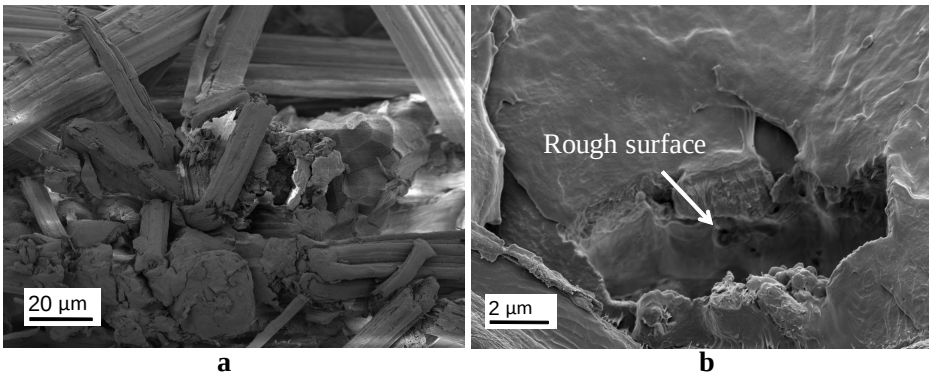


Figure 5.58: (a) Fibre breakage and (b) Matrix yielding and a rough cavity surface

5.3.3 Fatigue strength of kenaf/PP-MWCNT composites

Figures 5.59 through 5.61 illustrate the influence of the CNT concentration on the fatigue strength of kenaf/PP-MWCNT composites at different stress levels. The fatigue life of kenaf/PP-MWCNT composites are compared to that of alkali-silane treated kenaf/PP and glass/PP composites in order to evaluate the effect of the CNT inclusion.

A general observation can be made when viewing these figures: the fatigue life increases as the CNT concentration increases. There is, however, no clear evidence of improvement at 0.1% CNT, regardless the stress level. The fatigue life of the kenaf/PP-MWCNT compares well with that of an alkali-silane treated kenaf/PP specimen. This substantiates the proposal suggesting that the quantity of CNTs incorporated into the matrix at a concentration of 0.1% is inadequate to improve the strength of the material. The fatigue life improves slightly at 0.25% CNT and reaches a maximum at 0.5% and 0.75% CNT, illustrating the contribution of functionalized CNTs to the fatigue strength. For example, the fatigue life of 6AS-KF/30PP-0.5MWCNT and 6AS-KF/30PP-0.75MWCNT composites at 30% UTS is greater than that of GF/30PP by 7.5% and 5.7%, respectively. The failure mode of these composites is mainly characterized by fibre breakage in fibre dominated regions, whilst cracks, initiating in both fibre and matrix dominated regions, suggest strong adhesion between the fibres, matrix and the MWCNTs. Cracks initiating in matrix dominated region, are shown in

Figure 5.62. Matrix adhering to kenaf fibres of a 6AS-KF/30PP-0.5CMWNT specimen shows that the CNT functionalization process did not compromise the strength of the fibre-matrix interfacial adhesion.

As the CNT concentration rises above 0.75%, the fatigue life drops below that of unreinforced PP, at all stress levels. The main cause of the reduction is voids, caused by improper CNT dispersion at high CNT concentrations, subsequently acting as stress raisers.

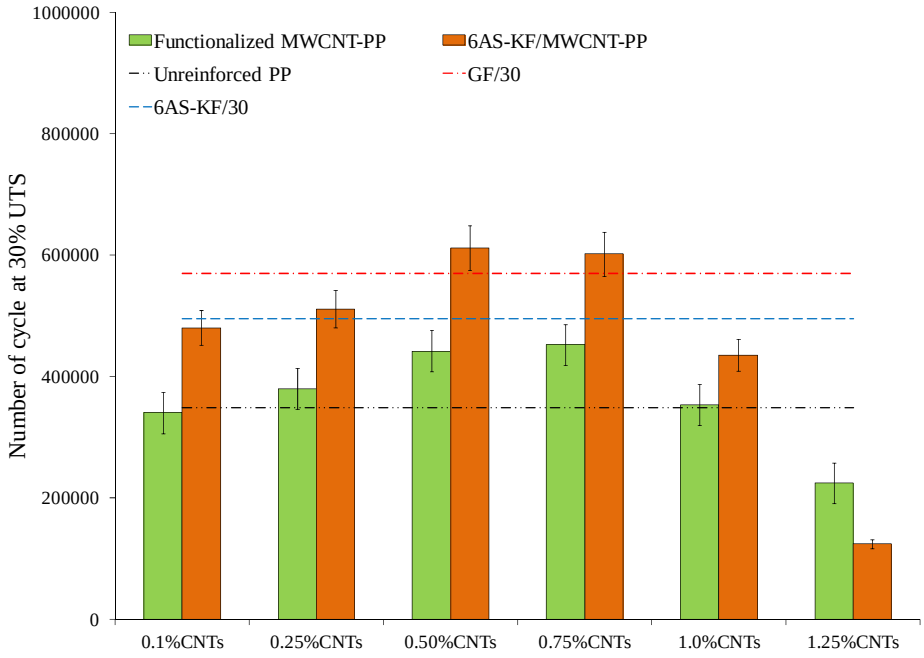


Figure 5.59: Fatigue life of alkali-silane treated kenaf/PP-MWCNT composites at 30% of UTS

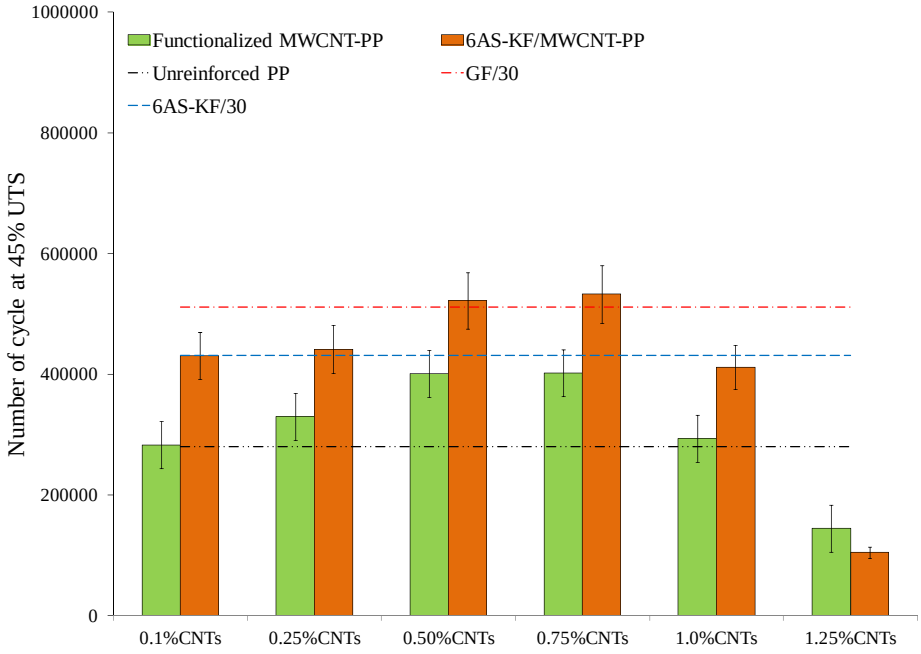


Figure 5.60: Fatigue life of alkali-silane treated kenaf/PP-MWCNT composites at 45% of UTS

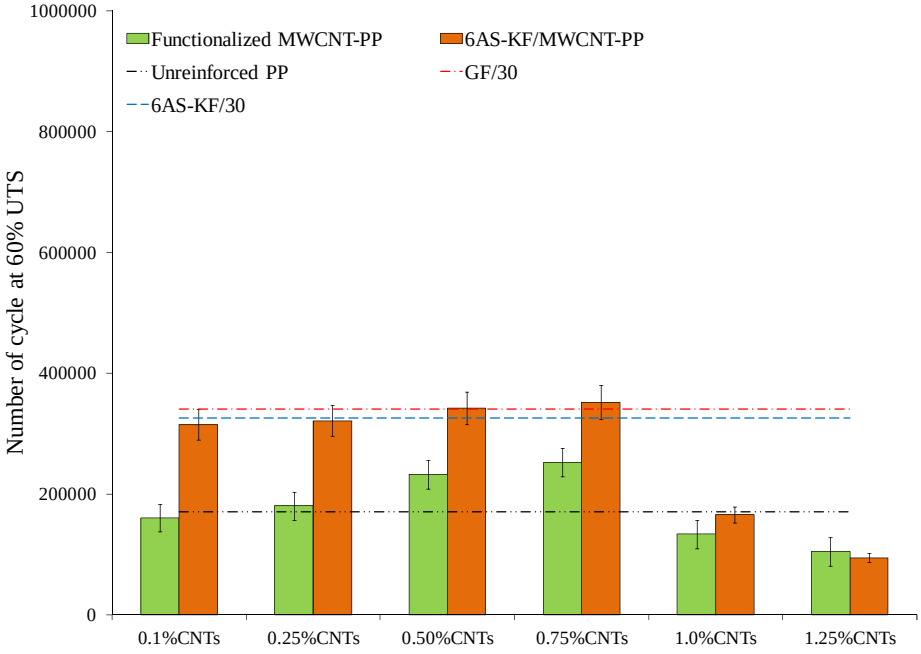


Figure 5.61: Fatigue life of alkali-silane treated kenaf/PP-MWCNT composites at 60% of UTS

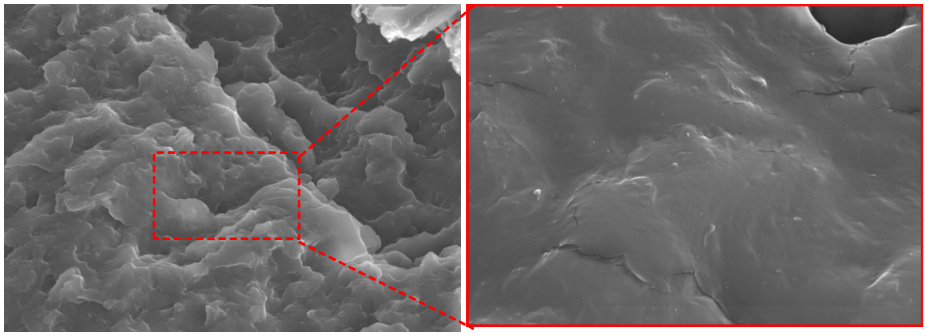


Figure 5.62: Cracks in matrix dominated region of 6AS-KF/30PP-0.5CMWNT composite

5.3.4 Izod impact strength of kenaf/PP-MWCNT-composites

Figure 5.63 shows that the impact strength increases with an increase in the CNT concentration. At 0.1% CNT, no increase is observed, and compares well with that of 6AS-KF/30PP. A fair increase is achieved at 0.25% CNT, obtaining a maximum value at 0.50% and 0.75%, resulting in effective load transfer between the matrix and fibres. Figure 5.63 also shows that the 6AS-KF/30PP-0.5CMWNT and 6AS-KF/30PP-0.75CMWNT composites perform well when compared to 6AS-KF/30PP and GF/30PP composites. For example, the impact strength of a 6AS-KF/30PP-0.5CMWNT specimen is 12.1% and 33.5% greater than that of 6AS-KF/30PP and GF/30PP specimens, respectively. The increase is attributed to the exceptional mechanical properties of the CNTs contributing to the mechanical strength of the composite.

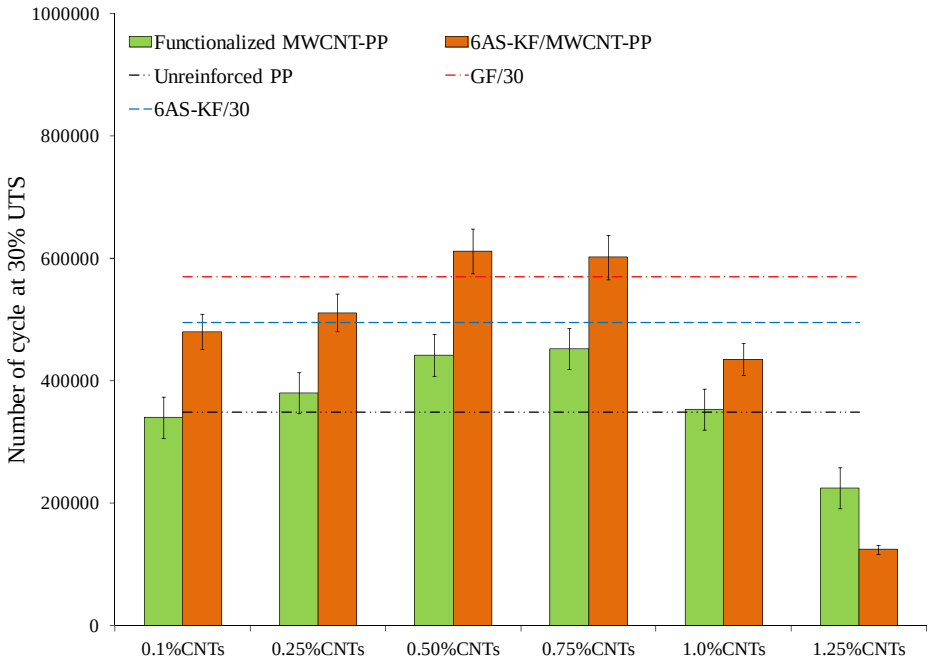


Figure 5.63: Impact resistance of Alkali-silane treated kenaf/PP-MWCNT composites

Splitting fibres (Figure 5.64) suggest that a considerable amount of the impact energy has been absorbed by the kenaf fibres, serving as an indication of a strong fibre-matrix interfacial adhesion. All the kenaf/PP-MWCNT specimens exhibited these failure modes. Brittle fractures were the main failure mode in the matrix dominated regions, Figure 5.65 (a). Where fibres pulled out of the matrix, yielding and rough cavity surfaces occurred, indicating that strong fibre-matrix interfacial adhesion was achieved, Figure 5.65 (b). This serves as proof that the smooth internal surface of the cavity, illustrated in Figure 5.38 (b), is evidence of poor fibre-matrix adhesion.

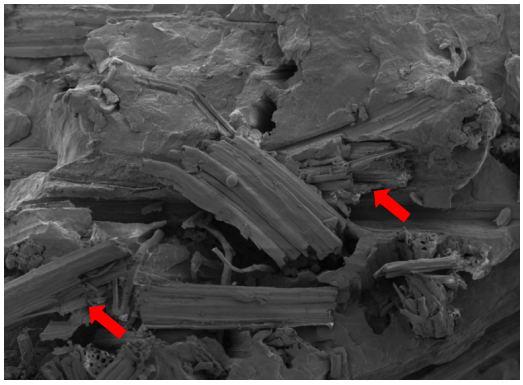
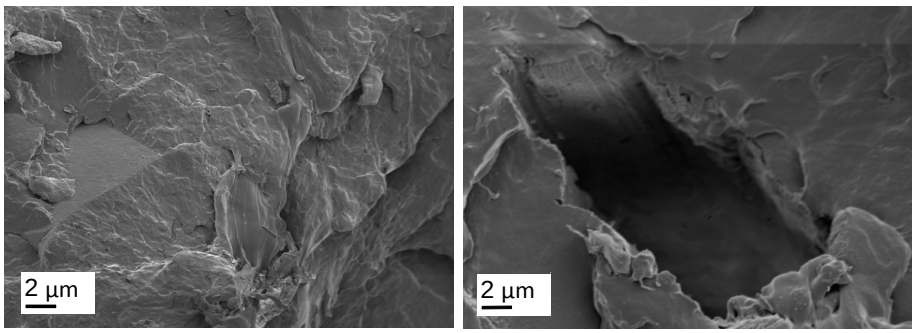


Figure 5.64: Fibre splits and breakage



a **b**

Figure 5.65: (a) Brightly facture and (b) Matrix yield and rough surface of the cavity

The results from the mechanical tests and microscopic examination presented in Section 5.3, allow the following conclusions to be drawn:

- The addition of multi-wall carbon nanotubes in sufficient quantities significantly increases the mechanical properties (e.g. tensile, flexural, fatigue and impact properties) of kenaf/PP composites. Findings indicate that 0.5% and 0.75% are the optimum CNT concentrations.

- The improved mechanical properties of alkali-silane treated kenaf/PP-MWCNT composites in comparison to glass/PP composites results from the exceptional mechanical properties of the CNTs and the functionalization process.

- Fibre breakage was found to be the prevalent failure mode in fibre dominated regions; cracks occurred mainly in matrix dominated regions.

- An optimal fibre content of 30% is required for improvement of the mechanical properties of kenaf/PP and kenaf/PP-MWCNT composites.

5.4 Effect of the inclusion of MWCNTs on the resistance to moisture absorption

The moisture content of raw MWCNT-PP, functionalized MWCNT-PP and kenaf/PP-MWCNT composites at saturation, $M_{S,}$ are shown in Table 5.3 and depicted in Figure 5.66, for various CNT concentrations. The moisture absorption characteristics are compared to that of unreinforced polypropylene, alkali-silane treated kenaf/PP and glass/PP composites in order to evaluate the effect of the CNTs.

Although slight discrepancies are noticed, Figure 5.66 shows that the moisture content of saturated MWCNT-PP and kenaf/PP-MWCNT specimens compare well and do not vary as a function of the CNT concentration. An maximum of 16% difference can be noted. This indicates that the incorporation of the CNT as a filler material does not affect the moisture absorption resistance of alkali-silane treated kenaf/PP composites. This is attributed to the hydrophobic nature of CNTs and the effective interfacial adhesion between the CNTs and the fibre and matrix. Paiken [99] also reported the increase of the moisture absorption rate with the increase of the carbon nanotubes in natural fibre reinforced polypropylene composites fabricated by compression moulding. The CNT's were not functionalized. He argued that the increase in moisture content was most likely due to the holes created in the matrix by the carbon nanotube agglomerates creating pathways for the water to diffuse through the thickness of the composite.

It is also noted that, Figure 5.66, kenaf/PP-MWCNT specimens absorb more water than glass/PP composites due to the hydrophilic nature thereof, regardless of the CNT concentration. As indicated in section 5.2, gaps and voids along the interfacial regions of the fibres were identified as the main cause of the moisture up take in glass/PP composites.

The laminate configuration also had an impact on the moisture behaviours of kenaf/PP composites are presented in section 5.2. A cross sectional view of a 6AS-KF/20PP-0.5MWCNT specimen is presented in Figure 5.67, showing the outer hydrophobic layers which act as moisture barriers.

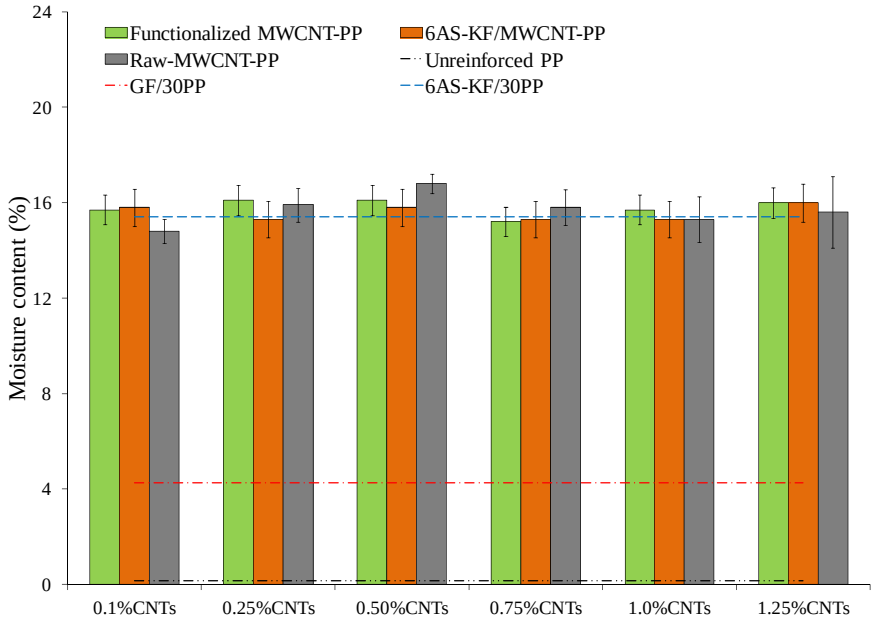


Figure 5.66: Moisture content of MWCNT-PP and kenaf/PP-MWCNT composites at saturation

Table 5.3: Moisture contents at saturation of MWCNT-PP and alkali-silane treated kenaf/PP-MWCNT

	Moisture content at saturation, M_S, (%)					
Composites	0.1%	0.25%	0.50%	0.75%	1.0%	1.25%
Raw MWCNT-PP	14.8	15.9	16.8	15.8	15.3	15.6
Functionalized MWCNT-PP	15.7	16.1	16.1	15.2	15.7	16.0
6AS-KF/MWCNT-PP	15.8	15.3	15.8	15.3	15.3	16.0

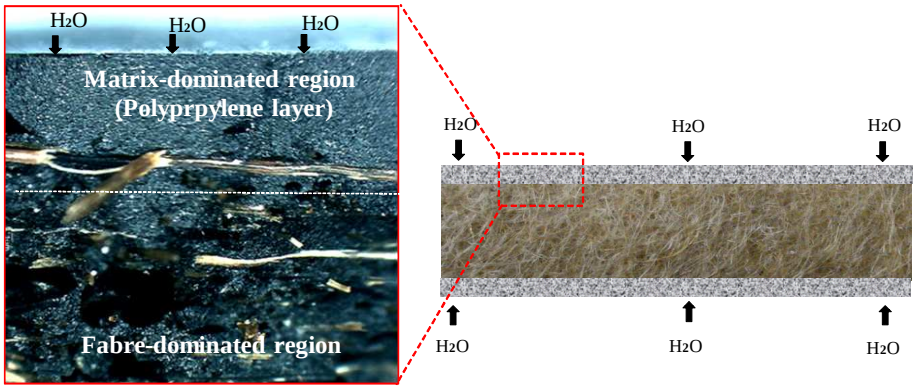


Figure 5.67: Fibre and matrix dominated regions of 6AS-KF/20PP-0.5MWCNT composite

The moisture absorption test results discussed in this Section 5.4, allow the following conclusions to be drawn:

- The resistance to moisture absorption is not altered by the addition of the multi-wall carbon nanotubes into the polypropylene matrix.
- The matrix rich layers on the outer surfaces of the kenaf/PP-MWCNT composite plates contribute to the moisture diffusion resistance.

6 CONCLUSIONS

The results of the mechanical tests and microscopic examinations discussed in the preceding chapters, allow the following conclusions to be drawn:

- Alkali treatments improve the mechanical properties (e.g. tensile, flexural, fatigue and impact properties) of kenaf/PP composites. However, the improvement due to the alkali-silane treatment is more significant (by 130%) because the additional silane treatment substantially enhances the fibre-matrix interfacial bonding strength.

- Alkali concentrations of 5% and 6% NaOH are optimal for increasing the surface roughness of the kenaf fibre and exposing more cellulose on the surface of the fibre to potential chemical bonding with the matrix material.

- Material failures in untreated kenaf/PP composites and alkali treated kenaf/PP composites are mainly characterized by fibres pulling out of the matrix, whereas fibre breakage are observed in alkali-silane treated kenaf/PP composites.

- The mechanical properties of glass/PP composites are generally greater than those of kenaf/PP composites. This is attributed to the exceptional tensile properties of glass fibre in comparison to those of kenaf fibre.

- Kenaf fibre/PP composites absorb more water than glass fibre/PP composites due to the hydrophilic nature of kenaf fibres. Improved moisture resistance of alkali-silane treated specimens in comparison to those of untreated and alkali treated specimens is attributed to the additional silane treatment. Alkali concentrations of 5% and 6% NaOH are found to be optimal for improving the moisture absorption resistance of kenaf/PP composites.

- Compression moulding using the film–stacking technique enables the manufacturing of kenaf/PP composite plates with matrix rich layers on both outer surfaces, contributing to the improvement of the moisture diffusion resistance.

- The addition of sufficient quantities of multi-wall carbon nanotubes significantly increases the mechanical properties (e.g. tensile, flexural, fatigue and impact properties) of kenaf/PP composites. Results show that the optimal concentrations are 0.5% and 0.75% CNT. Fibre breakage was found to be the prevalent failure mode in fibre dominated regions, matrix cracks occurred mainly in matrix dominated regions.

- The exceptional mechanical properties of multi-wall carbon nanotubes, as well as the functionalization process, resulted in improved mechanical properties (e.g. tensile, flexural, fatigue and impact properties) of alkali-silane treated kenaf/PP-MWCNT composites in comparison to that of glass/PP composites.

- A fibre content of 30% is optimal for the improvement in the mechanical properties of kenaf/PP and kenaf/PP-MWCNT composites.

- The impregnation of kenaf and fibre glass mats with polypropylene powder facilitated a uniform material distribution and lower manufacturing temperature (122.5°C), thereby preventing the thermal degradation of the kenaf fibres and silano functional groups.

- The moisture absorption resistance ok kenaf/PP-MWCNT composites is not altered by the addition of multi-wall carbon nanotubes to the polypropylene matrix.

7 RECOMANDATIONS

The experimental work conducted in this study showed that the fibre treatment and inclusion of carbon nanotubes as filler material improved the mechanical properties of kenaf fibre reinforced polypropylene composites. It is recommended that an investigation be launched into the cost of the improvement.

The combined effect of mechanical stress (e.g. tensile stresses) and a hostile environment (e.g. ultra-violet radiation, moisture) can cause plasticization and lead to a transition from ductile to brittle behaviour. Investigation into the influence of the environmental conditions on the mechanical properties (e.g. impact strength, etc.) of kenaf fibre reinforced polypropylene composites is therefore recommended.

In this study, Izod pendulum impact tests were conducted to evaluate the effect of the manufacturing variables on the impact strength. It is proposed that the design of kenaf fibre reinforced polypropylene composites, with specific focus on the prevention of crack initiation and subsequent propagation under high and low speed impact loads, be investigated. This will require high speed puncture tests using load and displacement sensors.

REFERENCES

1) M Zampaloni, F Pourboghrat, SA Yankovich, B.N. Rodgers, J. Moore, L.T. Drazal, A.K. Mohanty and M. Misra. Kenaf natural fiber reinforced polypropylene composites: A discussion on manufacturing problems and solutions. Composites: Part A, 38:1569–1580, 2007.
2) P Wambua, J Ivens and I Verpoest. Natural fibres: can they replace glass in fibre reinforced plastics? Composites Science and Technology, 63: 1259–1264, 2003.
3) BC Suddell. Industrial Fibres: Recent and Current Developments. Proceedings of the symposium on natural fibres, page 71-82, Rome, 20 October 2008.
4) AK Mohanthy, M Misra, LT Drzal. Surface modifications of natural fibers and performance of the resulting biocomposites: An overview. Compos Interface, 8(5):313–43, 2001.
5) COP 17 Summary of Outcomes, 17th session of the Conference of Parties http://www.sarva.org.za/sadc/workshops/cop17 - 19 April 2013.
6) LT Drzal, AK Mohanty, R Burgueno and M Misra. Biobased structural composite materials for housing and infrastructure applications: opportunities and challenges. NSF-PATH, 2001, Award No. 0122108.
7) RG Reid, OML Asumani and R. Paskaramoorthy. The effects of alkali-silane treatment on the tensile and flexural properties of short fibre nonwoven kenaf reinforced polypropylene composites. Composites: Part A, 43:1431–1440, 2012.
8) AK Mohanty. Natural Fibers, Biopolymers, and Biocomposites 2005; CRC Press, pp. 41.
9) Y Liu and MT Labuschagne. The influence of environment and season on stalk yield in kenaf. Industrial crops and products, 29: 377-380, 2009.
10) PK Mallick. Fibre-Reinforced Composites, Materials, Manufacturing and Design – Third edition, CRC Press, 2008.
11) EC Ramires and E Frollini. Tannin–phenolic resins: Synthesis, characterization, and application as matrix in biobased composites reinforced with sisal fibers, Composites: Part B, 43: 2836-2842, 2012.

12) Hideki Sato and Hiroyuki Ogawa. Review on Development of Polypropylene Manufacturing Process, R&D Report, Sumitomo Kagaku, volume 2. 2009.
13) Xue Li, G Lope Tabil and Satyanarayan Panigrahi. Chemical treatments of natural fiber for use in natural fiber-reinforced composites: A Review. J Polym Environ, 15:25–33, 2007.
14) R Andrews and MC Weisenberger. Carbon nanotube polymer composites. Current Opinion in Solid State and Materials Science, 8:31-37, 2004.
15) Rupesh Khare and Suryasarathi Bose. Carbon nanotube based composites – A review. Journal of Mineral & Materials Characterization & Engineering, 4(1):31 – 46, 2005.
16) Zhen Zhou, Shifeng Wang, Lan Lu, Yinxi Zhang and Yong Zhang .Functionalization of multi-wall carbon nanotubes with silane and its reinforcement on polypropylene composites. Composites Science and Technology, 68:1727–1733, 2008.
17) SH Aziz and MP Ansell. The effect of alkalization and fibre alignment on the mechanical and thermal properties of kenaf and hemp bast fibre composites: Part 1 – polyester resin matrix. Compos Sci Techno, 64:1219–1230, 2004.
18) W Liu, LT Drzal, AK Mohanty, M Misra. Influence of processing methods and fiber length on physical properties of kenaf fiber reinforced soy based biocomposites. Compos: Part B, 38:352–359, 2007.
19) RM Rowell, RA Young and JK Rowell. Paper and Composites from Agro-Based Resources. Library of Congress TS1109.P1713; pages 330–380, 1996.
20) AK Mohanty, M Misra, and LT Drzal. Sustainable Bio-Composites from Renewable Resources: Opportunities and Challenges in the Green Materials World, Journal of Polymers and the Environment, volume l. 10, Nos. 1/2, April 2002.
21) Aimin Liu. World production and potential utilization of jute, kenaf and allied fibres. Proceeding of the 2000 International Kenaf Symposium, page 139-143, Hiroshima. 13 October 2000.
22) Opportunities in Natural Fiber Composites http://www.lucintel.com/ - 10 October 2013.
23) Fibre Reinforced Plastic http://en.wikipedia.org/wiki/ - 13 November 2013

24) Kenaf harvesting and processing http://www.kenaf-fiber.com/en/coltivazione.asp - 30 April 2010.
25) Kenaf http://www.hort.purdue.edu – 12 May 2010.
26) L Charles, Webber and KV Bledsoe. Plant maturity and kenaf yield components. Industrial Crops and Products, 16: 81–88, 2002.
27) K.E.F.I. Fibre Naturali http://www.kenaf-fiber.com - 01.August.2010.
28) Ting Zhang. Improvement of kenaf yarn for apparel applications. Master's dissertation, Beijing University of Chemical Technology, 2000.
29) R Rowell, A Sanadi, D Caulfield and R Jacobson. Utilization of Natural Fibers in Plastic Composites: Problems and Opportunities in Lignocellulosic Plastics Composites,A.L. Leao, F.X. Carvalho and Frolline edition, USP and UNESP, Brazil, 1997.
30) IS Aji, SM Sapuan, ES Zainudin and K Abdan. Kenaf fibres as reinforcement for polymeric composites: a review. International Journal of Mechanical and Materials Engineering (IJMME), 4 (3):239-248, 2009.
31) Jute, Kenaf, Sisal, Abaca, Core and Allied Fibres, Statistics June 2010 http://www.fao.org/economic/est/publications/jute-hard-fibres-publications/en/ - 10 November 2013.
32) Stefan Rassmann. Mechanical and water absorption properties of resin transfer moulded kenaf fibre reinforced composites, Master's dissertation, University of the Witwatersrand, Johannesburg, 2010.
33) Polypropylene http://www.lenntech.com/polypropylene.htm - 01 November 2013.
34) Brendan McGuigan, What is Polypropylene http://www.wisegeek.com/ what is polypropylene.htm – 25 April 2011.
35) TA Osswald, E Baur, S Brinkmann, K Oberbach and E Schmachtenberg. International plastics handbook: The resource for plastics engineers – 4th edition, Carl Hanser Verlag, 2006.
36) ASM International, Characterization and Failure Analysis of Plastics, Edition 2003.

37) Use of Natural Fibres in Composites to Grow Rapidly http://composite.about.com/library/PR/2000/blkline1.htm - 18 November 2013.
38) Doan Thi Thu Loan. Investigation on jute fibres and their composites based on polypropylene and epoxy matrices, PhD Dissertation, Dresden University of Technology, 2006.
39) J George, SS Bhagawan, S Thomas. Effects of environment on the properties of low-density polyethylene composites reinforced with pineapple-leaf fiber. Composite Science Technology, 58:1471–85, 1998.
40) Mohd Edeerozey, Hazizan Md Akil, AB Azhar and MI Zainal Ariffin. Chemical modification of kenaf fibers. Materials Letters, 61: 2023–2025, 2007.
41) FG Torres and ML Cubillas. Study of the interfacial properties of natural fibre reinforced polyethylene. Polymer Testing, 24:694-698, 2005.
42) MS Huda, LT Drzal, AK Mohanty and Manjusri Misra. Effect of fiber surface-treatments on the properties of laminated biocomposites from poly(lactic acid) (PLA) and kenaf fibers. Composites Science and Technology, 68: 424–432, 2007.
43) Failure Analysis http://failure-analysis.info/2010/05/analyzing-material-fatigue - 15 July 2012.
44) Morten Rask, Bo Madsen, BF Sorensen, JL Fife, K Martyniuk, EM Lauridsen. In situ observations of microscale damage evolution in unidirectional natural fibre composites, Composites: Part A, 43(10):1639-1649, 2012.
45) Jochen Gassan. A study of fibre and interface parameters affecting the fatigue behaviour of natural fibre composites. Composites: Part A, 33:369-374, 2001.
46) AN Towo and MP Ansell. Fatigue of sisal fibre reinforced composites: Constant-life diagrams and hysteresis loop capture. Composites Science and Technology, 68:915-924, 2006.
47) TG Kannan, Chang Mou Wu and Kuo Bing Cheng. Effect of different knitted structure on the mechanical properties and damage behavior of Flax/PLA (Poly Lactic acid) double covered un-commingled yarn composites, Composites: Part B, 43:2836-2842, 2012.

48) American Society of Testing and Materials. ASTM D256 – 10: Standard Test Methods for Determining the Izod Pendulum Impact Resistance of Plastics, Edition 2010.
49) American Society of Testing and Materials. ASTM D6110 – 10: Standard Test Methods for Determining the Charpy Impact Resistance of Notched Specimens of Plastics, Edition 2010.
50) Han-Seung Yang, MP Wolcott, Hee-Soo Kim, Sumin Kim, Hyun-Joong Kim. Effect of different compatibilizing agents on the mechanical properties of lignocellulosic material filled polyethylene bio-composites. Composite Structures, 79:369-375, 2007.
51) BA Kamal, S Pang and MP Staiger. Long-term moisture absorption and thickness swelling behaviour of recycled thermoplastics reinforced with Pinus radiata sawdust. Chem Eng Journal, 142:142:190–98, 2007.
52) CPL Chow, XS Xing and RKY Li. Moisture absorption studies of sisal fibre reinforced polypropylene composites. Compos Sci Technol, 67:306–313, 2007.
53) Yunn-Tzu Yu and Kishore Pochiraju. Three-Dimensional Simulation of Moisture Diffusion in Polymer Composite Materials. Polymer-Plastics Technology and Engineering 42(5):737-756, 2003.
54) S Laurenzi Albrizio and M Marchetti. Modelling of Moisture Diffusion in carbon braided Composites. International Journal of Aerospace Engineering; Article ID 294681:10, 2008.
55) COMPOSITE AGENCY Analysis and Simulation Expertise, <. http://www.composite-agency.com/messages/4643.html> [02.0609] – 05 July 2012.
56) HN Dhakal, Z.Y. Zhang and M.O.W Richardson. Effect of water absorption on the mechanical properties of hemp fibre reinforced unsaturated polyester composites. Compos Sci Technol, 67:1674–83, 2007.
57) Samit Roy. Modelling of Anomalous Moisture Diffusion in Polymer Composites: A Finite Element Approach. Journal of Composite Materials, 33(14):1318, 1999.

58) EL Cusseler. Diffusion: Mass transfer in Fluid system, Third Edition, Cambridge University Press, 1997.

59) Byoung-Ho Lee, Hee-Soo Kim, Sena Lee, Hyun-Joong Kim and John R. Dorgan. Bio-composites of kenaf fibers in polylactide: Role of improved interfacialadhesion in the carding process. Compos Sci Technol, 69:2573–2579, 2009.

60) N Sgriccia, MC Hawley, M Misra. Characterization of natural fiber surfaces and natural fiber composites. Compos: Part A, 39:1632–1637, 2008.

61) SH Aziz, MP Ansell, SJ Clarke and SR. Panteny. Modified polyester resins for natural fibre composites Comps Sci Technol, 65:525-535, 2005.

62) Ana Espert, FranciscoVilaplana and Sigbritt Karlsson. Comparison of water absorption in natural cellulosic fibres from wood and one-year crops in polypropylene composites and its influence on their mechanical properties. Compos: Part A, 35:1267–76, 2004.

63) Moe Thwe and Kin Liao. Effects of environmental aging on the mechanical properties of bamboo-glass fibre reinforced polymer matrix hybrid composites. Compos part A, 33:43-52, 2002.

64) GL Hornyak, J Moore, HF Tibbals and J Dutta. Fundamental of Nanotechnology. CRC Press, 2009.

65) Vikas Mittal. Optimization of Polymer Nanocomposite Properties. WLEY-VCH Verlag GmbH & C0. KGaA, 2010.

66) Peng Cheng Ma, Jang-Kyo Kim and Ben Zhong Tang. Functionalization of carbon nanotubes using a silane coupling agent. Carbon, 44:3232 – 3238, 2006.

67) Ya-Ping Sun, Kefu Fu, Yi Lin and Weijie Huang. Functionalized Carbon Nanotubes: Properties and Applications. Acc. Chem. Res, 35:1096 – 1104, 2002.

68) K Prashantha, J Soulestin, MF Lacrampe, M Claes, G Dupin, P Krawczak. Multi-walled carbon nanotube filled polypropylene nanocomposites based on master batch route: Improvement of dispersion and mechanical properties through PP-g-MA addition. eXPRESS Polymer Letters, 2(10):735–745, 2008.

69) SD Mhlanga, C Mondal, R Carter, J Witcomb and Neil J Coville. The Effect of Synthesis Parameters on the Catalytic Synthesis of Multiwalled Carbon Nanotubes using Fe-Co/CaCO3. Catalysts. S. Afr. J. Chem, 62:67-76, 2009.

70) FH Gojny, MHG. Wichmann, U Köpke, B Fiedler and K Schulte. Carbon nanotube-reinforced epoxy-composites: enhanced stiffness and fracture toughness at low nanotube content. Composites Sciences and Technology, 64:2363-2371, 2004.

71) J Clayden, N Greevs, S Warren and P Wothers. Organic chemistry, 2nd Edition. Oxford University Press, 2012.

72) BG Demczyk, YM Wang, J Cumings, M Hetman, W Han, A Zettl, and RO Ritchie. Direct mechanical measurement of the tensile strength and elastic modulus of multiwalled carbon nanotubes. Materials Sciences and Engineering, A334:173-178, 2002.

73) Min-Feng Yu, Oleg Lourie, J Dyer, Katerina Moloni, F Kelly and Rodney S. Ruoff. Strength and Breaking Mechanism of Multiwalled Carbon Nanotubes Under Tensile Load. Science, 287:637-640, 2000.

74) AK Kaw. Mechanics of Composite Materials. CRC Press, Boca Raton, FL, 2nd edition, 2006.

75) International Standards Organization. ISO: 527, Plastics: Determination of tensile properties, Part 4, 2001.

76) American Society of Testing and Materials. ASTM D3039/ D3039 M: Standard Test Method for Tensile Properties of Polymer Matrix Composite Materials, 2008.

77) International Standards Organization. ISO 178, Plastics: Determination of flexural properties – 4th ed., 2001.

78) American Society of Testing and Materials. ASTM D790: Flexural Properties of Unreinforced and Reinforced Plastics and Electrical Insulating Materials, 2010.

79) American Society of Testing and Materials. ASTM D792: Density and Specific Gravity of Plastics by Displacement, 2008.

80) American Society of Testing and Materials. ASTM D3379: Standard Test Method for Tensile Strength and Young's Modulus for High-Modulus Single-Filament Materials, 1975.
81) Aart van Vuure .Natural Fibre Composite; Recent Developments, i-SUP natural fibre composites, 2008.
82) Animesh Bose and William B. Eisen. Hot consolidation of powders & particulates, Metal powder industries federation, Princeton, New Jersey, 2003.
83) Chao-Xuan Liu and Jin-Woo Choi. Improved Dispersion of Carbon Nanotubes in Polymers at High Concentrations. Nanomaterials, 2:329-347, 2012.
84) British Standards. BS ISO 13003: Fibre-reinforced plastics – Determination of fatigue properties under cyclic loading conditions, Edition 2003.
85) American Society of Testing and Materials. ASTM D3479/D 3479M: Standard Test Method for Tension-Tension Fatigue of Polymer Matrix Composite Materials, Reapproved 2007.
86) American Society of Testing and Materials. ASTM D5766/D5766M – 11: Standard Test Method for Open-Hole Tensile Strength of Polymer Matrix Composite Laminates, 2011.
87) American Society of Testing and Materials. ASTMD D466: Standard Practice for Conducting Force Controlled Constant Amplitude Axial Fatigue Tests of Metallic Materials, 2011.
88) International Standards Organization. ISO:62, Plastic – Determination of water absorption,
89) American Society of Testing and Materials. ASTMD D5229 / D5229M: Standard Test Method for Moisture Absorption Properties and Equilibrium Conditioning of Polymer Matrix Composite Materials, 2007.
90) MS Gockenbach. Partial Differential Equations: Analytical and Numerical Methods. Michigan Technology University Houghton, Michigan 2002.
91) Xu Chen Shufeng Zhao and Linda Zhai. Moisture Absorption and Diffusion Characterization of Molding Compound. 460 / Vol. 127, December 2005 Copyright © 2005 by ASME Transactions of the ASME.

92) Petra Po¨tschke, Arup R. Bhattacharyya, Andreas Janke, and Sven Pegel. Melt Mixing as Method to Disperse Carbon Nanotubes into Thermoplastic Polymers. Fullerenes, Nanotubes, and Carbon Nanostructures, 13: 211–224, 2005.
93) Kravchenko P Ye. Fatigue Resistance, Pergamon Press, 1964.
94) Richard Francis Creed. High cycle tensile fatigue of unidirectional fibreglass composite tested at high frequency, Master's dissertation, Montana State University, 1993.
95) Shinichi Shibata, Yong Cao and Isao Fukumoto. Press forming of short natural fiber-reinforced biodegradable resin: Effects of fiber volume and length on flexural properties. Polymer Testing, 24:1005–1011, 2005.
96) AK Mohanty, LT Drzal, M Misra. Novel hybrid coupling agent as an adhesion promoter in natural fiber reinforced powder polypropylene composites. Journal of Material Science, 88:21:1885–88, 2002.
97) D Cho, HS Lee and SO Han. Effect of fiber surface modification on the interfacial and mechanical properties of kenaf fiber-reinforced thermoplastic and thermosetting polymer composites. Compos Interf, 16:711–29, 2009.
98) I Van de Weyenberg, J Ivens, A De Coster, B Kino, E Baetens, I Verpoest. Influence of processing and chemical treatment of flax fibres on their composites. Compos Sci Technol, 63:1241–6, 2003.
99) Lance Daniel Paiken. The effects of alkali-silane treatment and filler materials on the tensile and water absorption properties of hemp fibre reinforced polypropylene, Master's dissertation, University of the Witwatersrand, Johannesburg, 2013.